



HEINRICH HEINE
UNIVERSITÄT DÜSSELDORF

Studies on ABC Transporters from Human Liver in Heterologous Expression Systems

Inaugural-Dissertation

zur Erlangung des Doktorgrades
der Mathematisch-Naturwissenschaftlichen Fakultät
der Heinrich-Heine Universität Düsseldorf

vorgelegt von

Jan Stindt

aus Kiel

Düsseldorf, 2010

Studies on ABC Transporters from Human Liver in Heterologous Expression Systems

Inaugural-Dissertation

zur Erlangung des Doktorgrades
der Mathematisch-Naturwissenschaftlichen Fakultät
der Heinrich-Heine Universität Düsseldorf

vorgelegt von

Jan Stindt

aus Kiel

Düsseldorf, im Dezember 2010

Aus dem Institut für Biochemie
der Heinrich-Heine-Universität Düsseldorf

Gedruckt mit der Genehmigung der
Mathematisch- Naturwissenschaftlichen Fakultät
der Heinrich-Heine-Universität Düsseldorf.

Referent: Prof. Dr. Lutz Schmitt

Koreferent: PD Dr. Ulrich Schulte

Tag der mündlichen Prüfung:

»...hier können wir die Hände bis an den Ellenbogen in das stecken, was man Abenteuer nennt.«

- Miguel de Cervantes (1605) El ingenioso hidalgo Don Quixote de la Mancha

meiner Familie

Summary

Today, the physiological function of canalicular export systems of the human liver in detoxification, bile generation and secretion is clearly defined. Most membrane proteins taking part in this function are members of the ATP binding cassette (ABC) transporter family and perform primary active substrate transport energized by ATP hydrolysis. On a molecular level, little knowledge exists about the relation between mutations in these membrane proteins and the diseases they are associated with. Convenient *in vivo* systems are limited and cannot answer many questions of molecular function. To gain mechanistic insights into both wild type and mutated transporters, *in vitro* systems are indispensable that are of a very limited availability.

The aim of this thesis was to establish suitable *in vitro* systems for human ABC transporters that are expressed in the apical membrane of polarized hepatocytes. Here, the human bile salt export pump (BSEP, ABCB11) and the multidrug resistance protein 3 (MDR3, ABCB4) play an important role in bile secretion, and their malfunction is associated with severe hereditary diseases like Progressive Hereditary Intrahepatic Cholestasis (PFIC) type 2 and 3. Heterologous overexpression is a vital necessity for *in vitro* studies, because membrane proteins, especially those from human, are quite unstable and of rather low abundance in their native tissue. In contrast to mammalian cell culture, the yeasts *Saccharomyces cerevisiae* and *Pichia pastoris* provide comparatively easy and well-characterized expression systems for polytopic membrane proteins. A challenge associated with BSEP and MDR3 is the instability of their coding sequences in *Escherichia coli* that has been a strong limiting factor in previous studies on both, and especially on clinically relevant mutations in these, as the latter are not easily generated. The results of this thesis can be summarized as follows:

I) The first-time heterologous expression in *S. cerevisiae* yeast of both human BSEP and MDR3 was achieved, both chromosomally and from plasmid. For the low-expressing BSEP, an expression screen was devised that did not lead to an improved expression. The compatible osmolyte glycerol was found to function as a chemical chaperone for BSEP, leading to an estimated twofold increase in expression. For MDR3 it was found that the his tag position had a dramatic impact on expression levels.

II) In *S. cerevisiae*, the C-terminally his-tagged MDR3 could be expressed at a level comparable to MDR1 which yields milligram amounts per litre of culture. Human MDR3 could be detergent-solubilized and purified to amounts that for the first time allowed its detection on a Coomassie-stained SDS-PAGE gel.

III) The yield of BSEP could be improved substantially by switching the expression host from *S. cerevisiae* to *P. pastoris*.

IV) In order to establish expression in both yeast systems, a complete workflow was designed and implemented that allows the cloning of the unstable *BSEP* and *MDR3* coding sequences without the use of *E. coli*. Instead, the cloning strategy can completely rely on the powerful homologous recombination machinery of *S. cerevisiae*. The workflow includes a new site-directed mutagenesis procedure that is also independent of *E. coli* usage and enables the rapid recreation of clinically relevant BSEP and MDR3 mutations in both mammalian cell culture and the yeast expression systems. This has previously been a complicated and time-consuming procedure as the attempt to introduce targeted mutations regularly led to random deletions within the constructs.

As a result of this work, clinically relevant mutants of BSEP and MDR3 are now generated much faster, and several BSEP variants are currently being studied in mammalian cell culture and *in vitro*.

Zusammenfassung

Die physiologische Funktion kanalikulärer Transportsysteme in der menschlichen Leber ist heute klar definiert. Die Mehrheit der beteiligten Membranproteine gehören zur Familie der ATP-Bindekassette (ABC)-Transporter und vermitteln den primär-aktiven Transport ihrer Substrate unter ATP-Hydrolyse. Auf molekularer Ebene sind die Beziehungen zwischen Mutationen in diesen Membranproteinen und den damit assoziierten Krankheiten noch weitgehend unverstanden. *In vivo*-Systeme sind für die Untersuchung vieler Fragestellungen auf molekularer Ebene ungeeignet. Um mechanistische Einblicke in die Funktionsweise von Wildtyp als auch mutierten Transportern zu erlangen, werden *in vitro*-Systeme benötigt.

Ziel dieser Doktorarbeit war, geeignete *in vitro*-Systeme für humane ABC-Transporter bereitzustellen, die in der kanalikulären Membran der Hepatozyten lokalisiert sind. Die Gallensalzexportpumpe (BSEP, ABCB11) und das Multidrogenresistenzprotein 3 (MDR3, ABCB4) nehmen wichtige Rollen bei der Sekretion von Gallenbestandteilen ein. Ihre Fehlfunktion ist mit schweren erblichen Erkrankungen wie der Progressiven Familiären Intrahepatischen Cholestase (PFIC) Typ 2 und 3 verbunden. Ihre heterologe Überexpression ist eine wichtige Voraussetzung für *in vitro*-Studien, da Membranproteine recht instabil sind und in ihrem nativem Gewebe oft nur in geringer Menge vorkommen. Im Gegensatz zu Säugetierzellkultur sind die beiden Hefen *Saccharomyces cerevisiae* und *Pichia pastoris* leicht handzuhabende und gut charakterisierte Expressionssysteme für Membranproteine. Eine Herausforderung in bezug auf BSEP und MDR3 ist die Instabilität der kodierenden DNS-Sequenzen in *Escherichia coli*, die in vorherigen Studien ein limitierender Faktor war. Speziell Studien an Transportermutationen gestalten sich schwierig, da die Mutagenese der kodierenden Sequenzen stark erschwert ist. Die Ergebnisse dieser Doktorarbeit können wie folgt zusammengefaßt werden:

I) Die erstmalige heterologe Expression von BSEP und MDR3 in Bäckerhefe gelang sowohl chromosomal als auch plasmidgebunden. Da hier die Expression von BSEP nur sehr gering war, wurde ein Expressionstest verschiedener Promotoren durchgeführt, der zu keiner Expressionssteigerung führte. Der Zusatz von Glycerin, einem kompatiblen Osmolyten, zu den Hefekulturen bewirkte eine zweifache Expressionssteigerung von BSEP. Glycerin diente hier als eine chemische Faltungshilfe. Für MDR3 wurde gezeigt, daß die Position des Histidin-Affinitätsanhängsels die Expression signifikant beeinflusste.

II) Ein carboxyterminal mit einem Histidin-Affinitätsanhängsel fusioniertes MDR3 konnte in Bäckerhefe in Mengen exprimiert werden, die mit denen hier für humanes MDR1 erzielten vergleichbar sind. MDR3 konnte mit Detergenzien solubilisiert und anschließend in Mengen aufgereinigt werden, die erstmalig die Detektion auf einem mit Coomassie-Farbstoff gefärbten SDS-Proteingel ermöglichten.

III) Die Ausbeute an rekombinantem BSEP konnte durch Wechsel des Expressionssystems von der Bäckerhefe auf die methylotrophe Hefe *Pichia pastoris* deutlich erhöht werden. Aus diesem kann BSEP jetzt in präparativen Mengen solubilisiert und aufgereinigt werden.

IV) Zur Etablierung der Expression in beiden Hefesystemen wurde ein kompletter Arbeitsablauf realisiert, der die Klonierung der instabilen kodierenden DNS-Sequenzen von BSEP und MDR3 ohne *E. coli* ermöglicht. Die Strategie macht sich stattdessen die effiziente Maschinerie von *S. cerevisiae* zur homologen Rekombination von DNS-Sequenzen zunutze. Der Arbeitsablauf beinhaltet außerdem eine neue Methode zur zielgerichteten DNS-Mutagenese, die ebenfalls ohne *E. coli* funktioniert und die schnelle Herstellung klinisch relevanter BSEP- und MDR3-Mutationen sowohl in Säugetierzellkultur

als auch in den Hefeexpressionssystemen ermöglicht. Dieses war bisher sehr zeitaufwendig, da die Einführung von Mutationen auf DNS-Ebene regelmäßig zu zufälligen Deletionen in den Konstrukten führte.

Aufgrund dieser Arbeit können klinisch relevante Mutationen in beiden Transportproteinen nun ungleich schneller und leichter realisiert werden, und diverse BSEP-Varianten werden derzeit sowohl in Zellkultur als auch *in vitro* untersucht.

Summary of Contents

Summary	I
Zusammenfassung	II
Summary of Contents	IV
1 Introduction	1
1.1 Membrane Transport	1
1.2 ATP Binding Cassette Transporters - the Largest Family of Primary Active Transporters.....	2
1.3 Structure and Function of ABC transporters.....	3
1.4 The Human ABC Transporter Superfamily.....	11
1.5 Active Transport and Detoxification Processes in the Liver.....	14
1.6 The Role of Human Hepatic ABC Transporters in Bile Formation.....	19
1.7 Eukaryotic Expression Systems for Human ABC Transporters	21
Aims and Objectives	23
2 Materials and Methods	24
2.1 Materials	24
2.2 Methods	36
3 Results	63
3.1 The <i>BSEP</i> and <i>MDR3</i> cDNA Sequences are unstable in <i>E. coli</i>	63
3.2 A Set of Cassette Vectors for the Chromosomal Overexpression of both yeast and non-yeast genes in <i>Saccharomyces cerevisiae</i>	65
3.3 Expression in <i>S. cerevisiae</i> of the Human Bile Salt Export Pump and Multidrug Resistance Protein 3 by Use of Homologous Recombination.....	72
3.4 Expression of BSEP and MDR3 from Plasmid in <i>S. cerevisiae</i>	77
3.5 A Recombination-Based Expression Plasmid Screen for BSEP	82
3.6 The Use of the Compatible Solute Glycerol as a Chemical Chaperone to Increase BSEP Expression in <i>S. cerevisiae</i>	89
3.7 Subcellular Localization of Human BSEP and MDR3 in <i>S. cerevisiae</i>	92
3.8 Testing for a Cellular Resistance Phenotype of BSEP and MDR3 in <i>S. cerevisiae</i>	93
3.9 Initial Purification of Human BSEP and MDR3 from <i>S. cerevisiae</i>	101
3.10 Moving Expression of BSEP from <i>S. cerevisiae</i> to <i>Pichia pastoris</i>	106
3.11 The Site-Directed Mutagenesis of Human <i>BSEP</i> by a New, <i>E. coli</i> -Independent Approach..	110
3.12 Rapid Site-Directed Mutagenesis and Expression Analysis of a Yeast-Enabled Mammalian BSEP Expression Vector	115
4 Discussion	117
4.1 The Impact of Affinity Tag Position on the MDR3 Fusion Protein demonstrates the Empirical Value of Expression Screens.....	117
4.2 Overexpression of Human BSEP	119
4.3 Further Steps towards <i>In Vitro</i> Studies of BSEP and MDR3	120
4.4 Lack of a Cellular Phenotype of BSEP Expression in <i>S. cerevisiae</i>	121
4.5 The M800I Variant of MDR3	122
4.6 Lack of MRP2 Expression in <i>S. cerevisiae</i>	124
4.7 DNA Cloning and Manipulation in <i>S. cerevisiae</i>	125
Outlook	133
References	134
Abbreviations	150
Danksagung	153
Erklärung.....	155
Lebenslauf	156

1 Introduction

Cells have evolved compartments of distinct and regulated composition [1]. Biological membranes, which are selectively permeable barriers, keep these various compartments separate from each another and also segregate the interior of the cell from the extracellular environment. These membranes are composed of a lipid bilayer, which due to its hydrophobic nature is a barrier to charged, hydrophilic, and large molecules. Only very small hydrophobic or neutral compounds such as oxygen and carbon dioxide can permeate such a bilayer, while the diffusion of other molecules such as metal ions or metabolites and enzymes away from their point of biogenesis, function, and turnover is limited. In contrast, cellular membranes permit the selective uptake and accumulation of diverse nutrients, while secreting metabolic waste products. Across each of these membranes, the directional and selective transport of a wide variety of both macro- and micromolecules is carried out [2,3].

1.1 Membrane Transport

This selective and highly regulated transport is mediated by integral membrane proteins [1]. These or domains of these membrane proteins reside in the lipid bilayer by presenting hydrophobic and aromatic side chains at the protein-lipid interface. Here, they facilitate the transmembrane passage of the most diverse substances [4,5,6]. For example, aquaporins, large alpha barrel membrane proteins, are highly selective channels for water molecules that allow their quick diffusion across the membrane [7]. Carrier proteins bind and shield the charges of their substrate to facilitate its passive diffusion across the membrane. Secondary active transporters that transport molecule "a" are driven by the concentration gradient of molecule "b" across a membrane. Other membrane proteins in turn create and maintain this concentration gradient which then can then be used to fuel the co-transport of another compound against its own concentration gradient. Symporters either transport their substrate in the same, antiporters in the opposite direction of the energy-providing molecule gradient.

Primary active transporters, that establish these energizing gradients, are often fueled by the hydrolysis of adenosine triphosphate (ATP). The phosphodiester bond within this molecule contains 57 kilojoules per mol of Gibbs free energy stored in the covalent linkage of the gamma to the beta phosphate, a phosphoric acid

anhydride [8]. The yeast plasma membrane ATPase Pmal is a primary active transporter that uses this energy to create a proton gradient from the exterior to the cytosol [9,10,11]. The sodium potassium pump is another ATP-dependent primary transporter [12,13]. It is an electrogenic pump as it generates a membrane surface charge separation and helps create the plasma membrane resting potential that is vital for e. g. signal transduction by neuronal cells [1]. The action of the sodium potassium pump also fuels secondary active transport processes and plays a role in cell volume regulation. Apart from ATP, redox energy (the mitochondrial electron transport chain) or light (bacteriorhodopsin [14], and the photosystems of the thylakoid membranes in chloroplasts) can serve to fuel primary active transport across biological membranes [1].

1.2 ATP Binding Cassette Transporters - the Largest Family of Primary Active Transporters

ATP binding cassette (ABC) transporters are probably the largest group of primary active membrane transporters [15]. In 1982 the group of Giovanna Ames cloned the first ABC transporter gene, the histidine permease from *Escherichia coli* [16]. Today, 78 ABC-encoding genes are described within its genome [17], 31 in the yeast *Saccharomyces cerevisiae* [18] and 48 in human [19,20]. ABC transporters are old in evolutionary terms as they are found in archaea, eubacteria, in plant and animal eukaryotes [21]. Sequence analyses indicate that while about 4 % of all genes in *Escherichia coli* and *Bacillus subtilis* encode membrane proteins, 2 % of the genome, or half the membrane protein genes, encode ABC transporters [22]. They function as im- or exporters of an astonishing variety of substrates, both natural and synthetic, ranging from heavy metal ions or small molecules like sugars, amino acids, vitamins, osmolytes or short peptides to xenobiotics, antifungals and drugs to whole proteins [15]. Some recognize a single specific substrate, while others bind and translocate a wide variety of in part chemically diverse substrates [23,24,25]. Members of the latter group such as the multidrug resistance protein 1 (MDR1 or P-glycoprotein, P-gp), the breast cancer resistance protein (BCRP), and multidrug resistance associated protein (MRP) 1 are the main cause of chemotherapy (multidrug) resistance of cancer cells [26,27].

1.3 Structure and Function of ABC transporters

Domain organization of ABC transporters

A functional ABC transporter consists of two nucleotide binding domains (NBDs) and two transmembrane domains (TMDs, Figure 1). The two TMDs interact as homo- or heterodimers to form a passage through a membrane and thus facilitate the transport of various substrates which in turn is energized by the ATPase activity of the two NBDs. In archaea and eubacteria, the different transporter components are usually encoded by separate genes (Figure 1, upper and middle panel). Importers and exporters can readily be discriminated by virtue of sequence analysis. Only importers contain the highly conserved EAA motif in an intracellular loop of their TMDs which most likely interacts with a specific region of the NBD [28,29]. ABC importers containing this motif are found in archaeal and bacterial organisms only. Here, the substrate first interacts with its cognate substrate binding protein (SBP), which is another exclusive feature of ABC import systems. In Gram-positive bacteria, this is additionally anchored to the cytoplasmic membrane by a lipid moiety where it acquires substrate molecules and directs them to the TMDs. Anchoring to the plasma membrane by a short, transmembrane alpha helix has been found exclusively in archaea until now [30]. In eukaryotic genomes, one NBD and one TMD occur as one fused gene, e. g. TMD-NBD (termed half-size transporter), or the complete functional unit is encoded by one structural gene, e. g. (TMD-NBD)₂ (termed full-size transporter; Figure 1, lower panel) [21]. The organization of domain elements can be either (TMD-NBD)₂ (regular) or (NBD-TMD)₂ (inverse topology) and additional transmembrane segments have been described in addition to the core helices of MRP-type ABC transporters like the multidrug resistance-associated protein 2 [30,31,32].

ABC Protein Family Characteristics and the Nucleotide Binding Domains

All ABC proteins share highly conserved sequence motifs within their NBD (see Figure 2) [33]. The P-loop, also termed the Walker A motif (consensus sequence GXXGX(G)KST, X for any amino acid residue), the Walker B motif ($\phi\phi\phi\phi$ D, ϕ for any hydrophobic residue) and the C-loop or ABC signature motif (LSGGQ) between these two are specific for the NBD [21,34].

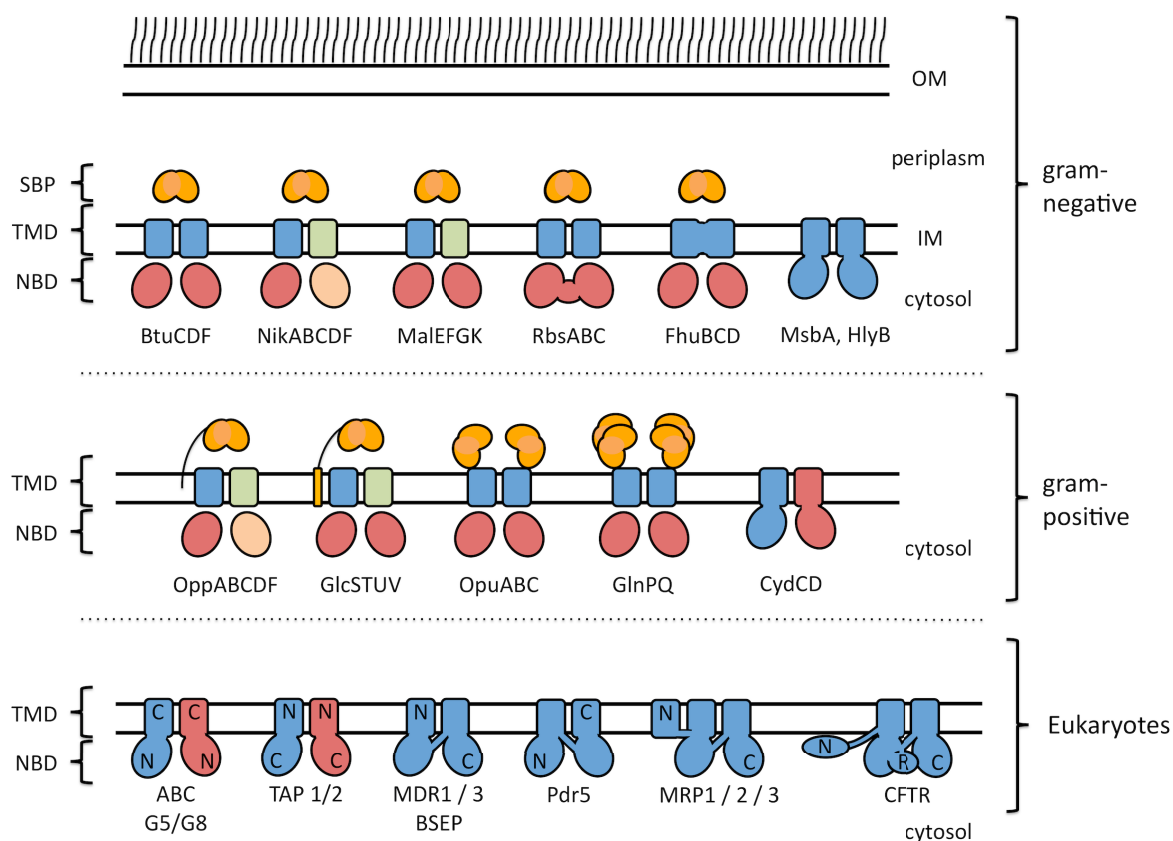


Figure 1. The domain organization of different ABC transporter systems. The functional unit of an ABC transporter consists of two TMDs and two NBDs. These can be fused onto a single polypeptide chain in full-size transporters. One TMD and NBD are fused to each other in half-size transporters, and all four subunits can also be encoded by separate genes. This is only encountered in prokaryotes. ABC importers bind their cognate substrate binding protein (SBP), which in gram-negative bacteria is contained in the periplasmic space by the outer membrane. In gram-positive organisms, this is either anchored in the membrane by a lipid moiety or a transmembrane segment (exclusive to archaea). Adapted from [30].

After these core ABC motifs comes the D-loop (SALD), and C-terminal to that is a conserved histidine residue essential for ATP hydrolysis [35]. These motifs reflect structural features of the NBD and conserved functions *in vivo*: the Walker A motif/P-loop constitutes a loop binding the phosphate moiety of ATP [36]. Walker B is part of a beta sheet and participates in the coordination of the catalytically important Mg^{2+} cation.

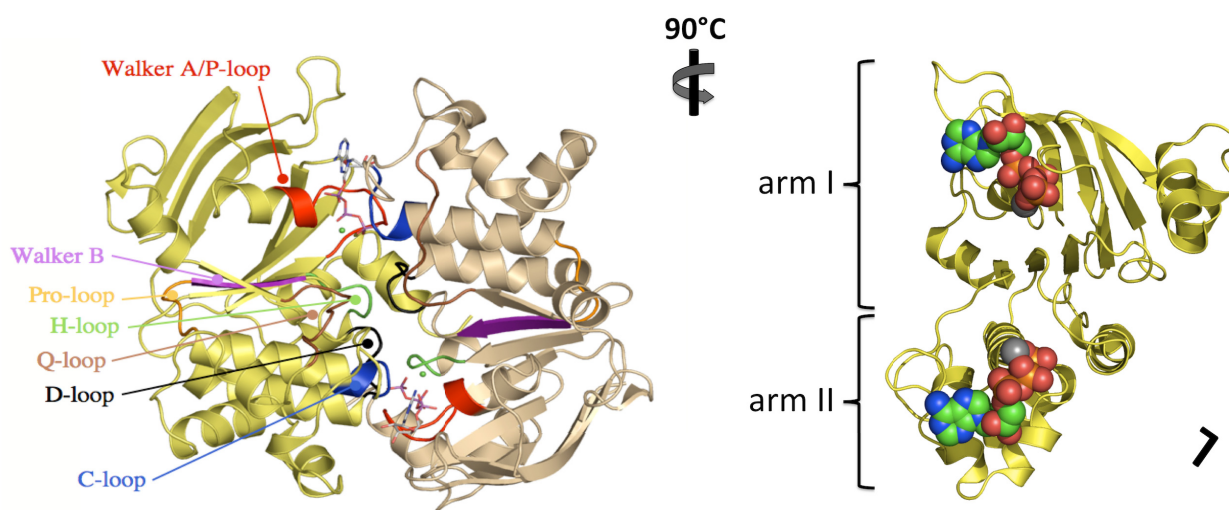


Figure 2. **Crystal structure of the haemolysin B NBD dimer.** **Left** The dimer of the H662A variant of the HlyB NBD is shown with bound ATP (stick molecules) and Mg^{2+} (green spheres). For ease of viewing, the two NBDs are individually coloured. Conserved motifs are marked in different colours on the left NBD. Both NBD monomers contribute to each of the ATP binding sites with the Walker A and B motif residing on one and the C-loop on the opposite NBD. Through its coordination by these three motifs in the two sites, ATP functions as a "molecular glue" in the process of NBD dimerization [35,37,38]. **Right** View of the yellow HlyB NBD monomer from the interface plane. The L-shaped architecture of the two arm domains is shown. Both bound ATP molecules and both Mg^{2+} ions are indicated as calotte models and spheres, respectively. Adapted from [35].

It plays an important role in the hydrolysis of the anhydride bond between the gamma- and beta-phosphate. The Q-loop serves as a gamma-phosphate sensor [35]. It is generally hypothesized that during hydrolysis both NBDs at least transiently form a dimer [39]. Solved structures of the DNA repair enzyme Rad50, the HlyB-NBD ATP-bound dimer [35], and the full-length vitamin B₁₂ transporter BtuCD show that the ATP binding pockets are formed by the Walker A and B of one NBD and the signature motif of the opposite NBD [40,41]. Here, the serine residue of the C-loop is in close contact with the gamma-phosphate of the bound ATP [42]. ATPase domains of ABC transporters show similarity to the F₁-ATPase [43] and RecA [44]. The structure of the NBD is that of an L-shape (Figure 2, right side): the larger domain

(arm I) has structural homology to RecA and other nucleotide binding proteins and consists of alpha helices and beta strands (alpha/beta fold). It contains the Walker A, B motifs and the Q-, H- and D-loop described above (left side). The smaller domain (arm II) exclusively consists of alpha helices and contains the ABC signature motif or C-loop. All atomic structures solved so far show the same overall architecture. Comparison of structures solved with bound ATP [35,45,46,47,48] to those with bound Mg/ADP [47,49,50,51,52] suggests the release of hydrolysis products by a rotational movement of arm II. How exactly binding and hydrolysis of ATP are coupled to transport remains yet to be elucidated.

The transmembrane domains

While NBDs share an average 30 % of amino acid sequence identity, the same does not apply to the highly diverse TMDs. The high sequence conservation among NBDs suggests a common mode of providing and transferring chemical energy derived from ATP hydrolysis to the variable TMD units. Still, the sequence heterogeneity of the TMDs is generally assumed to reflect the wide spectrum of the various substrates that differ as much in structure, shape and size as their respective cognate TMDs.

Studies on both bacterial and mammalian ABC transporters and hydrophobicity plots argue in favor of six transmembrane helices per TMD as a general core functional unit. The six-helices architecture was confirmed by solving full-length transporter structures such as the bacterial lipid flippase MsbA [53], the SAV1866 putative MDR pump [54], and more recently, the mouse P-glycoprotein (the murine homologue of the human MDR1 multidrug efflux pump [55]). In contrast, other hydrophobicity plots of mostly eukaryotic transporters such as the transporter associated with antigen processing (TAP), a half-size heterodimer, predict a composition of 10 (TAP1) and 9 (TAP2) transmembrane helices, respectively [31,32]. Deletion studies have shown that the C-terminal six transmembrane helices of both TAP TMDs form an essential channel complex while the others are not engaged in its formation [31,56]. Instead, the additional three and four helices of the ER-resident TAP heterodimer have been proposed to facilitate the binding of tapasin (TAP ASSociated proteIN), the central interface component in the peptide loading complex (PLC), that recruits empty MHC class I heterodimers to TAP for loading with peptides derived from the proteasome on the cytosolic side. Here, the additional component helices function as interaction modules for other molecules engaged in the same

pathway [31,32]. More importantly, the crystal structure of the vitamin B₁₂ transporter BtuCD clearly showed ten TM helices in each TMD [41], indicating that additional TMD architectures exist. Functions of NBD and TMD in ATP hydrolysis, substrate recognition and transport are, however, not always mutually exclusive, as was shown for the haemolysin transport complex of uropathogenic *E. coli*. Here, the substrate HlyA was shown to interact with the NBD of HlyB [57].

The catalytic cycle of the NBDs and its coupling to substrate transport

Several functional mechanisms have been postulated for ABC transporters. A general working mechanism for substrate transport by membrane pumps was postulated already in 1966 by Jardetzky [58]. In this model, a transporter can in general assume two basic conformations: one that is open towards one side, and one that is open towards the other side of the membrane. As a result, the substrate binding site is accessible from only one side of the membrane at a time (Figure 3).

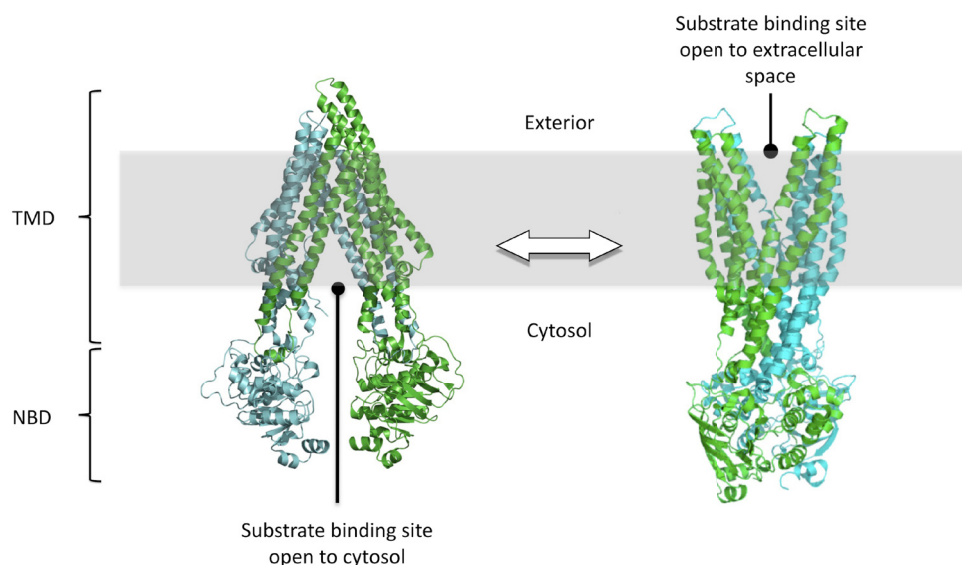


Figure 3. The Alternating Access Model of ABC transporter function. Already suggested by Jardetzky in 1966 [58] as a principal mode of operation for membrane pumps, this mechanism can also be postulated from the currently available structural data. **Left** The mouse P-gp structure [55] displays a large cavity accessible from both cytosol and inner membrane leaflet. **Right** The Sav1866 structure [54] represents an outward open conformation with potential access to the outer membrane leaflet. Adapted from [23].

Two available crystal structures of ABC exporters are thought to represent both alternate, either inward (mouse P-gp, left side) or outward open (Sav1866, right side) conformations [54,55]. On the premise of the alternating access concept, the "ATP Switch" [39] and "Processive Clamp" [59] models of substrate transport have been described. In the first model, the binding of two ATP molecules is the switch that induces dimerization of the NBDs and, upon hydrolysis of both, dimer dissociation. The second model postulates the sequential hydrolysis of the two bound ATP molecules. Recent biochemical and structural studies (reviewed in [39]) suggest that the energy released by ATP hydrolysis is not directly translated into substrate translocation by conformational changes in the TMDs and thereby does not serve as the "power stroke" in the catalytic cycle as had been postulated previously [60]. Rather, ATP binding itself induces the necessary conformational changes for substrate translocation by NBD dimerization, and subsequent hydrolysis resets the transporter to its original conformation. Based on the general, "Alternating Two-Site Access" mechanism postulated for membrane pumps [58], a catalytic cycle can be assembled that integrates these biochemical findings. Figure 4 depicts the "Processive Clamp" transport cycle of an ABC exporter: in the initial state, the NBDs are monomers allowing nucleotide exchange and binding, and the high-affinity substrate binding site is exposed by the inward open conformation of the TMDs (step 1). After substrate and ATP binding, the nucleotide-induced dimerization of the NBDs effects the conformational change to the outward open TMD configuration and concomitant substrate translocation across the membrane (step 2), where it is released from its low affinity binding site (step 3). ATP hydrolysis (step 4) then effects the dissociation of the NBD dimer (step 5), which drives the conformational change of the TMDs back to the inward open conformation. The hydrolyzed nucleotide can be exchanged against fresh ATP, which completes the catalytic cycle (step 6).

This model of the catalytic cycle nicely integrates the biochemical and structural findings of both isolated NBDs and full transporters. NBDs have been overexpressed and purified in isolation for crystallization and *in vitro* studies. Some of these subunits display a basal ATPase activity, e. g. HisP or HlyB-NBD [61,62], or the cloned NBD of P-gp from mouse, contradicting the argumentation that hydrolysis occurs only in the presence of bound substrate.

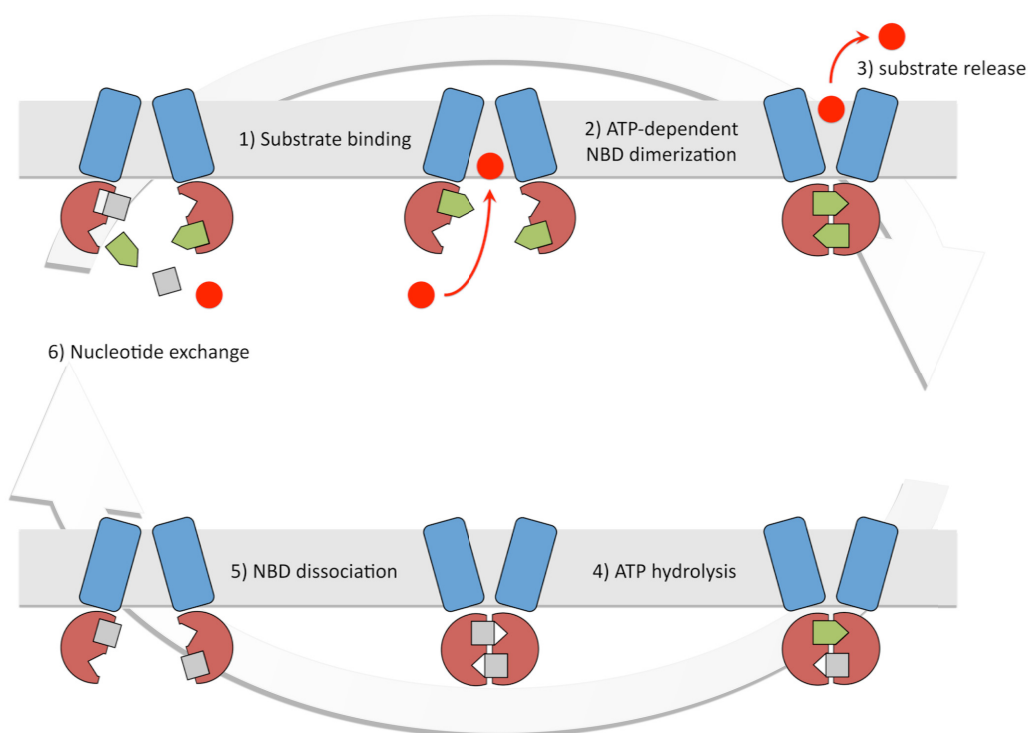


Figure 4. The "Processive Clamp" model of the ABC transport cycle. 1) The translocation channel formed by the two TMDs is open towards the cytosol, and the NBDs are monomeric and can exchange nucleotides. 2) After substrate binding to the high affinity site, bound nucleotide induces NBD dimerization and changes translocation channel to outward open conformation. 3) Substrate is released from the low affinity binding site. 4) Nucleotides are hydrolyzed, 5) which triggers NBD dissociation and subsequent change back to the inward open conformation of the translocation channel. 6) Hydrolyzed nucleotides can be exchanged in the monomeric NBDs, and a new cycle can be initiated. Adapted from [23].

Interestingly though, ATPase activity of the histidine permease NBD (HisP) is abolished by addition of the corresponding TMDs. In such a setting, hydrolysis can be measured again only after substrate addition [63,64]. In the intact scaffold of the transporter structure, hydrolysis of ATP in the NBDs is tightly coupled to substrate recognition and binding in the TMDs. But how is the binding event in the TMDs relayed to the NBDs in order to allow ATP binding, and how is the dimerization event translated into the proposed conformational changes in the TMDs? Mutagenesis studies on the maltose importer system identified the EAA motif in the fourth cytosolic loop of the TMD unit that mediated assembly of the separately encoded TMD and

NBD subunits but failed to do so when mutated [29]. This conserved loop was subsequently found to interface with its adjacent NBD in the solved structures of complete transporters [41,54,55,65,66,67,68] and is generally thought to play an important role in the interdomain crosstalk during the transport cycle (Figure 5).

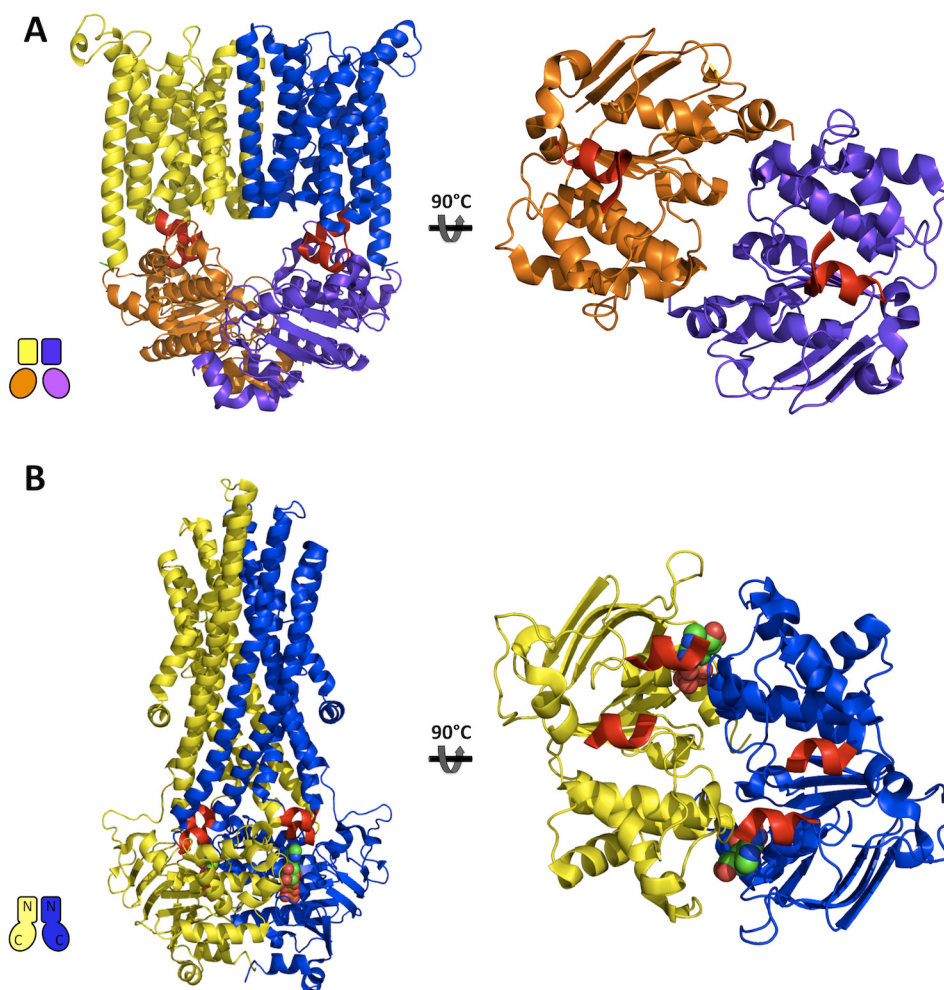


Figure 5. Crosstalk between TMDs and NBDs. **A, left** The vitamin B₁₂ importer BtuCD consists of two identical NBDs and two identical TMDs that each comprise 10 transmembrane helices. The proposed coupling helices of each TMD (coloured in red) interface with the NBD directly below. **B** Sav1866 is a homodimeric half-size exporter with 6 transmembrane helices. Here, two cytosolic loops in each TMD are candidates for interdomain communication: one helix interfaces with the *cis*-NBD (on the same polypeptide chain as the TMD) while the other is the classic coupling helix that interfaces with the *trans*-NBD. The denoted helices are assumed to couple substrate recognition and transport to hydrolysis of ATP or, in other words, mediate the crosstalk between TMDs and NBDs during the catalytic cycle. The bound ADP molecules in the Sav1866 structure are depicted as calotte models.

1.4 The Human ABC Transporter Superfamily

Based on phylogenetic analysis, the 48 ABC genes found in human are divided into seven subfamilies, ABCA to ABCF [19]. Many of the human ABC transporters have been discovered in studies on hereditary diseases in which they are implicated (Table 1). A prominent example is cystic fibrosis, the most common fatal inherited human disease [69].

Subfamily ABCA (ABC1) contains twelve full-size transporters and the largest human ABC genes, some of which encode proteins longer than 2100 amino acids. Mutations in two A subfamily genes are associated with hereditary diseases: ABCA1 is connected with Tangier disease and functions in cholesterol transport and high-density lipoprotein (HDL) biosynthesis [70,71,72,73]. Mutations in ABCA4 cause Stargardt disease, a progressive macular degeneration [74,75,76]. ABCA4 transports a retinal precursor in the outer rod segment of photoreceptor cells that is cytotoxic upon accumulation.

A unique feature of the B (MDR/TAP) subfamily is that it comprises both full- (four) and half-size (seven) transporters. ABCB1 (MDR1, P-gp) was the first cloned and studied human ABC transporter [77,78,79,80,81]. It was identified as the cause of a multidrug resistance phenotype in tumour cells. It can be found in many tissues including the blood–brain barrier and the liver. ABCB4 and ABCB11 proteins are both located in the liver and are involved in the secretion of bile components [82,83,84]. ABCB2 and ABCB3 form the TAP heterodimer that exports peptides derived from the proteasome in the cytosol into the endoplasmic reticulum (ER) for MHC I antigen presentation on the cell surface. Other members function in mitochondrial iron metabolism and Fe/S cluster transport [85].

The ABCC (MRP/CFTR) subfamily encompasses the MRP (multidrug resistance related proteins), the sulfonylurea receptors (SUR) 1 and 2 and the cystic fibrosis transmembrane conductance regulator (CFTR). It is the biggest ABC subfamily [86], containing twelve full-size transporters with diverse functions such as ion transport (CFTR), cell surface receptor (SUR), and toxin extrusion (MRP1 and 2). The chloride ion channel CFTR participates in exocrine secretion, and mutations in CFTR cause cystic fibrosis, the most common mutation being the $\Delta F508$ deletion leading to protein misfolding and degradation (reviewed in [87]). ABCC8 and ABCC9 (SUR1 and 2) bind sulfonylurea and regulate potassium channels involved in modulating insulin secretion [88]. Of the nine MRP-related genes, ABCC1, ABCC2,

and ABCC3 transport drug conjugates to glutathione and other organic anions. ABCC4, ABCC5, ABCC11 and ABCC12 lack an additional N-terminal TMD0 that is comprised of five transmembrane helices (reviewed in [89]). The TMD0 segment has been found to be irrelevant for transport function [90]. ABCC4 and ABCC5 proteins confer resistance to nucleosides including PMEA and purine analogs that are used in antiviral treatment.

The ABCD (ALD) subfamily contains four genes. The yeast subfamily members Pxa1 and Pxa2 form a heterodimer involved in peroxisomal very long chain fatty acid (VLCFA) oxidation [91]. All members are half-size peroxisomal transporters participating in the regulation of VLCFA transport.

The ABCE (OABP) and ABCF (GCN20) subfamilies contain genes that have ATP-binding domains that are clearly derived from ABC transporters but have no TMDs and are not known to be involved in any membrane transport functions. The only ABCE member is the oligo-adenylate binding protein [92]. Oligo-adenylate is produced in response to infection by certain viruses [93]. ABCE has been suggested to be part of the innate immune system as it is found in multicellular eukaryotes, but not in yeast. ABCF genes code for a pair of NBDs. In yeast, Gcn20 mediates activation of the eIF-2 α -kinase [94]. Studies on its human homolog ABCF1 have shown association with the ribosome, proposing similar function [95].

The human ABCG (White) subfamily is comprised of six half-size transporters that, in contrast to all other human ABC superfamily members, possess an inverted topology (i. e. NBD-TMD instead of TMD-NBD). The name White is derived from the ABCG gene at the white locus of *Drosophila*. Here, the white protein participates in transport of the eye pigment precursors guanine and tryptophan [96]. In contrast, mammalian ABCG1 is associated with cholesterol transport regulation [97]. The multidrug efflux pump BCRP (ABCG2, also known as MXR, mitoxantrone resistance protein) and the ABCG5/G8 heterodimeric cholesterol transporter of liver and intestine are prominent ABCG members associated with tumor MDR and sitosterolemia, respectively [98]. Next to MDR1 and MRP1 and other MRP members, ABCG2 mediates multidrug resistance in a variety of tissues.

Table 1. Human ABC transporter genes and their associated hereditary diseases

ABC Gene	Associated disease	Physiological function	Reference
<i>ABCA1</i>	Tangier disease, FHDLD	Export/loading of cholesterol and phospholipids onto HDL	[70,71,72,73]
<i>ABCA4</i>	Stargardt disease, FFM, RP, CRD, CD, AMD	Translocation of N-retinylidene-PE, an all-trans-retinal precursor	[74,75,76]
<i>ABCB1</i>	Ivermectin susceptibility, Digoxin uptake	Resistance against various cytotoxic compounds	[77,78,79,80,81]
<i>ABCB2</i>	Immune deficiency	Peptide import into ER lumen	[99,100,101,102,103]
<i>ABCB3</i>	Immune deficiency	Peptide import into ER lumen	
<i>ABCB4</i>	PFIC3, ICP	bile formation; PC floppase	[82,83,104,105,106]
<i>ABCB7</i>	XLSA/A	mitochondrial iron transport?	[107,108]
<i>ABCB11</i>	PFIC2	bile formation; bile salt export	[109,110]
<i>ABCC2</i>	Dubin-Johnson syndrome	export of GSH- and glucuronic acid-conjugated substances; bilirubin export	[111,112]
<i>ABCC6</i>	Pseudoxanthoma elasticum	transport of GSH-conjugates?	[113]
<i>ABCC7</i>	Cystic fibrosis, CBAVD	Chloride channel	[114,115,116]
<i>ABCC8</i>	FPHHI	K ⁺ -channel regulation?	[117]
<i>ABCD1</i>	Adrenoleukodystrophy	peroxysomal VLCFA transport?	[118]
<i>ABCG5</i>	Sitosterolemia	Bile formation; cholesterol export	[119,120,121]
<i>ABCG8</i>	Sitosterolemia	Bile formation; cholesterol export	

FHDLD, Familial High-Density Lipoprotein Deficiency (= Hypoalphalipoproteinemia); FFM, Fundus Flavimaculatis; RP, Retinitis Pigmentosa; CRD, Cone-Rod Dystrophy; CD, Corneal Dystrophy; AMD, Age-related Macular Degeneration; PFIC 2/3, Progressive Familial Intrahepatic Cholestasis Type 2/3; ICP, Intrahepatic Cholestasis of Pregnancy; XLSA/A, X-Linked Sideroblastic Anemia and Ataxia; CBAVD, Congenital Bilateral Aplasia of Vas Deferens; FPHHI, Familial Persistent Hyperinsulinemic Hypoglycemia of Infancy. PE, Phosphatidyl Ethanolamine; ER, Endoplasmic Reticulum; PC, Phosphatidyl Choline; HDL, High-Density Lipoprotein; VLCFA, very long chain fatty acid

1.5 Active Transport and Detoxification Processes in the Liver

A plethora of endogenic and exogenic substances are excreted by the liver (for a short description of liver morphology see Figure 6), which carries out many metabolic reactions of exogenic importance [122]. Enzymes and active membrane transport systems are the two fundamental components carrying out this task [123]. However, the fundamental importance of the transport systems has only recently been established (reviewed in [124]). A wide range of specialized transport systems catalyzes the uptake of amphipatic, polar and lipophilic substances [125] from the blood. These are localized in the basolateral or sinusoidal membrane of the polarized hepatocytes (Figure 7) [126]. In contrast, ABC transporters localized in the apical or canalicular membrane mediate the active and energy-dependent secretion of bile salts, drugs and metabolic end products against a steep gradient into the canaliculi or bile ductules that ultimately converge in the gall bladder [124].

In general, hepatic elimination of xenobiotics is a complex sequence of uptake, intracellular metabolization and export [123]. Export can be directed towards two ways (Figure 7): across the basolateral membrane into the blood and subsequently to the kidneys, where the drug is cleared from the blood and excreted as part of the urine, or across the apical membrane into bile fluid, by which it is first secreted into the duodenum and finally disposed of via the feces. By virtue of hepatocyte polarity, substrate excretion is controlled [123]. The membrane domains are separated by tight junctions and are distinctly targeted by the cellular protein trafficking machinery, so that each has a separate repertoire of membrane proteins.

All import processes at the basolateral membrane are mediated by members of the solute carrier (SLC) family [127,128]. These are the sodium (Na^+) taurocholate cotransporter (NTCP) and the organic anion transporters (OATPs). In contrast, all export from the hepatocyte into bile or blood is exerted by ABC transporters. Export into blood is mediated by the Multidrug Resistance-related Protein (MRP) 1 and MRP3 [129,130], export into the canalicular lumen by MRP2, BSEP, MDR1, MDR3, the breast cancer resistance protein (BCRP), the ABCG5/G8 heterodimer, and others [124,130,131].

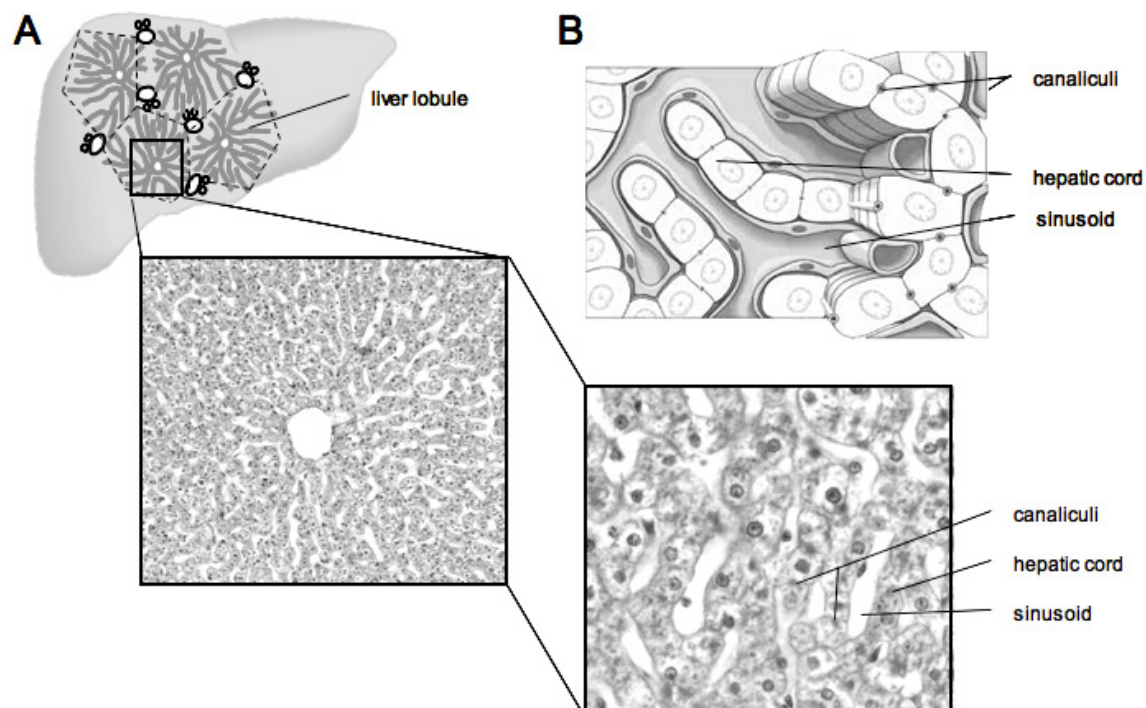


Figure 6. Morphology of the human liver. **A** Liver tissue is organized into lobules, roughly hexagonal fields of liver parenchyma surrounding the central vein. These form the functional units of the liver. The set of inlay micrographs shows the centre of a lobule with the central vein (left) and the cellular morphology (right). Blood flows through the sinusoid, and hepatocytes are organized into hepatic cords connected to each other by the apical or canalicular membrane while the basolateral or sinusoidal membranes flank the adjacent sinusoids. **B** Cartoon of cell morphology as depicted in micrograph inset below. Liver section micrographs adapted from [132], cartoon adapted from [133].

The Bile Salt Export Pump (BSEP, ABCB11)

ABCB11 belongs to the B subfamily of ABC transporters and was discovered in 1995 in Vancouver [134]. At the same time, another group in Zurich could demonstrate the ATP-dependent bile salt export from the liver [135]. Initially, the *ABCB11* gene was termed *sP-gp* (sister of P-glycoprotein) and connected to chemotherapeutic resistance of certain cell types [134]. However, Gerloff and coworkers could establish the function of ABCB11 or BSEP (bile salt export pump) in hepatic bile salt export [135].

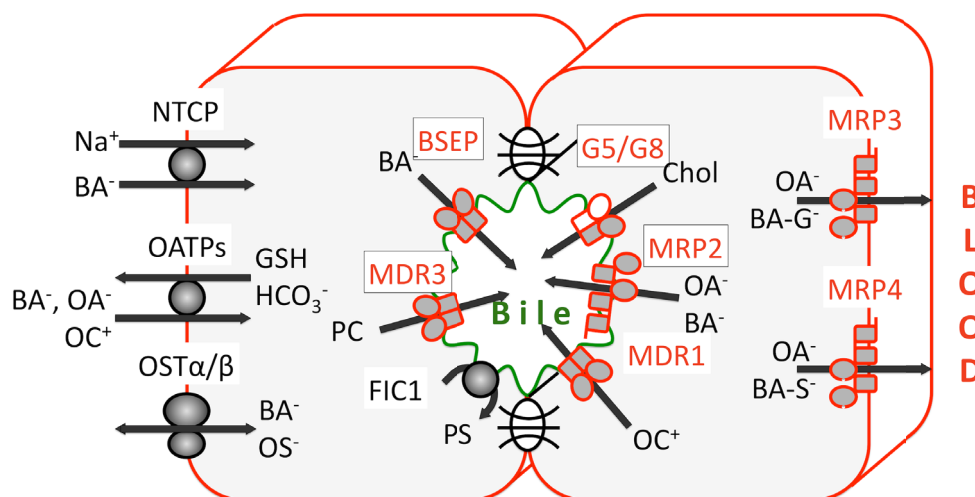


Figure 7. Localization of active transport systems in hepatocytes. The apical membranes of two hepatocytes together form a canaliculus that is separated from the basolateral membranes by tight junctions. All primary active export systems are ABC transporters, which have to work against steep concentration gradients (in red letters). All transporters contributing to bile formation are set in boxes. NTCP, sodium taurocholate cotransporting polypeptide; OATP; organic anion transporting polypeptide; G5/G8, ABC G5/G8, the half-size, heterodimeric cholesterol exporter; BA, bile acid; OA, organic anion; OC, organic cation; GSH, reduced glutathione; Chol, cholesterol; BA-G/S, glyco-/ S-conjugated bile acid. Adapted from [136].

Hydrophobicity analyses classify BSEP as a classic full-size transporter, consisting of two homologous halves with 6 transmembrane helices each, and cytosolically located NBDs (Figure 8) [131]. The C-loop of the C-terminal NBD features the amino acid sequence LSRGEK instead of the expected LSGGQ consensus. In addition, the glutamate residue C-terminal to the Walker B motif is missing in the N-terminal NBD. Its postulated function is the stabilization of the catalytically essential histidine of the H-loop in a conformation productive for hydrolysis [35]. This shows a degeneration of one of the two ATP binding sites which has already been reported for other ABC transporters like Pdr5 in *S. cerevisiae*, and the human CFTR and TAP [137,138,139].

BSEP is expressed almost exclusively in the canalicular membrane and subcanalicular vesicles of the liver [135], under tight translational and posttranslational control. Interestingly, a high concentration of bile salts effects BSEP expression [140] by binding to the nuclear farnesoid X receptor (FXR) [141]. FXR is,

in the heterodimeric complex with retinoic X receptor (RXR), a bile salt activated receptor. In addition to this translational control, the insertion of BSEP-containing vesicles in the canalicular membrane is, for instance, controlled by the cellular status of hydration [142] or the BSEP substrate tauroursodeoxycholate [143]. Isoforms of the protein kinase C (PKC), phosphoinositide kinase or p38 MAP kinase also control the transport from the Golgi apparatus to the canalicular membrane [144]. BSEP activity also depends on its phosphorylation status. Bile salt transport is upregulated eighteenfold by the presence of phorbol esters, while the inhibition of phosphorylation by activation of PKC ϵ apparently reduces BSEP transport efficiency [145].

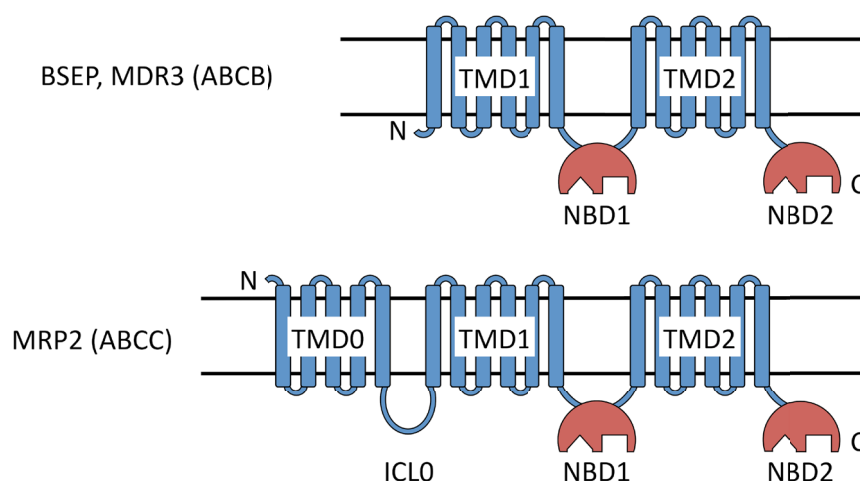


Figure 8. Domain topology of BSEP, MDR3 and MRP2. While all three are full-size transporters, MRP2 belongs to the ABC C subfamily of the human ABC transporter subfamily. Several members of this subfamily have an additional N-terminal transmembrane domain consisting of five membrane-spanning helices. This TMD0 is also referred to as NTE (N-Terminal Extension). Blue, TMDs; red, NBDs. N- and C-termini are indicated. Black lines indicate the membrane.

Progressive Familial Intrahepatic Cholestasis Type 2

Mutations in BSEP effect one type of hereditary cholestasis, termed progressive familial intrahepatic cholestasis (PFIC) type 2 [109,110]. So far, over 140 mutations have been described in associated with PFIC2, their majority resulting in truncated proteins or being missense mutations. In those forms of PFIC2, no BSEP protein can be detected in the canalicular hepatocyte membrane. Experimental evidence

suggests that BSEP mutations and changes in BSEP expression levels play an important role in induced cholestasis of the liver [110]. Here, a frequent mutation or allelic variant in the caucasian population is the V444A allele of BSEP that is associated with drug-induced liver cholestasis [146]. PFIC2 patients eventually suffer from organ failure and need a liver transplant for long-term survival.

The Multidrug Resistance Protein 3 (MDR3, ABCB4)

ABCB4 (syn. Multidrug resistance protein 3, Mdr3) is a full-size transporter also localized to the canalicular or apical membrane of hepatocytes and functions as a phosphatidylcholine (PC) floppase that specifically translocates its lipid substrate from the inner to the outer membrane leaflet [147,148]. In the canalicular lumen this lipid, together with cholesterol, forms mixed micelles with the bile salts excreted by BSEP. In these mixed micelles, their strong detergent capacity is neutralized.

Progressive Familial Intrahepatic Cholestasis Type 3

Mutations in *MDR3* lead to progressive familial intrahepatic cholestasis type 3 (PFIC3). Here, no phosphatidylcholine is detectable in the bile fluid and the strong bile salt detergent activity leads to severe cellular damage. PFIC3 ultimately results in liver cirrhosis and subsequent organ failure, necessitating liver transplantation. To date, over 45 mutations have been associated with this hereditary condition [149,150,151].

The Multidrug Resistance-related Protein 2 (MRP2, ABCC2)

The function of MRP2 (or cMOAT for canalicular multispecific organic anion transporter, [152]) is the secretion of organic anions such as bilirubin, leukotriene C₄, divalent bile salts and glutathione, glucuronide and sulfate conjugates [129]. MRP2 is localized in the canalicular hepatocyte membrane and mediates protection towards toxic substances, antibiotics and heavy metals [153,154]. MRPs are special in that most of them possess a third transmembrane domain N-terminal to the classic (TMD-NBD)₂ core unit, giving them the topology TMD₀-(TMD-NBD)₂. Hydrophobicity analyses suggest a number of five transmembrane helices in the TMD₀ domain while the other TMDs represent the standard, six transmembrane helix topology (shown in Figure 8). The (TMD-NBD)₂ core is rather conserved among MRPs. Interestingly, and

in contrast to this finding, the MRP-specific TMD0 segment is the one least conserved in this subfamily [155]. Its exact function remains to be determined, as MRP mutants lacking the TMD0 are still functional. However, deletion of this domain results in loss of targeting to the apical membrane of MRP2 [156]. The deletion of the intracellular connecting loop between TMD0 and adjoining the core part results in inactive proteins [157,158].

The Dubin-Johnson Syndrome (DJS)

Mutations in MRP2 are responsible for the relatively mild Dubin-Johnson syndrome, an autosomal recessive defect in bile acid secretion [111]. To partially compensate for defects in MRP2, expression of MRP3 is upregulated. In contrast to MRP2, MRP3 resides in the basolateral membrane [159]. This finding reinforces the concept that secretorial direction in the liver is regulated by the activity of the corresponding ABC transporters. Clinical symptoms include mild jaundice that can become more severe by estrogen-based contraceptive drugs, and chronic conjugated hyperbilirubinemia [111]. The deposition of black pigment in the hepatocytes of DJS patients can be observed [160].

1.6 The Role of Human Hepatic ABC Transporters in Bile Formation

Bile is a vital secretion and essential for intestinal digestion and absorption of lipids. In addition, it is an important way of elimination for xenobiotics like environmental toxins, carcinogens, drugs and their metabolites. Endobiotics such as bilirubin and hormones are also secreted via the bile fluid.

The normal formation of bile is a finely tuned process of both osmosis and concerted transport action from the hepatocyte into the canalicular lumen. Bile is mainly composed of water, cholesterol, conjugated bile salts, lipid, and bilirubin, as well as several conjugated or unconjugated compounds [161]. All membrane pumps involved in this active, vectorial transport are ABC transporters that maintain and work against steep gradients of their substrates across the canalicular membrane. The osmotic force of these gradients comes mainly from bile salts (BSEP) and glutathione (MRP2) and generates a water flow through aquaporins and the tight junctions delimiting the canaliculus. The drug transporters MDR1, MRP2, and BCRP mediate drug elimination as the second physiological function of bile.

The functionally active components in bile are cholesterol, bile salts and phosphatidylcholine. This phospholipid is moved from the inner to the outer canalicular membrane leaflet by MDR3, while cholesterol is translocated by the cholesterol floppase ABCG5/G8 (Figure 9) [119,162,163]. In the outer leaflet, both sterol and lipid are further concentrated by the inward flip of phosphatidylserine by the PS flippase FIC1 (ATP8B1, a P4-Type ATPase, [164]). Here, the bile salts exported by BSEP extract PC and cholesterol, forming mixed micelles in the process. In these micelles the strong bile salt detergents are neutralized, so that cellular damage to the tissue surrounding the bile canaliculi is prevented [161]. At the same time, the depletion of PS from the outer leaflet also favours the formation of laterally separated membrane microdomains (lipid rafts) by the highly enriched cholesterol and sphingomyelin as the potential microdomain constituents [165,166,167,168]. These are believed to stabilize the canalicular transporters themselves against the high luminal concentration of bile salts. Indeed, ABC transporters have been found to be associated with membrane microdomains [169], and loss of the underlying asymmetric lipid distribution has been associated with their reduced activity [170].

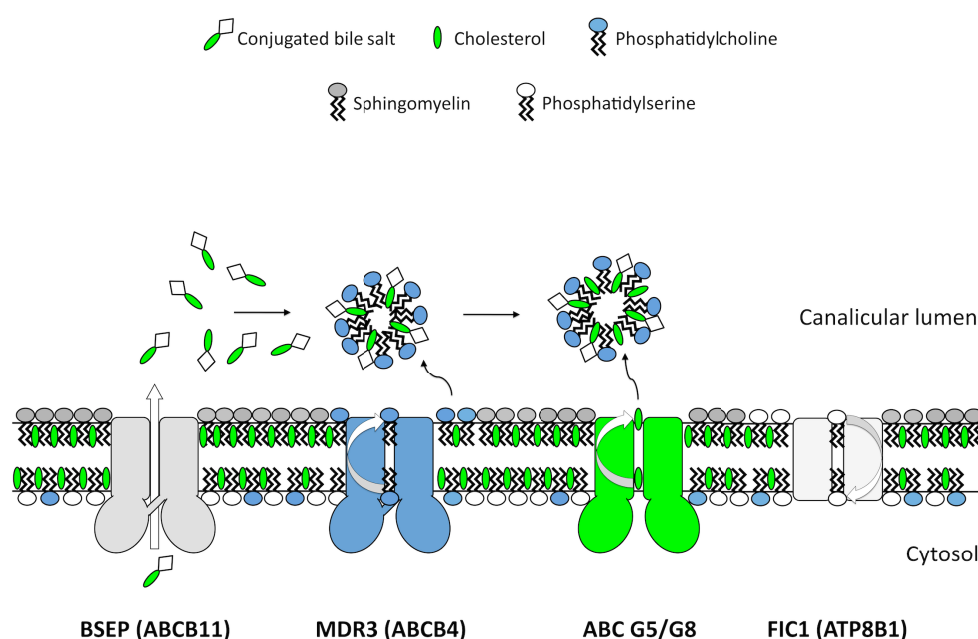


Figure 9. Current model of bile formation at the canalicular membrane of hepatocytes. All involved processes are primary active and dependent on ATP hydrolysis. FIC1 is a phosphatidylserine flippase. Its action is proposed to concentrate cholesterol and phosphatidylcholine in the outer membrane leaflet and provide additional protection of the membranes against the strong detergent effect of bile salts. Adapted from [171].

1.7 Eukaryotic Expression Systems for Human ABC Transporters

As described, fundamental processes of both normal and diseased physiology such as multidrug resistance (MDR) and bile formation are mediated by a number of identified ATP binding cassette (ABC) transporters. The major bottleneck in mechanistic studies of both wild type and disease-associated mutated variants of the transporters is obtaining sufficient amounts of these membrane proteins. Cultivation of liver-derived cell lines such as HepG2 in order to obtain suitable amounts of the ABC transporters involved in bile formation is not feasible: slow cell division rates (six to eight hours) and the general low abundance of these transporters in their native tissue forbid their use in large-scale protein production [172]. Heterologous overexpression in a suitable host is a frequent attempt to overcome this limitation [173]. However, the expression of BSEP and MDR3 in insect cells, while providing functional protein, requires extensive culturing for two to three days after infection with the recombinant baculovirus, which has to be generated first [174,175]. Cell culture-based systems may generally be suitable for addressing questions of a cellular phenotype, protein trafficking, and modification or protein interaction and can even provide the basis for some *in vitro* approaches. One example for this is the purification and biochemical characterization of human MRP2 from human embryonal kidney (HEK) 293 cells [176,177]. For both structural and mechanistic *in vitro* studies on purified and membrane-reconstituted protein, much larger amounts are needed. In general, some yeasts species have been found to provide suitable functional expression systems for mammalian membrane proteins [173,178].

Saccharomyces cerevisiae (*S. cerevisiae*)

The unicellular eukaryote *S. cerevisiae* is a well-characterized expression system for eukaryotic membrane proteins [179]. Five of the seven human ABC transporter subfamilies can be found in this yeast species [180], among these the ABCB (MDR/TAP) and ABCC (MRP/CFTR) subfamilies that in human contain BSEP, MDR3, and MRP2, respectively. Previously, *S. cerevisiae* has been used to express both functional MDR1, a BSEP homologue [181,182], and human MRP1, a homologue of the conjugate efflux pump MRP2 [183,184]. Taken together, these studies indicate the potential of *S. cerevisiae* for heterologous overexpression of BSEP, MDR3, and MRP2 in *S. cerevisiae*. Two key advantages of *S. cerevisiae* in foreign gene expression are its easy cultivation and the well-established genetic

manipulation. In rich medium, a yeast cell in logarithmic growth phase on average divides every ninety minutes [185], thus providing substantial cell mass in a short time.

A good example for the levels of expression obtainable in *S. cerevisiae* is the Pleiotropic Drug Resistance (PDR) ABC transporter Pdr5 which could be overexpressed and studied in a haploid *S. cerevisiae* strain that carries a mutated transcriptional factor, Pdr1 (*pdr1-3*) [186,187]. The mutated factor is constitutively active and drives strong Pdr5 expression up to 8 % of the total yeast plasma membrane protein during mid-log growth phase [188]. The yeast pleiotropic drug resistance network is under tight control of the transcriptional factors Pdr1p and Pdr3p [18,188,189,190]. Mutations in both genes can effect the constitutive expression of PDR components. Under control of the *PDR5* promoter in the *pdr1-3* strain background, the yeast membrane proteins Yor1, Rsb1, Mdl1, and Drs2 could also be overexpressed [191]. It has also successfully been used by other groups for membrane protein overexpression in yeast [192,193,194].

Pichia pastoris (*P. pastoris*)

The methylotrophic yeast *P. pastoris* has already been successfully used for expression of human MDR1 [195] and MRP1 [196]. Several human ABC transporters have been expressed in this system to date [195]. Remarkably, the heterologous overexpression of the human, heterodimeric half-size cholesterol transporter ABCG5/G8 could be established and used to study its biochemistry *in vitro* [197,198]. Recently, the expression of 25 human ABC transporters has been reported [199]. Expression in the *Pichia* system is frequently accomplished from the chromosomal *AOX1* locus. The strong promoter natively drives the expression of the alcohol oxidase enzyme up to 25 % of total soluble protein [200]. The most poignant advantage of this yeast, however, is its rapid growth in comparison with mammalian cell culture, to densities that allow harvesting more than 400 grams of wet weight of cell mass from one litre under controlled fermentation. With *Pichia*, kilogram amounts of cell mass can routinely be harvested from a single, middle-sized fermenter run. Thus, while the expression level of a heterologous gene, and especially a human polytopic membrane protein, may not be very high, the abundant cell mass that is obtained by *Pichia* fermentation can compensate this shortcoming [200].

Aims and Objectives

The reported, disease-associated mutations in human ABC transporter genes like *BSEP* and *MDR3* can be grouped as follows: the first group of mutations can be silent and even reside outside the protein-coding exons of the gene structure on the chromosome. These impair the correct splicing of the gene into a mature mRNA and result in loss of its expression. The second group are nonsense mutations that result in truncated and non-functional protein. The third group consists of missense mutations that result in single amino acid substitutions in the mature protein. They can influence its function, proper folding or correct localization to the canalicular membrane. Several of these are found in the TMDs or outside of the conserved motifs in the NBDs.

Cell culture systems are limited in that they may allow for studies on mutation-related trafficking defects, but being complex, they cannot give insight into the mechanistic impact of a mutation on the function of the protein itself. This can only be investigated *in vitro*. The system of choice for this is the functionally reconstituted ABC transporter in a proteoliposome. In such a defined *in vitro* environment, kinetic parameters such as ATPase or substrate binding and transport can be studied on both wild type and mutant variants. For these *in vitro* studies, purified and functional protein is needed. However, in their native tissue, the liver ABC transporters are not present in sufficient amounts, and therefore cannot, for example, be obtained by purification from a liver-derived human cell line such as HepG2 (a human liver tumor-derived cell line). The **first aim** of this thesis is therefore the heterologous overexpression in a suitable host. As detailed above, yeast species are potential candidates to be tested.

Since eukaryotic coding sequences are sometimes inefficiently cloned, which has been shown to be particularly difficult for *BSEP* and *MDR3*, a system is desirable that allows their easy handling and, preferably, also their targeted mutagenesis. The **second aim** of this thesis is therefore the development of a general and flexible system to clone and manipulate the corresponding coding sequences. This system should also enable the rapid exchange of sequences between different expression hosts such as, for instance, mammalian cell culture and yeast to facilitate the investigation of clinically relevant mutations both in cell culture and *in vitro*.

2 Materials and Methods

2.1 Materials

2.1.1 Chemicals and Reagents

Acetic acid, glacial	Normapur
5-bromo-4-chloro-3-indolyl-beta-D-galactopyranoside (X-Gal)	Carl Roth
Acrylamide/bisacrylamide (37.5:1) 30 % solution	Carl Roth
Agar	Serva
Agarose, GTQ	Carl Roth
Ammonium peroxodisulfate (APS)	Carl Roth
Ammonium sulfate	J.T. Baker
Bromophenol blue	Sigma-Aldrich
Carbenicilline	Carl Roth
Cobalt chloride	Fluka
Coomassie Brilliant blue R-250	Carl Roth
Dimethyl sulfoxide (DMSO)	Carl Roth
Dithiothreitol (DTT)	ICN
dNTPs (10 mM)	Fermentas
Ethanol	Carl Roth
Ethidium bromide	Carl Roth
Ethylenediamine tetraacetic acid (EDTA)	AppliChem
Formaldehyde, 37 % (wt/wt) solution	Carl Roth
Glucose	Caesar & Loretz
Glycerol (98 % (v/v))	Grüßing
Hydrochloric acid, 37 % (w/v)	Riedel-de Haën
Isopropanol	Carl Roth
Isopropyl-beta-D-thiogalactoside (IPTG)	Carl Rohl
L-amino acids	Serva, Fluka, Carl Roth, Sigma-Aldrich, Merck
Lithium acetate	Fluka
Methanol	Carl Roth
Non-fat dried milk powder (Blotting Grade)	Carl Roth
Polyethylenglycol 4000 (PEG 4000)	Fluka
Ponceau S	Sigma-Aldrich

Protease inhibitor cocktail tablets, EDTA-free	Roche
Sodium acetate	Fluka
Sodium azide	Fluka
Sodium chloride	J.T. Baker
Sodium hydroxide	J.T. Baker
Sorbitol	Carl Roth
Tetramethylethyldiamin (TEMED)	Merck
Trichloroacetic acid (TCA)	Fluka
Tris-(hydroxymethyl)-aminomethan (Tris)	Sigma-Aldrich
Tryptone/peptone from caseine	Carl Roth
Urea	Grüßing
Yeast extract	Carl Roth
Yeast nitrogen base (YNB)	Difco
β -mercaptoethanol	Carl Roth

2.1.2 Detergents

CYMAL 5	Glycon
Decyl- β -D-maltopyranoside (DM)	Glycon
Dodecyl- β -D-maltopyranoside (DDM)	Glycon
Fos-choline 14 (FOS-14)	Anatrace
Fos-choline 16 (FOS-16)	Anatrace
Sodium dodecylsulfate (SDS)	Serva
Tween 20 / 80	Carl Roth

2.1.3 Antibodies

MLE	[201]
M ₂ III-6	[202]
K24	[174]
K168	[203]
C219	Abcam
pentaHis	Qiagen
α -Dpml	Molecular Probes/Invitrogen
α -Pdr5	[204]

goat α -rabbit IgG, HRP-coupled	Sigma-Aldrich
goat α -mouse IgG, HRP-coupled	Pierce

2.1.4 Antibiotics

Ampicilline	Carl Roth
Carbenicilline	Carl Roth
Kanamycin	Carl Roth

2.1.5 Drugs

Cycloheximide	Fluka
Doxorubicine	Sigma-Aldrich
FK506 (Tacrolimus)	Alexis
Fluconazol	Sigma-Aldrich
Ketoconazole	Sigma-Aldrich
Lovastatin	15 % (v/v) ethanol, 250mM NaOH
Pravastatin	Sigma-Aldrich
Taurocholate	Sigma-Aldrich
Taurodeoxycholate	Sigma-Aldrich

2.1.6 Enzymes, proteins, and kits

Enzymes and proteins

Calf intestinal alkaline phosphatase (CIAP)	Fermentas
T4 DNA ligase	Fermentas
T4 polynucleotide kinase	New England Biolabs
Bovine serum albumin Fraction V (BSA)	Carl Roth

All polymerase-based reactions were performed with the Phusion® High Fidelity DNA polymerase (Finnzymes) and the supplied HF buffer. Restriction enzymes were either from NEB or Fermentas.

Kits

Plasmid Miniprep kit	Qiagen
Plasmid Midiprep kit	Qiagen
Nucleobond Xtra Midiprep kit	Macherey & Nagel
DNeasy Blood and Tissue Kit	Qiagen
Ni-NTA slurry	Qiagen

2.1.7 Markers

PageRuler Plus prestained protein ladder	Fermentas
GeneRuler 1 kb DNA ladder	Fermentas
6X His protein ladder	Qiagen

2.1.8 Plasmids

pRE2	[205]
pRE3	[205]
p10HISHA	This study
p2HA	This study
p10HisSfil	This study
p14HisSfil	This study
pCDNA3.1- <i>MRP2</i>	[206]
pbluebac4.5- <i>BSEP</i>	[207]
pbluebac4.5- <i>MDR3</i>	Kind gift of Prof. Kenneth Linton
YEphIS	[182]
YEpMDR1HIS	[182]
YEpNHIS	This study
YEpNHIS <i>BSEP</i>	This study
YEpCHIS <i>BSEP</i>	This study
YEpNHIS <i>MDR3</i>	This study
YEpCHIS <i>MDR3</i>	This study
YEpCHIS <i>MRP2</i>	This study
p426-GPD, -TEF, -MET25, -CYC, -GAL1	ATCC No. 87669 [208], and ATCC No. 97670 [209]

p426-GPD-N6HISBSEP	This study
p426-GPD-C6HISBSEP	This study
p426-TEF-N6HISBSEP	This study
p426-TEF-C6HISBSEP	This study
p426-MET25-N6HISBSEP	This study
p426-MET25-C6HISBSEP	This study
p426-CYC-N6HISBSEP	This study
p426-CYC-C6HISBSEP	This study
p426-GAL1-N6HISBSEP	This study
p426-GAL1-C6HISBSEP	This study
pPIC3.5	Invitrogen
pPIC3.5-CHISBSEP	This study
pEYFP-N1-BSEP	[210]

The YEpHIS and YEpMDR1HIS plasmids were the kind gift of Prof. Marwan Al-Shawi (Department of Molecular Physiology and Biological Physics, University of Virginia, Charlottesville, USA). The BSEP and MDR3 cDNA were the kind gift of Prof. Kenneth J. Linton (Barts and The London School of Medicine and Dentistry, Institute of Cell and Molecular Science, Queen Mary University of London, UK). For the sake of clarity, the YEpHIS plasmid encoding the C-terminal his₈ tag is referred to as YEpCHIS throughout this work.

2.1.9 Strains

Escherichia coli

DH5alpha	F ⁻ endA1 <i>glnV44 thi-1 recA1 relA1 gyrA96 deoR nupG</i> $\Phi 80$ lacZ Δ M15 Δ (lacZYA-argF)U169, <i>hsdR17</i> (r _K ⁻ m _K ⁺), λ -
DH10b	F ⁻ endA1 <i>recA1 galE15 galK16 nupG rpsL</i> Δ lacX74 $\Phi 80$ lacZ Δ M15 <i>araD139</i> Δ (<i>ara, leu</i>)7697 <i>mcrA</i> Δ (<i>mrr-hsdRMS-mcrBC</i>) λ ⁻
XL1blue	endA1 <i>gyrA96</i> (nal ^R) <i>thi-1 recA1 relA1 lac glnV44</i> F' [::Tn10 proAB ⁺ lacI ^q Δ (lacZ)M15] <i>hsdR17</i> (r _K ⁻ m _K ⁺) Invitrogen

XL10Gold	<i>endA1 glnV44 recA1 thi-1 gyrA96 relA1 lac Hte Δ(mcrA)183 Δ(mcrCB-hsdSMR-mrr)173 tet^R F'[proAB lac^fZΔM15 Tn10(Tet^R Amy Cm^R)]</i> Stratagene
S.U.R.E.	<i>endA1 glnV44 thi-1 gyrA96 relA1 lac recB recJ sbcC umuC::Tn5 uvrC e14- Δ(mcrCB-hsdSMR-mrr)171 F'[proAB⁺ lac^f lacZΔM15 Tn10]</i> Stragagene
S.U.R.E.2	<i>endA1 glnV44 thi-1 gyrA96 relA1 lac recB recJ sbcC umuC::Tn5 uvrC e14- Δ(mcrCB-hsdSMR-mrr)171 F'[proAB⁺ lac^f lacZΔM15 Tn10 Amy Cm^R]</i> Stratagene

Saccharomyces cerevisiae

ΔPP	<i>MAT_α; ura3–52; trp1-1; leu2–3,112; his3–11,15; ade2-1; pdr1-3; ΔPDR5prom, Δpdr5::TRP</i> [205]
AD1-8U ⁻	<i>MAT_α; PDR1–3; ura3; his1; yor1::hisG; snq2::hisG; pdr5::hisG; pdr10::hisG; pdr11::hisG; ycf1::hisG; pdr3::hisG; pdr15::hisG</i> [192]

Pichia pastoris

GS-115	Invitrogen
--------	------------

2.1.9 Oligonucleotides

The Clone Manager Suite 6 (Sci-Ed Software) was used to design all oligonucleotides and calculate annealing temperatures of the primer pairs. All oligonucleotides were ordered from Eurofins MWG Operon (Ebersberg, Germany).

Oligonucleotide	Sequence 5'-3' (relevant restriction sites in underlined italics and point mutations indicated in bold letter)
-----------------	--

Oligonucleotides for the construction of the expression cassette plasmids

N2HA-FOR	TCATCACTACCCATACGATGTTCCAGATTACGCTGGTTACCCATACGATG TTCCAGATTACGCTGGTTAAT
----------	---

N2HA-REV	TAAACCAGCGTAATCTGGAACATCGTATGGGTAACCAGCGTAATCTGGAA CATCGTATGGGTAGTGATGATGCA
N10HIS1HA-FOR	TCATCACCATCATCACCATCATCACCATGGTGGTGGTTACCCATACGATG TTCCAGATTACGCTGGTTTAAT
N10HIS1HA-REV	TAAACCAGCGTAATCTGGAACATCGTATGGGTAACCACCACCATGGTGTGAT GATGGTGTGATGGTGTGATGATGCA
N10HIS- <i>SfiI</i> -FOR	TCATCACCATCATCACCATCATCACCATGGTGGTGGTATTGAAGGCCGCT CTGGCCAGTTAAT
N10HIS- <i>SfiI</i> -REV	TAAGTGGCCAGAGCGGCCCTTCAATACCACCACCATGGTGTGATGGTGA TGATGGTGTGATGCA
N14HIS- <i>SfiI</i> -FOR	TCATCACCATCATCACCATCATCACCATCATCACCATGGTGGTGGTAT TGAAGGTAGAATGCCCGAGGCCTTAAT
N14HIS- <i>SfiI</i> -REV	TAAGGCCTCGGGCATTCTACCTTCAATACCACCACCATGGTGTGATGATGAT GGTGTGATGGTGTGATGGTGTGATGCA

Oligonucleotides for the silent mutagenesis of SfiI sites in the pRE2 plasmid backbone and in the MRP2 cDNA.

pRE2- <i>SfiI</i> rem-FOR	TATCAGATCCACTAGT <u>GGCCTATGCGGT</u> CGCGGATCTGCC
pRE2- <i>SfiI</i> rem-REV	GGCAGATCCGCG <u>ACCGCATAGGCC</u> ACTAGTGGATCTGATA
MRP2- <i>SfiI</i> rem-FOR	TAAGGTCTTGG <u>GCCCAATGGT</u> CTGTTGAAAGGCAAGACTCGACTC
MRP2- <i>SfiI</i> rem-REV	GAGTCGAGTCTTGCCTTTCAACAG <u>ACCATTGGGGCCCAAGACCTTA</u>

Oligonucleotides for SfiI-based cloning of the lacZ fragment and the MRP2 cDNA into p14HisSfiI

MRP2- <i>SfiI</i> -S1	GGGCT <u>GGCCGCTCTGGCC</u> TGGAGAAGTTCTGCAACTCTA
MRP2- <i>SfiI</i> -S2	GGGGT <u>GGCCAGAGCGGCC</u> CTAGAATTTTGTGCTGTTACAT
<i>lacZ</i> - <i>SfiI</i> -S1	GGGCT <u>GGCCGCTCTGGCC</u> ATTGAGCGCAACGCAATTAATGTGAGT TAG
<i>lacZ</i> - <i>SfiI</i> -S2	GGGCAG <u>GGCCAGAGCGGCC</u> CTCAATTCGCCATTCAGGCTGCGCAACT GTT

Cassette oligonucleotides for the generation of the YEpNHIS plasmid

YEpNHISFor	GATCCTTTAATTATCAAACAATATCAATATGCATCATCACCATCATCA CCATCATCACCATCATCATCACCATGGTGGTGGTATTGAAGGTAGA CCCGGGTAGA
YEpNHISRev	CGCGTCTACCCGGGTCTACCTTCAATACCACCACCATGGTGTGATGAT GATGGTGTGATGGTGTGATGGTGTGATGCATATTGATATTGTTT GATAATTAAAG

Oligonucleotides for the cloning of MRP2, BSEP, and MDR3 into the YEpCHIS and YEpNHIS plasmids by homologous recombination

<i>BSEP-YEpHISN-S1</i>	TCACCATCATCATCACCATGGTGGTGGTATTGAAGGTAGATCTGAC TCAGTAATTCTTCGAAGTATAAAG
<i>BSEP-YEpHISN-S2</i>	GAATAAGGTAAACATGGTAGCGATGTCGACCTCGAGACGCGTCTAA CTGATGGGGGATCCAGTGGTGACT
<i>BSEP-YEpHISC-S1</i>	ATAAGAAGATAGGATCCTTTAATTATCAAACAATATCAATATGTCTGA CTCAGTAATTCTTCGAAGTAT
<i>BSEP-YEpHISC-S2</i>	CGATGTCGACCTCGAGACGCGTCTAATGGTGATGGTGATGGTGAT GGTGACCACTGATGGGGGATCCAGTGGTGACT
<i>MDR3-YEpHISN-S1</i>	TCACCATCATCATCACCATGGTGGTGGTATTGAAGGTAGAGATCTT GAGGCGGCAAAGAACGGA
<i>MDR3-YEpHISN-S2</i>	GAATAAGGTAAACATGGTAGCGATGTCGACCTCGAGACGCGTCTAT AAGTTCTGTGTCCCAGCCTGGACACTGACCATT
<i>MDR3-YEpHISC-S1</i>	ATAAGAAGATAGGATCCTTTAATTATCAAACAATATCAATATGGATCT TGAGGCGGCAAAGAACGGA
<i>MDR3-YEpHISC-S2</i>	CGATGTCGACCTCGAGACGCGTCTAATGGTGATGGTGATGGTGAT GGTGACCTAAGTTCTGTGTCCCAGCCTGGACACTGACCATT
<i>MRP2-YEpHISC-S1</i>	TCACCATCATCATCACCATGGTGGTGGTATTGAAGGTAGATCTGGC CTGGAGAAGTTCTGCAACTCTA
<i>MRP2-YEpHISC-S2</i>	GAATAAGGTAAACATGGTAGCGATGTCGACCTCGAGACGCGTCTAG AATTTTGTGCTGTTACATTCTCAA

Oligonucleotides for the cloning of BSEP into the p426 plasmid set by homologous recombination for the expression screen

<i>BSEP-p426-NHis-HR S1</i>	TCTAGAACTAGTGGATCCCCCGGGCTGCAGGAATTCGATAATGCAT CATCACCATCATCACTCTGACTCAGTAATTCTTCGAAGTATAAAG
<i>BSEP-p426-CHis-HR S2</i>	ATAACTAATTACATGATATCGACAAAGGAAAAGGGGCCTGTCTAACT GATGGGGGATCCAGTGGTGACT
<i>BSEP-p426-CHis-HR S1</i>	TCTAGAACTAGTGGATCCCCCGGGCTGCAGGAATTCGATAATGTCT GACTCAGTAATTCTTCGAAGTATAAAG
<i>BSEP-p426-CHis-HR S2</i>	ATAACTAATTACATGATATCGACAAAGGAAAAGGGGCCTGTCTAATG GTGATGGTGATGATGACTGATGGGGGATCCAGTGGTGACT

Oligonucleotides for the cloning of BSEP into the pPIC3.5 plasmid set by homologous recombination for expression in Pichia pastoris

OriLeu-pPIC3.5-NdeI-S1	AACTATGCGGCATCAGAGCAGATTGTA CTGAGAGTGCACCATATGC GAGGCCCTTTCGTCTTCAAGAATTA ACTGTGGGA
OriLeu- pPIC3.5-NdeI-S2	GTATTTCTCCTTACGCATCTGTGCGG TATTTACACCCGCATATGAT CTGTGCGGTATTTACACCCGCATAT ATCG
BSEP-pPIC3.5-S1	AATTATTCGAAGGATCCTACGTAGA ATTCCCTAGGGCGGCCGCATG TCTGACTCAGTAATTCTTCGAAGT ATAAAGAAAT
BSEP-pPIC3.5-S2	TGAGGAACAGTCATGTCTAAGGCGA ATTAATTCGCGGCCGCCTAAT GGTGATGGTGATGGTGATGGTGAC CACTGATG

Oligonucleotides for the E. coli-free site-directed mutagenesis of BSEP for introduction of an extra BstBI restriction site

BSEP-BstBImut-S1	AGCTC <u>TTCGA</u> AGAGCCTTCTCTTAC ACCCCAAGTTATGCAAAGCTA AA
BSEP-BstBImut-S2	AGAAGGCTC <u>TTCGA</u> AGAGCTGTTG CACTCAGTACAACCTGCAGAGAT CAC

Oligonucleotides for the addition of a Ori/Leu sequence into the AflII restriction site of the mammalian BSEP expression construct pEYFP-N1-BSEP by homologous recombination

OriLeu-pEYFP-AflII-S1	TCTAGTTGTGGTTTGTCCAAACTCAT CAATGTATCTTAAGCGAGGCC CTTTCGTCTTCAAGAATTA ACTGTGGGA
OriLeu-pEYFP-AflII-S2	ATTTTAACAAAATATTAACGCTTACA ATTTACGCCTTAAGATCTGTGC GGTATTTACACCCGCATATATCG

Oligonucleotides for sequencing and of MRP2, BSEP, and MDR3 and colony PCR

MRP2-FWD-Seq1	AGGACCAAGAGATCCTCTAC
MRP2-FWD-Seq2	GCTACAAGCGTCCTCTGACA
MRP2-FWD-Seq3	CTTATTCAGTGGCTCTCA
MRP2-FWD-Seq4	TGCGATACTGTCCACCAAGA
MRP2-FWD-Seq5	GGAAGCCACAGTCCGAGATG
MRP2-FWD-Seq6	GCAGTGGATGCTCATGTAGG
MRP2-FWD-Seq7	AGCCTGAAGGAAGACGAAGA
MRP2-FWD-Seq8	AGTCCTTGCGCAGCTGGATT
MRP2-FWD-Seq9	AACTGGCTGGTGAGGATGAC

<i>MRP2-FWD-Seq10</i>	TCTGGAAGCCTGAGGATGAA
<i>MRP2-FWD-Seq11</i>	GGTCCTAGACAACGGGAAGA
<i>MRP2-SeqREV</i>	CATTCTCAATGCCAGCTTCC
<i>MRP2-REV-Seq1</i>	AGAGCGGCCTTCAATACCAC

<i>BseqFOR1</i>	CATGTGTGAATAACACCATTGTA
<i>BseqFOR2</i>	TAGGAGAATAATGAGAATGGA
<i>BseqFOR3</i>	TTACGGACTATGAGCTGAAG
<i>BSEP-FWD-Seq3</i>	CCATCGCTTGTCCACCATCC
<i>BseqFOR4</i>	AGTGTCATAGTAGGAGCTT
<i>BseqFOR5</i>	TAGAGATCAGATTGGGATA
<i>BseqFOR6</i>	AGAGCTGCAGATACCATCAT
<i>BseqFOR7</i>	CATTAGCTGTTGTAGATCATA
<i>BseqFOR8</i>	GAGCATTGACAACAAGACTT
<i>BseqFOR9</i>	GATGTTGACAGGATTTGC
<i>BseqFOR10</i>	GTGATCTCTGCAGTTGTAC
<i>BSEP-REV-Seq5'</i>	CCAACCTAACGCCATCACC
<i>BseqREV1</i>	GACAGCAATTCCAGCATAGTA
<i>BseqREV2</i>	AACCACAGATGGTCGAGGTCAT
<i>BseqREV3</i>	ATCTGGACAAGGGTTCCAG
<i>BseqREV4</i>	TAAGAGAGCGAATGTCATG
<i>BseqREV5</i>	TATGATCTACAACAGCTAATG
<i>BseqREV6</i>	AAGTCTTGTTGTCAATGCTC
<i>BseqREV7</i>	GATGACCAGGCTCAGCT
<i>BseqREV8</i>	GTCTCAAGTGCTTCAATG
<i>BseqREV9</i>	GTTCCAACAGCTGAATGCT
<i>BseqREV</i>	CTGGCCATTCTGACTCAGTA

<i>MDR3-SeqFor1</i>	GGCCATAGCTCACGGATCAG
<i>MDR3-SeqFor2</i>	CTCAATACGCGGCTAACAGA
<i>MDR3-SeqFor3</i>	GGCCATCAGGACTGTGATAG
<i>MDR3-SeqFor4</i>	TCAACCTGAAGGTGCAGAGT
<i>MDR3-SeqFor4.5</i>	AAGAGGCCAACGCCTATGAG
<i>MDR3-SeqFor5</i>	GATGAGGCCACGTCAGCATT
<i>MDR3-SeqFor6</i>	AATGTGCCACCAGTGTCTT
<i>MDR3-SeqFor7</i>	AGTCCAAGGAGCCACAGGAA
<i>MDR3-SeqFor8</i>	TGGACATATGCGCTTCAGAG
<i>MDR3-SeqFor9</i>	CAGTGCTTCTCGATGGTCAA
<i>MDR3-SeqFor10</i>	GCCGCACCTGCATTGTGATT
<i>MDR3-SeqREV1</i>	TGCAATGGCGATCCTCTGCT
<i>MDR3-SeqREV1.5</i>	GCATTTGGACCGTAGACAG

5'-locus	AATTATCGTCACAATCTAATCA
3'-locus	GTCAGCCTGCCGTATGTCAA
checkprom_pRK3	TTGGCAACTAGGAACTTTTCG [205]
Heukan2	GTCAAGACTGTCAAGGAGGG
Heukan3	CATCATCTGCCCAGATGCGAAG
p426-Promoterseq	TATGCTTCCGGCTCCTATGT
p426-SeqRev	GCGCGTAATACGACTCACTA
YEpHISsSeq	AAAATATACCCCAGCTAGTT
YEpHISasSeq	GACACGGACGACAGTAACAA

Oligonucleotides for the site-directed mutagenesis of the cryptic prokaryotic promoter motif (TATAAT box) as in [174]

BSEP-cryptmut-FOR	GAGTCAGATAAATCATACAACAATGATAAGAAATCAAGG
BSEP-cryptmut-REV	CCTTGATTTCTTATCATTGTTGTATGATTTATCTGACTC

2.1.10 Technical devices

Avanti J-20xp	Beckman Coulter
ÄKTA Prime / Basic / Explorer / Purifier	GE Healthcare
Balances EMB 2200-0/ 440-47N/ ALS 220-4	Kern
Bead beater	Biospec
Centrikon T-124	Kontron
ChemiGenius2 imaging system	Syngene
CO8000 Cell density meter	WPA Biowave
Gel electrophoresis apparatus	Custom-made
Incubator	Bachofer
LSM 510	Zeiss
Megafuge 1.0R	Heraeus
Multiwell plate reader Polarstar Galaxy	BMG Labtech
Nanodrop ND-1000 spectrophotometer	Peqlab
pH meter	Schott
Pharmacia ECPS 3000-150 power supply	Pharmacia
Power Pac Basic power supply	Bio-Rad
SDS-PAGE apparatus	Custom-made / Bio-Rad
Semidry Western Blot apparatus	Bio-Rad

Sonorex ultrasonic water bath	Bandelin
Sorvall Evolution RC / Discovery 90 SE and 120 SE	Thermo Fisher
Sterile cleanbench Lamin Air LB-48-C	Heraeus
Tabletop microcentrifuge 5415C/ 5417R/ 5415D	Eppendorf
Thermocycler	Biometra
Thermomixer	Eppendorf
Ultracentrifuge L7-65	Beckman Coulter
Unitron shaking incubator	Infors
Vortex Genie 2	Scientific Instruments
Wild M5A stereo microscope	Wild Heerbrugg

Chromatography media

5 ml IMAC column	GE Healthcare
Superdex 200 10/300 GL column	GE Healthcare

Consumables

0.5 mm Glas-Beads	BioSpec Products
1.5 and 2 ml reaction tubes SafeSeal and Easy Cap	Sarstedt
15 and 50 ml conical ("falcon") tubes	Sarstedt
96well microtiter plate, non sterile	Greiner
Amicon Ultra 15 (MWCO 100 kDa)	Millipore
Biomax Films MS/XAR	Kodak
Nitrocellulose membranes	Schleicher & Schüll/Pall Gelman
Pipette tips (10, 200, and 1000 µL)	Sarstedt
Whatman 3MM filter paper	Whatman

2.2 Methods

Unless stated otherwise, all buffers and solutions were made from double-distilled water.

2.2.1 Methods of molecular biology and microbiology

All microbiological steps were performed under at least semi-sterile conditions, using either a cleanbench for *S. cerevisiae* and *P. pastoris* or a bunsen burner environment for working with *E. coli*.

2.2.1.1 Cultivation of *E. coli*

Lysogeny broth (LB, low salt)

10 g/L Tryptone/Peptone from caseine
5 g/L yeast extract
10 g/L NaCl

LB agar

LB medium supplemented with
1.5 % (w/v) agar

1000X Carbenicilline Stock

50 mg/ml Carbenicilline sodium salt in
50 % (v/v) ethanol

E. coli cells were cultivated in LB medium with either 50 µg/ml Carbenicillin or 30 µg/ml Kanamycin at 37 °C and 200 rpm shaking in baffled Erlenmeyer flasks. For propagation of unstable plasmids, the temperature was strictly kept at 30 °C. Liquid media were always inoculated with single, freshly grown colonies from LB agar plates with the appropriate antibiotic. For the small-scale isolation of plasmids, liquid cultures of 5 ml volume were incubated overnight at the appropriate temperature. For large-scale plasmid isolation, 150 ml medium were used.

For long-term storage of *E. coli* cells, aliquots of overnight cultures were taken, adjusted to 15 % (v/v) glycerol, and snap-frozen in liquid nitrogen. These glycerol stocks were stored at -80 °C. For recultivation, a sterile plastic pipette tip was used to transfer frozen material to a room-temperature LB plate, and the thawed bacterial solution was spread with a inoculum needle.

2.2.1.2 Cultivation of *S. cerevisiae*YP (Yeast extract, Peptone)

20 g/L Tryptone/Peptone from Caseine
10 g/L Yeast extract
(dissolved in 900 ml dd. water and autoclaved)

20 % (w/v) Glucose

(autoclaved)

YPD (YP Dextrose)

YP supplemented with
2 % (w/v) Glucose
(900 ml YP + 100 ml 20 % (w/v) glucose)

YPD agar

YPD medium supplemented with
2 % (w/v) agar
(autoclaved as YP agar; glucose is added after autoclaving)

2X Dropout stock medium (740 ml)

3.4 g Yeast nitrogen base
2.86 g Amino acid mix
5 g Ammonium sulfate
(adjusted with KOH to a pH 5.6 and autoclaved)

Dropout medium and agar (-HIS, -LEU, -URA)

185 ml 2X Dropout stock medium
3 X 5 ml of 100X Histidine stock and/or
100X Leucine stock and/or
100X Tryptophane stock and/or
100X Uracil stock
250 ml sterile dd. water or 4 % (w/v) agar
50 ml 20 % (w/v) glucose
(e.g. -HIS: Leu, Trp, and Ura are added, His is left out)

100X Histidine / Leucine / TryptophaneStock (100ml)

0.6 g Histidine
2.6 g Leucine
0.4 g Tryptophane
0.4 g Uracil
(100X Tryptophane is sterile filtered (0.4µ filter), all other stocks are autoclaved and stored at 4°C; precipitate formation is dissolved by short sonication and brief heating in a microwave oven)

Amino acid mix (14.5 g)

0.4 g Adenin
0.2 g L-arginine
0.3 g L-tyrosine
0.3 g L-isoleucine
0.5 g L-phenylalanine
1 g L-glutamic acid
1 g L-aspartic acid
2 g L-threonine
4 g L-serine
1.5 g L-valine
1.5 g L-methionine
1.8 g L-lysine

S. cerevisiae cells were cultivated at 25 or 30 °C and 200 rpm shaking in the appropriate liquid medium, using only baffled Erlenmeyer flasks for better aeration. Yeast cells on solid media were maintained at 30 °C for a maximum time of one week before restreaking onto a fresh plate. Small-scale cultures were of 3-5 ml for expression or drug resistance tests, and 5 or 50 ml culture volumes were used for plasmid recovery experiments. Preparative Plasmid isolation from yeast was always from 1 L overnight cultures.

Glycerol stocks of important cultures were made in analogy to *E. coli*, but at a final glycerol concentration of 30 (v/v). For recultivation, glycerol stock material was streaked out on the appropriate solid medium, and plates were incubated for 2-4 days for colony formation.

2.2.1.3 Cultivation of *P. pastoris*

MD agar

13.4 g/L yeast nitrogen base

1.5 % (w/v) agar

added sterile after autoclaving:

0.4 mg/L biotin

2 % (w/v) glucose

MGY and MMY medium

10 g/L yeast extract

20 g/L peptone from caseine

13.4 g/L yeast nitrogen base

0.4 mg/L biotin and

1 % (v/v) glycerol (MGY) or

0.5 % (v/v) methanol (MMY)

P. pastoris cells were cultivated like *S. cerevisiae* with the exception that they were shaken at 250 rpm. Cultivation was also in YPD or on YPD plates for simple propagation purposes, or

2.2.1.4 Chemical Transformation of *E. coli*

E. coli were made chemically competent by the method of Hanahan [211] or used directly in a competent form as part of a kit. For transformation by heat shock, aliquots of competent cells were thawed on ice for 10 min and split into 50 µl aliquots. Regularly, 10-100 ng of plasmid DNA were used in a maximal volume of 5 µl that was added to the cell suspension and mixed by gentle stirring with a sterile pipette tip.

After 20 min incubation on ice, cells were subjected to a heat shock at 42 °C for 60 sec, cooled on ice for 2 min, and were mixed with 800 µl of sterile, prewarmed LB medium without any antibiotic. For transformation of normal plasmids, all following steps were carried out at 37 °C, and 30 °C was used for all unstable constructs. The cells were incubated for 1 h at 200 rpm shaking, pelleted by centrifugation at 8.000 rpm for 2 min in a table top microcentrifuge, and the supernatant was discarded by decantation. Cells were carefully resuspended in the remaining medium and plated out on LB agar containing the suitable antibiotic. At 37 °C, plates were incubated overnight, and at 30 °C, incubation was for two days to allow colony formation of the slow-growing transformants.

2.2.1.5 Measurement of optical density of cell suspensions

The optical density in cultured cell suspensions was measured at a wavelength of 600 nm in disposable cuvettes in a cell density meter (CO8000). Water was used for calibration in the case of dilute samples, and the appropriate medium for non-dilute samples.

2.2.1.6 Chemical transformation of *S. cerevisiae*

10X TE

100 mM Tris pH 7.5

10X LiAc

1 M Lithium acetate pH 7.5

50 % (w/v) PEG 4000

dd. sterile water

LATE buffer

1 ml 10X TE

1 ml 10X LiAc

8 ml dd. sterile water

PLATE buffer

1 ml 10X TE

1 ml 10X LiAc

8 ml 50 % (w/v) PEG 4000

For the preparation of competent *S. cerevisiae* cells, a single freshly grown yeast colony was used to inoculate an 5 ml YPD culture. After overnight growth, the OD₆₀₀ was measured, and 5 ml YPD in a small baffled Erlenmeyer flask were inoculated to an OD₆₀₀ of 0.2 and allowed to grow to 0.8-1. The cells were harvested in an sterile

50 ml falcon tube (5 min at 4000 rpm and 4 °C in a Megafuge 1.0R), washed once in 30 ml of ice-cold, sterile water and resuspended in 1 ml LATE. After transfer to a sterile 1.5 ml reaction tube, the cells were pelleted by brief centrifugation at 10.000 rpm at room temperature, and resuspended in 50 µl LATE per 10 OD₆₀₀ equivalent. Cells were stored for a maximum of four days before transformation with plasmid DNA. For use in homologous recombination, freshly made competent cells were always used.

50 µl aliquots were used for chemical transformation. To these, a maximum of 10 µg linear expression cassette DNA was added, or usually several hundred ng of plasmid DNA, and the suspension was mixed by pipetting up and down a few times. After addition of 300 µl PLATE buffer and careful yet thorough mixing of the reaction, the cells were incubated at 30 °C for 20 min. They were then heat-shocked by a 20 min incubation at 42 °C. During heat shock, the cells were resuspended every 5 min by gentle inversion. Finally, after harvest by brief centrifugation at 13.000 rpm, the supernatant was completely removed by pipetting the cells were carefully resuspended in 100 µl of sterile water and plated out onto appropriate Dropout plates. The plates were incubated at 30 °C for up to five days in order to allow the growth of sufficiently large colonies that were then restreaked onto the same plate type for a second round of selection.

2.2.1.7 Transformation of *P. pastoris* by electroporation

1 M sorbitol

500 ml YPD medium were inoculated from an overnight culture to an OD₆₀₀ of 0.2 and grown to OD₆₀₀ 1.3-1.5. Cells were harvested by centrifugation for 5 min at 1.500 x g and 4°C and then washed twice with 500 ml of ice-cold, sterile dd. water. The cells were resuspended in 20 ml of ice-cold 1 M sorbitol, transferred to a sterile 50 ml falcon tube and collected by centrifugation (5 min at 1500 rpm and 4 °C in a Megafuge 1.0R). The cell pellet was resuspended in 1.5 ml of ice-cold 1 M sorbitol and stored at 4 °C for use on the same day.

80 µl of this cell suspension were transferred into a sterile electroporation cuvette with a electrode gap of 2 mm and mixed with 5 to 10 µg of linearised vector

DNA. For electroporation, DNA has to be salt-free. For BSEP expression in *P. pastoris*, the pPIC3.5BSEP construct was linearized by restriction digest with *Sall* and salt/ethanol-precipitated to remove salts. The cells were incubated with the DNA on ice for 5 min and then electroporated for 5 ms at 1500 V. Immediately after, 1 ml of ice-cold 1M sorbitol was added to the cells by gentle inversion, and 300 µl of the cell suspension were plated out on MD agar plates. These are devoid of histidine and select for histidine prototrophy of the transformants by the *HIS4* marker on the linearized plasmid that is only maintained in *P. pastoris* by homologous recombination into the *AOX1* locus of the histidine auxotrophic strain GS-115. Transformants that were obtained after 4 days of growth and restreaked onto MD agar for a second round of selection.

2.2.1.8 DNA precipitation by sodium acetate/ethanol

It was found that freshly precipitated DNA resulted in better transformation of *S. cerevisiae* cells. For *in vivo* homologous recombination, the corresponding fragments were mixed in an equimolar ratio to an amount in the µg range and coprecipitated by addition of 1/10 volume of 3M sodium acetate and 2 volumes of pure, -20 °C cold ethanol followed by thorough mixing. The DNA was allowed to precipitate either at -20 °C overnight or at -80 °C for 1 h. The precipitate was collected by centrifugation for 30 min at 13.000 rpm and 4 °C, and residual salt was washed out with 500 µl of -20 °C 70 % (v/v) ethanol. The DNA pellet was dried under the cleanbench for 10 min at room temperature with the reaction tube lying on the side to prevent pellet loss. After that, the DNA was directly resuspended in the 50 µl of competent yeast cells and used for transformation. For electroporation, DNA was resuspended in 10 µl of sterile dd. water.

2.2.1.9 Plasmid recovery from *S. cerevisiae*

Yeast cells in the logarithmic growth phase were harvested and the cell wall was digested with Zymolyase 100T for 30 min at 37 °C in the presence of 2 mM DTT. The spheroblasted cells were then subjected to chemical lysis as described for *E. coli*.

2.2.1.10 Plasmid isolation from *E. coli*

Plasmid isolation was carried with the Qiagen pasmid mini- and midiprep kits and the Macherey-Nagel Nucleobond Xtra Midi kit according the manufacturers' guidelines. *E. coli* cultures for were either grown overnight at 37 °C or for 48 h at 30 °C to allow the generation of enough bacterial mass and plasmid. For plasmid miniprep, 2 ml of cell suspension were either harvested in 2 ml reaction tubes. For plasmid midiprep, 150 ml medium were cultured and harvested in 50 ml falcon tubes. The cell pellets were either directly resuspended and processed or stored at -20 °C until preparation. DNA was always resuspended in elution buffer (10 mM Tris/HCl pH 8.5) and stored at 4 °C for a short period or at -20 °C indefinetely. DNA quantity and purity was measured on a Nanodrop ND-1000 spectrophotometer.

2.2.1.11 DNA sequencing

Sequencing of plasmids and PCR products was carried out at the service unit of the Biologisches-Medizinisches Forschungszentrum (BMFZ) at the University of Duesseldorf.

2.2.1.12 Manipulation of DNA with enzymes *in vitro* and agarose gel electrophoresis

Restriction digest of DNA

Restriction endonucleases were either from Fermentas of New England Biolabs and were used according to the manufacturers' guidelines. Analytical restriction digests were regularly performed in microtiter plates in a reaction volume of 10 µl with approximately 100 ng of DNA and a maximum of 0.3 units per restriction enzyme. As most restriction endonucleases are delivered in a concentration of 10 units/µl, this corresponds to 0.3 µl. As a rule, the volume of restriction enzyme stock solution never exceeded 10 % (v/v) of the final reaction volume as too high glycerol concentrations of glycerol can inhibit restriction enzyme activity. The plates were covered with their lid, after sterile water was pipetted in each of the plates edges to saturate the air and prevent sample evaporation. The plates were sealed with parafilm and put into an incubator at the optimal restriction temperature for 1 h.

Preparative restriction digests were carried out in final volumes that were the double of the used DNA solution to digest. Accordingly, 25 or 30 μ l were digested in a final volume of 50 and 60 μ l, respectively. Depending on the amount of enzyme used, preparative digestion was performed for 2 to 4 h or overnight for complete digestion unless a restriction enzyme was used that was prone to star activity upon overdigestion.

Agarose gel electrophoresis of DNA

50X TAE buffer

2 M Tris

1 M acetic acid

100 mM EDTA

(pH 8.1)

EDTA stock

0.5 M EDTA

(adjusted to pH 8)

6X DNA sample buffer

40 % (v/v) glycerol

0.25 % (w/v) Bromophenol blue

0.25 % (w/v) Xylene cyanole

in 10X TAE buffer

For purposes of analysis or purification of digested DNA, samples were mixed with 6X DNA sample buffer to a final concentration of 1X and separated by agarose gel electrophoresis. DNA fragments were usually separated on 1 % (w/v) agarose gels (prepared in 1X TAE buffer) at 140 V (about 14 V/cm) for 30-60 min. Separation of larger fragments was improved by using 0.8 % (w/v) agarose gels. After electrophoresis, the relevant parts of the gels were incubated in an ethidium bromide bath (40 μ l of a 10 % EtBr stock solution in 400 ml of dd. water) for DNA visualization and documentation on a UV light unit (Chemigenius 2). For the preparative excision of DNA, the gels were exposed to UV light as short as possible (few seconds) to prevent excessive DNA damage. The DNA fragment was then separated from EtBr and agarose by using the Qiagen gel extraction kit. Elution from the spin column was increased by incubation of the membrane with elution buffer for 3 min before elution.

Dephosphorylation of DNA ends

The enzyme calf intestinal alkaline phosphatase (CIAP) was used to remove the terminal 5'-phosphate at the ends of DNA fragments. This prevents a ligation of the dephosphorylated 5' strand end to the terminal hydroxyl group of the 3' strand of a compatible end. After the restriction digest of a plasmid at a single site, CIAP treatment prevents a religation of the resulting DNA ends. An insert however, can still ligate to such ends as it has intact 5'-phosphate-carrying termini.

Ligation of DNA

Depending on the concentration of the fragments to be ligated, the reaction volume was between 10 and 20 μ l. A typical reaction consisted of 50-100 ng total DNA in an 15 μ l reaction with 0.5 to 1 μ l of T4 DNA ligase and corresponding ligase buffer from Fermentas that was allowed to proceed for 1 to 2 h at room temperature before heat inactivation of the enzyme at 65 °C for 10 min. 1 to 5 μ l of this mixture were then used for chemical transformation of *E. coli* cells.

2.2.1.13 Generation of a system of expression cassette vectors for chromosomal overexpression of genes in *S. cerevisiae*

10 μ l of a plasmid miniprep of the pRE2 vector were digested in 50 μ l reaction volume with 20 units *Nsi*I and 20 units *Pac*I for 3 h at 37°C. The vector backbone was then purified on a preparative 0.8 % (w/v) agarose gel and was gel extracted. DNA was eluted in 30 μ l elution buffer. Each pair of the forward and reverse oligonucleotides encoding the different tags, 3X glycine linker, optional *Sfi*I restriction site and factor Xa protease cleavage site was pooled (1 μ l per oligonucleotide solution 100 pmol/ μ l in water, in 100 μ l 1X PNK reaction buffer), heated to 94 °C in the metal block of a thermal incubator for 1 min, and allowed to anneal by slow passive cooling of the metal block to room temperature for 30 min. The ends of 20 μ l annealed cassette oligonucleotide were then phosphorylated by the addition of 1 μ l of T4 polynucleotide kinase and incubation for 1 h at 37 °C. After inactivation of the enzyme for 20 min at 65 °C, the finished cassette fragment was ligated into the double-digested pRE2 backbone (1 μ l cut pRE2, 1 μ l cassette fragment in 15 μ l 1X ligase reaction buffer and 1 μ l T4 DNA ligase) for 2 h at room temperature. The

ligation mixture was inactivated for 10 min at 65 °C, and 5 µl were used to transform *E. coli* strain DH5α. Transformants were selected on LB agar supplemented with 100 µg/ml ampicilline, and plasmid preparations from these were subjected to analytical restriction digest with *Nsi*I and *Pac*I. Positive clones were digested into backbone and cassette insert.

2.2.1.14 The *Sfi*I cloning strategy

Principle

For *Sfi*I-mediated cloning of any gene of interest (GOI), a PCR product is generated from the GOI with primers that each encode a *Sfi*I restriction site on their 5' overhangs. The *Sfi*I sequence on the p10- and p14His*Sfi*I plasmids is:

5'-GGCCGCTC/TGGCC-3'.

Primer design

Since *Sfi*I digestion takes place at 50 °C the DNA ends of the GOI PCR product are expected to "breathe", i. e. to partially become single-stranded. To prevent this, the PCR primers should be designed with some additional G and C bases upstream of their *Sfi*I restriction site. Examples are given in the oligonucleotide table in the Materials section for *MRP2* and the *lacZ* fragment.

2.2.1.15 Blue/white screening of *E. coli* colonies

LB-IPTG/X-Gal agar (25 ml)

100 µl 2 % (w/v) X-Gal in dimethyl formamide

40 µl 0.1 M IPTG

The presence of the *lacZ* insert in p14His*Sfi*I was tested blue/white screening. *E. coli* XL1blue cells were chemically transformed with the inactivated ligation reaction and plated out onto LB agar containing IPTG and X-Gal. The *lacZ*-encoded beta galactosidase was induced by IPTG and catalyzed the formation of a blue dye from X-Gal in cells that carried the plasmid with the insert.

2.2.1.16 Construction of MDR3 and BSEP expression vectors by homologous recombination and the recombination-based BSEP expression screen

Generation of PCR products and preparation of vectors for homologous recombination in S. cerevisiae

The YEpHIS and YEpMDR1HIS vectors [182] were the kind gift of Marwan Al-Shawi. All PCR reactions were performed with the Phusion® DNA polymerase in HF buffer according to the manufacturers recommendations. 50 µl reactions usually contained 1.5 µl of DMSO, except for yeast colony PCR. PCR conditions were: 2 min initial denaturation, 50 sec cycle denaturation, 50 sec annealing, 20 sec per kbp of extension for 35 cycles, followed by 7 min of final extension. For homologous recombination, all vectors were linearized by restriction digest as indicated during which they also were dephosphorylated with calf intestinal alkaline phosphatase (Fermentas). YEpMDR1HIS was double-digested with *Bam*HI and *Bsm*II, YEpHIS was cut with *Bam*HI and *Mlu*I to remove the C-terminal his tag [182]. The oligonucleotides YEpNHISFor and YEpNHISRev encoding an N-terminal his₁₄ tag followed by a factor X_a cleavage site were mixed in equimolar amounts, heated to 95 °C for 5 min and allowed to anneal by slow cooling to room temperature. After T4 polynucleotide kinase (NEB) treatment, the phosphorylated synthetic insert was ligated into the gel-purified linearized YEpHIS plasmid. *BSEP* PCR products with fitting overlaps were generated with the primer pairs *BSEP*-YEpHISN-S1 / -S2 and *BSEP*-YEpHISC-S1 / -S2, respectively.

2.2.1.17 The two-step, recombination-based BSEP expression screen

For the two-step expression screen, p426-GPD, -TEF, -CYC1, -MET25 from ATCC vector set No. 87669 [208], and p426-GAL1 from set No. 97670 [209] were used. Preparative digest of the p426-MET25 plasmid was carried out in a volume of 80 µl with 20 units of the indicated restriction enzymes following the manufacturers' recommendations. *BSEP* cDNA was amplified with primer pair *BSEP*-p426-CHis-HR-S1 / -S2 for homologous recombination into the first plasmid of the set, p426-MET25. All DNA fragments were gel-purified, mixed together in equimolar amounts (final amount before precipitation: 2 - 4 µg), and co-precipitated with salt / ethanol. The pellet was briefly dried and directly used to transform 50 µl of competent yeast cells.

Transformants arising from the selection procedure were directly used to screen the BSEP expression from YEX whole cell lysates.

2.2.1.18 Plasmid recovery from *S. cerevisiae*

Small- (5 - 10 ml for *E. coli* transformation) or large-scale (0.5 - 1 l for obtaining preparative plasmid amounts) overnight yeast liquid yeast cultures were harvested, washed in cold water once, and then resuspended in Zymolyase incubation buffer (see above, with 1.2 M sorbitol). The yeast cell wall was digested with occasional gentle inversion for 30 min at 37 °C, cells were then lysed by alkaline lysis generally as described in [212], with the exception that the Macherey-Nagel midiprep kit was used. 0.5 - 1 µl of this preparation was used to transform chemically competent *E. coli* strain XL1blue. After heat shock, bacteria were shaken for 1 h at 30 °C and 200 rpm to prevent the loss of unstable construct. After plating out on low salt LB media containing 50 µg/ml Carbenicillin, plates were incubated at 30 °C. Carbenicillin allows for a tighter and longer lasting selection as it hydrolyzes much slower than ampicillin. 150 ml low salt LB with Carbenicillin were then directly inoculated with a single colony and allowed to grow for 36 to 48 hours at 30 °C and 200 rpm. Cells were harvested and plasmid prepared from these. The plasmids were sequence-verified.

2.2.1.19 Isolation of genomic DNA from *S. cerevisiae*

Total genomic DNA was isolated from *S. cerevisiae* using the DNeasy Blood and Tissue kit (Qiagen) and the additional kit protocol "Purification of total DNA from yeast".

2.2.1.20 Polymerase chain reaction

The polymerase chain reaction was used to amplify DNA sequences for analytical detection or recombinant DNA work. The Phusion HiFi DNA polymerase was used to minimize nucleotide misincorporation during PCR. PCR reactions were set up on ice in total volumes of 50 or 30 µl according to the product guidelines.

	<u>50 μl Rxn</u>	<u>30 μl Rxn</u>
5X HF buffer (final conc. 1.5 mM Mg ²⁺)	10 μ l	6 μ l
10 mM dNTPs	1 μ l	0.6 μ l
optional: DMSO	1.5 μ l	0.9 μ l
optional: 50 mM MgCl ₂	1 μ l	0.6 μ l
Primers (10 pmol/ μ l)	3 μ l each	1.8 μ l
Template	10-50 ng	10-50 ng / one small bacterial colony
water, molecular biology grade	to 49.5 μ l	to 29.7 μ l
Phusion polymerase	0.5 μ l	0.3 μ l

The PCRs were performed as hot start, except for colony PCR setups. The hot start procedure was found to improve yields, especially with primers that have long and overlapping 5'-ends.

Yeast colony PCR

Freshly growing transformant colonies were picked and restreaked onto selective agar plates. The rest of the material was treated with Zymolyase for 45 min at 37 °C in 50 μ l reaction volume (0.1 M sodium phosphate buffer pH 7.4, 2 mM DTT, and 5 - 10 mg/ml of Zymolyase T-100 (ICN)). After heating the reactions to 95 °C for 10 min, the material was frozen at -20 °C for 10 min and thawed again. 5 μ l of this were used as template for colony PCR (30 μ l reaction in Phusion HF buffer: 2 mM final conc. of MgCl₂, 20 pmol/primer, 200 μ M dNTPs, 1.5 units Phusion® DNA polymerase).

Restriction analysis of colony PCR products from the BstBI mutagenesis

10 μ l of the reaction was directly digested with *Bst*BI (15 μ l reaction, 8 units restriction enzyme) for 1 h at 37 °C and then resolved on a 1 % agarose gel.

2.2.1.21 Standard site directed mutagenesis (SDM)

Classic site-directed mutagenesis was performed with the Quikchange II XL site-directed mutagenesis kit according to the manufacturers' protocol for silent removal of the *SfiI* sites in the *MRP2* cDNA and the plasmid backbone of p10- / p14HisSfiI.

2.2.1.22 The new, *E. coli* independent site-directed mutagenesis procedure

For introduction of the missense, *BstBI* mutation into *BSEP* constructs, the mutagenesis primer pair *BSEP-BstBI*mut-S1 / -S2 was used. Cycling conditions were as in the classic SDM protocol, with 18 cycles to minimize PCR-induced errors, and with the annealing temperature strictly being kept at 60 °C to ensure the generation of ds-ended mutagenesis product (for a detailed description of the procedure, see Results 3.10). Reactions were set up with the Phusion DNA polymerase, as this proofreading enzyme has a low error rate practically identical to the enzyme used in the Stratagene SDM kits (according to the manufacturers' datasheets: 4.4×10^{-7} for Phusion High Fidelity Polymerase, 4.3×10^{-7} for PfuUltra HF Polymerase). Extension time was 1 min per kb to allow for complete extension. This seems to be a very important factor in the successful generation of mutagenesis product. The recommended elongation time for Phusion polymerase is 15 - 30 seconds per kbp, and an extended incubation at the elongation step was found to be paramount for a successful exponential product generation, probably because it ensures the quantitative integrity of the ends that serve as priming sites in subsequent cycles. 10 ng of template was used, and the reaction was initiated after heating the reaction to 98 °C (hot start) with 0.5 µl of Phusion polymerase. The finished reaction was precipitated with sodium acetate and ethanol, and directly resuspended in 20 µl (= 4 OD₆₀₀ equivalents) of fresh competent yeast cells in LATE buffer. This assures an optimal ratio of mutagenesis product to yeast cells. The transformation was carried out as described above by addition of 120 µl PLATE buffer (40 % (v/v) PEG 4000, 0.1 M lithium acetate, 10 mM Tris-HCl pH 8, 1 mM EDTA).

2.2.1.23 Drug agar resistance assays of *S. cerevisiae*

<u>Compound</u>	<u>Solvent</u>
Taurocholate	dd. sterile water
Taurodeoxycholate	dd. sterile water
FK506	DMSO
Cycloheximide	dd. sterile water
Fluconazol	DMSO
Ketoconazole	DMSO
Doxorubicin	ethanol
Lovastatin	15 % (v/v) ethanol, 0.25 % (w/v) NaOH*
Pravastatin	dd. sterile water

*hydrolyzed at 60°C for 1 h as described in [213]

Drug agar plates were prepared as follows: the indicated liquid agar medium was allowed to cool down to about 60 °C and kept liquid by slow mixing on a magnetic stirrer (a stirring bar was autoclaved in the agar). Serial dilutions of the tested drugs were made either in sterile dd. water or the indicated solvent. For each concentration, the same volume of drug solution was then pipetted into a sterile 50 ml falcon tube, mixed with some of the warm medium by gentle inversion and then filled up to 50 ml. The same volume of solvent was used as a control. The amount of ethanol or DMSO never exceeded 0.5 % (v/v). After mixing by repeated careful inversion to avoid air bubbles, the drug-containing medium was poured in two equal parts into two petri dishes. The drug agar plates were allowed to solidify and stored at room temperature in the dark until their use on the same day.

S. cerevisiae cells from 5 ml overnight cultures were used to inoculate 5 ml of liquid medium to an OD₆₀₀ of 0.2. At the OD₆₀₀ of 1, the cultures were put on ice until all strains for an experiment were collected. If the time between the first and the last culture was more than an hour, the experiment was abandoned and repeated. For this reason, every strain was inoculated twice. Aliquots of the cultures were diluted to an OD₆₀₀ of 0.2 in sterile ice-cold reaction caps, and from these, serial 1:10 dilutions were made in the culture medium. Using a printed template, 3 µl aliquots of the serial dilutions were spotted onto the different drug agar plates.

2.2.2 Methods of protein biochemistry

2.2.2.1 Preparation of whole cell lysates of *S. cerevisiae* by chemical lysis

YEX (Yeast EXtraction) buffer [214]

1.85 M NaOH

7.5 % β -ME

50 % (w/v) trichloroacetic acid (TCA)

double-distilled water

1 M Tris/HCl pH 8

All solutions must be ice-cold. 2 OD₆₀₀ of cells were harvested by centrifugation for 1 min at 13.000 rpm and 4 °C in a tabletop microcentrifuge. The cell pellet was washed once in 1 ml water, then resuspended in the same volume of water. 150 μ l of YEX buffer were added, the samples were briefly, but thoroughly mixed and incubated for 10 min on ice. After addition of 150 μ l of 50 % (w/v) TCA and mixing as above, they were incubated for an additional 10 min in ice. Precipitated proteins were collected by centrifugation for 10 min at 13.000 rpm and 4 °C, and supernatants were discarded. Initially, 1 ml of ice-cold acetone was then used to remove any remaining TCA. Since this made the protein pellets more fragile and resulted in random loss of sample, this step was changed: after removal of the supernatant, the reaction tubes were allowed to dry for 10min upside down on tissue paper. Residual TCA was neutralized by addition of 10 μ l of 1 M Tris/HCl pH 8, and the samples were resuspended in 40 μ l of 1X SDS special sample buffer per OD₆₀₀ equivalent. Samples were incubated at 65 °C for 10 min, briefly allowed to cool down and cellular debris was removed by short centrifugation (30 sec at 13.000 rpm at room temperature). 20 μ l of lysate corresponding to 0.5 OD₆₀₀ equivalents of cells were then analyzed by SDS-PAGE.

2.2.2.2 Sodium dodecylsulfate polyacrylamide gel electrophoresis (SDS-PAGE) of proteins

Separating gel buffer

SDS 4 g/L

Tris-HCl 1.5 M pH 8.85

Stacking gel buffer

SDS 4 g/L

Tris-HCl 0.5 M pH 6.8

10X SDS electrophoresis buffer

Glycine 1.9 M

Tris-HCl 0.25 M

SDS 10 g/L

final pH of this solution is 8,8 and does not need to be adjusted.

Western blot transfer buffer

100 ml 10X SDS electrophoresis buffer

700 ml double-distilled water

200 ml methanol

5X SDS special sample buffer [214]

10 ml Stacking gel buffer

10 ml 16 % (w/v) SDS

5 ml 0.2 % (w/v) Bromophenol blue

8 M Urea (concentration in 50 ml final volume)

Reducing SDS special sample buffer

960 µl 5X SDS special sample buffer

40 µl 1M DTT

(stored at -20 °C)

Components are mixed in an 50 ml falcon tube and then Urea is added. Finally, glycerol is added to 50ml final volume.

Separating gel (for 9 gels)

	<u>7 %</u>	<u>8 %</u>	<u>9 %</u>	<u>10 %</u>	<u>12 %</u>	<u>15 %</u>
dd. water	38.75 ml	36.25 ml	33.75 ml	31.25 ml	26.25 ml	18.75 ml
Separating gel buffer	18.75 ml	18.75 ml	18.75 ml	18.75 ml	18.75 ml	18.75 ml
Acrylamide/ Bis-acrylamide (37.5:1)	17.5 ml	20 ml	22.5 ml	25 ml	30 ml	37.5 ml
10 % (w/v) APS	300 µl	300 µl	300 µl	300 µl	300 µl	300 µl
TEMED	70 µl	70 µl	70 µl	70 µl	70 µl	70 µl

Stacking gel (for 9 gels)

	<u>4.5 %</u>
Stacking gel buffer	5 ml
Acrylamide/Bisacrylamide (37.5:1)	5.25 ml
dd. water	28 ml
10 % (w/v) APS	210 µl
TEMED	70 µl

APS and TEMED were added to initiate polymerization. The SDS gels were cast (40 min polymerization for separating, 1 h for stacking gel) and stored up to one week at 4 °C wrapped in wet paper. For BSEP and MDR3, 7 % SDS gels were used. Since most membrane proteins irreversibly aggregate at high temperatures, samples were incubated in reducing SDS special sample buffer at 65 °C for 10 min. After brief centrifugation to remove insoluble material, the protein samples were separated at 150 V using 1X SDS electrophoresis buffer.

2.2.2.3 Coomassie staining of SDS gels

Coomassie staining solution

100 ml glacial acetic acid
 500 ml dd. water
 400 ml methanol
 0.25 % (w/v) Coomassie brilliant blue R-250

Destaining solution

100 ml glacial acetic acid
 500 ml dd. water
 400 ml methanol

Proteins in SDS gels were stained by incubation in Coomassie staining solution for 30 min to 1 h. The gels were rinsed briefly with dd. water and incubated in several rounds of destain solution until protein bands were clearly visible against the background.

2.2.2.4 Silver staining of SDS gels

Fixing solution

30 % (v/v) ethanol
 10 % (v/v) glacial acetic acid

Thiosulfate buffer

0.1 M sodium acetate pH 6
 30 % (v/v) ethanol

Silver nitrate solution

0.5 g/L AgNO₃
 (immediately before use, add 12.5 µl
 37 % (wt/wt) formaldehyde)

Developing solution

2.5 % (wt/v) Na₂CO₃
 (immediately before use, add 25 µl of 37
 % (wt/wt) formaldehyde)

37 % (w/v) Formaldehyde solution

Glacial acetic acid

After electrophoresis, SDS gels were fixed for 15 min under gentle agitation in fixing solution. After incubation in thiosulfate buffer for 15 min, the gels were washed 2 x 10 min in dd. water. The gels were incubated for 25 min in silver nitrate solution, washed in water for 1 min and then submerged in developing solution. Development of bands was stopped by addition of 1 ml glacial acetic acid, a few minutes of gentle agitation, and transfer into dd. water. 50 ml per gel were used of each solution.

2.2.2.5 Western blot and immunodetection of proteins

Western blot transfer buffer

100 ml 10X SDS gel electrophoresis buffer
700 ml dd. water
200 ml methanol

Ponceau S solution

0.1 % (w/v) Ponceau S in
3 % TCA

TBS(-T)

20 mM Tris/HCl pH 8
250 mM NaCl
(0.1 % (v/v) Tween 20)

Blocking solution

5 % (w/v) non-fat dried milk powder in
TBS-T
0.05 % (w/v) sodium azide

Stripping buffer

15 g/L glycine
1 g/L SDS
1 % (v/v) Tween 20
pH adjusted to 2.2

Proteins separated by SDS-PAGE were transferred onto nitrocellulose membranes by semi-dry Western blot transfer in a Biorad apparatus. For this, the glass plates surrounding the polyacrylamide gels were gently pried apart with a broad plastic wedge or spatula SDS, and the gels were sandwiched between nitrocellulose membranes and presoaked Whatman filter paper in the following order, from bottom to top: 3 layers of whatman paper, the nitrocellulose membrane, the SDS gel including the stacking gel part, and three layers of whatman paper. For optimal

electrotransfer of the proteins, the filter paper and the membranes were cut to the gel size and extensively soaked in transfer buffer for 10 min. The stacking gel area was also transferred onto the membrane to check for possible membrane protein aggregation, which however was not an issue due to use of the SDS special sample buffer. Proteins were electrotransferred at 110 mA per gel for 1.5 h to achieve maximum transfer.

Ponceau S staining

The transfer was checked by reversible Ponceau S staining of the nitrocellulose membrane after blotting. The membranes were covered in Ponceau S solution and incubated for 3-5 min under gentle agitation. The solution was recovered for reuse, and excessive stain was removed by repeated gentle rinsing with dd. water. Complete removal of the stain was achieved by simple blocking of the membranes in blocking solution.

Immunodetection of nitrocellulose membranes

The membranes were blocked for 30 min in blocking solution. Primary antibodies were used in volumes of 10 ml of blocking buffer per membrane at concentrations of 1:2500 (K24), 1:2000 (K168), 1:1000 (C219), 1:10.000 (anti Pdr5), and 1:1500 (anti Dpml), respectively. The blocked membranes were incubated in the primary antibody for 1 h, rinsed shortly with TBS-T after antibody solution recovery (the primary antibody solutions can be reused several times and were stored at 4 °C between uses), and washed three times in TBS-T for 5 min under gentle agitation. Then the membranes were incubated with the appropriate secondary antibodies at a dilution of 1:10.000 in 10 ml of blocking solution without sodium azide for 1 h. Sodium azide inhibits the horseradish peroxidase that is coupled to the secondary antibodies for detection. After 2 wash steps in TBS-T and one wash step in TBS, proteins marked by antibodies were detected with the ECL Advanced Western blot detection kit according to the manufacturers' guidelines. All incubation and washing steps were under gentle agitation.

His tag immunodetection

The pentaHis antibody from Qiagen was used to detect his-tagged proteins according to the manufacturers' guidelines, with the following deviations: membranes were blocked in blocking solution instead of TBS-T with 3 % (v/v) BSA. After blocking, membranes were rinsed briefly in TBS-T, then washed 2 x 5 min in TBS-T and 1 x 5 min in TBS. After incubation in the primary antibody solution (pentaHis diluted 1:1000 in TBS + 3 % (w/v) BSA), membranes were subjected to the same washing regime and incubated with the secondary antibody solution (goat anti-mouse, HRP-coupled, diluted 1:10.000 in TBS + 10 % non-fat dried milk). The washing regime was repeated, and the blot membranes were detected as described above.

Stripping and reprobing of membranes

During stripping, bound antibodies and detection reagents are removed from the blot membrane. The binding of the antibodies is disrupted by the low pH of the solution. As an internal control for some of the Western blots that were made of the sucrose gradients to investigate the subcellular localization of the human ABC transporters in *S. cerevisiae*, these membranes were stripped by two incubation steps with 15 ml of stripping buffer for 10 min. After this, membranes were washed 2 x 10 min in TBS, then 2 x 5 min in TBST. After incubation in blocking solution for 30 min, the membranes were ready for redetection. In the case of the sucrose gradients, membranes were reprobated with anti Dpml.

2.2.2.6 Subcellular fractionation of membranes from whole *S. cerevisiae* Cells*Incubation medium*

200 mM Tris/HCl pH8.0
20 mM EDTA
1 % (v/v) β -mercapto ethanol
5 mM NaN_3
5 mM NaF

Spheroblast medium

SD or YPD medium adjusted to
1 M sorbitol
5 mM NaN_3
5 mM NaF

(150 ml per cell pellet: 50 ml for cell wall)

(50 ml per cell pellet)

digestion, 2 x 50 ml for wash steps)

Hyposmotic buffer

50 mM Tris/HCL pH7.5

200 mM Sorbitol

1 mM EDTA

one Roche Protease inhibitor cocktail
tablet per 50 ml(1 µg/ml Aprotinin, 1 µg/ml Leupeptin, 1
µg/ml Pepstatin, 5 µg/ml Antipain, 1 mM
Benzamidin, 1 mM PMSF)(4-6 ml per cell pellet, can be stored at -
20 °C)Sucrose gradient

Sucrose solutions 22-60 % (w/w) in

10 mM HEPES/KOH pH7.2

1 mM EDTA

0.8 M sorbitol

Gradients were always pipetted in
duplicates for balancing during the
ultracentrifugation step. Concentration
steps were as follows:

0.5 ml	60%
1 ml	40%
1 ml	37%
1.5 ml	34%
2 ml	32%
2 ml	29%
1.5ml	27%
1.5ml	22%

500 ml yeast cultures were harvested at an OD₆₀₀ of 1 by centrifugation at 4000 rpm and 4 °C (MegaFuge 1.0R) for 11 min and. The pellet was resuspended in 50 ml Incubation medium and incubated with 0.9 mg/ml Lysing Enzymes. The cells were then incubated for 30 min at 30 °C, cooled on ice and washed twice with ice-cold Spheroblast medium (4000 rpm, 5min at 4°C). All subsequent steps were carried out at 4 °C. Spheroblasts were resuspended in 4-6ml ice-cold Hypoosmotic buffer and disrupted in a small Dounce homogenizer with 15 strokes. This lysate was then transferred into 15 ml Falcon tubes and centrifuged for 5 min at 500 x g to remove cellular debris. The supernatant was centrifuged for 10 min at 13.000 x g (10.500 rpm in A8.24 rotor). Complete membranes were then harvested from the resulting supernatant by ultracentrifugation (100.000 x g, Ti60 rotor) for 1 h. During the centrifugation step, the gradients were pipetted. Membrane pellets were

resuspended in 2 ml ice-cold Hypoosmotic buffer with protease inhibitor cocktail and carefully layered on top of the sucrose gradient. The different membrane species were then separated by ultracentrifugation for 18 h at 130.000 x g (32.100 rpm in a SW40Ti rotor). The gradients were separated into 600 µl aliquots by carefully pipetting from the top. Equal volumes were then directly analyzed by SDS-PAGE and Western blot.

2.2.2.7 Preparation of whole cell membranes from *S. cerevisiae*

1 M Tris/acetate pH 7.5

Acid washed glass beads

(in water)

500 mM EDTA pH 8

TEG

(adjusted with NaOH)

10 mM Tris/acetate pH 7.5

0.2 mM EDTA

20 % (v/v) glycerol

Membrane buffer

20 mM Tris/Hcl pH 8

75 mM NaCl

15 % (v/v) glycerol

All steps of this procedure were carried out at 4 °C with ice-cold buffers. *S. cerevisiae* cells carrying YEpHISBSEP or -MDR3 were grown in 10 L DO-LEU medium supplemented with 10 % (w/v) glycerol overnight at 25 °C and 200 rpm shaking. The next morning, at an OD₆₀₀ of 1 to 1.5, they were harvested by centrifugation for 11 min at 6000 x g. The cell pellet was washed once in ice-cold dd. water and cells were stored in 50 ml falcon tubes at -20 °C until use.

For membrane preparation, frozen cell pellets from 10 L were dislodged from their falcon tube with 20 ml of cold dd. water on a rotational shaker. Pellets were pooled in a glass cylinder and filled up to 84 ml, then 5 ml 1 M Tris/acetate pH 7.5 and 1 ml 500 mM EDTA pH 8 were added. Cells were disrupted in a bead beater (Biospec): the precooled container unit was first filled with 200 ml of acid-washed glass beads, then two protease inhibitor cocktail tablets and the cell suspension (cell

pellets don't need to be completely dissolved) were added. The rest of the glass beads was added, and the remaining space of air in the container was filled with a bit of ice-cold dd. water. The container was closed, and the cells were disrupted by 5 cycles of a 1 min burst followed by 1 min of cooling phase to prevent sample overheating. The lysate and glass beads were separated by gentle vacuum filtration through a porous glass filter, and the beads were washed twice with 30 ml of TEG buffer. Cell debris of the pooled lysate was removed by centrifugation for 10 min at 5.000 x g. Whole cell membranes were collected from the supernatant by ultracentrifugation (1.5 h at 180.000 x g in a Ti60 rotor) The Pellet was resuspended in 10 ml membrane buffer with a Dounce homogenizer, snap-frozen in liquid nitrogen, and stored at -80 °C.

2.2.2.8 Preparation of highly enriched plasma membranes

1 M sodium acetate

(pH 5.2)

2.5 M Tris/acetate pH 7.5

50 mM HEPES pH 7

(one tablet of protease inhibitor cocktail
in 50 ml)

This method is a combination of two preparation methods by L. Serrano [215] and A. Goffeau [216,217] and was initially developed for selective enrichment of the *S. cerevisiae* ABC transporter Pdr5 [205]. All steps were carried out at 4°C and with ice-cold buffers. One preparation usually was from cell pellets of 4 L culture. Cells were grown, harvested and disrupted as in 2.2.2.7. Cell debris was removed in three centrifugations: 2 x 5 min at 1.000 x g, 1 x 5 min at 3.000 x g. The resulting supernatant was centrifuged for 40 min at 20.000 x g, and the resulting pellet was resuspended in 12 ml TAE buffer with protease inhibitor cocktail. The suspension was adjusted to a protein concentration of 5 mg/ml. Under constant mixing on a magnetic stirrer, this suspension was brought to a pH of 5.2 with 1 M sodium acetate. The acidification results in the massive precipitation of mainly mitochondrial membranes. The precipitate was immediately removed by centrifugation for 5 min at 6.900 x g, and the supernatant was quickly adjusted to pH 7.5 with 2.5 M Tris/acetate buffer. Highly enriched plasma membranes were collected by centrifugation for 30

min at 26.500 x g and resuspended in 1-2 ml of 50 mM HEPES pH 7 with protease inhibitor cocktail. The concentration was adjusted to 10 mg/ml and the suspension was snap-frozen in aliquots and stored at -80 °C

2.2.2.9 Protein quantification using the Bradford Assay

The protein content of samples was measured using the Coomassie Plus protein assay reagent kit (Biorad) which is based on the method of Bradford [218]. Samples were taken in several dilutions made with their buffer, and this buffer served as the empty control. Briefly, 10 µl of diluted protein sample or control were pipetted in duplicates into flat bottom, 96well plates and mixed with 200 µl of the assay reagent. The plates were covered for protection against dust, and colour development was allowed for 8 min at room temperature. Measurements were taken on a multiwell plate reader (Polarstar Galaxy) at 562 nm. Multiple serial dilutions of BSA in water were used as a quantitative reference. Only sample dilutions that gave values in the linear area of the BSA reference curve were used to calculate sample protein concentration.

2.2.2.10 Solubilization of BSEP and MDR3

Membrane proteins were solubilized from plasma membrane preparations for the initial affinity purifications of BSEP and MDR3. For the solubilization trials for BSEP and MDR3 from purified plasma membrane purifications, or MDR3 from whole cellular membranes, 300 µl aliquots of the respective membrane preparation at the indicated concentration were brought to their final detergent concentration from 10 % (w/v) freshly made stock solutions (prepared in dd. water) and incubated for 1 h at 4 °C on an overhead tumbler under slow inversion. Insoluble material was pelleted by ultracentrifugation (1 h at 180.000g and 4 °C), and the supernatant was transferred into a reaction tube, while the pellet was resuspended in 300 µl of membrane buffer. Equal volumes of both supernatant and resuspended pellet were then analyzed by SDS-PAGE and Western blot for solubilization efficiency. For the preparative purification of MDR3, whole cell membranes were adjusted to 2 mg/ml with membrane buffer, and Fos-choline was added from a 10 % (w/v) stock solution to a final concentration of 0.5 % (w/v). Membranes were solubilized for 1 h at 4 °C under gentle stirring, and insoluble material was removed by ultracentrifugation (1 h at

180.000g and 4 °C). The supernatant contained the solubilized material and was used for affinity purification.

2.2.2.11 Purification of human MDR3 by IMAC on ÄKTA systems

Buffer A

20 mM Tris/Hcl pH 8

75 mM NaCl

15 % (v/v) glycerol

0.001325 % (w/v) Fos-choline 16

10 mM imidazole

Imidazole stock solution

500 mM imidazole pH 8

(adjusted with NaOH)

Buffer B

Buffer A with

300 mM imidazole

All steps were carried out at 4 °C and with precooled buffers. A 5 ml IMAC column equilibrated in 100mM cobalt chloride was used to purify solubilized MDR3. The supernatant from the Foscholin 16 solubilization was adjusted to 10 mM imidazole and applied to the column at a flow rate of 2 ml/min, and the flow-through was collected. The column was washed with buffer A until a stable baseline was reached, and proteins were eluted in 1 ml fractions in steps of 20, 40, 60, 80, and 100 % (fraction of Buffer B mixed into Buffer A, corresponding to 58, 116, 174, 232, and 300 mM imidazole concentration, respectively).

2.2.2.12 Protein concentration using Amicon filter devices

An 15 ml Amicon spin concentrator with a molecular weight cutoff of 100 kDa was prewetted with dd. water and then preequilibrated with Buffer A by centrifugation at 4000 rpm at 4 °C (Megafuge 1.0R). The sample was concentrated in the equilibrated unit in centrifugation steps of 15 min until the desired concentration was reached. For the preparative MDR3 purification, all fractions from the protein elution peaks 2-4 were pooled and concentrated up to a volume of 250 µl.

2.2.2.13 Gel filtration of affinity-purified MDR3

A Superdex 200 10/300 GL gel filtration column was preequilibrated with buffer A. 100 µl concentrated MDR3 from the affinity purification were applied to the column and eluted with buffer A at a flow rate of 0.2 ml/min. The eluate was collected in fractions of 1 ml.

2.2.2.14 IMAC purification of BSEP and MDR3 with Ni²⁺-NTA slurry

BSEP and MDR3 were purified from purified plasma membranes (see 2.2.2.8) that came from 1 L of cells. The membranes were diluted with purification buffer (50 mM Tris/HCl pH 8, 150 mM NaCl, 10 % (v/v) glycerol). After solubilization (see 2.2.2.10), the supernatant was mixed with 500 µl of 50 % (v/v) Ni²⁺-NTA slurry (Qiagen) that was pre-equilibrated to the purification buffer. The slurry was then batch-loaded for 1 h at 4 °C under gentle agitation, and purification was performed at 4 °C by gravity flow. All further steps involved 2 column volumes of the respective buffers: the gravity-packed column was washed twice (purification buffer + 5 mM imidazole) and elution was in steps of 30, 60, 100, 150, 200, and 300 mM imidazole.

2.2.2.15 Transfection of cell lines with wild type and *Bst*BI-mutated BSEP-eYFP and fluorescence microscopy

pEYFP-N1-*BSEP* was made yeast-compatible as described for pPIC3.5 by addition of an Ori / Leu PCR product made from YEplac3.5 with primer pair OriLeu-pEYFP-*Afl*I-S1 / -S2. The Ori / Leu fragment can be removed completely and without trace by *Afl*I digestion (see above) which was not necessary. HepG2 cells were cultured in Dulbecco's modified Eagle's medium Nutrimix F12 (DMEM-F12; Invitrogen), HEK293 cells were cultured in DMEM and MDCK cells were cultured in MEM with Earle's Salts, each containing 10 % fetal calf serum (PAA, Coelbe, Germany), in a humidified, 5 % CO₂-atmosphere at 37 °C. The indicated *BSEP*-YFP plasmid DNA was transfected using FuGENE HD (Roche) according to the manufacturer's guidelines. For fluorescence microscopy (LSM 510, Zeiss, Oberkochen, Germany) cells were fixed and permeabilized with methanol (100 %, 4 °C, 1 min) and nuclei were stained with Hoechst 34580 (Invitrogen). Cell culture and microscopy was kindly handled by Dr. Claudia Stross (Department of Gastroenterology, Hepatology and Infectiology, Heinrich Heine University Düsseldorf).

3 Results

In this thesis, overexpression of both human BSEP and MDR3 is established in two yeast species as a foundation for future *in vitro* studies. MRP2, that does not express in *P. pastoris* [199], is also found not to express in *S. cerevisiae*. Accordingly, the Results section is divided into two parts that address two central aspects of the *in vitro* theme: the first part consists of the experiments that were necessary to obtain an overexpression of both proteins. The cloning of the corresponding, unstable coding sequences was a major hurdle that had to be solved first. The second part is dedicated to show how these *in vitro* systems can be connected to clinical *in vivo* data of disease-causing mutations in both transporters. For this, mutations need to be transferred quickly between the biochemical and clinical world, e. g. between recombinant expression (for functional studies) and mammalian cell culture systems (cell biology).

3.1 The *BSEP* and *MDR3* cDNA Sequences are unstable in *E. coli*

Expression screening plays an important role in the first steps of recombinant membrane protein expression. Depending on the pursued strategy, an expression screen consists of several expression systems, their vectors, promoters, purification tags and tag positions. In essence, screening involves substantial recombinant DNA work to create the necessary expression constructs. Standard techniques of molecular biology, however, become limiting when working with gene sequences that are unstable in *Escherichia coli*. Several circumstances can account for the fact that a certain sequence is toxic to or unstable in its bacterial host [219,220]. However, comprehensive approaches to create, maintain, and manipulate such a construct are limited, and studies on the actual cloning of such unstable or toxic genes for expression are rare [221]. Unfortunately, both the *MDR3* and *BSEP* cDNA were shown to be unstable in several *E. coli* vectors [174,175,207,222].

Genes and DNA sequences in general can be unstable in their bacterial host for a variety of reasons, including: extensive secondary structure (e. g. z-DNA [223]), inverted or direct sequence repeats, encoding a gene product toxic to host metabolism, or carrying unintended prokaryotic signal sequences [174,224]. A close comparison of the *MDR1* with the *MDR3* and *BSEP* sequences revealed 79 and 49 % DNA sequence identity, respectively (Figure 1), but no obvious reason for the

difference in toxicity, one exception being a cryptic prokaryotic promoter motif within the *BSEP* cDNA that has previously been suggested to destabilize it in *E. coli* [174]. However, silent mutagenesis of this motif as published did not abolish the instability of the *BSEP* coding sequence and was not easily accomplished. Also, reduction of the incubation temperature to 30 °C as described [174] or even to room temperature had no positive effect on any cloning efforts for *BSEP* in *E. coli*.

In essence, the integration of *BSEP* or *MDR3* containing DNA fragments into the expression cassette vectors or any other of many tested commercial or non-commercial plasmids failed, either as blunt-ended PCR products or as DNA fragments resulting from restriction digest. Topo-TA cloning trials were as unsuccessful as the application of several low-copy plasmids for subcloning of the unstable DNA at more tolerable copy numbers.

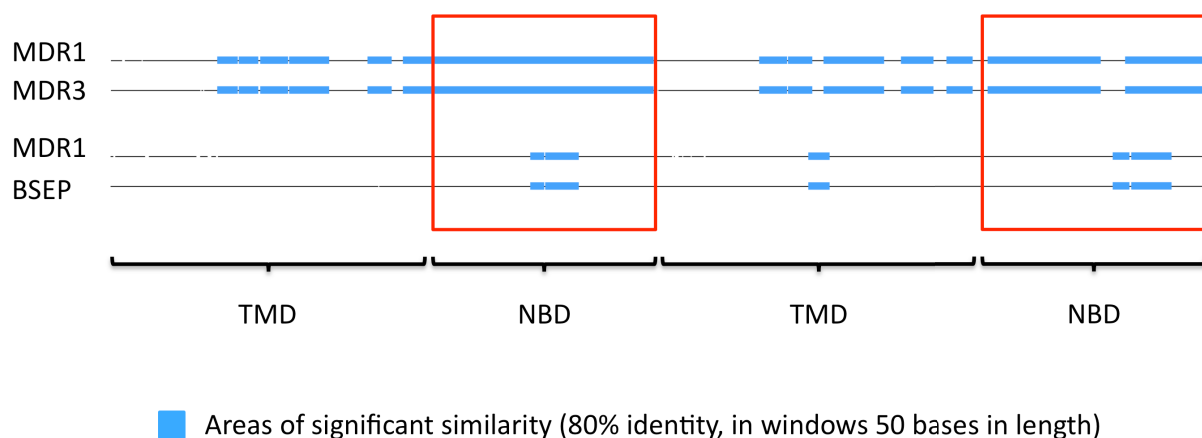


Figure 1. Pairwise assembled sequence alignment of MDR1/MDR3 and MDR1/BSEP. The coding sequences of the human ABC transporters (MDR1, NM_000927.3; Mdr3, NM_000443.2; BSEP, NM_003742.2) were aligned with the Clone Manager Software V.7 (Fast Scan, Maximum Quality, and default algorithm values). The assembled sequence alignment algorithm is used for pairwise comparison of sequences with some similar and some different regions such as ABC transporters (conserved NBDs, divergent TMDs). The significance threshold was set to 80 % identity for display of only significant local homologies. MDR3 is clearly more related to MDR1 (79 % DNA sequence identity) than BSEP (49 %) as significant local sequence conservation is found (blue bars). Not surprisingly, the only significant local homologies to MDR1 are found in the BSEP NBDs (red boxes indicate the corresponding sequences).

In none of these attempts, plasmids containing the full transcripts were obtained, only rarely small fragments of *BSEP* or *MDR3* were contained in the plasmids, with no obvious preference for a certain backbone, restriction site(s) or bacterial strain. The attempt to obtain the desired constructs by stepwise cloning of pieces of both cDNAs also failed, as did efforts to construct plasmids with a *BSEP* insert by ligation-independent cloning (LIC). Because of this instability, the cloning, expression, and mutagenesis of human BSEP and MDR3 remains a tedious and complicated task, and biochemical studies on these ABC transporters in recombinant expression continue to be severely limited: the only heterologous expression of BSEP and MDR3 so far was accomplished in insect cells [174,175,222].

3.2 A Set of Cassette Vectors for the Chromosomal Overexpression of both yeast and non-yeast genes in *Saccharomyces cerevisiae*

There are two basic strategies to overexpress a gene of interest (GOI) in *S. cerevisiae*: either from a chromosomal locus or from a plasmid. Both strategies have mutually exclusive advantages. The biggest advantage of chromosomal expression is the genetic stability: the expression cassette is stably propagated along with its host chromosome upon cell division, without the need of selection agents or chemically defined media allowing the selection of prototrophy markers in order to maintain a plasmid. With chromosomal expression, every cultured cell has the genetic information needed for expression of the recombinant gene. A plasmid on the other hand, is a highly flexible autonomous container of genetic information, that is easily manipulated. It can also be present in several copies per cell, thus increasing the gene copy number from one (chromosomal expression in a haploid *S. cerevisiae* strain) up to 60, depending on the construct used [225,226].

A System of Expression Cassette Vectors for S. cerevisiae

As the N-terminally 14xhistidine (his_{14})-tagged Pdr5 ABC transporter of *S. cerevisiae* could be overexpressed at high level from its native chromosomal locus [186], this setting was also attempted for the expression of BSEP, MDR3, and MRP2. For availability of several types and combinations of affinity tags for protein production and purification, the expression cassette plasmid pRE3 [205] was modified and expanded into a set of several plasmids (Figure 2) that allow to chromosomally tag any *S. cerevisiae* gene of interest (GOI) for homologous overexpression [191], and

also to introduce any foreign GOI into the genome of *S. cerevisiae*. After chromosomal integration, expression is driven from the strong constitutive *PDR5* promoter in the cassette. In the set, several affinity tags are available: a his₁₀ or his₁₄ tag, a his₁₀ / hemagglutinin (HA) tag combination, and a double HA tag. The considerable length of the his₁₄ tag allows for a more stringent washing step during affinity purification, which minimizes co-purification of potential contaminants.

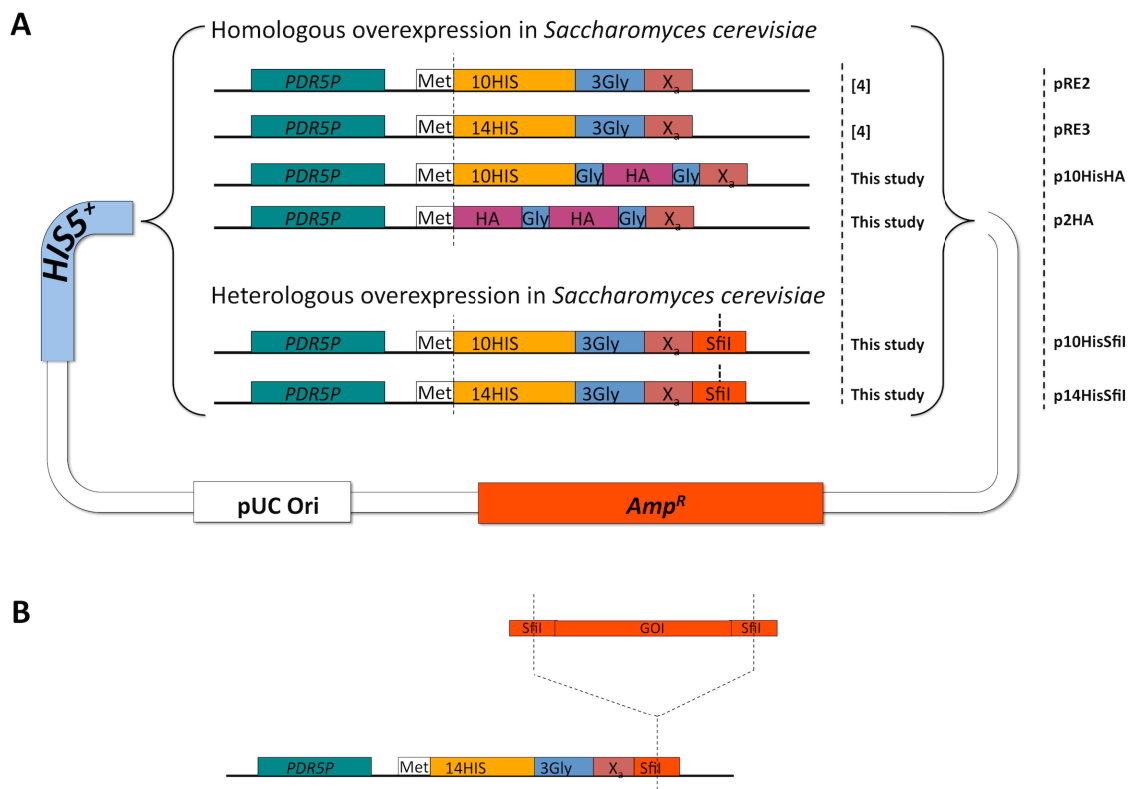


Figure 2. **A system of expression cassette vectors for *S. cerevisiae*.** Two variants are available: a set for the *in situ* tagging of any open reading frame (ORF) in the *S. cerevisiae* genome, and a set for the directed insertion of a non-*S. cerevisiae* gene of interest into the *SfiI* restriction site of the cassette on the plasmid (detail in **B**). In both cases, the expression cassette is prepared for site-specific recombination via PCR-primer-encoded terminal 40 bp overlaps. The tagging cassettes are then put upstream in frame to the *S. cerevisiae* gene of interest, while the expression cassette containing the non-*S. cerevisiae* GOI is recombined into the targeted locus. Successful integration results in histidine prototrophy of the transformants (*HIS5*⁺). In this study, a custom-designed strain with a modified *PDR5* locus was used [186].

All affinity tags are designed to be flexible via insertion of a short linker: a stretch of three glycines prevents interference with protein folding by random steric obstruction and assures accessibility to their respective ligand during affinity purification. The sequence encoding these features was introduced by ligation of one synthetic double-stranded oligonucleotide per construct downstream of the *PDR5* promoter into pRE2 [205]. For directional cloning of a GOI into the cassette, a *SfiI* restriction site was inserted downstream of the his₁₀ or his₁₄ tag on the p10- or p14His*SfiI* plasmid. The directional cloning of a DNA fragment is possible because the Type IIs restriction endonuclease *SfiI* recognizes a non-palindromic sequence (5'-GGCCNNNN↓NGGCC-3', N for any nucleotide) [227]. To adapt the pRE2 plasmid to the *SfiI* cloning strategy, a *SfiI* restriction site in the backbone was removed by silent mutagenesis. While directional cloning with a single restriction site is a very convenient method, it has been reported that *SfiI* requires two recognition sites *in cis*, i. e. on the same plasmid for efficient digestion as two sites are bound and cut simultaneously by this enzyme [228]. To evaluate the efficiency of the *SfiI* cloning step with a single site *in cis*, a small insert of about 500 bp was cloned that contains the beta galactosidase gene along with its promoter (Figure 3A). As small fragments ligate much more efficiently due to cloning bias of size [229], nearly all properly *SfiI*-cut plasmids are expected to receive an insert, and only religated or uncut plasmids will result in the formation of white colonies after transformation. To minimize background due to religation of the single-cut plasmids, their free ends were dephosphorylated. In essence, the amount of ligation mirrors the amount of digestion. The ligation efficiency was then determined by blue-white screening of the resulting transformant colonies (Figure 3A). The digestion of the p14His*SfiI* vector was found to be almost complete as judged from the screening plate that shows almost exclusively blue (insert present = was properly digested) and only few white bacterial colonies (undigested or religated). Next, the cloning efficiency of the large (4700 bp) *MRP2* cDNA was tested. Ten clones resulting from transformation of a 1 h ligation with equimolar amounts of vector and insert were picked and analyzed. Nine out of ten carried the correct plasmid as established by *XhoI* restriction digest, which only cuts once and within the *MRP2* insert. This demonstrates the efficient insertion of DNA with compatible ends into the p14His*SfiI* vector (Figure 3B).

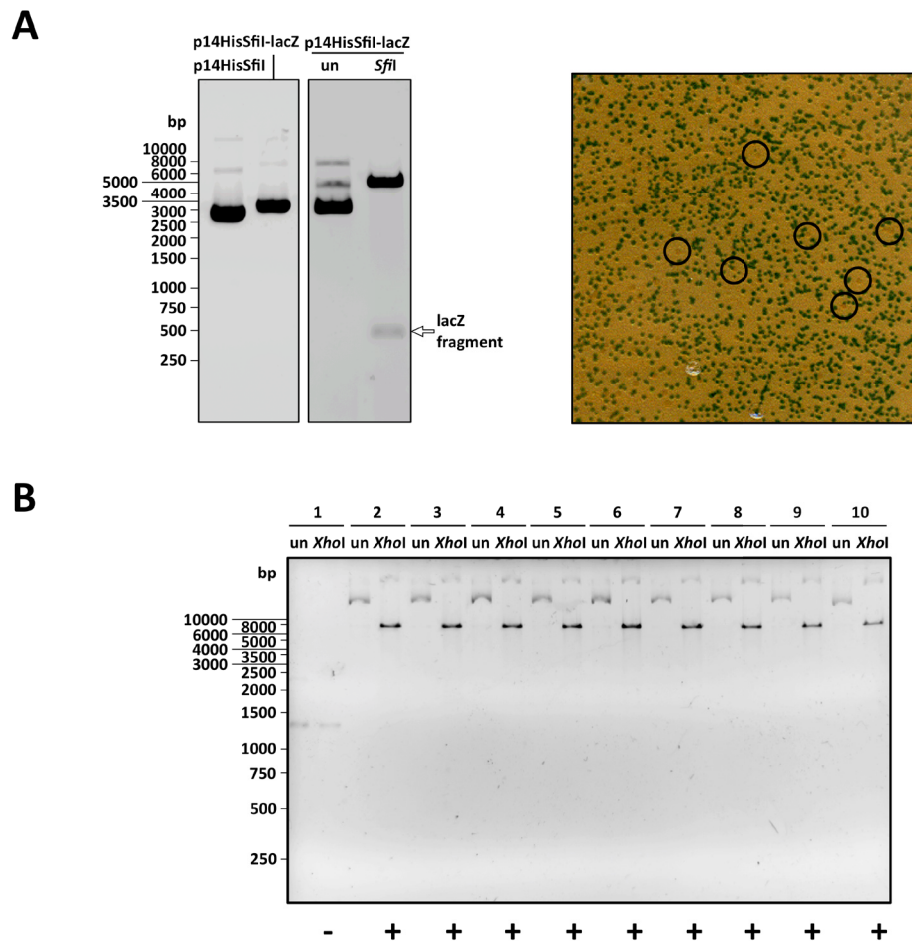


Figure 3. Proof of concept for the *SfiI* cloning strategy with the expression cassette vector p14HisSfil. **A, left panel A fragment containing the *lacZ* gene and promoter from *E. coli* ("lacZ fragment") was directionally cloned into the *SfiI* restriction site on p14HisSfil. **Right panel** *E. coli* cells capable of blue/white screening (XL1blue) were transformed with a ligation reaction containing the dephosphorylated *SfiI*-cut vector with an equimolar amount of a lacZ fragment carrying compatible *SfiI* cohesive ends. Black circles denote examples of white colonies. **B** *SfiI*-based cloning of the *MRP2* cDNA. This proof of concept shows that even without a second *SfiI* restriction site *in cis* (= on the same plasmid), the p14HisSfil vector can be efficiently digested by this type II_S enzyme. un, undigested; *XhoI/SfiI*, digested with the respective restriction enzyme.**

The use of the *SfiI* site is based on the analysis of all human ABC transporter coding sequences (Figure 4A). The analysis shows that the vast majority (77 %) of all cDNA variants do not contain any, and only few (23 %) contain one or more *SfiI* recognition sites. From the 1024 ((4 bases)^(5 nucleotide positions)) possible *SfiI* recognition sequences 64 ((4 bases)^(3 nucleotide positions)) different cohesive ends can originate that often would

be different from the one used on the p10- and p14HisSfil plasmids. Even a cleaved ABC gene could then properly religate with itself and the vector backbone in the correct order. However, ligation efficiency also decreases with the number of participating fragments [229], and the *MRP2* cDNA was one of the few transcripts to contain a (different) *Sfil* site that interfered with its efficient cloning. It was removed by silent mutagenesis (Figure 4B).

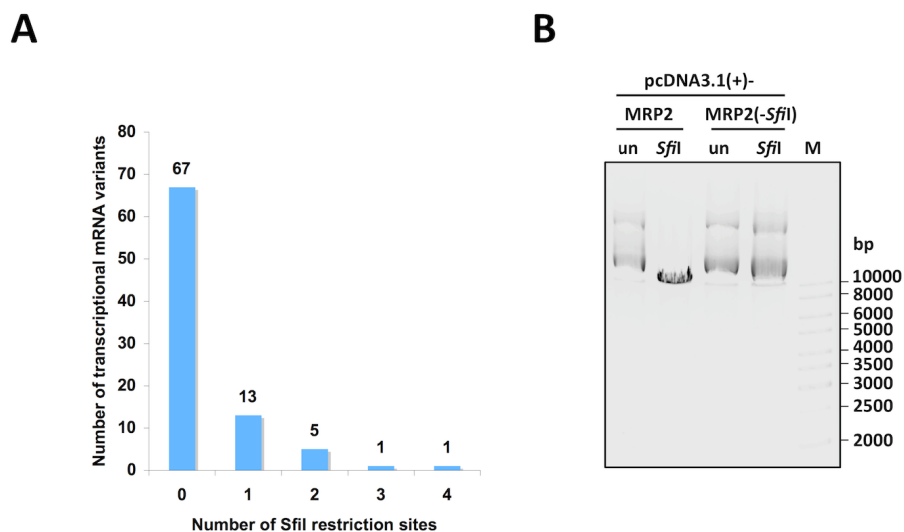


Figure 4. The *Sfil* cloning strategy. **A** *Sfil* restriction site frequency in the 87 transcriptional mRNA variants of the 49 human ABC genes. The majority of the predominant variants carries no *Sfil* site and can readily be inserted into the custom expression cassette plasmid as a *Sfil*-digested PCR product. **B** The *MRP2* cDNA is one of few human ABC protein transcripts containing a *Sfil* restriction site. It was removed via silent site-directed mutagenesis.

Integration of the MRP2 Expression Cassette into the Chromosomal PDR5 Locus of S. cerevisiae

After generation of the *MRP2* cassette plasmid (p14HisSfil-*MRP2*, Figure 3B) and sequence verification of the complete expression cassette, the latter was amplified with overlap-containing primers that target the *PDR5* locus on chromosome XV of *S. cerevisiae* (Figure 5). The yeast strain used for expression has two important characteristics: the *pdr1-3* transcriptional *gain of function* mutation that turns the

strong, but highly regulated *PDR5* promoter into a constitutive promoter, and the deletion of both this promoter and the *PDR5* structural gene from the chromosomal locus by its replacement with a tryptophan prototrophy cassette [186]. Due to the latter deletion the strain was designated Δ PP. The removal of the *PDR5* promoter is necessary to avoid interference with the *PDR5* promoter on the cassette during homologous recombination.

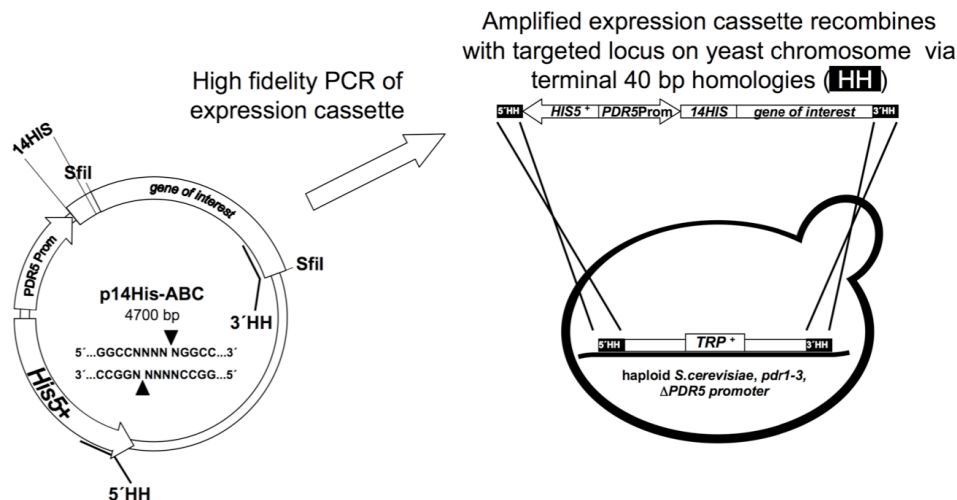


Figure 5. Targeting of the chromosomal *PDR5* locus of *S. cerevisiae*. The cassette vector (p14His*SfiI*-*MRP2*) serves as the template used for amplification of the expression cassette containing the gene of interest. Here, the target locus for integration can be chosen by design of the 40 base pair long homologies on the primers used to amplify the cassette. *S. cerevisiae* is then transformed with the expression cassette and transformants are selected on minimal medium via the *His5⁺* prototrophy marker.

As shown in Figure 6, human *MRP2* expression could not be detected in whole cell lysates of yeast transformants with two different antibodies. The polyclonal *MRP2* antiserum MLE (used in Figure 6A) was raised against a synthetic oligopeptide comprising the N-terminal 26 amino acids of the protein [201]. To exclude possible interference by the fusion of the N-terminal *his*₁₄ tag and linker sequence to this epitope with its immunodetection, the samples were reprobated with a second *MRP2* antibody, the monoclonal mAb M₂III-6 (Figure 6B) [202]. Three control lysates from liver samples (kind gift of Dr. Verena Keitel) were included as a positive control for *MRP2* and showed an immunoreactivity of approximately 180 kDa, which corresponds to the glycosylated form of *MRP2* (Figure 6A and B, lanes 1 to 3).

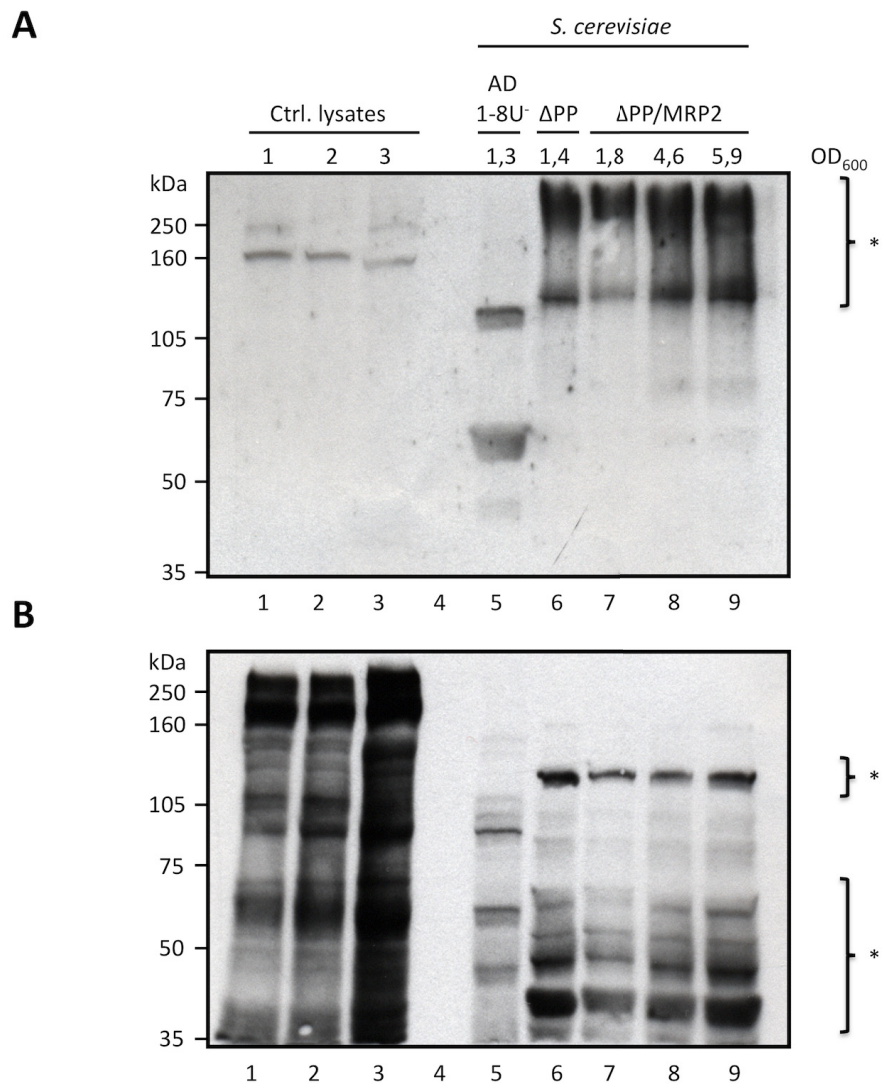


Figure 6. Expression of human MRP2 is not detected in *S. cerevisiae*. Equal amounts of whole cell lysates from small-scale liquid yeast cultures of the indicated optical density (OD) were separated on an 8 % SDS gel and electroblotted. **A** Western blot detection with the polyclonal anti-MRP2 antiserum MLE [201]. **B** Stripped membrane from A reprobed with the monoclonal MRP2 antibody M₂III-6 [202]. *Cross-reactivity.

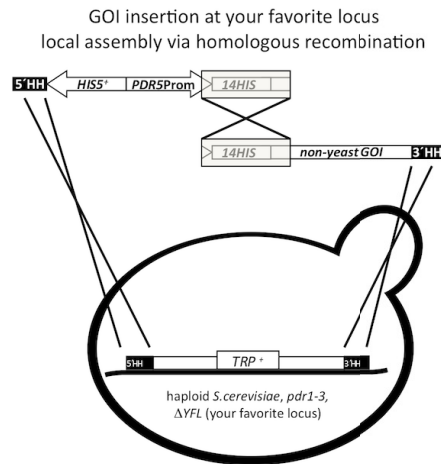
In a previous study on the close homologue MRP1, expression of the human transporter was detectable in *S. cerevisiae* throughout the exponential phase of growth [184]. Accordingly, a liquid yeast culture of a yeast clone with a fully sequence-verified recombinant *PDR5/MRP2* locus was used to sample MRP2 expression at corresponding culture densities (Figure 6A and B, lanes 7 to 9). Both antibodies show a marked signal at a molecular weight of about 150 kDa that might

be mistaken as MRP2-specific, since underglycosylation of MRP2 in *S. cerevisiae* could be anticipated from previous studies [182,184]. The high molecular weight of the native protein, in contrast, results from its substantial glycosylation [230]. However, the same quality and quantity of immunoreactivity was found in the empty parental Δ PP strain (lane 6), indicating lack of MRP2 expression. Since MRP-type ABC transporters are also found in *S. cerevisiae*, one or more of these membrane proteins could cross-react with both antibodies due to sequence conservation. This was confirmed by testing a whole cell extract from strain AD1-8U⁻ [192], which lacks the yeast ABC transporter genes *YOR1*, *SNQ2*, *PDR5*, *PDR10*, *PDR11*, *YCF1*, and *PDR15* (as well as the transcription factor gene *PDR3*). Here, the signal found in the Δ PP background from 150 kDa upwards was not detected (Figure 6A and B, compare lanes 5 and 6 to 9). In summary, the N-terminally his₁₄-tagged human MRP2 could not be expressed in *S. cerevisiae*.

3.3 Expression in *S. cerevisiae* of the Human Bile Salt Export Pump and Multidrug Resistance Protein 3 by Use of Homologous Recombination

While the human *MRP2* cDNA could readily be cloned into the expression cassette, this was not the case for the unstable coding sequences of BSEP and MDR3. Their insertion into the designed expression cassette plasmids either by *Sfi*I-based or any other means of bacterial cloning was ultimately unsuccessful. Instead, the expression cassette was constructed at the *PDR5* locus by employing a "local assembly" strategy (Figure 7). Here, the two parts of the cassette that could not be spliced together by conventional cloning were combined *in vivo* by multiple homologous recombination (HR; Figure 7A): the *HIS5*⁺ prototrophy marker, *PDR5* promoter, start codon and his₁₄ tag on one, and the coding sequence on the other segment. Both parts were generated by high fidelity PCR, adding 40 (termini) or 60 (overlap of both) bp of sequence overlap for HR. Only the combination of both fragments resulted in formation of transformant colonies on the Dropout-HIS agar plates, which select for the capability of the transformants to grow in the absence of histidine (Figure 7B).

A



B

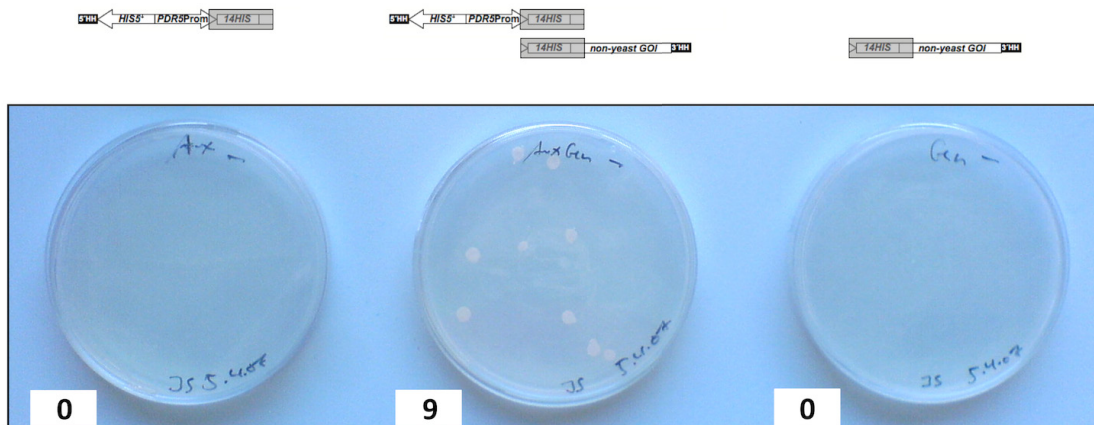


Figure 7. The homologous recombination-based, "local assembly" strategy leads to recombinant *S. cerevisiae* expression strains for human BSEP. **A** Two fragments are generated via PCR, carrying overlaps (40 bp) to both up- and downstream chromosomal sequence targeting the chromosomal locus of choice (YFL, Your Favorite Locus). Both fragments are also made to overlap with each other (60 bp) to allow HR-mediated joining. **B** Actual experiment of A carried out for human BSEP. Competent *S. cerevisiae* cells were transformed with either one or both of the expression cassette fragments and plated onto Dropout-HIS agar plates. Only the combination of both fragments (middle) leads to the formation of colonies of histidine-prototrophic transformants.

Importantly, the fragment carrying the histidine prototrophy marker could not integrate by itself (left side) due to the *PDR5* promoter and gene deletion in the Δ PP strain. This "local assembly" strategy, which entails a triple homologous crossing-

over event, allowed for the generation and analysis of *S. cerevisiae* strains that express human BSEP and human MDR3 (Figures 8 and 9). Both *BSEP* and *MDR3* transformants were tested for the correct local assembly of the complete expression cassette by colony PCR: primer pairs were used that generate PCR products overlapping all *de novo* formed junctions (Figure 8A). All nine BSEP clones (the same as from Figure 7) and three arbitrarily picked MDR3 clones showed the correct product for each of the three junctions (front, junction, back) thus proving the correct cassette generation on the chromosome.

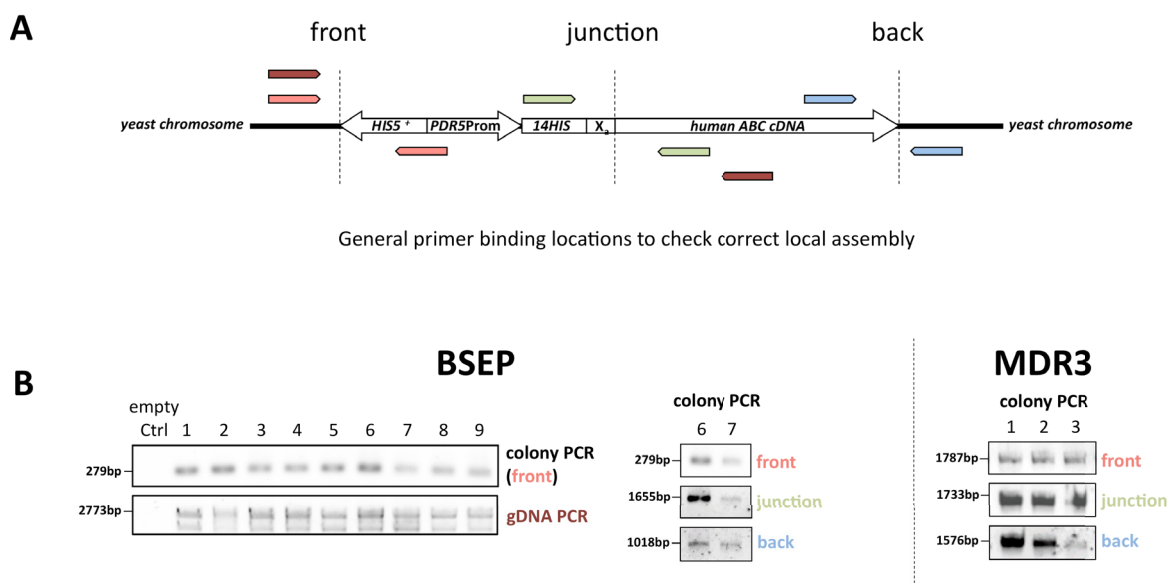


Figure 8. Genetic analysis confirms the successful "local assembly" of the *BSEP* and *MDR3* expression cassettes. **A** Cartoon of the chromosomal recombinant PDR locus carrying the recombinant expression cassette. Primer pairs are colour-coded. The exact primer binding sites are not indicated as these vary for BSEP and MDR3. Instead, the general priming location relative to the three covalent recombinant junctions (indicated by the broken lines) is shown. Each primer pair product spans at least one of these junctions and is only generated (and then at the expected size) if correct recombination at these sites has taken place. **B** Using primer pairs corresponding to the colour-coding in A, all tested *S. cerevisiae* transformants yield PCR products of the expected size and thus show the correct local assembly of the expression cassettes containing either the unstable *BSEP* (left panel) or *MDR3* cDNA (right panel).

Western blot analysis of these clones showed a signal at approximately 130 kDa for both BSEP and MDR3 (Figure 9), which is considerably smaller than the 160 kDa of the native proteins coming from human cell lines [176,177]. However, this is expected given the fact that the closely related MDR1 of the same polypeptide length as both was found to be only core-glycosylated in *S. cerevisiae* and thereby migrate at 130 kDa [182] while having a native apparent molecular weight of approximately 190 kDa in human cells [231]. A clear difference can be seen between the immunodetection of BSEP and MDR3: the *polyclonal* rabbit BSEP antiserum K24 [174] shows several signals at various apparent molecular weights that are unspecific cross-reactions, because they also occur in the control lane with whole cell lysate from the empty parental *S. cerevisiae* strain (Figure 9, left panel, compare clones 1 to 9 and empty control, also middle panel).

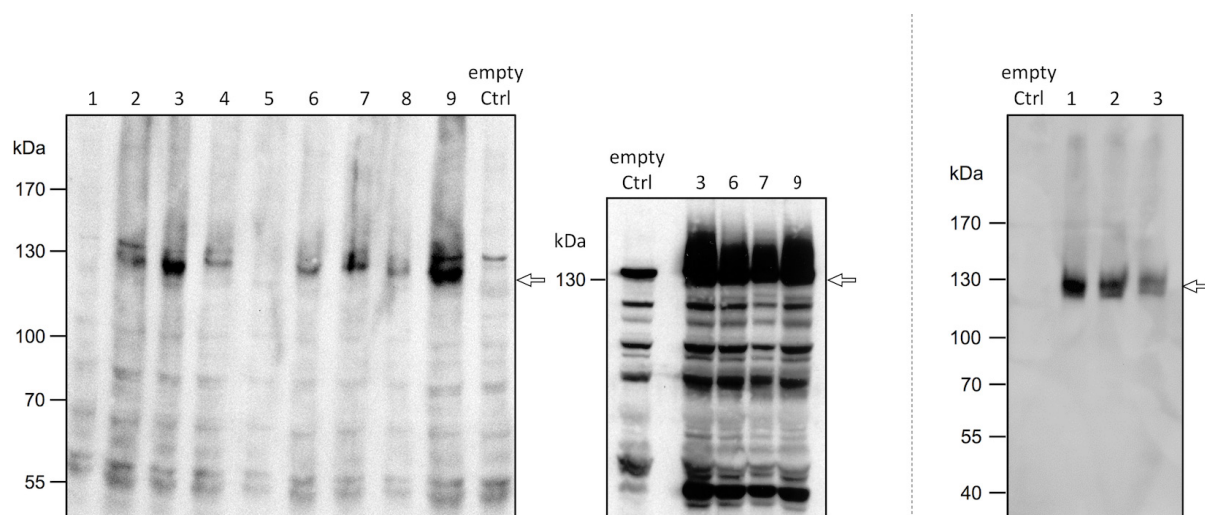


Figure 9. The "local assembly" strategy leads to the first heterologous expression of human BSEP and MDR3 in *S. cerevisiae*. Western blot analysis of *S. cerevisiae* whole cell lysates harvested in the early log-phase (OD_{600} of 1) showed the constitutive expression of BSEP (with the polyclonal rabbit antiserum K24 [174]) and MDR3 (with the monoclonal antibody C219 [232]). **Left panel** All nine obtained BSEP clones were tested, and at least five of these express the human membrane protein (clone 2, 3, 6, 7, 9). Clones 3, 6, 7, and 9 were reprobbed for expression with light sensitive film material. **Right panel** Three arbitrarily picked clones of more than 50 obtained from transformation were tested for correct cassette assembly (B, right panel) and showed MDR3 expression.

In contrast, the *monoclonal* P-glycoprotein antibody C219 [232], which detects a stretch in the first NBD conserved in both MDR1 and MDR3, showed only a single band of the full-length protein (right panel).

Not all clones, however, seemed to express BSEP, and those which did, seemed to do so at varying levels (Figure 9, left panel, clones 2, 3, 6, 7, 9). This variation was probably the result of partial protein loss during sample preparation (for details on this and a subsequent modification of the corresponding protocol, see Materials and Methods 2.2.2.1). To clear this issue, the Western blot was repeated for the four expressing clones 3, 6, 7, and 9 from fresh *S. cerevisiae* cultures (Figure 9, middle panel), and all four clones were now found to express BSEP at similar levels. Several confirmed expression clones were checked for the sequence integrity of the expression cassette. In all cases except one, the obtained sequence of the complete chromosomal expression cassette was found to completely replicate the *in silico* constructed sequence. The MDR3 clone 3 carried a missense mutation that resulted in an amino acid substitution from methionine to isoleucine at position 800. Unless stated otherwise, BSEP clone 9 and MDR3 clone 2 (carrying the wild type sequences) were used for all subsequent studies on the chromosomally expressed transporters.

Since the expression cassette could rapidly be generated by multiple homologous recombination *in vivo*, this "local assembly" strategy qualified as a suitable alternative to attempts of conventional cloning of the unstable BSEP and MDR3 cDNAs for expression. Judging from the Western blot signals, however, the expression levels were quite low and therefore insufficient for purification and biochemical studies. Several reasons for this were considered or excluded: I) The N-terminal his tag demanding fourteen consecutive histidines could, under conditions of high translational activity, lead to the local depletion of tRNAs carrying histidine so that the ribosome stalls and subsequently translation into protein is abrogated (a quantitative study of this phenomenon found in [233]). This seems unlikely as the same his tag configuration in the same cassette allowed a dramatic Pdr5 overexpression [186]. Accordingly, the tag has been designed using both available histidine codons (CAC and CAT) in alteration to balance codon usage. II) The N-terminal his tag position could lead to mistargetting of the protein. Therefore, C-terminally tagged versions of both BSEP and MDR3 would be of closer interest. Human MDR1 has been successfully overexpressed with a C-terminal his₈ tag to

purifiable amounts [182]. Importantly, this MDR1 fusion protein conferred a cellular multidrug resistance phenotype, indicating at least a partial localization to the *S. cerevisiae* plasma membrane for its proper function. III) The proteins are intrinsically unstable or mistargeted in the *S. cerevisiae* environment and thus rapidly turned over, leading to low levels of detected expression. As both MDR3 and BSEP are detectable at their full molecular weight, they are expected to reside in a membrane environment and thus to be folded properly. In essence, mistargeting due to an unfavourable his tag position or a general sequence incompatibility (e. g. codon usage [234]) remained as two possible reasons for the unsatisfactory expression levels of BSEP and MDR3. An obvious solution was the shift of the his tag to the C-terminus of the fusion protein. If this is unsuccessful, an increase in gene copy number may help to increase protein yield [200,235].

3.4 Expression of BSEP and MDR3 from Plasmid in *S. cerevisiae*

The impact of his tag position and copy number can be studied by the direct expression of both tag configurations from a multicopy plasmid: chromosomal (single copy) and plasmid-based (multicopy) expression of the very same tag configuration can then directly be compared. At the same time, expression of the two tag configurations from the same expression vector can be tested. For these reasons, *BSEP* and *MDR3* expression vectors were constructed with both his tag configurations by direct homologous recombination in *S. cerevisiae*. Homologous recombination-based plasmid construction in *S. cerevisiae* has been well-documented [236,237,238]. In general, *S. cerevisiae* can rely on sequence overlaps as short as 20 base pairs (bp) to generate a selectable circular plasmid from one, two, or several fragments after transformation. This is used to easily shuffle large fragments between constructs [237,238,239]. Next to the "local assembly" strategy, this method is another convenient way to circumvent cloning in *E. coli*. It allowed the rapid construction of a set of plasmids expressing N- and C-terminally his-tagged wild-type BSEP or the V444A allele of BSEP (Figure 10). The V444A allele has been described as both a natural allelic variant and a clinically relevant mutation that has been associated with drug-induced cholestasis and reduced BSEP protein levels [146,222,240,241]. V444A BSEP constitutes the first non-wild type BSEP variant expressed in *S. cerevisiae*. The YEpHIS expression vector was chosen because the

BSEP and MDR3 homologue MDR1 (human P-glycoprotein) could functionally be overexpressed from this construct in *S. cerevisiae* [182] as well as human MRP1 [184], a close relative of MRP2 from the same ABC transporter subfamily (ABCC). For clarity, it is referred to as YEpCHIS throughout this work.

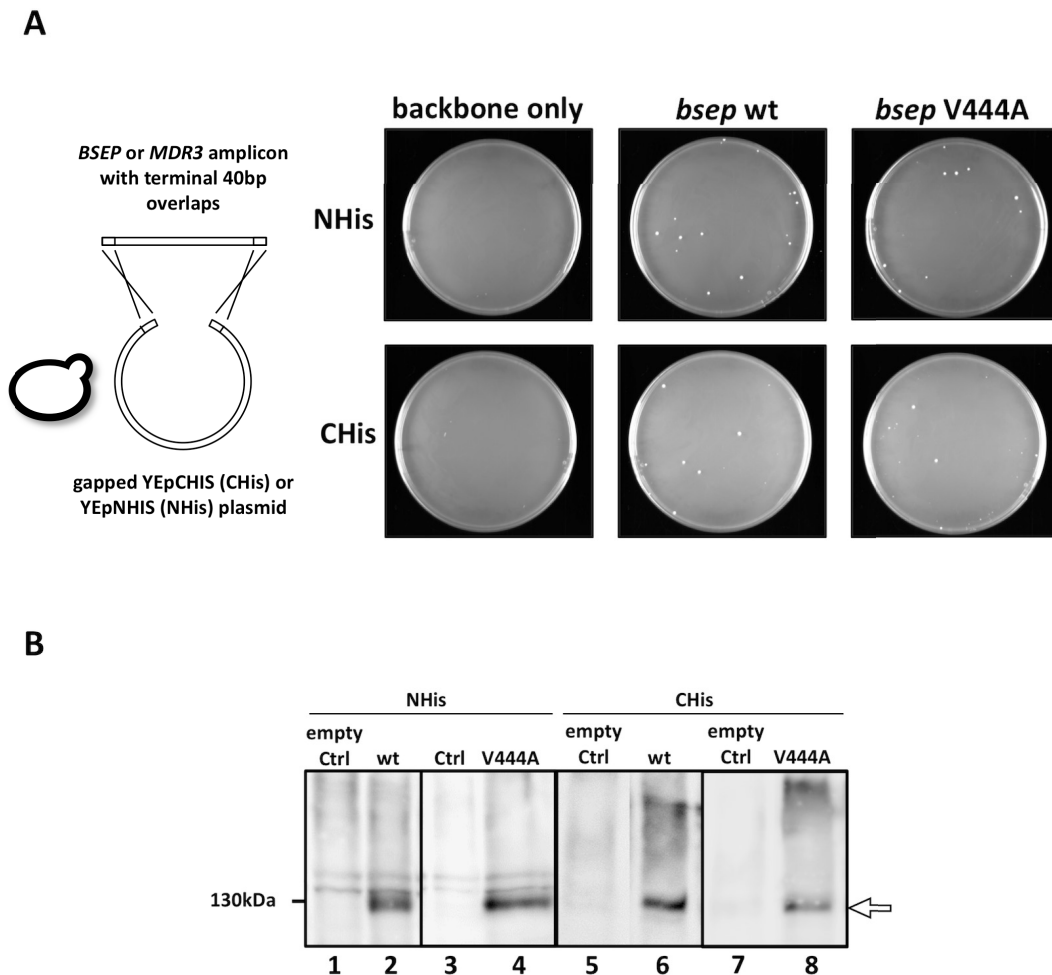


Figure 10. Plasmid-based expression of two human BSEP variants in *S. cerevisiae*. **A, left panel** Homologous recombination was used to construct the unstable *BSEP* expression vectors in *S. cerevisiae*. **Right panel** The gapped plasmid backbone and *BSEP* PCR products carrying 40 bp terminal overlaps were co-transformed into competent *S. cerevisiae* cells. Only Co-transformation of both backbone and insert resulted in transformant colony formation. **B** Resulting transformants were picked and directly used to screen the expression of BSEP from small-scale, mid-log liquid cultures. Equal amounts of whole *S. cerevisiae* cell extracts were resolved on SDS gels, electroblotted and probed with the polyclonal BSEP antiserum K168 [203]. NHIS / CHIS, N- or C-terminal his tag position; empty Ctrl, strain transformed with the corresponding empty expression plasmid.

Since the original YEpHIS vector exclusively encodes a C-terminal his₈ tag, a version of this plasmid with a N-terminal his₁₄ tag followed by a 3 x glycine linker and a factor X_a protease cleavage site was constructed and designated as YEpNHIS. The gapped plasmid backbone of both tag variants was then co-transformed into *S. cerevisiae* with a PCR product of the coding insert with terminal 40 bp overlaps (Figure 10A, left panel). Since under selection only the circular plasmid is propagated, only recombinants with the insert survive (Right panel). The transformants obtained were analyzed by Western blot from small-scale liquid cultures, and Figure 10B shows the expression of both wild-type and V444A variant BSEP from representative clones. All four recombinant BSEP variants were found to express roughly in similar amounts (lanes 2, 4, 6, and 8). More importantly, however, both tag positions did not differ in terms of expression levels. The only observable difference was that the C-terminally his₈-tagged fusion proteins (lanes 6 and 8) seemed to give a slight high molecular smear that was less pronounced in the lanes with the N-terminally tagged BSEP variants (lanes 2 and 4). From this comparison it could be concluded that the position of the polyhistidine affinity tag is not the limiting factor in the low BSEP expression levels.

Expression of N- and C-terminally His-tagged MDR3 from plasmid in S. cerevisiae

In analogy to BSEP, both MDR3 tag variants were constructed based on the YEpHIS and YEpNHIS construct. In order to facilitate a direct discrimination between the impact of the tag position and the impact of gene copy number (chromosomal versus plasmid-based expression), chromosomally expressed N-terminally his₁₄-tagged MDR3 was included on the Western blot (Figure 11). For a proper comparison, the corresponding *S. cerevisiae* strain was grown in the same synthetic complete medium as the plasmid-based expression strains, with the difference that an appropriate amount of leucine was included that was left out in the other media for plasmid selection.

As seen for MDR3 expressed from the YEp plasmids (Figure 11), the tag position seems to be a vital determinant of its expression levels in *S. cerevisiae* as the N-terminal tag variant (lane 3) expressed much less than the chromosomal version of the same tag configuration and length (lane 2). The C-terminal tag variant

on the other hand (lanes 4 and 5 show two arbitrarily picked clones) expressed to levels comparable with MDR1 (lane 6). The direct comparison of expression levels between the chromosomal, single copy N-His and the plasmid-based, multicopy C-His version of human MDR3 showed a roughly two- to threefold difference of expression in favor of the latter.

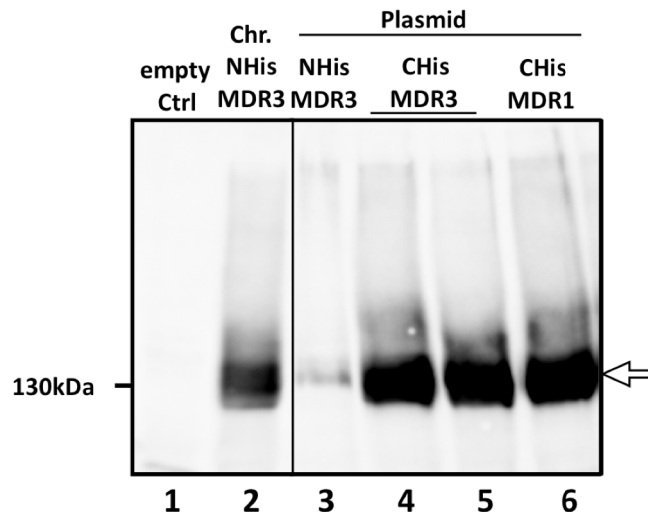


Figure 11. Plasmid-based expression of human MDR3 in *Saccharomyces cerevisiae*. As in Figure 10, MDR3 expression vectors were constructed by homologous recombination from the YEpHIS and YEpNHIS plasmids. Equal amounts of whole *S. cerevisiae* cell extracts from mid-log growth phase liquid culture were resolved on SDS-PAGE, electroblotted and probed with the monoclonal C219 P-gp antibody that detects both MDR1 and MDR3 P-glycoproteins. Chr., chromosomal expressio; NHis / CHis, N- or C-terminal his tag position; empty Ctrl, strain transformed with empty YEpHIS expression plasmid.

In summary, the shift from chromosomal to plasmid-based expression showed that the low BSEP expression was not alleviated by a change of the his tag position. For MDR3, the tag position has a pronounced influence on protein levels. In comparison to the chromosomal, N-terminal his₁₄ tag fusion protein, the same tag configuration from plasmid resulted in a drastic decrease of detectable MDR3, while the C-terminally his₈-tagged MDR3 expressed about two- to threefold better.

In light of these findings a direct comparison between both MDR3 and BSEP expression levels became interesting: how great is the difference in expression between the both in *S. cerevisiae* or, more specifically, is the MDR3 P-glycoprotein expressed much better, perhaps as it is more closely related to the well-expressing MDR1 than BSEP? The C219 antibody does not recognize human BSEP in *S. cerevisiae* (own observation). Instead, the protein levels of recombinant human BSEP and MDR1 in *S. cerevisiae* with the same his tag position and length that were expressed from the same construct (YEPhIS) were analyzed with a his tag antibody (Figure 12). BSEP (lane 3) was found to express at a much lower level than MDR1 (lane 2). Since MDR1 and MDR3 are expressed at roughly the same amount (see Figure 11), this means that the BSEP expression is also much lower than that of MDR3. This direct comparison of MDR1 and BSEP yields showed the clear need for further optimization of BSEP expression conditions in *S. cerevisiae*.

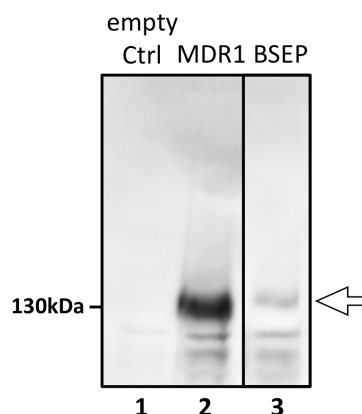


Figure 12. Direct comparison of MDR1 and BSEP expression in *S. cerevisiae*. Human BSEP is much less expressed in *S. cerevisiae* than human MDR1. Equal amounts of whole *S. cerevisiae* cell extracts from mid-log, small-scale liquid culture expressing C-terminally his₈-tagged MDR1 or BSEP were probed with a monoclonal anti his tag antibody. As in Figure 7, all shown lanes come from the same blot membrane and detection. Irrelevant lanes have been omitted for the sake of clarity.

3.5 A Recombination-Based Expression Plasmid Screen for BSEP

Since recombinant BSEP expression in *S. cerevisiae* was, irrespective of the affinity tag position, shown to be inadequate for further biochemical or structural studies, other ways of increasing protein yield were explored. To test the impact of different promoters, an expression screen was developed that addressed the following requirements:

I) A set of different (strong, weak, inducible, repressible) promoters was to be tested against both available terminal affinity tag positions. For subsequent cost-effective purification, a short, his₆ tag was chosen that could easily be encoded on either of the overlap-containing primers.

II) It must, as all previous successful efforts to clone BSEP, be as independent of *E. coli* usage as possible in order to circumvent the problems encountered when working with the unstable *BSEP* coding sequence.

Recovery of the Unstable BSEP and MDR3 Plasmids from S. cerevisiae

Plasmids generated in *S. cerevisiae*, as was done for *BSEP* and *MDR3*, can be recovered from yeast cells [212]. For lysis to occur, the rugged outer cell wall is either disrupted by mechanical force (vortexing with glass beads) or by treatment with a cell wall-digesting enzyme mix such as zymolyase or lyticase. Then the *S. cerevisiae* cells are subjected to a standard alkaline lysis procedure just as *E. coli* [212], yielding plasmid of sufficient quantity and purity. As plasmid copy number in *S. cerevisiae* is generally much lower than in *E. coli* [225,226], larger culture volumes are required to partially compensate for this difference [212]. From a 1 L overnight yeast culture, several micrograms of plasmid can be purified. For comparison, a 100 ml overnight bacterial culture can easily yield 100 micrograms of a multicopy plasmid.

The *BSEP*- and *MDR3*-containing YEp vectors were recovered from *S. cerevisiae* and used to transform several *E. coli* strains (DH5alpha, DH10b, XL1blue, XL10Gold, S.U.R.E., S.U.R.E.2). It was found that all tested bacterial strains could maintain the intact vectors stably as long as the incubation temperature was strictly kept at the permissive temperature of 30 °C [174]. At 37 °C none of the constructs could be stably propagated. As in previous attempts to construct *BSEP* and *MDR3* plasmids in *E. coli*, the lowered temperature was kept at every step following the heat shock used for transformation, including the regeneration phase in antibiotic-free

medium. Figure 13 shows the plasmid recovery of the YEpHIS constructs with the *MDR1*, *BSEP* (V444A), and *MDR3* insert, respectively, in XL1blue *E. coli* cells. The YEpHIS vector is maintained by ampicilline selection in bacteria. The much slower hydrolyzing beta-lactam carbenicilline was used to ensure a tighter selection pressure on the bacteria for better maintenance of the intact plasmid during the prolonged time of incubation. Additionally, the transformed bacteria were strictly cultured under low salt conditions. The integrity of the constructs could in all cases be verified by DNA sequencing. Only rarely (about one in ten), clones were picked that carried single random point mutations.

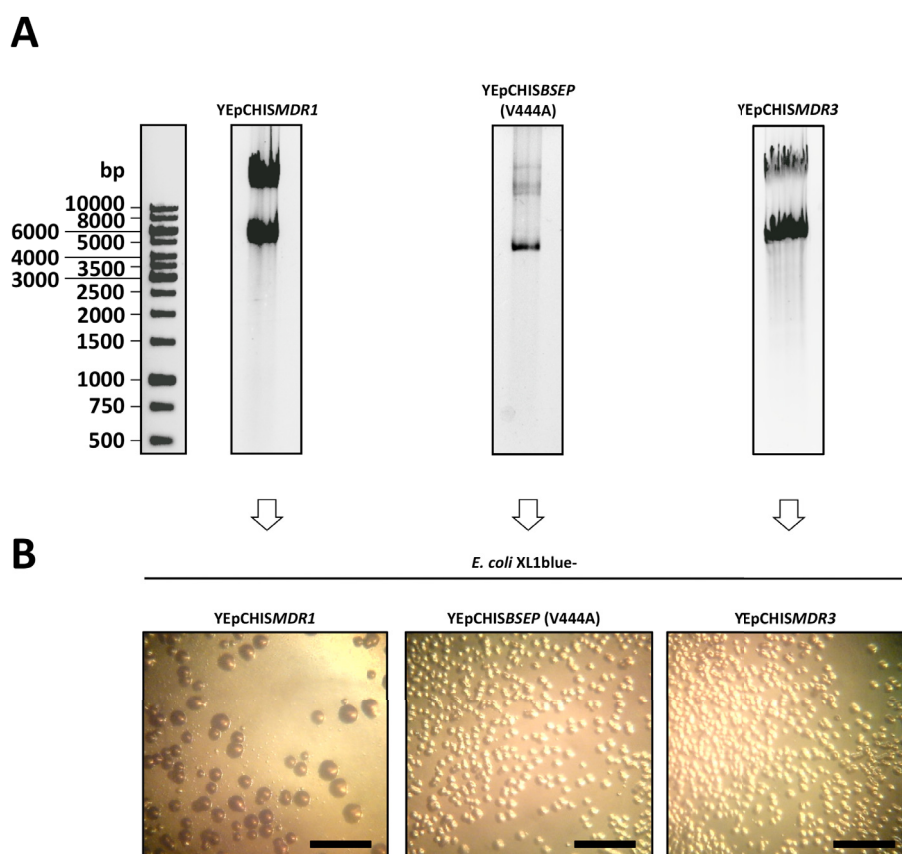


Figure 13. Intact toxic *BSEP* and *MDR3* plasmids can be recovered from *S. cerevisiae* and propagated in *E. coli* under suitable conditions. **A** Analytical agarose gel of the plasmid preparation coming directly from *S. cerevisiae*. **B** *E. coli* XL1blue cells were transformed by heat shock with the preparations from A and grown at 30 °C on low salt LB agar plates containing carbenicillin, and pictures were taken after incubation for 48 h. *BSEP*- and *MDR3*-containing plasmids result in slower bacterial growth than *MDR1*. Black bars = 0.3 mm.

At this point, it should be noted that, although some groups have ultimately succeeded in creating full-length human *BSEP*, their generation in *E. coli* has never been a straightforward, let alone quick procedure due to the reported instability of the *BSEP* cDNA [174,207]. It could be observed that the bacterial colonies resulting from *BSEP* and *MDR3* plasmid transformations are slow-growing in comparison to the closely related, stable and non-toxic *MDR1*-containing YEpHIS plasmid, indicating that *E. coli* is impaired by the presence of *BSEP* and *MDR3* coding sequences (Figure 13B).

Screening of BSEP Expression in S. cerevisiae: a Two-Step Strategy for the Generation of Unstable Plasmids

Combining *in vivo* homologous recombination to first generate and plasmid recovery to then amplify the intact toxic *BSEP* constructs in *E. coli* at 30 °C, a rapid *BSEP* expression screen was established. A subset of multicopy vectors with inducible (GAL1), repressible (MET25), and constitutive promoters of varying strength (GPD, TEF, CYC), was taken from two *S. cerevisiae* expression vector sets available in the public domain (ATCC nos. 87669 [208] and 87670 [209], respectively). As all the vectors share a common backbone, the same terminal insert overlaps added by PCR can be used for recombination into all of these.

While the generation of the *BSEP* inserts for recombination via PCR was straightforward, optimizing the product yield was not as uncomplicated. The following circumstances had to be taken into account to ensure a fool-proof routine for the screen: first, the transformation of *S. cerevisiae* has to be chemical because this requires less hands-on time and is much less error-prone (in terms of handling) than *S. cerevisiae* spheroplast electroporation. For an efficient chemical transformation of *S. cerevisiae* cells for homologous recombination, more DNA is needed than for bacterial transformation, i. e. in the range some hundred nanograms [238]. These are contained in a few pooled PCR reactions that have to be gel-purified in order to remove secondary products that otherwise could compete with the desired insert during HR. The purification results in a reduced yield of product. This is either compensated by pooling and purifying more reactions or by optimization of PCR conditions. The design of the primers for HR in general is, however, often rather fixed: start and end of the coding sequence to be inserted have to serve as priming

sites, and the 5'-overhangs consist of the overlaps necessary for targeted recombination, usually around 40 bp. If either of the primers is to encode additional information like a his tag or a protease cleavage site then the oligonucleotide overhangs that do not prime become too long and may interfere with the PCR by unproductive binding to stretches of random complementarity. The main feature of variability about such primers is the length of the priming stretch which is adjusted to avoid unfavourable properties such as primer dimerization. This however can only be done within a certain range as the primers should not be too long. What can be optimized instead is the reaction itself by additives like DMSO, which promotes template DNA denaturing, or increasing the amount of free Mg^{2+} , which is needed for polymerase activity. The primers for *BSEP* amplification both carried 40 bp of homology stretches to the ends of the gapped target plasmid, and, in each of the two used primer pairs, one encoded the his₆ tag. The features of the primers allowed for a limited optimization of PCR product yield (Figure 14). In the depicted example, DMSO was the central component in optimizing PCR product yield.

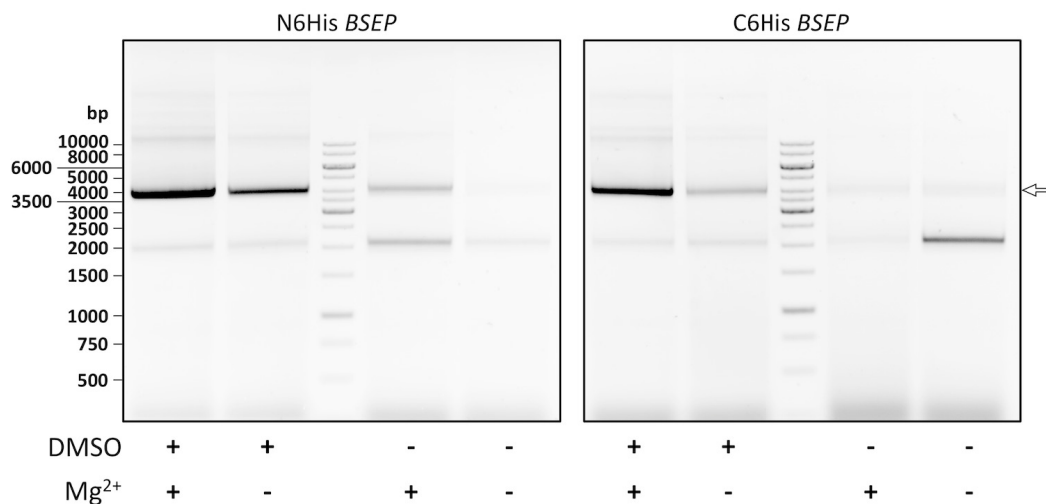


Figure 14. Overlap-carrying primers limit the yield of PCR product for HR. Optimization of PCR conditions can not always compensate for limitations in primer performance that are dictated by the necessary 5'-overlaps and custom features such as encoded tags. Shown here is a sparse optimization strategy to increase *BSEP* product (indicated by the arrow) yield under such conditions by addition of dimethyl sulfoxide and / or magnesium. Several such PCR reactions have to be pooled (eight in the case of *BSEP*) for an efficient co-transformation of *S. cerevisiae*.

This essentially means that more reactions have to be pooled to obtain enough product after gel purification, and for this reason the construction of the whole set of screening plasmids was divided into two phases (Figure 15):

- I) Initially, the two his tag configurations of the p426-MET25-*BSEP* vector were created by *in vivo* recombination in *S. cerevisiae* (Figure 15, Box I).
- II) After plasmid recovery, amplification in *E. coli* and sequence verification, preparative amounts of these were then used for restriction digest to obtain the inserts for immediate recombination into the remaining screening set vectors (Figure 15, Box II).

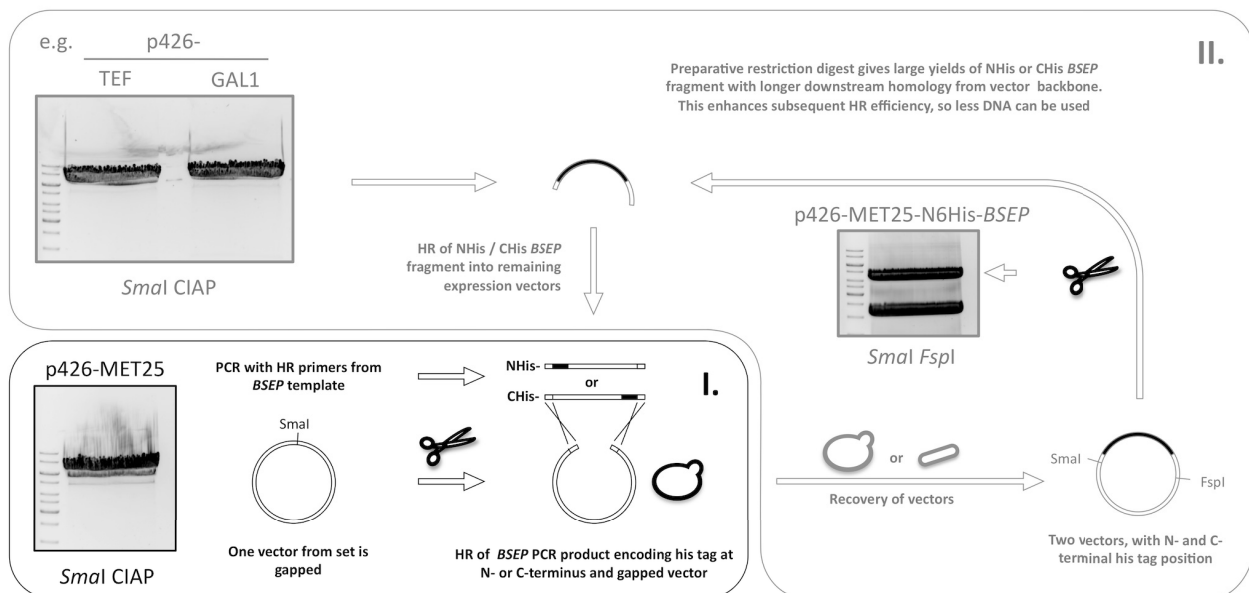


Figure 15. A simple, two-step screening strategy is used to construct and test *BSEP* expression from a set of different expression vectors. The construction of the vector set is carried out in two steps: I. Overlap-generating primers are used to generate two wild type *BSEP* PCR products covering both terminal his tag positions. The first screening plasmid is then gapped and used to construct both *BSEP* variants by homologous recombination in *S. cerevisiae* (black box). II. Plasmids are harvested either from *S. cerevisiae* or *E. coli* culture. *BSEP* cDNA with terminal sequence overlaps is then obtained by preparative restriction digest (RSI = *SmaI*, RSII = *FspI* for the vector set used) and recombined into the remaining gapped vectors of the screening set (grey box).

The resulting *S. cerevisiae* clones in each step were directly used to screen expression. All obtained clones were found to uniformly express BSEP; examples from both phases of the screen are given in Figure 16.

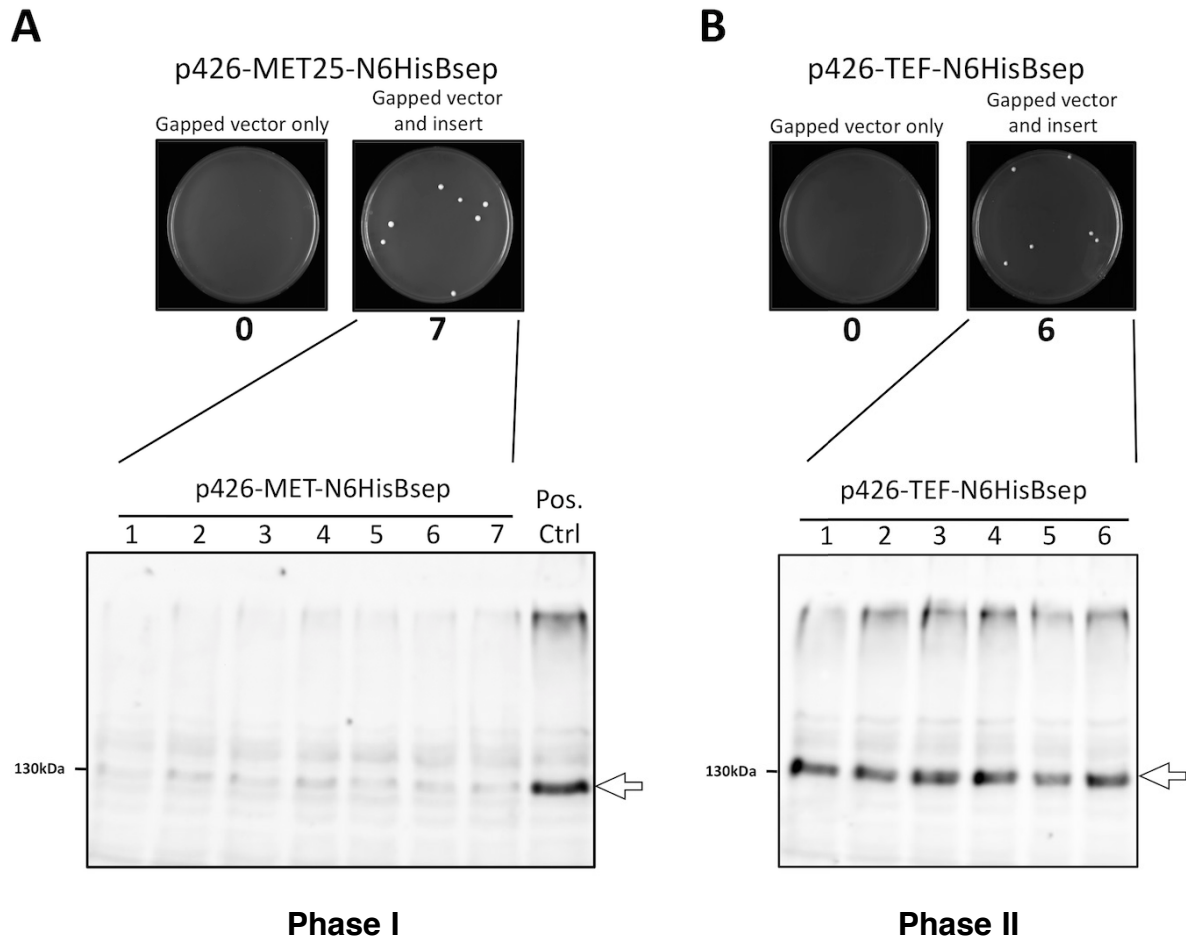


Figure 16. Homogeneity of expression among transformants in the plasmid-based screen. Representative examples of Western blots from both steps of the screen show that every transformant clone obtained expresses BSEP. **A** Performance of the N-terminally his₆-tagged BSEP construct made in step I of the expression screen. **B** Performance of the TEF promoter / N-terminal his₆ tag from step II of the screen. Pos. Ctrl, YEpCHIS-BSEP as expression reference.

The results of the screen have been compiled in Figure 17: the strong constitutive GPD and TEF promoter constructs showed the strongest BSEP expression (lanes 1 to 4), while the weak CYC promoter did not lead to detectable BSEP levels (lanes 5 and 6). From the regulatable promoters, both MET25-driven variants expressed at quite low levels, while under induction only the N-terminally his₆-tagged GAL1-BSEP

construct shows expression (lanes 7, 8, 9, and 10). In all cases, the *BSEP* sequence on these constructs was verified by sequencing, including the correct upstream junction and promoter. In summary, by following this two-step strategy a set of vectors could be used to rapidly screen the influence of promoter strength and his tag position on expression from the unstable *BSEP* cDNA. However, no combination of these led to a notable increase in *BSEP* expression.

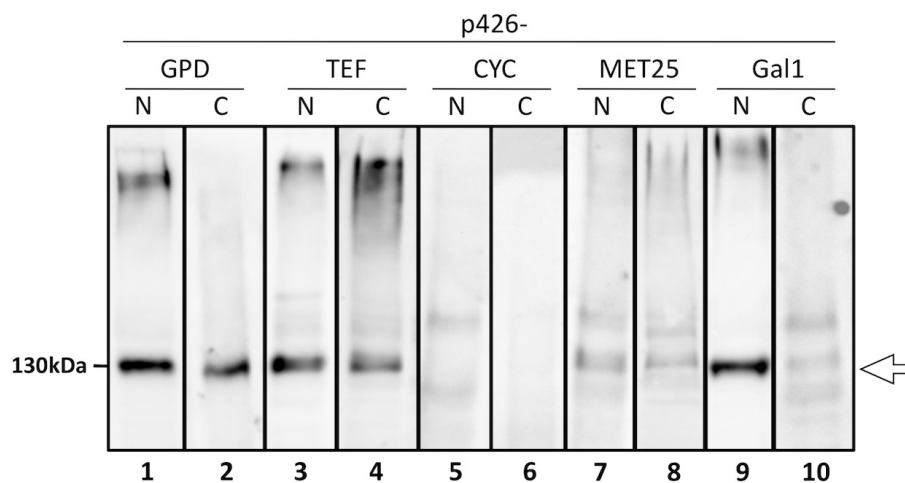


Figure 17. BSEP expression from a set of different expression vectors constructed with the two-step, HR screening strategy. **A** The construction of the vector set is carried out in two steps: **I.** Overlap-generating primers are used to generate two wild type *BSEP* PCR products covering both terminal his tag positions. The first screening plasmid is then gapped and used to construct both *BSEP* variants by homologous recombination in *S. cerevisiae* (black box). **II.** Plasmids are harvested either from *S. cerevisiae* or *E. coli* culture. *BSEP* cDNA with terminal sequence overlaps is obtained by preparative restriction digest (RSI = *Sma*I, RSII = *Fsp*I for the vector set used) and recombined into the remaining gapped vectors of the screening set (grey box). **B** The expression screen showed a correlation of promoter strength and *BSEP* expression. Mid-log *BSEP* expression was assessed by probing Western blots of whole *S. cerevisiae* cell extracts with K168 [203].

3.6 The Use of the Compatible Solute Glycerol as a Chemical Chaperone to Increase BSEP Expression in *S. cerevisiae*

Since the plasmid-based expression screen (Results 3.5) did not result in an increase of BSEP expression, an alternative approach was tested. If modifications on the genetic level fail, the expression conditions themselves can be adjusted. Two previous studies on the functional expression of human ABC transporters reported the successful use of glycerol as a small molecular chaperone to increase the amount of expressed MDR1 and MRP1 [182,184]. Glycerol is a non-toxic compound that mixes well with water, and, more importantly, is not metabolized in *S. cerevisiae* while glucose is present. It has already been used as a chaperone in eukaryotic cell culture [242]. Glycerol is thought to stabilize and facilitate the proper folding of nascent polypeptide chains, thus increasing the amount of active and non-degraded protein in the cell [242,243].

For MDR1, Figler and colleagues found an addition of 10 % (v/v) glycerol to be optimal in stabilizing the recombinant membrane protein [182]. This concentration was also tested for the MDR1 homologues BSEP and MDR3, and the expression of both membrane proteins was indeed sustained by use of this chemical chaperone. Two observations can be derived from the Western blots depicted in Figure 18: for both variants of plasmid-expressed BSEP (wild type and V444A) and chromosomally expressed MDR3, the *de facto* expression was detectably increased, and the time of expression during exponential growth phase was significantly prolonged. This may help to partially compensate low yield with cell mass: more protein is obtained from more cells. Through the use of the chemical chaperone glycerol, the same culture volumes can now be grown to higher densities instead of having to scale up for compensation.

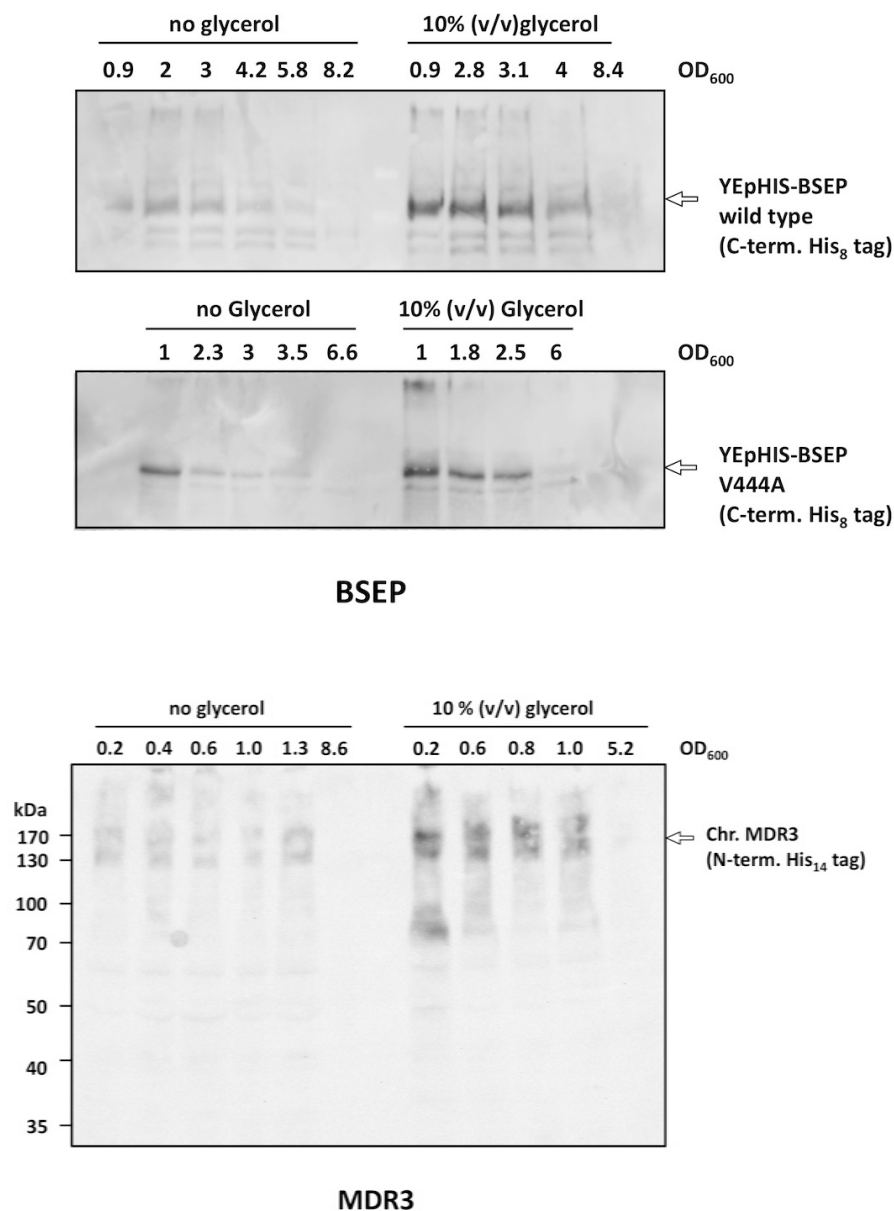


Figure 18. The chemical chaperone glycerol increases and extends the expression of both BSEP and MDR3. A Equal amounts of whole cell lysates from 1 L liquid cultures with or without 10 % (v/v) glycerol sampled at the indicated optical density were probed for BSEP expression with a monoclonal anti-his tag antibody. **B** Experiment as described in A for chromosomally expressed, N-terminally his₁₄-tagged MDR3. MDR3 appears on this blot as a double band, which is the result of using a 10 % SDS separating gel instead of 7 %. The signal's weakness in comparison with the other MDR3 Western blots is due to the use of the ECL+ detection solution instead of the more sensitive ECL Advanced reagent.

Since it was shown for MDR3 and BSEP as well as for MDR1 [182] that these proteins are most prominently expressed during exponential growth phase, the expression behaviour at the very onset of the exponential growth phase, after one cell division cycle, was investigated (Figure 19). At this point, cells expressing N-terminally his-tagged MDR3 from the chromosomal *PDR5* locus showed an increase in expression by glycerol (see Figure 18B, OD₆₀₀ 0.6 sample with glycerol).

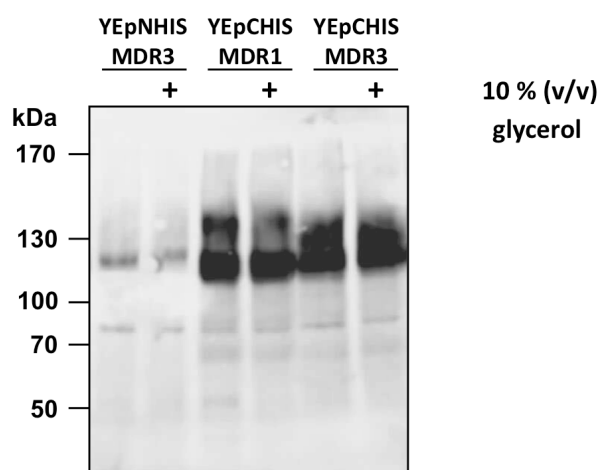


Figure 19. The chemical chaperone glycerol has no influence on the expression of the MDR3 plasmid constructs at the onset of the exponential growth phase. Whole cell lysates from cells harvested at OD₆₀₀ 0.5 were probed for protein expression with the C219 P-gp antibody that recognizes both MDR1 and MDR3. Cultures were inoculated at an OD₆₀₀ of 0.2. The Western blot shows that, after one cell division, glycerol had no effect on the expression. MDR1 and MDR3 expressed equally well and were not affected by glycerol. The low expression of the N-terminally his-tagged MDR3 expressed from YEpNHIS is not rescued, suggesting that this tag position does not result in an unstably folded fusion protein in *S. cerevisiae*.

The Western blot showed that, after one cell division, glycerol had no effect on MDR3 expression from any of the constructs, suggesting that the expression was at its maximum. Importantly, at this growth stage MDR1 and MDR3 expressed equally well and were not affected by the addition of glycerol. The low expression of the N-terminally his₁₄-tagged MDR3 expressed from YEpHIS was not rescued by the chemical chaperone.

3.7 Subcellular Localization of Human BSEP and MDR3 in *S. cerevisiae*

BSEP and MDR3 were then investigated with respect to their subcellular localization to see whether impaired trafficking could account for the low BSEP expression. For this, membranes were harvested from whole yeast cells in the early phase of logarithmic growth, and subjected to density fractionation through a multistep sucrose gradient [244]. Figure 20 shows the localization of the membrane proteins in the fractionated membranes. All tag variants of BSEP and MDR3 co-localized at least partially with Pdr5, which was exclusively found in the plasma membrane (PM) fractions (Figure 20, green box).

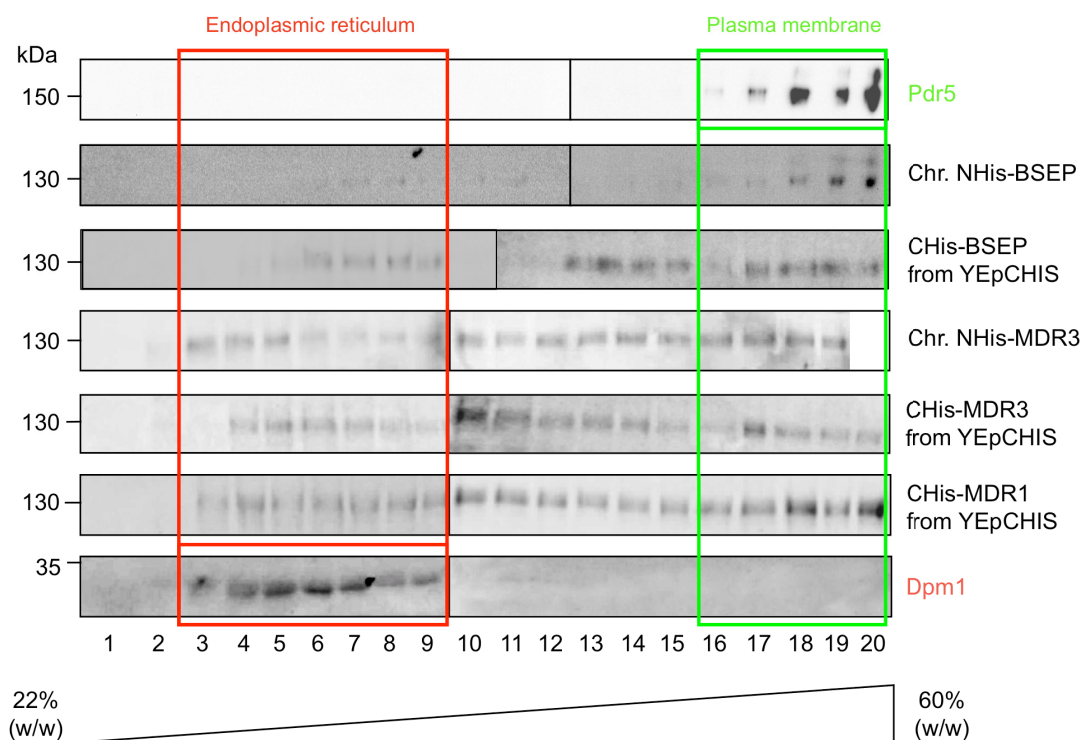


Figure 20. Subcellular localization of BSEP, MDR1 and MDR3 in early log-phase *S. cerevisiae*. Membrane vesicles prepared from whole *S. cerevisiae* cells were separated by ultracentrifugation through a multistep sucrose gradient. Dpm1 is a membrane-resident yeast enzyme marker for the endoplasmic reticulum (ER), while the Pdr5 transporter is a yeast plasma membrane marker. Both BSEP and MDR3 at least partially localized to the plasma membrane (PM). MDR3 and MDR1 shared a localization pattern throughout the sucrose gradient, while BSEP seems to consist of two populations, one residing in the ER, and the other localized to the PM.

One striking difference was observed between the low-expressing BSEP and the better expressing MDR3 and MDR1: the latter were found throughout all fractions from the endoplasmic reticulum (ER) to the PM, while both N- and C-terminal his tag variants of BSEP were found separated into two species: one resided in the ER (red box) while the other was targeted to the yeast plasma membrane. Whether the low level of BSEP protein is due to partial degradation in the ER is unclear. The high MDR1 and 3 expression levels, on the other hand, may result in these proteins being stuck in all stages of the secretory pathway, and it is uncertain whether a lower expression would result in an exclusive PM-localization or the bipartite pattern observed for BSEP.

3.8 Testing for a Cellular Resistance Phenotype of BSEP and MDR3 in *S. cerevisiae*

The expression of drug efflux pumps of both fungal and mammalian origin was frequently found to be functional in *S. cerevisiae* and often conferred cellular drug resistance [181,193,245,246,247,248,249,250]. As an example, the homologous over-expression of Pdr5 results in hyperresistance against the broad substrate spectrum of this PDR transporter such as azoles and cycloheximide [251,252]. Heterologous expression of human MDR1 also conferred a multidrug resistance phenotype against a broad spectrum of cytotoxic compounds that was easily detected in a $\Delta pdr5$ strain background (Figure 21) [181,253]. In contrast, MDR3, which is a close MDR1 homologue in terms of sequence conservation but not function, is a phosphatidylcholine floppase and not a multidrug efflux pump like MDR1. As expected, its expression in *S. cerevisiae* cells did not confer resistance against any of the tested drugs (Figure 21).

MDR3-associated Phenotype

Next, FK506 was tested as a compound that is an important MDR1 substrate in the context of transplantation medicine [254,255]. Also known as tacrolimus, FK506 is a potent immunosuppressant that additionally functions as an antifungal compound and in yeast has a cytotoxic effect [256]. In the blood-brain barrier, MDR1 mediates FK506 efflux back into blood plasma and protects the central nervous system from neurotoxic effects [257]. The compound is lipophilic, and its clearance from the body is highly dependent on liver function [258]. A drug resistance assay against FK506

was carried out to test whether MDR3, that is almost exclusively expressed in the apical membrane of liver parenchymal cells, also plays an active role in FK506 excretion. Indeed, MDR3 has been found to transport a small subset of the MDR1 spectrum, the relevance of which in biliary drug clearance, however, is likely to be low [175]. As FK506 was not among the tested substrates in that study, the compound was tested here. As seen in Figure 22, only MDR1 but not MDR3 expression conferred FK506 resistance to *S. cerevisiae* cells. A marginal resistance could be found and reproduced for a chromosomal MDR3 clone that carried an M800I missense mutation located in the cytoplasmic loop between TM helix 7 and 8 in the second TMD (Figure 22, Chr. N-his₁₄-MDR3 Clone 3). For the wild type MDR3 (clones 1 and 2), however, no resistance against FK506 was observed.

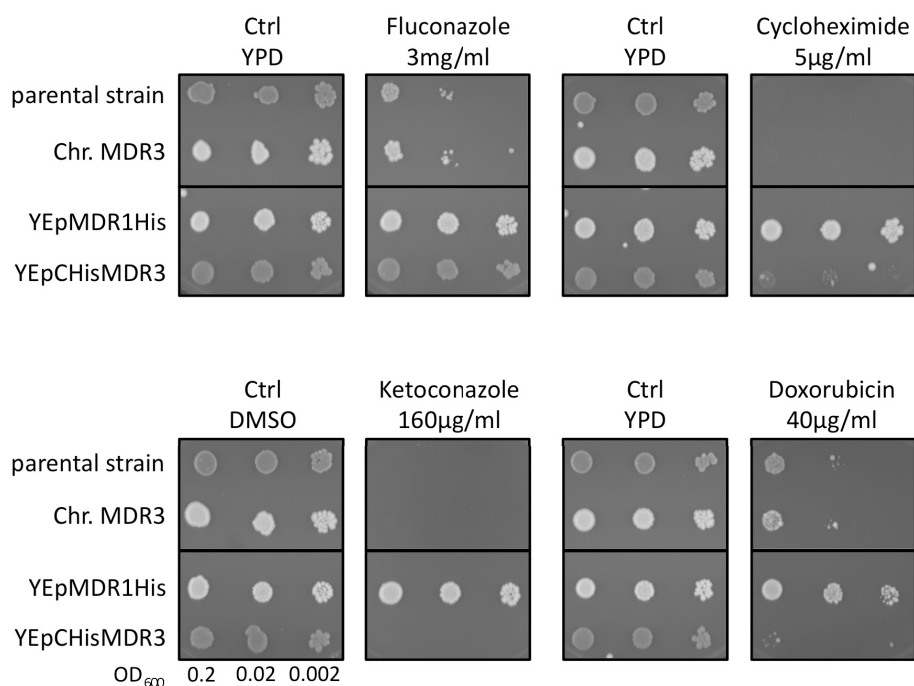


Figure 21. MDR1, but not MDR3 confers a cellular multidrug resistance phenotype in *S. cerevisiae*. Expression of the human P-glycoprotein (MDR1) protected the yeast cells against fluconazole, ketoconazole, cycloheximide, and doxorubicin. Human MDR3 failed to protect the cells against these compounds. Parental strain: Δ PP strain, that is devoid of Pdr5 expression.

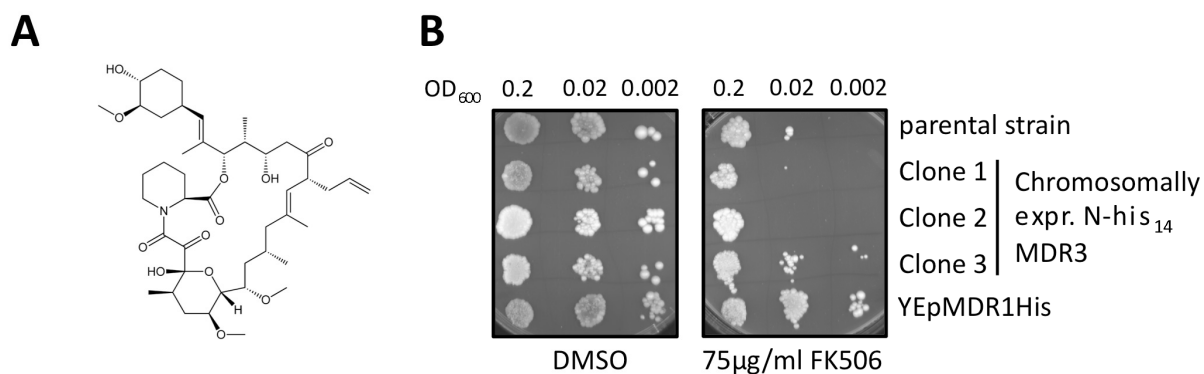


Figure 22. MDR1 confers resistance against FK506 in *S. cerevisiae*. One of the MDR3 clones (3) also mediates a marginal yet reproducible resistance. This clone carries a M800I missense mutation. Parental strain, Δ PP strain that is devoid of Pdr5 expression.

BSEP-associated Phenotype

Under aerobic conditions, exogenous sterol compounds are not taken up by *S. cerevisiae* cells, a phenomenon which is termed *aerobic sterol exclusion* [259]. However, the conjugated bile salts taurocholate (TC) and taurodeoxycholate (TDC) are major constituents of the bile salt pool that are sterol derivatives and have a strong detergent capacity owing to their more hydrophilic nature after conjugation. Unless neutralized in the bile as part of mixed micelles containing both cholesterol and phosphatidylcholine, they inflict substantial cellular damage in the liver by partitioning into and subsequently destroying the canalicular membrane by its lysis. In some PFIC3 patients, the canalicular systems are damaged so much that they can not be identified morphologically anymore [171]. The difference between TC and TDC is a single hydroxyl group at carbon position 7 in the B ring of the sterane core structure (Figure 23). Along with the taurine-conjugated form of chenodeoxycholic acid, they are the major species of bile salts found in human bile. The conjugation also permits a high canalicular (in the mixed micelles) and intestinal concentration without passive reabsorption that would occur with the more hydrophobic unconjugated forms. As both TC and TDC are BSEP substrates [174,207] and strong detergents, they were tested for their potential as cytotoxic compounds that impair yeast cell growth by compromising membrane integrity, and it was tested whether the expression of human BSEP conferred cellular resistance against them (Figure 24).

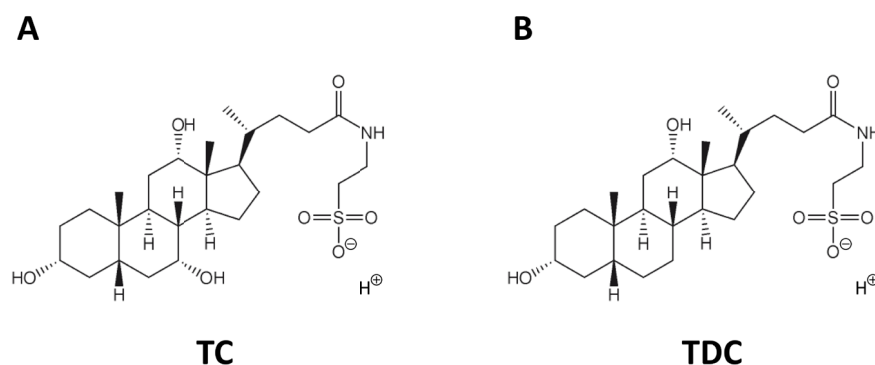


Figure 23. Chemical structures of taurocholate (TC) and taurodeoxycholate (TDC). Both are dominant forms of conjugated bile acids in the bile salt pool.

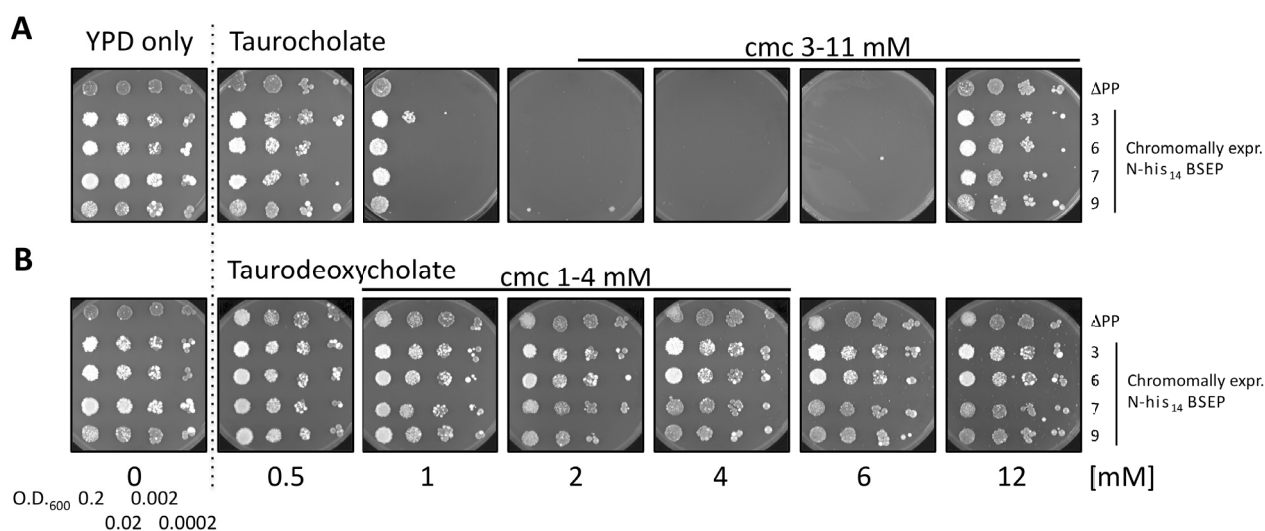


Figure 24. Resistance test of *S. cerevisiae* strains expressing BSEP against tauro- and taurodeoxycholate. **A** The bile salt taurocholate is growth-inhibiting starting from 1 mM. Surprisingly, its inhibitory effect diminishes with increasing concentration. **B** No effect on growth is seen over a range of taurodeoxycholate concentrations. The range of the respective bile salts' critical micellar concentration (cmc) is indicated. Serial dilutions of mid-log growth phase cells were spotted onto YPD plates with the indicated bile salt concentrations.

It was found that TC, but not TDC had a strong growth-inhibiting effect on *S. cerevisiae* cells. The effect was found in concentrations below and within the range of the critical micellar concentration (cmc) of TC (the cmc range is indicated for both TC

and TDC in Figure 24). Interestingly, *S. cerevisiae* cells returned to their full growth potential at concentrations above the cmc for TC. The cmc value of a detergent can be influenced by other additives in an aqueous system [260], which might explain the offset encountered between growth inhibition and theoretical cmc range. In addition, the broad cmc range of bile salts is not easily estimated as a mixture of different aggregates exists throughout this range and even well above the given cmc concentration [261]. The expression of BSEP in the four clones 3, 6, 7, and 9 (see Results 3.3) did not result in a resistance against TC. The slightly better growth of clone 3 at 1 mM TC (in Figure 24A) was not reproducible, when the relevant concentrations of taurocholate were used to test all available BSEP expressing *S. cerevisiae* clones (Figures 25 and 26, upper panels). The lack of resistance could again be reproduced for all nine clones (see Results 2.2) that contain the expression cassette for N-terminally his₁₄-tagged BSEP (Figure 25). Also, the expression of the wild type or the V444A allele of BSEP with either the N- or the C-terminal tag from plasmid did not lead to TC resistance (Figure 26, upper panels).

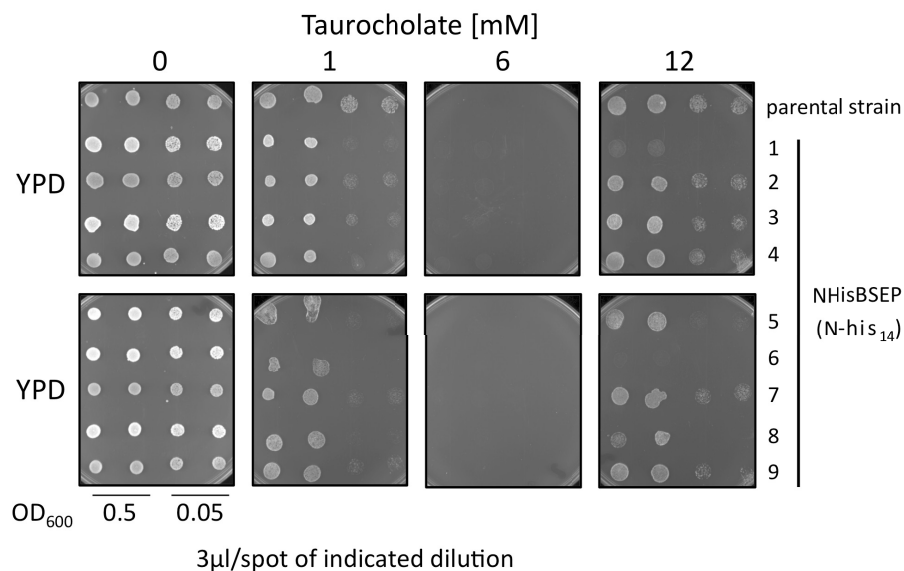


Figure 25. Taurocholate resistance test of *S. cerevisiae* strains expressing BSEP from the chromosomal *PDR5* locus. This experiment fully reproduces the results from Figure 24 as none of the nine clones that express Nhis₁₄-BSEP show resistance against TC.

Since MDR3 was shown to translocate phosphatidylcholine from the inner to the outer leaflet of the membrane [83], and this protects the canalicular membranes from bile salt-mediated damage, it was tested whether the expression of MDR3 conferred such a "secondary" resistance to the yeast plasma membrane by overloading it with phosphatidylcholine. However, the three yeast strains chromosomally expressing MDR3 were found to be as susceptible to TC as the control strain (Figure 26, lower panels). In all TC resistance experiments the onset and ceasing of the bile salts-mediated growth impairment was observed with increase in concentration, strongly suggesting that this effect is an inherent characteristic of this compound, and most likely cmc-related.

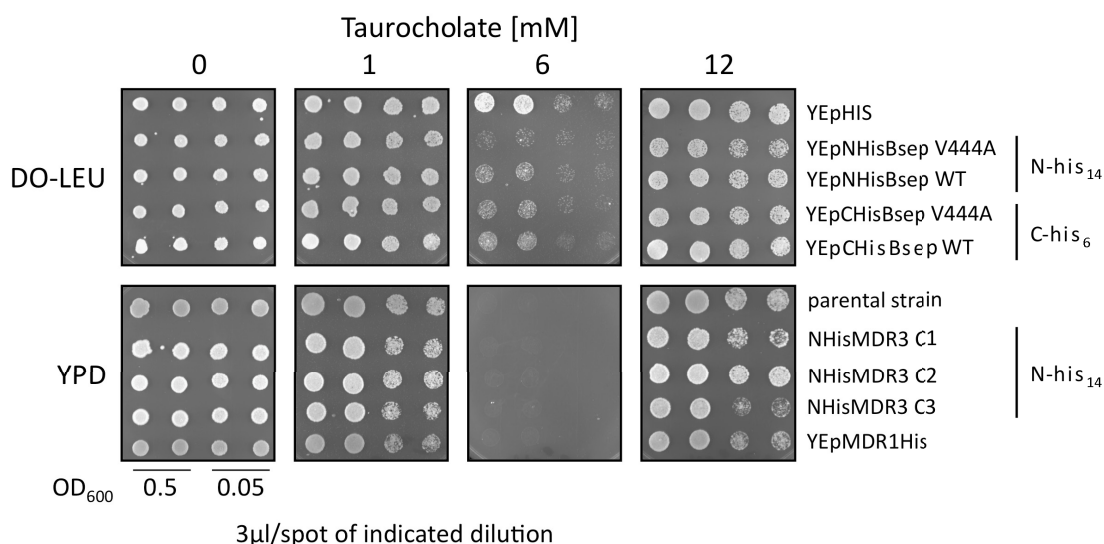


Figure 26. Taurocholate resistance test of *S. cerevisiae* strains expressing either BSEP from plasmid or MDR3 from the *PDR5* locus. Neither BSEP nor MDR3 mediate cellular TC resistance.

Analysis of Statins as S. cerevisiae Growth Inhibitors and BSEP Substrates

Statins are inhibitors of the 3-hydroxy-3-methylglutaryl (HMG) -CoA reductase, a key enzyme in the cholesterol biosynthesis pathway, by mimicking its substrate, HMGCoA [262]. Lovastatin (Figure 27) has been shown to also inhibit yeast HMGCoA reductase and thus growth of yeast cells. Another statin, pravastatin, has been reported to be a transported substrate of BSEP [263]. However, it is unclear whether

this compound can inhibit the *S. cerevisiae* HMG-CoA reductase and thus function in the selection of yeast cells expressing functional BSEP.

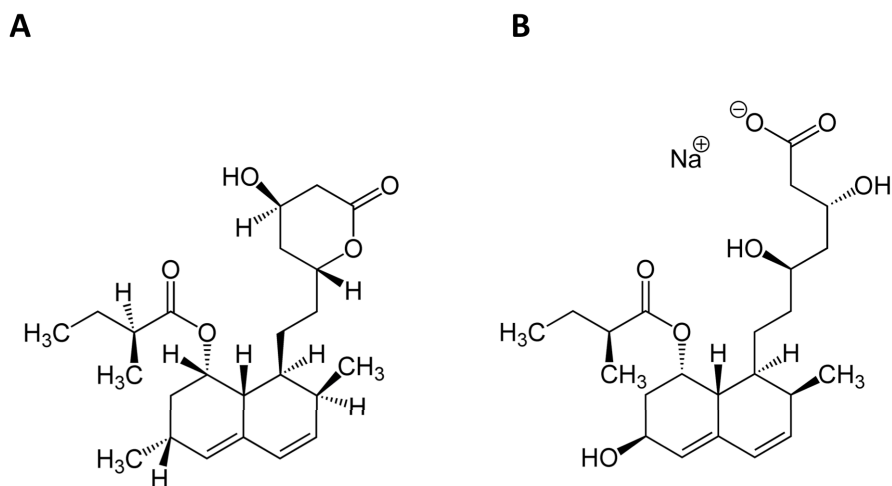


Figure 27. Chemical structures of statins. A Lovastatin is an inhibitor of the HMGCoA reductase of *S. cerevisiae* [213]. **B** Pravastatin is a BSEP substrate [263].

Both statins were tested as compounds selecting for active BSEP expression. Lovastatin, as an inhibitor of the yeast HMG-CoA reductase [213], was found to inhibit growth of all tested yeast strains irrespective of BSEP or MDR3 expression (Figure 28). As statins are drugs that may be cleared by efflux pumps such as MDR1, yeast cells expressing this transporter were included as a control. MDR1 in *S. cerevisiae*, however, did not transport Lovastatin (Figure 28), although this statin was found to interact with MDR1 in mammalian cell culture [264]. In the same study, pravastatin did not interact with MDR1, yet neither of these statins was tested for being an actual MDR1 transport substrate. MDR3 expression did not provide protection against the toxic effect of lovastatin (Figure 28). Since MRP2 is another apical efflux pump that could mediate statin efflux in hepatocytes, and which could not be expressed from the chromosomal *PDR5* locus with a N-terminal his₁₄ tag (see Results 3.2), an MRP2 expression plasmid with a C-terminal his tag was constructed by homologous recombination in *S. cerevisiae*. The sequence-verified construct showed no MRP2 expression, and no lovastatin resistance of *S. cerevisiae* cells carrying this plasmid could be detected (Figure 28).

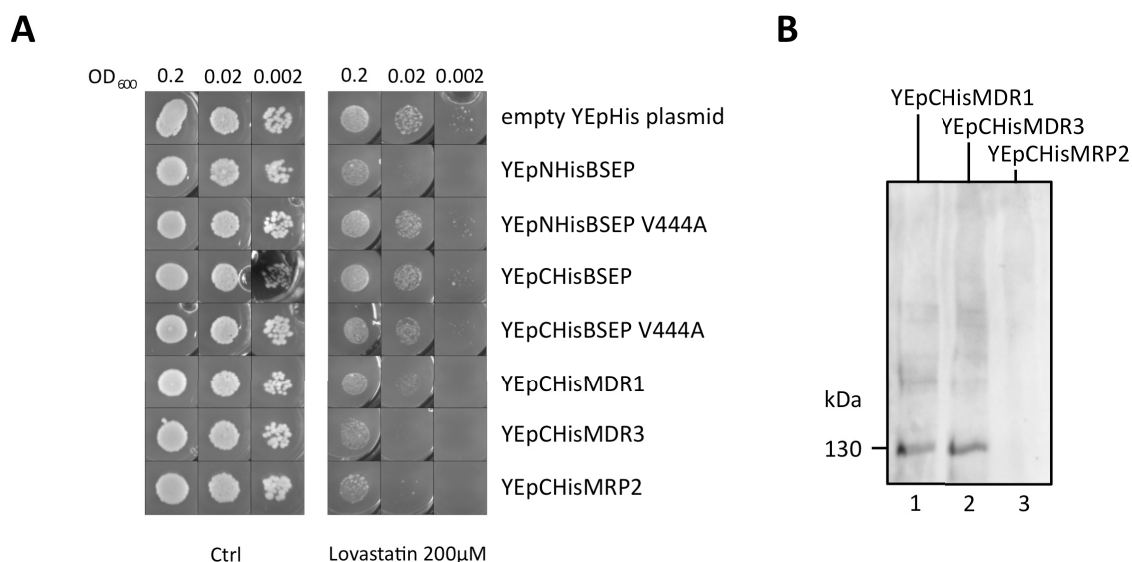


Figure 28. Lovastatin inhibits cellular growth but is not a BSEP substrate in *S. cerevisiae*. **A** MDR1 and MDR3 did not protect the cells from lovastatin. In addition, yeast cells carrying the YEp expression plasmid for carboxyterminally his₈-tagged MRP2 showed no resistance. **B** In Western blot analysis, no MRP2 expression from this plasmid was detected with a monoclonal his tag antibody. Ctrl, drug-free control medium (solvent only).

The other tested statin, pravastatin, showed no growth-inhibiting effect on any of the tested *S. cerevisiae* cells in a broad range of concentrations (Figure 29). In summary, no information about BSEP-, MDR3-, and MDR1-conferred resistance toward this substance in yeast cells could be gained.

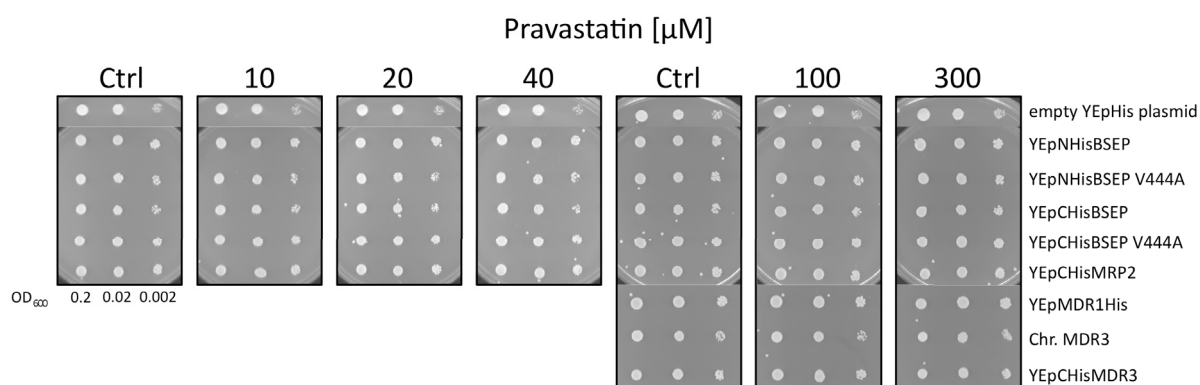


Figure 29. Pravastatin does not inhibit *S. cerevisiae* cell growth. Therefore, it could be used as a compound to confirm functional BSEP expression. Ctrl, drug-free control medium (solvent only).

3.9 Initial Purification of Human BSEP and MDR3 from *S. cerevisiae*

Nonetheless, a first analytical affinity purification of both human transporters was possible. An initial solubilization screen of membranes prepared from whole yeast cells pointed towards the stronger, ionic Fos-choline detergents and here, the best results for both MDR3 and BSEP were obtained with Fos-choline 16 that has the longer aliphatic chain (Figure 30). Using this detergent, the C-terminal his tag fusion proteins were taken for purification, since MDR3 gave the highest yield in this tag configuration. In this way, a direct comparison of the purification efficiency for both membrane proteins could be made.

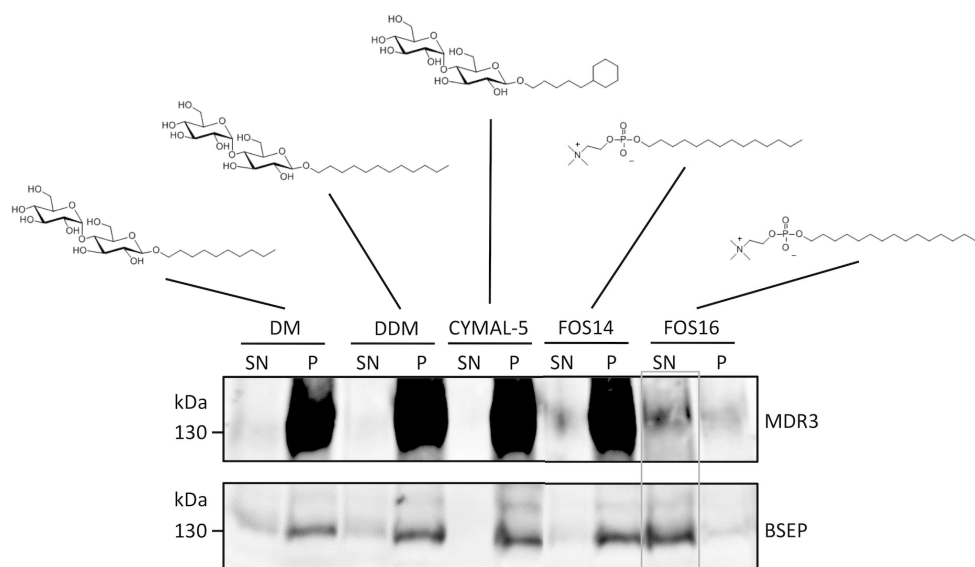


Figure 30. Initial solubilization screen for MDR3 and BSEP. A small selection of "popular" detergents in membrane protein biochemistry were screened for their capability to efficiently solubilize the human ABC transporters at a final concentration of 1 % (w/v) at 4 °C for 1 h. Fos-choline (FOS) 14 and 16 are stronger detergents in comparison to decyl-, dodecyl-maltoside and CYMAL-5 as they are ionic detergents. Only the stronger detergents could efficiently solubilize C-his₈-BSEP (detected with K168) and C-his₈-MDR3 (C219). For both membrane proteins, FOS16 gave the best results (indicated by grey box). SN, supernatant; P, pellet.

Although the amounts obtained were insufficient for any further studies, the his tags on both membrane proteins were clearly accessible to the IMAC column material and thus were not occluded by a detergent micelle or the protein itself (Figure 31).

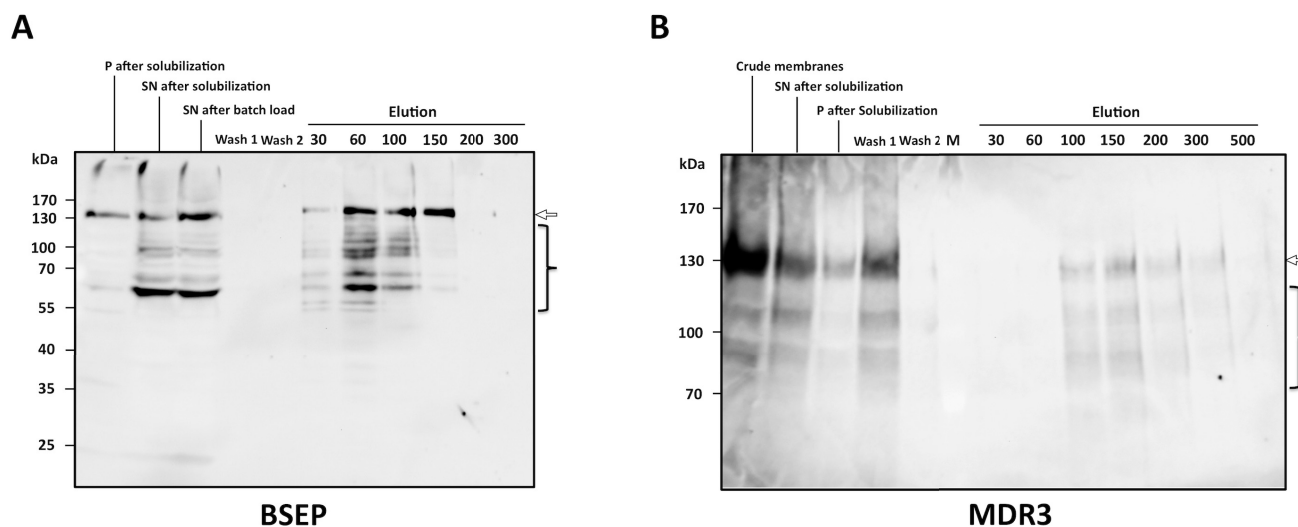


Figure 31. Affinity purification of C-terminally his₈-tagged human BSEP and MDR3. Both BSEP (A) and MDR3 (B) were solubilized with Fos-choline 16 from preparations of whole yeast cellular membranes, the column material (Ni²⁺-NTA agarose) was batch-incubated with the solubilized material. Packing, washing and elution steps were performed by gravity flow. Equal volumes of the indicated steps and fractions were separated on SDS gels, electroblotted, and detected with K168 (A) and C219 (B). Arrows indicate the full-length proteins, and brackets indicate degradation products. M, marker lane on MDR3 Western blot.

BSEP, once solubilized from its membrane, seemed to become the subject of substantial degradation (Figure 31A), although a cocktail of protease inhibitors was used. A major product of this degradation might contain both the his tag and the linker region between the two homologous TMD-NBD halves of BSEP as it was detected by the K168 antibody that recognizes aa residues 688-702. Although both proteins should be concentrated roughly 500-fold in this purification step, they could only be detected via Western blot. During MDR3 purification, Figure 31B, wash1).

As MDR3 expression gave high enough yields, its purification could be optimized further. First, the solubilization step was optimized by changing the mass ratio of membrane protein to detergent (Figure 32). Again, Fos-choline 16 was the most effective detergent for MDR3 solubilization. Here, a protein concentration of 2 mg/ml was found to be more favourable than 5 mg/ml at a final detergent concentration of 0.5 % (w/v).

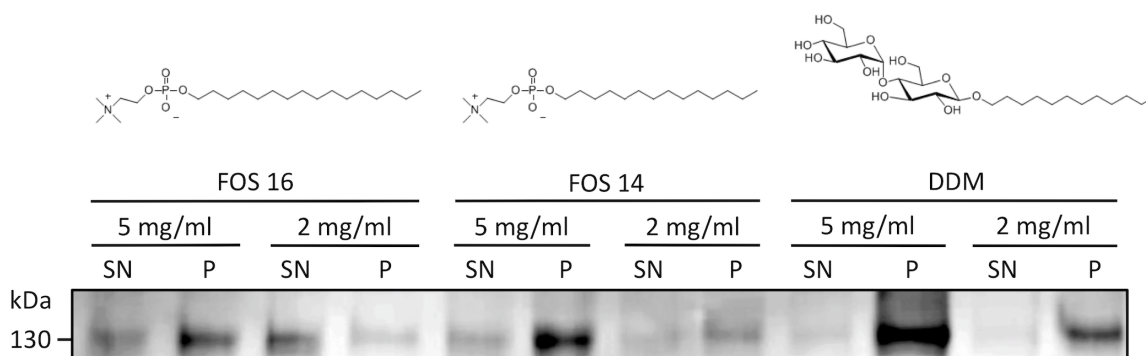


Figure 32. A sparse solubilization screen for MDR3 shows the impact of the protein:detergent ratio on solubilization. The concentration of the detergents indicated was set to 0.5 % (w/v) for the Fos-cholines and 1 % (w/v) for DDM. After solubilization for 1 h at 4 °C, unsolubilized material was removed by ultracentrifugation. This material was then resuspended in the initial volume of membrane buffer and used for comparison with the supernatant. The variations in signal intensity in the pellet (P) lanes come from inhomogenous resuspension of the insoluble material.

In addition to this change during solubilization, the purification was scaled up from analytical gravity flow columns and batch loading of the Ni²⁺-NTA slurry to a larger bed volume used in an ÄKTA liquid chromatography system, and cobalt was used as the loaded metal cation providing a higher affinity than nickel.

As a result of these optimizations, the affinity purification of MDR3 from yeast membranes now yielded more substantial amounts of protein that could even be detected on a Coomassie-stained SDS-polyacrylamide gel (Figure 33B). For this, cells from 10 L of yeast culture were grown in 10 % glycerol and used to prepare and solubilize whole cellular membranes, and the elution was with a step gradient from 0 to 300 mM Imidazol in five steps of 60 mM (Figure 33A, green trace). In the first elution step (at 60 mM Imidazole), a lot of unspecifically bound proteins were found to elute (red trace), while at the second and third peak the main fractions of the bound MDR3 were eluted (120 and 180 mM Imidazole, respectively; Figure 33B and C). Fractions containing MDR3 from peaks 2 to 4 were pooled (containing about 2 mg MDR3).

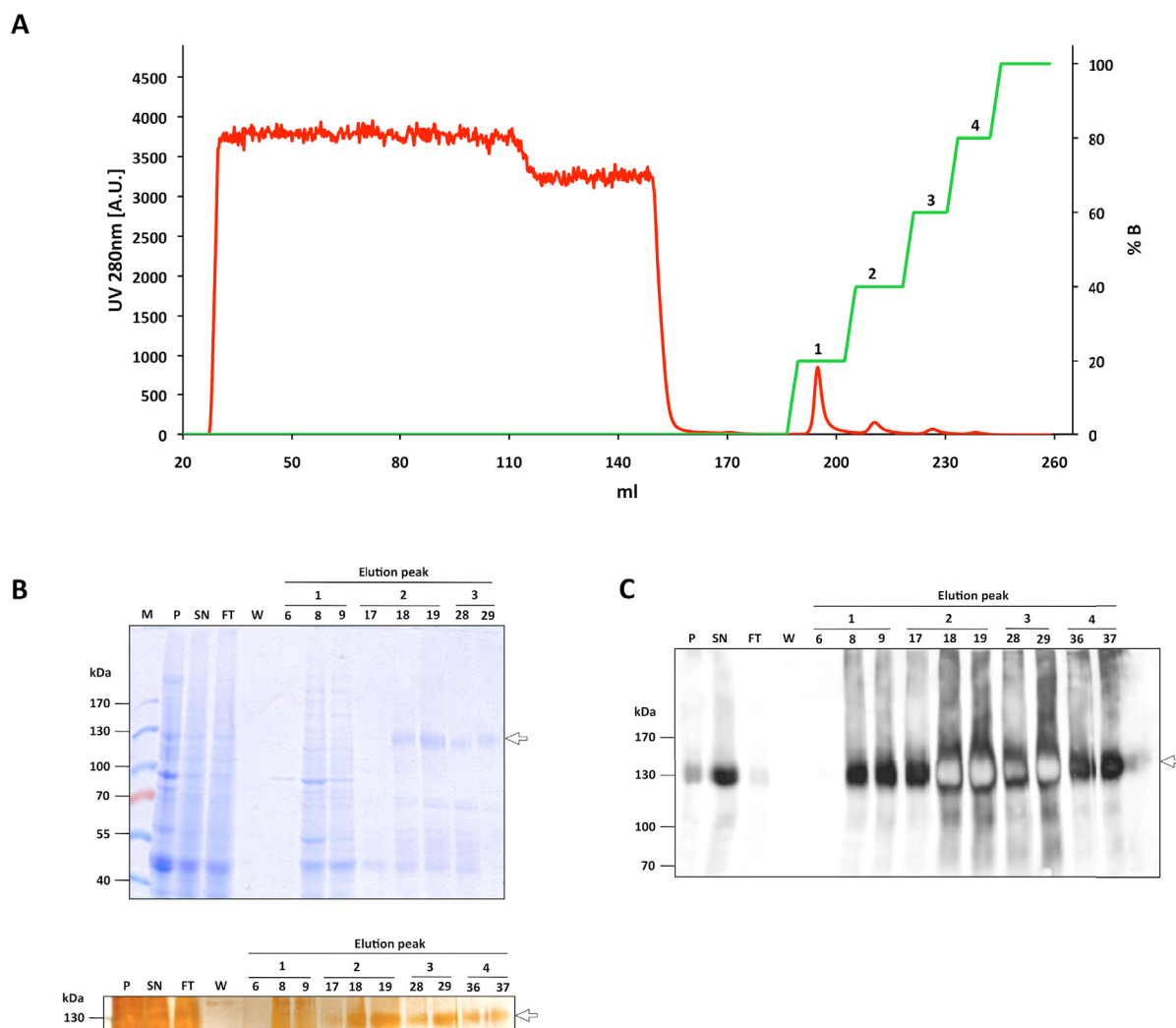


Figure 33. Optimized affinity purification of human MDR3. **A** Chromatogram of MDR3 IMAC purification. Red, UV signal at 280; green, elution buffer (300 mM). **B, upper panel** Coomassie stained SDS gel of the purification in A. **Lower panel** Silver stained SDS gel of the same. **C** Western blot of the IMAC samples.

The pooled eluate was concentrated (Figure 34A), and a portion of the concentrate was then subjected to gel filtration for further purification. The elution profile shows a sharp peak at the void volume (Figure 34B), indicative of substantial aggregate formation in the filtrated sample (fraction 4). This fraction was also found to contain MDR3, however, the main fraction of MDR3 eluted outside the void volume as a broad peak (Figure 34B and C). The width of the peak indicates that the MDR3 membrane protein together with detergent and yeast lipids forms a variety of micellar species of different size.

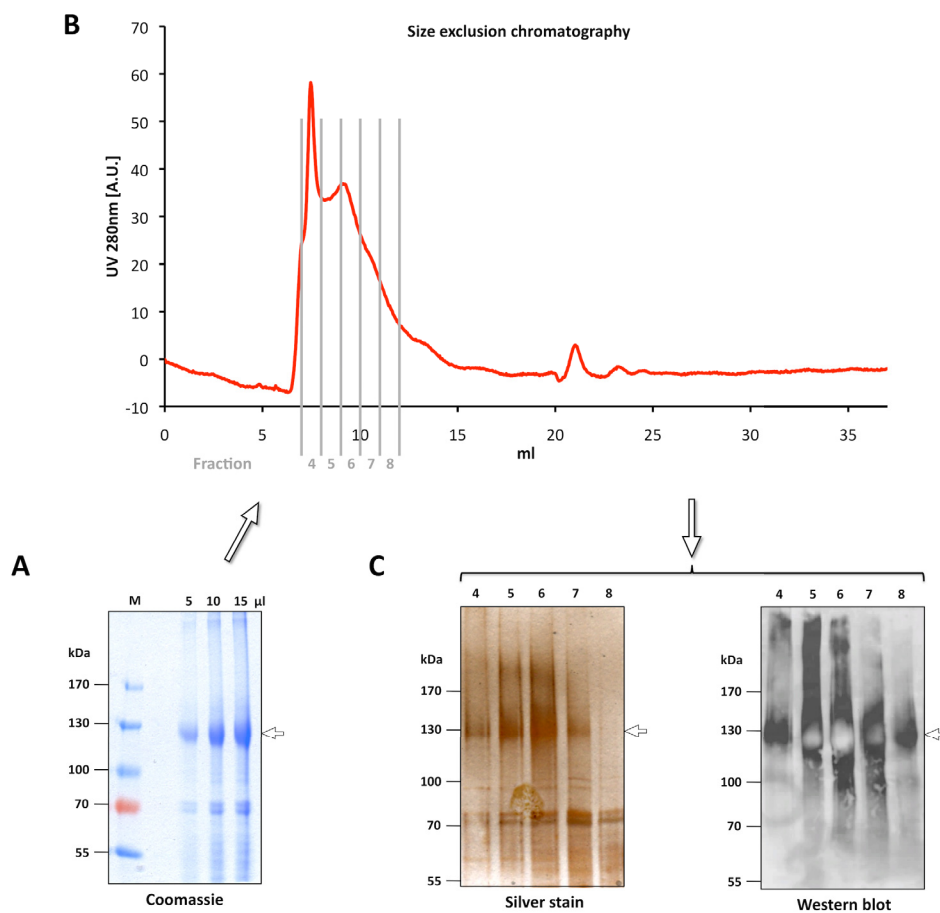


Figure 34. Gel filtration of affinity-purified MDR3. **A** Fractions containing recombinant human MDR3 eluted from the Co^{2+} -chelating material in Figure 32 were pooled and concentrated using a filter with a 100 kDa cutoff. **B** Using a Superdex 200 10/300 GL column, the material was gel filtrated. **C** The peak fractions were analyzed by SDS-PAGE and silver staining (left panel) or Western blot detection (right panel).

3.10 Moving Expression of BSEP from *S. cerevisiae* to *Pichia pastoris*

The screen of BSEP expression from several constructs with different promoters and his tag positions (see Results 3.5) did not lead to an expression suitable for the purification of preparative amounts. None of the used vectors in combination with either the N- or C-terminal his tag position led to a drastic increase in BSEP expression. Also, the use of the chemical chaperone glycerol (Results 3.6) did not increase the yield to a point where attempts to purify BSEP became a feasible option (Results 3.9).

Because of this, the expression system was changed to another eukaryotic expression system, the methylotrophic *S. cerevisiae Pichia pastoris*. This unicellular organism has, like *S. cerevisiae*, the necessary eukaryotic processing and trafficking machinery to accommodate mammalian membrane proteins. In addition, it can reach much higher cell densities than are normally possible with *S. cerevisiae*. *P. pastoris* has been shown to be very suitable for the heterologous overexpression of several human ABC transporters before, including human MDR1 P-glycoprotein [195,197,199,265]. Notably, in one of these studies the expression of 25 human ABC transporters could be detected [199]. Interestingly, Chloupkova and co-workers did not report the expression of BSEP or MDR3, most probably due to cloning issues in *E. coli* as they were applying a ligation-independent cloning (LIC) strategy in order to clone several human ABC transcripts in a high-throughput fashion. Also, MRP2 expression could not be detected in *P. pastoris* [199]. Notably, the crystal structure of recombinant mouse MDR3 (the murine MDR1 homologue) coming from *P. pastoris* was solved, as this expression system could provide the necessary quality and quantity of membrane protein [55].

BSEP Expression in Pichia pastoris

Expression in *P. pastoris* is frequently accomplished from the chromosomal *AOX1* locus. The necessary recombination cassette is created by cloning the gene of interest downstream of the *AOX1* promoter into one of several commercially available plasmids that can be maintained in *E. coli*, but not in *S. cerevisiae*. They contain the upstream sequence of the strong inducible *AOX1* promoter followed by a multiple cloning site and a stretch of downstream *AOX1* sequence so that the gene of interest (GOI), after cloning into this vector is flanked by sequences that surround the

AOX1 structural gene on its chromosomal locus. *AOX1* is then replaced by the GOI via homologous recombination. Here, the *P. pastoris* integration vector pPIC3.5 was used. However, in order to achieve the chromosomal integration of the unstable *BSEP* cDNA along with the necessary vector-encoded sequences of the expression cassette, local assembly was deemed to be an impractical option as *P. pastoris* needs larger overlaps for an efficient site-specific recombination [266]. Such long overlaps are not easily added to the unstable GOI just with primers but instead require delicate fusion PCR reactions to splice together the whole linear expression cassette *in vitro*. In the light of the abundant clinical *BSEP* variants, such an approach is impractical.

Another point to be considered is that, by a local assembly strategy (see Results 3.3), multiple cassette integration events at the targeted chromosomal locus that are the basis of high-expressing clones [200] would become practically impossible. Three parts have to be recombined into the *AOX1* locus in the *Pichia* genome to form the expression cassette: upstream *AOX1* sequence, GOI, and downstream *AOX1* sequence. This entails four crossing-over events; multicopy integrants, however, depend on efficient integration of a first copy of the expression cassette followed by tandem integration events. The need for four recombination events to generate just one copy at the targeted locus is incompatible with the occurrence of multiple integration events.

3.10.1 The *Pichia pastoris* Integration Vector pPIC3.5 is made maintainable in *S. cerevisiae* for Recombination-Based Plasmid Construction

In essence, it would be favourable, if the pPIC3.5 vector could be made viable in *S. cerevisiae*, that is, maintainable and selectable. In a previous study, Vu and coworkers constructed a yeast-mammalian shuttle vector by integrating a mammalian expression cassette into the multiple cloning site of a *S. cerevisiae* plasmid [221]. In contrast, pPIC3.5 was prepared for manipulation in *S. cerevisiae* by integration of only the relevant sequence that is necessary for maintenance and selection in *S. cerevisiae* (Figure 35).

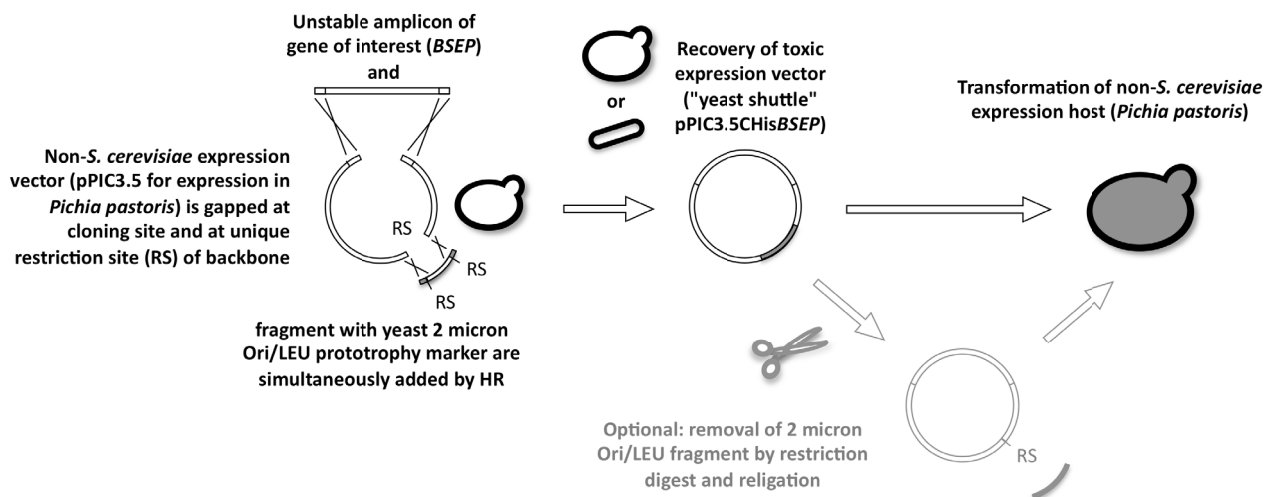


Figure 35. Moving BSEP expression from *Saccharomyces cerevisiae* to *Pichia pastoris*. A Toxic or unstable expression plasmids can be made for any system in *S. cerevisiae* by adding the necessary sequence to the plasmid backbone. In order to move BSEP expression from *S. cerevisiae* to *Pichia pastoris*, the pPIC3.5 recombination vector was double-digested to allow the simultaneous insertion of both the unstable *BSEP* coding sequence and a PCR-generated fragment of the YEphIS plasmid carrying the 2 micron origin (Ori) of replication and the leucine (LEU) prototrophy marker by homologous recombination (RS = *NdeI*). The plasmid was recovered from yeast and obtained in preparative amounts from *E. coli* by cultivation at 30 °C. The sequence necessary for propagation and selection in yeast was then removed by restriction digest and religation to avoid possible interference after chromosomal insertion in *P. pastoris*.

For this, a PCR product comprising the Ori and LEU marker region from the YEphIS plasmid was recombined into the single *NdeI* restriction site of pPIC3.5 simultaneously with a *BSEP* PCR product carrying a C-terminal his₈ tag and terminal overlaps to the sequence around the vector's *BamHI* cloning site (step 1). As this his tag location did not interfere with the expression of several other human ABC transporters in *P. pastoris* [199], it was also selected for BSEP. The resulting derivative pPIC3.5-CHISBSEP is identical to the construct that would be obtained by conventional bacterial cloning, with the exception that the backbone enhancement allows its maintenance and manipulation in *S. cerevisiae*. This construct was recovered from yeast and amplified in *E. coli*, taking the precautions described in Results section 3.5 (Figure 35). Prior to transformation and integration into the

chromosomal *Pichia AOX1* locus, the yeast Ori/LEU marker sequence was removed by digestion and religation of the vector. Abundant *Pichia* transformants were obtained and twelve of these tested for BSEP expression (Figure 36).

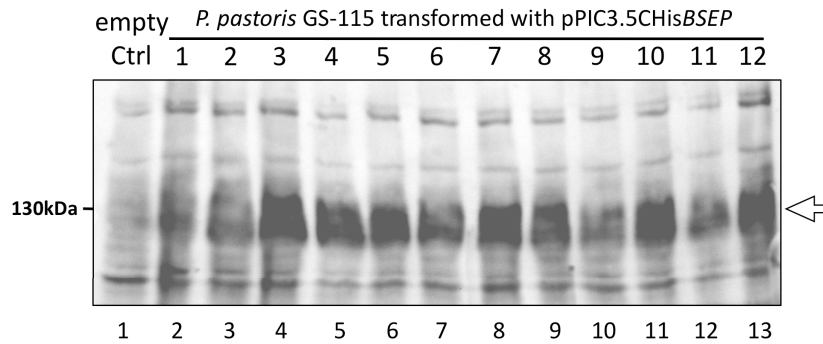


Figure 36. Human BSEP is expressed in *P. pastoris*. pPIC3.5-CHISBSEP was constructed as described in A and used to transform *P. pastoris* strain GS-115 by electroporation. Equal amounts of whole cell extracts from small-scale liquid cultures harvested after 48h after induction were resolved by SDS-PAGE, electroblotted and probed with K168 [203]. Empty Ctrl, parental *P. pastoris* GS-115 strain.

As shown by Western blot, all of the tested clones expressed BSEP at various levels (Figure 36 lanes 2 to 13) as compared to the control (lane 1). The level of BSEP expression achieved in highly expressing *P. pastoris* clones was found to be suitable for further purification and subsequent biochemical studies in our lab (see Discussion).

3.11 The Site-Directed Mutagenesis of Human *BSEP* by a New, *E. coli*-Independent Approach

One of the most common methods to generate targeted mutations is the site-directed mutagenesis (SDM) procedure [267]. In this method, a pair of oligonucleotides carrying the intended sequence mutation is used in which one primer is the exact reverse complement of the other. The product of this SDM reaction exists in a non-covalently closed circular form in which the full length of both primers comprises the annealed single-stranded overlaps. The nicks in the phosphodiester backbone of both strands are repaired after transformation of the mutagenesis product into *E. coli* [267]. As a result of this primer complementarity, the SDM reaction is a linear copying and not an exponential amplification of the template plasmid. The product of one SDM cycle can not serve as a template in the next one (Figure 37, left side), and thereby polymerase-introduced sequence errors are kept at a minimum. For introducing directed mutations into toxic or otherwise unstable DNA such as the *BSEP* and *MDR3* coding sequences, a different approach than standard SDM is needed as its product is a linearized, unstable plasmid that would perish in *E. coli*.

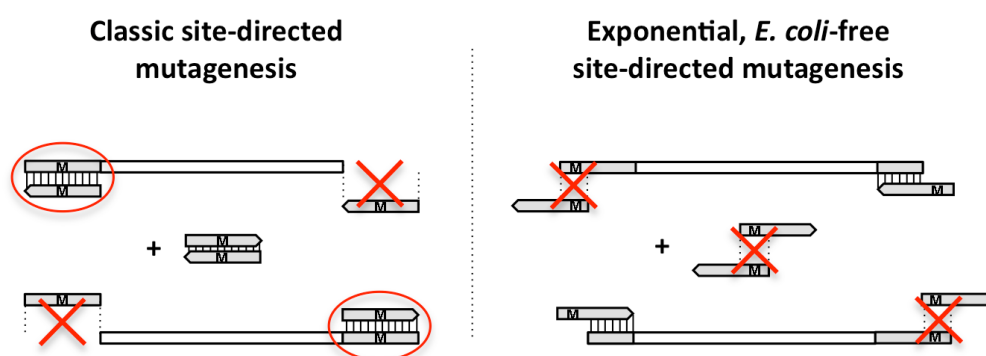


Figure 37. Primer binding on the mutagenesis products determines yield and the nature of the product termini. **Left** SDM product does not serve as template in the reaction. Absolute complementarity of the mutagenesis primers results in additional protection of the single-stranded termini (red circles) during annealing and extension steps due to their high T_m . **Right** SDM product is exponentially generated, from both template and product from previous cycles. The 20 bp 5'-complementarities of the primers have a lower T_m and do not protect single-stranded ends by annealing. This decreases unproductive 5' primer dimers, aiding in the exponential generation of product.

The new primers are constructed according to the following guidelines: both primers are about 50 bp in length, with the 5'-end consisting of 20 bp sequence overlap between the primers. This stretch is a minimum requirement for the later intramolecular homologous recombination that turns the mutagenesis PCR product into a circular plasmid in *S. cerevisiae*. Due to the exponential nature of the new site-directed mutagenesis, the number of cycles is strictly kept at 18 as in the classic SDM protocol [272] in order to minimize PCR-introduced errors. In addition, a proofreading DNA polymerase is used with an error rate equal to that of the *Pfu* Ultra enzyme in the commonly used Stratagene kit [273].

Proof of Concept:

Targeted Mutagenesis of BSEP and MDR3 Constructs in S. cerevisiae

As proof of principle and to establish the efficiency of the yeast-based mutagenesis, the unstable, 12 kbp YEpHISBSEP plasmid was mutated with the new site-directed mutagenesis method, completely avoiding the use of *E. coli*. A primer pair was designed according to the devised guidelines that carried a missense mutation. This changes a glycine at amino acid position 1032 to arginine (G1032R), thus introducing an additional *Bst*BI recognition site into the vector (Figure 39). For comparison, SDM was also performed with a mutagenesis primer pair of classic design that contained the same mutation, which is a single nucleotide exchange at position 3094 (counted from the A of the *BSEP* cDNA start codon) from G to C. The shift to an exponential product generation can clearly be seen in Figure 39A (compare middle and right panel). As an additional control, a mock-treated SDM reaction (thermocycled without DNA polymerase) was included in the experiment. In both control and SDM, neither template nor product was detectable, and only a slight smear could be observed. This is not uncommon, as the standard SDM yield especially of large template plasmids not always permits visual detection on an agarose gel [272]. In addition, the repeated thermocycling is expected to result in the stepwise degradation of template. Nonetheless, competent yeast cells were directly transformed with all of the reactions. The mock-treated (left) and the standard SDM reaction (middle) did not result in the formation of yeast colonies, and only the modified site-directed mutagenesis protocol yielded abundant colonies. Classic SDM products can in theory be nick-repaired by yeast [274], while the modified product is recircularized by homologous recombination of its double-stranded ends. Clearly, the classic SDM

product yield was then insufficient for a successful chemical transformation of *S. cerevisiae*. In contrast, a single mutagenesis reaction of the new design was enough to give ~ 100 colonies after transformation (Figure 39A, right panel). 25 of the resulting transformants were picked and the targeted plasmid region was first amplified by colony PCR, then directly subjected to *Bst*BI digestion (Figure 39B).

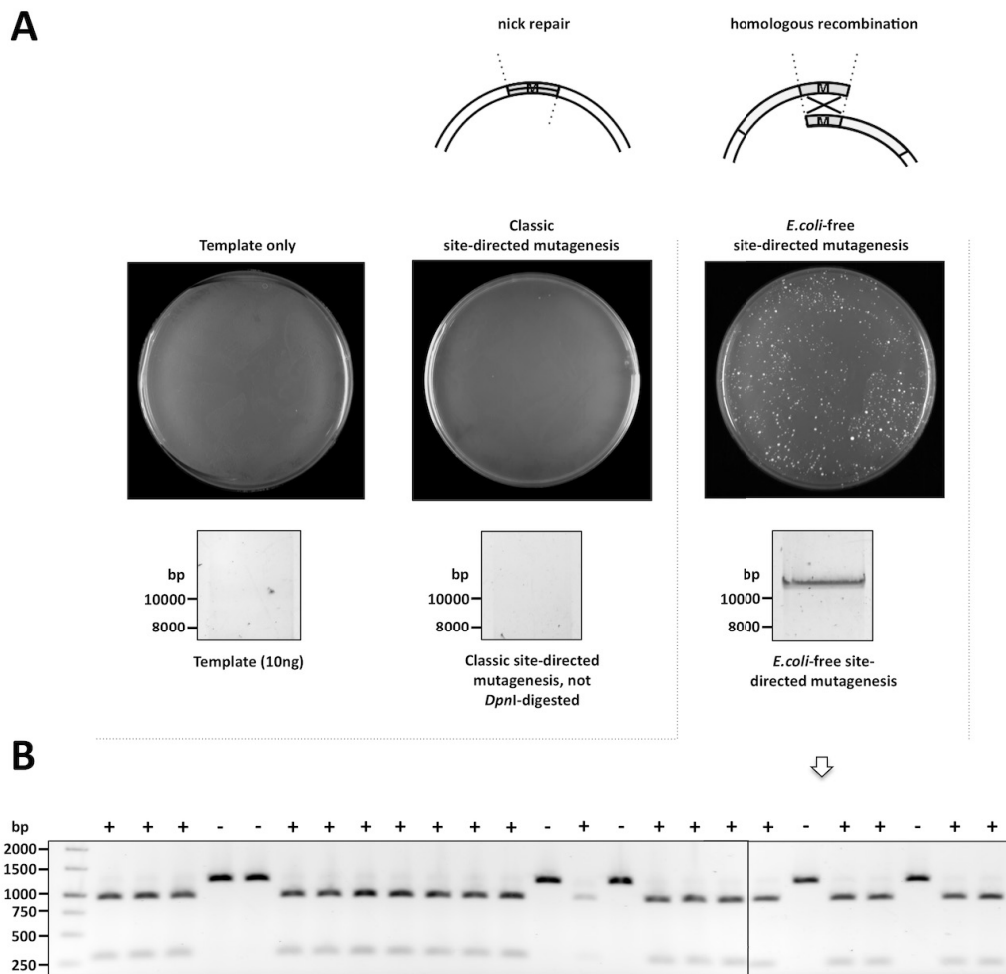


Figure 39. An unstable *BSEP*-plasmid is mutated with high efficiency, without the use of *E. coli*. **A** Only the modified SDM results in colony formation after direct transformation of yeast (right), whereas a mock-treated (without polymerase, left) and a standard SDM reaction (middle) do not yield transformants. **B** Successful mutagenesis results in the addition of a *Bst*BI restriction site into the *BSEP* coding sequence. Colony PCR of the resulting transformants was performed with primers surrounding the mutagenesis site, and the resulting product was digested with *Bst*BI. 19 of 25 clones carried the additional restriction site, corresponding to an mutagenesis efficiency of 76 %.

From these 25 clones, 19 could be digested and thereby carried the introduced mutation, corresponding to a mutagenesis efficiency of 76 %. This is well in the range of the 80 % efficiency reported for the *E. coli*-based SDM by the kit manufacturer [272]. The plasmids from two randomly picked, *Bst*BI-positive yeast clones were recovered and, after amplification in *E. coli*, the integrity of the complete *BSEP* coding region could be confirmed by sequencing.

The functionality of the new mutagenesis method was additionally tested on the YEpHIS*MDR3* construct. Here, an E558Q mutant of *MDR3* was generated that inactivates one of the ATP binding cassettes in the NBDs (see Introduction 1.3). Primers were again designed according to the described guidelines, and the resulting transformants were sequenced. As shown in the electropherograms in Figure 40, this mechanistically relevant mutant could be constructed as described for the clinical *Bst*BI mutation in Figure 39. Again, the integrity of the *MDR3* coding region could be sequence-verified.

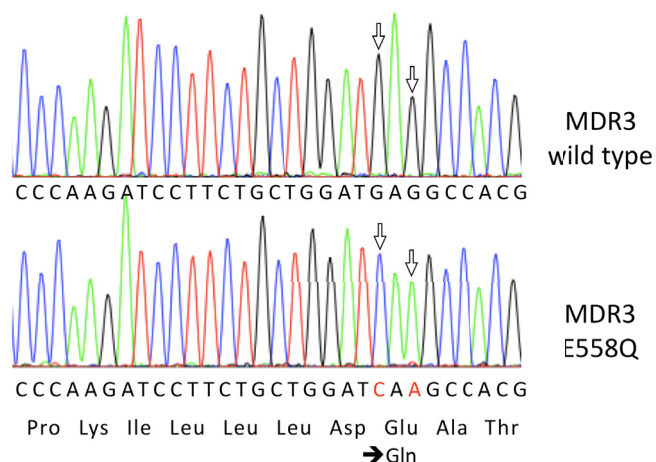


Figure 40. Sequence analysis of the E558Q YEpHIS*MDR3* missense mutation created with the *E. coli* free SDM. Upper panel Wild-type *MDR3* sequence. Lower panel Sequence from *MDR3* (E558Q). Arrows indicate the corresponding base changes. This mutation removes the catalytically important glutamate residue in the Walker B motif of the first NBD of *MDR3* (see Introduction 1.3).

3.12 Rapid Site-Directed Mutagenesis and Expression Analysis of a Yeast-Enabled Mammalian BSEP Expression Vector

Essentially, the recombinant DNA techniques used and developed so far for the unstable *BSEP* and *MDR3* sequences allow their cloning, maintenance, and mutagenesis in yeast. As many human membrane proteins are studied using mammalian cell lines, a consecutive step was to combine all established methods into a complete workflow that allowed the potential manipulation (see Results 3.10) and mutagenesis (Results 3.11) of plasmids used to express proteins in cell culture. This allows the study of aspects such as the localization of the transporter in a native cellular setting (i. e. human cell lines). Therefore, a yeast-compatible derivative of the mammalian *BSEP* expression vector pEYFP-N1-*BSEP* [210], that is used to study transporter localization in human cell lines, was created in analogy to the *P. pastoris* vector modification shown in Results 3.10.1 (see Figure 35). After sequence verification, the "yeast shuttle" construct could successfully be transfected into HEK293 cells with comparable efficiency as the parental non-yeast shuttle plasmid (Figure 41). The cell culture work and fluorescence microscopy was kindly performed by Dr. Claudia Stross (Department of Gastroenterology, Hepatology and Infectiology, Heinrich Heine University Düsseldorf) as part of a cooperation on the generation and analysis of clinically relevant *BSEP* mutations. Detection of the fluorescent eYFP-tag in the *BSEP* fusion protein showed the same localization of the ABC transporter expressed from both constructs to the plasma membrane (Figure 41A, B). From these observations, it could be concluded that the presence of the additional backbone sequence does not influence the properties of the construct in cell culture. In the yeast-enabled construct, the missense *Bst*BI mutation was then introduced by the new *E. coli*-free SDM method described above. After plasmid recovery and subsequent transient transfection, the *Bst*BI construct variant expressed in HEK293, MDCK, and HepG2 cells (Figure 41C). Comparison of the *Bst*BI to wild type *BSEP* expression showed a different localization pattern: although the plasma membrane was consistently fluorescent in HEK293, MDCK and HepG2 cells, the cytoplasm showed a clear fluorescence that was not present in HEK293 cells transfected in the control or yeast-enabled wild type. This suggested an at least partial defect in trafficking of the mutated *BSEP* fusion protein to its cellular target location, the plasma membrane.

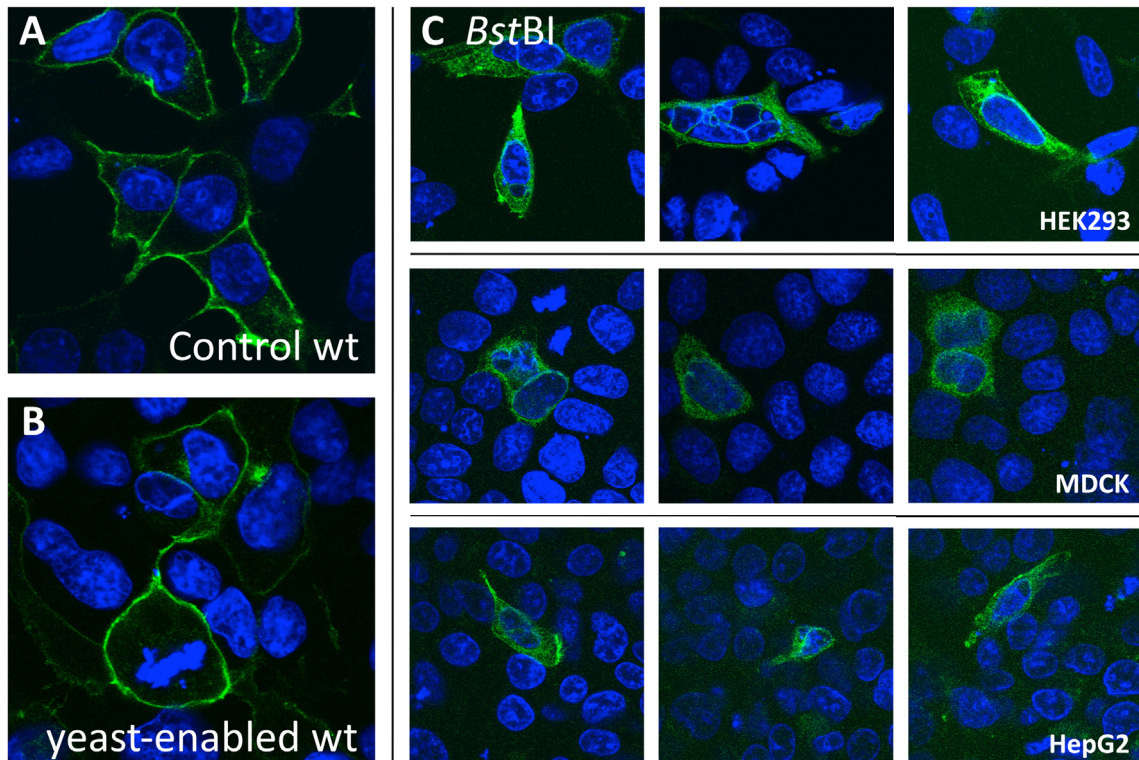


Figure 41. The yeast-maintainable mammalian *BSEP* expression construct is functionally indistinguishable from the non-yeast parental plasmid in cell culture. **A** HEK293 cells transfected with pEYFP-N1-*BSEP* [210]. **B** HEK293 cells transfected with pEYFP-N1-OriLeu-*BSEP*. Equimolar amounts of both constructs showed the same transfection efficiency as shown by FACS analysis. **C** HEK293 (upper panel), MDCK (middle), and HepG2 cells (lower panel) were transfected with the *Bst*BI mutation in pEYFP-N1-OriLeu-*BSEP* that was introduced with the *E. coli*-free site-directed mutagenesis method. All cells were transfected with equimolar amounts of the respective constructs via the Fugene reagent according to the manufacturer's guidelines. After fixation, nuclei were stained with Hoechst 34580 (blue), and the fluorescence (green) of the eYFP tag in the *BSEP* fusion protein was observed.

4 Discussion

The bile salt export pump and the multidrug resistance protein 3, two human ABC transporters connected with severe hereditary diseases of the liver, could be overexpressed in two yeast species for the first time (Results 3.3 and 3.10). As a result of this work, *in vitro* biochemical studies on the purified BSEP and MDR3 ABC transporters can now be engaged. A constant source of protein is now available, from unicellular eukaryotes that, unlike mammalian or insect cell culture, can deliver substantial cell mass in a short amount of time. Equally important, the recombinant protein can now easily be adjusted to any arising needs: mutations of both clinical and mechanical relevance can be and have been generated with ease in the unstable *BSEP* and *MDR3* coding sequences with an *E. coli*-independent site-directed mutagenesis method (Results 3.11 and 3.12). With the *Bst*BI (BSEP) and the EQ (MDR3) mutations, both a clinically and a mechanistically relevant mutation could be realized without any of the problems previously encountered when attempting mutagenesis in *E. coli*. Together with the means of *in vivo* homologous recombination in *S. cerevisiae* (Results 3.3, 3.4, 3.5, and 3.10), this constitutes a complete workflow that permits the generation of constructs from and manipulation of these unstable sequences without the use of a bacterial organism if this is required.

4.1 The Impact of Affinity Tag Position on the MDR3 Fusion Protein demonstrates the Empirical Value of Expression Screens

An unexpected finding was the drastic decrease in protein levels of the N-terminally his-tagged MDR3 upon change from chromosomal to plasmid-based expression. Both fusion proteins are, on the genetic level, identical, including the recombinant N-termini. The chromosomal expression clearly shows that the recombinant protein itself is not intrinsically destabilized by the his tag at the N-terminus. It was, as all other expressed variants of both MDR3 and BSEP, associated with the membrane fraction, and MDR3 co-localized with the plasma membrane-resident Pdr5 (Results 3.7, Figure 20). Here, the comparison of both his tag positions on MDR3 showed an identical pattern of subcellular distribution, and thereby a mistargeting of the N-terminal tag fusion can be ruled out. In support of this, the M800I mutant of MDR3 conferred a weak cellular resistance in *S. cerevisiae* against the antifungal compound FK506 (Results 3.8, Figure 22), which also indicates a functional protein at the

plasma membrane. Also, the chemical chaperone glycerol did not rescue the low plasmid expression of Nhis₁₄-MDR3 (Results 3.6, Figure 19). All this is indicative of a properly folded and targeted integral membrane protein. What then remains to explain this difference in expression of two identical proteins? Both the *PDR5* and *PMA1* promoter are highly active during the exponential growth phase and were found to be of comparable strength in the *pdr1-3* strain background used throughout this study, because in highly enriched plasma membranes of *pdr1-3 S. cerevisiae* cells Pdr5 and Pma1 were two dominant protein bands of comparable intensity [186]. The nature of the two mRNAs expressed from chromosome or plasmid may be very different with respect to translational activity or lifetime. Figler and colleagues added a short stretch of the 5'-untranslated region (5'-UTR) of the highly expressed *PMA1* gene [11] to their YEpHIS construct downstream of the *PMA1* promoter and found an increased MDR1 expression [182]. In the empirical approach to obtain overexpression, the levels of the two mRNA species were not quantified and leave potential differences in mRNA stability to speculation.

The unexpected impact of the same affinity tag in different settings in any case illustrates the value of empirical screening approaches in the attempt to push the expression of a given protein: a single-copy, N-terminal fusion protein expression leads to higher expression than the multi-copy version, against expectations that would be the result of an "educated guess". Expression levels for MDR3 with a C-terminal his tag reach those that are achieved for MDR1 in *S. cerevisiae* [182]. Here, a yield of milligram amounts per L of mid-log growth phase culture was reported. The C-terminal tag variant of MDR3 expressed from plasmid in the same range of yield and could be preliminary affinity-purified to an amount of about 2 mg from a 10 L culture (Results 3.9). One potential way to further increase MDR3 yield in *S. cerevisiae* is the reintroduction of the corresponding coding sequence into the *PDR5* locus. First, chromosomal expression of MDR3 with a C-terminal tag can be expected to result in higher yields, because every cell in the culture carries the expression cassette as a part of its genome. This is not the case in plasmid-based expression, where the plasmid copy number in the cell population can fluctuate throughout the fermentation process [275]. Additionally, the metabolic cost of plasmid selection on the cells is abolished (growth in the presence of antibiotics, or the need to synthesize an amino acid missing in the growth medium), and in the case of *S.*

cerevisiae, rich media can be used for the expression of stably integrated coding sequences.

4.2 Overexpression of Human BSEP

Low BSEP Expression in S. cerevisiae

In contrast to the strong influence of the tag position on MDR3 expression, the low expression of BSEP from the *PDR5* locus with a N-terminal his₁₄ tag was found to be independent on tag position. A shift from the N- to the C-terminal tag configuration did not increase the expression from the same construct that was also used for MDR3 (Results 3.4). An expression screen probing the combination of both his tag positions with a set of different promoters failed to produce an overexpressing *BSEP* vector (Results 3.5). The strain background was strictly kept to the Δ PP strain for two reasons: several native yeast membrane proteins could be overexpressed from the *PDR5* locus [191], and the absent major PDR transporter PDR5 does not interfere with cellular drug assays (Results 3.8). The most influential strain characteristic with respect to heterologous protein production is likely to be the cellular repertoire of chaperones that facilitate protein folding and proteases that remove misfolded proteins. While there is a number of protease-deficient available *S. cerevisiae* strains, degradation did not seem to be a problem as judged from Western blots of whole cell lysates (Results 3.3 and 3.4). For the BSEP transporter, that is less homologous to the good "yeast-expresser" MDR1 than the better-expressing MDR3, *S. cerevisiae* may simply be a suboptimal choice. The bile salt export pump may need specific interacting proteins (such as human chaperones [276]), or the mRNA might be translated with limited efficiency due to differences in codon usage. Obvious differences in *BSEP* codon utilization that might give rise to problems after the switching from human to expression in yeast were not found. Under such vague circumstances, that are commonplace when starting to work on a membrane protein of interest (reviewed in [276]), a first empirical screening approach should always encompass different expression systems in order to produce a first "hit". *S. cerevisiae* proved to be such a first hit on the way to the large-scale (i. e. mg/L) protein production of BSEP. The test of other yeast species may change the repertoire of chaperones and proteases (along with a plethora of other parameters) in favour of a better target protein expression.

BSEP can be purified from Pichia pastoris

The usefulness of *P. pastoris* as a suitable host for membrane protein overexpression is firmly established (see Introduction 1.7). Supporting this notion, human BSEP could be brought to overexpression in *P. pastoris* (Results 3.10). The affinity purification of BSEP from this source was subsequently accomplished and is currently under optimization (personal communication by M.Sci. Philipp Ellinger). For this, the expression cassette was changed from a C-terminal, single his₈ tag to a dual tag configuration that comprises both a his₈ and a calmodulin binding peptide (CBP) tag [199]. This allowed for a tandem affinity purification procedure which yields preparative amounts of protein of high purity in two steps.

4.3 Further Steps towards *In Vitro* Studies of BSEP and MDR3

The example of MDR3 shows the next necessary steps: further purification and reconstitution into proteoliposomes of both wild type and relevant mutant protein variants. Gel filtration of detergent-solubilized MDR3 resulted in the separation of aggregates in the void volume of the column and a broad peak that contained the protein along with other impurities, that at least partially are derived from MDR3 itself (Results 3.9). Upon concentration by filter membranes with a proper molecular weight cutoff these impurities remained, suggesting that these MDR3 fragments were residing in detergent micelles that could not pass the pores of the filter device. This assumption is supported by the observed molecular weight of the two main fragments which correspond to about half the size of the full-length protein and therefore most likely contain transmembrane segments. A similar cleavage pattern was observed for BSEP upon solubilization in Fos-choline 16 (Results 3.9, Figure 31). The continued state of solubilization in micelles of this comparatively strong detergent may facilitate the degradation of MDR3 throughout the purification process. To solve this problem, an exchange on the IMAC column to a more gentle detergent such as DDM may be helpful [277]. The exchange to gentler detergents may lead to micelles in which the membrane protein is more protected from proteases and its native conformation is less compromised. In addition, a detergent that keeps the protein "happy" in solution can have substantial impact on the homogeneity of the protein-micelle population and thereby facilitate purification by forming a sharper elution peak during gel filtration than found with the initial, solubilizing detergent (Results 3.9, Figure 34).

Functional, Cysteine-Free, and Glycosylation-Deficient Mutants

Another step that is directed more towards potential structural studies of MDR3 and BSEP is an increased homogeneity of the purified proteins themselves. This can either be achieved by generating non-functional, "dead" mutants in which the catalytically relevant glutamate residues in the non-degenerate NBDs (one in BSEP, two in MDR3) are substituted by glutamine residues [35,59]. A bound substrate or inhibitor may be capable of locking these protein variants in one or a narrow ensemble of similar conformations. Another way to limit conformational diversity of a protein in heterologous systems is the generation of a cysteine-free version of the wild-type protein. Cysteines can form disulfide bridges *in vivo*, and heterologous expression into the ER of a host that may not be able to facilitate their correct formation can result in a heterogeneity of protein conformations, which in turn prevents ordered formation of a crystal lattice. A functional cysteine-less mutant of mouse P-gp was generated and expressed in *P. pastoris* [278]. Erroneous glycosylation may be another source of protein microheterogeneity, which may be abolished by mutation of the residues (asparagine and arginine in N-glycosylation). Hyperglycosylation may also be an impediment to overexpression in some cases [276]. Using the new SDM method, any of these mutations can be introduced with little effort into *BSEP* and *MDR3* expression constructs.

4.4 Lack of a Cellular Phenotype of BSEP Expression in *S. cerevisiae*

The finding that the BSEP substrate taurocholate inhibited *S. cerevisiae* growth already at a concentration below 1 mM, while BSEP expression from none of the constructs conferred resistance against this conjugated bile salt (Results 3.8), gives rise to several questions. According to subcellular fractionation experiments (see Results 3.7), intact BSEP is at least partially located at the yeast plasma membrane. The lack of mammalian glycosylation patterns in either *S. cerevisiae* or *P. pastoris* is highly unlikely to result in an inactive protein as several MDR efflux pumps that feature various degrees of glycosylation in their native tissue could be functionally expressed in both yeast species [181,182,183,184]. Human MDR1, which in this study was used as an expression control, was fully functional in *S. cerevisiae* and conferred a multidrug resistance phenotype (Results 3.8, Figure 21). Why then is no taurocholate resistance observed? The mode of taurocholate-mediated cytotoxicity is

assumed to be the disruption of the yeast plasma membrane by solubilization. The low expression levels of its cognate export pump may simply be insufficient to protect the cells against the toxic effect of TC. Future resistance assays conducted on BSEP-expressing *Pichia* recombinants may prove more conclusive, although expression during growth on solid media may differ significantly from that achieved by fermentation. A prerequisite for these resistance assays is the correct localization of BSEP to the plasma membrane of *Pichia* which can be investigated by subcellular localization.

4.5 The M800I Variant of MDR3

A mutated, N-terminally his₁₄-tagged MDR3 that had a methionine to isoleucine exchange at amino acid position 800 conferred a weak resistance against the antifungal compound FK506 in *S. cerevisiae* (Results 3.8, Figure 22). The wild type protein, in contrast, failed to protect the yeast cells, although both variants are expressed to the same extent (Results 3.3, Figure 9). This was an unexpected and intriguing finding, since this mutation seems to result in an at least partially altered substrate spectrum of this highly specific phosphatidylcholine translocase [83]. Although MDR3 was shown to transport a few compounds in polarized monolayers of transfected cells to some extent [175], this compound was not tested in that study. The M800I mutation has not yet been described in a clinical or mechanistic context. A multiple alignment of MDR1, MDR3, and BSEP from mouse, rat and human shows that this residue is located in a conserved sequence stretch (Figure 1) that comprises the intracellular loop between transmembrane helices 7 and 8 in the structure of the closely related mouse MDR1 (Figure 2). In human MDR1, this position is occupied by a valine residue, and in all other cases an isoleucine is found at this position.

Interestingly, this loop has previously not been implicated in interdomain crosstalk (see Introduction 1.3). For this, the interface made by the coupling helix and the structurally diverse region of the NBDs was the central candidate [279]. If this mutation has mechanistic relevance and causes not some random pleiotropic effect, then this highly conserved residue has a role in interdomain communication: its mutation allows the triggering of the catalytic export cycle by ATP binding in the NBDs in response to FK506 binding which is assumed to take place in the central cavity formed by the two TMD segments.

```

KSMLRQDIISWFDHKNSTGSLTTRLASDASSVKGAMGARLAVVTQNVANLGTGVILS--L 849 MDR1_MOUSE
KSMLRQDIISWFDHKNSTGSLTTRLASDASNKVGAMGSRRLAVVTQNVANLGTGIILSLVL 851 MDR1_RAT
RSMLRQDVSWFDDPKNTTGALSTRRLANDAAQVKGAIGSRLAVITQNIANLGTGIIIS--F 851 MDR1_HUMAN
KAMLRQDMSWFDHKNSTGALSTRLATDAAQVQGATGTKLALIAQNTANLGTGIIIS--F 847 MDR2_MOUSE
KAMLRQDMSWFDHKNSTGALSTRLATDAAQVQGATGTRLALIAQNTANLGTGIIIS--F 849 MDR2_RAT
KAMLRQDMSWFDHKNSTGALSTRLATDAAQVQGATGTRLALIAQNTANLGTGIIIS--F 850 MDR3_HUMAN
KAMLRQDIISWFDLKNPNPGLTTRLATDASQVQGATGSQVGMVNSFTNIFVAVLIA--F 894 ABCBB_MOUSE
KAMLRQDIISWFDLKNPNPGLTTRLATDASQVQGATGSQVGMVNSFTNIIAALLIA--F 894 ABCBB_RAT
RAMLGQDIISWFDLKNPNPGLTTRLATDASQVQGAAGSQIGMIVNSFTNIVTVAMIIA--F 894 ABCBB_HUMAN
::** **:.**** :*..* *:****.*:.*** *:::..... :*: ..... :

```

Figure 1. Multiple alignment of MDR1, MDR3, and BSEP from mouse, rat, and human. Alignment made with ClustalW2 on the ExPasy website (www.expasy.ch). M800 is found in a highly conserved stretch of sequence that comprises the intracellular loop between the transmembrane helices 7 and 8 of the second TMD. Mouse MDR1 is the murine ABCB1.



Figure 2. Putative localization of the M800I mutation on the mouse P-glycoprotein. The crystal structure comes from mouse ABCB1, the murine functional homologue of the human MDR1 efflux pump [55]. **Left side** Overall structure of mouse P-gp. Four helices of the *cis* and two of the helices from the *trans* TMD in this inward opened structure form a clustered transmembrane segment interfacing each of the NBDs. **Right side** Detail of the TMD loops interfacing with the NBD. The mutation is located in the connecting loop between TM helices 7 and 8 of the *cis* helix bundle part in the second NBDs' TM segment. Amino acid position 800 is in the center of a stretch of residues conserved in mouse ABCB1, human MDR1 and MDR3 P-glycoproteins. Interestingly, only MDR3 has a methionine at position 800, while both the mouse and human efflux pumps have a valine in this position (the corresponding residue is depicted in the structure in green).

Further studies based on systematic mutations in this loop and in its counterpart helix in the other TMD unit are needed to pinpoint the exact mechanistic role of this residue and the cytosolic helix it resides in.

4.6 Lack of MRP2 Expression in *S. cerevisiae*

The lack of MRP2 expression in *S. cerevisiae* is likely to be an intrinsic characteristic of this transporter in general, as both a C- and an N-terminal tag position were tried and found not to express (Results 3.2 and 3.8, Figures 6 and 28, respectively). Interestingly, *MRP2* also did not express in *Pichia pastoris* (supplementary material to [199]). In general, *S. cerevisiae* should be capable to correctly fold and traffic a membrane protein of MRP-type topology as its genome contains several MRP-type ABC transporters [180]. One (empirical) option that might lead to expression is the removal of the extra, N-terminal TMD0 segment of MRP2. This five transmembrane-helix domain was found to be dispensable for transporter function [157,158], although it was necessary for apical membrane sorting for MRP2 [156]. After its deletion on an expression plasmid, both his tag configurations can again be tested for a detectable expression. In this context, either a suitable antibody has to be found that does not detect any of the native ABC transporters in *S. cerevisiae* that shape its wild-type repertoire, or a more suitable strain should serve to probe for MRP2 expression in future attempts. Interestingly, the background detected by both the MLE and the M₂III-6 antibodies was not present in the AD1-8U⁻ strain that is devoid of seven PDR and compound efflux related ABC transporters (Results 3.2, Figure 6). Since both yeast strains lack the *PDR5* gene, this ABC transporter can be ruled out as the source of the intrinsic immunoreactivity. Pdr5 is, at any rate, not a MRP-type ABC transporter. Of the transporters that are absent in AD1-8U⁻, only Yor1 and Ycf1 belong to the MRP/CFTR-subfamily of *S. cerevisiae* ABC proteins [280]. Yor1 lacks the TMD0 segment, but has a large, N-terminal cytosolic loop that is found between the TMD0 and TMD1 domains in human MRP1, 2, and Ycf1 of *S. cerevisiae*. A sequence analysis indicates similar C-terminal portions of Yor1, Ycf1, and MRP2 that might all be recognized by the monoclonal M₂III-6 antibody, while the N-terminus of MRP2 recognized by the polyclonal MLE antiserum is not conserved in Yor1 and Ycf1. So most likely the cross-reaction comes from one of these ABC transporters.

4.7 DNA Cloning and Manipulation in *S. cerevisiae*

4.7.1 Yeast Recombination as a Flexible Tool in High-Throughput Applications

As shown in this work, recombination-based cloning in *S. cerevisiae* has tremendous potential for high-throughput expression screening (for example, see [281]), because cloning and expression can be accomplished in the same cell, and the resulting transformants can instantly be screened for protein expression. The construction and expression test of the first yeast *BSEP* expression plasmids (Results 3.4) can, from obtaining the gapped plasmid backbones by restriction digest and performing the *BSEP* PCRs to the final Western blot detection, be completed in as little as six days, which may be considered a short time-frame when working with such unstable constructs. A complete recombinatorial expression screen as shown for *BSEP* can be achieved in as little as two weeks (Results 3.5, Figure 15). Currently, several sets of *S. cerevisiae* expression vectors are available that include different promoters and a variety of available tags at both ends (for a good overview, see <http://web.uni-frankfurt.de/fb15/mikro/euroscarf/>). Most, if not all of these sets are built in a similar fashion, meaning that with a single primer pair for the insert all vectors in the set can be used.

4.7.2 Non-Yeast Plasmids and their Manipulation in *S. cerevisiae*

In order to use any given plasmid for direct cloning in yeast, it has to be properly maintained, replicated, and selected for in this organism. This is easily accomplished by the addition of a yeast 2 micron ori and prototrophy marker sequence as shown for the pPIC3.5 vector (Results 3.10.1, Figure 35) and the mammalian expression vector pEYFP-N1-*BSEP* (Results 3.12). Notably, it was subsequently found for the pPIC3.5 construct that the Ori/LEU sequence could be left in the backbone as its presence on the chromosomal *AOX1* locus did not seem to impact on *BSEP* expression or the viability of *P. pastoris*.

4.7.3 Recovery of Unstable Plasmids from Yeast and Propagation in *E. coli*

Genes and DNA sequences in general can be unstable in their bacterial host for a variety of reasons, including: extensive secondary structure (e.g. z-DNA [223]), inverted or direct sequence repeats, encoding a gene product toxic to host metabolism, or carrying unintended prokaryotic signal sequences as was the case for

BSEP [174]. *BSEP* plasmids were, once constructed in yeast, found to be sufficiently stable in *E. coli* at 30 °C. Plasmid integrity could be verified by analytical restriction digest and DNA sequencing. In this context, it should be noted that, although some groups have at succeeded in creating full-length human *BSEP* constructs, their generation in *E. coli* has not been a straightforward procedure due to the instability of the *BSEP* and MDR3 cDNAs [174,175,207,222]. Another issue regarding their handling is the seemingly random loss of bits of the coding sequence when trying site-directed mutagenesis using *E. coli*. This most probably arises due to bacterial selection of incomplete, dysfunctional plasmid species that are stable und thus retain the encoded selection marker upon recircularization in their host. While the amplification of an intact construct in bacteria is highly unlikely to be a general option when attempting this for other unstable or toxic coding sequences, changing the host back to *E. coli* after yeast recombination has one advantage: unlike in a ligation mixture that contains a heterogenous mix of linearized vector, insert, partial and complete vector-insert ligations, the unstable plasmid recovered from yeast is in a nick-free and intact form. Several *E. coli* strains that are custom-tailored to meet diverse requirements can then be tested for their propagation properties, starting from the common basis of an intact construct.

4.7.4 General Advantages of *S. cerevisiae* as a Cloning Tool

In bacterial cloning, a large (i. e. in the range of several kbp) insert already is prone to inefficient cloning due to size bias [229], while generally being of no concern in yeast recombination. For the efficient, high-throughput cloning of such inserts in *E. coli*, ligation-independent cloning (LIC) [282] is often applied to streamline the process and optimize cloning efficiency [283]. This necessitates the introduction of LIC linker sequences that, depending on the strategy, can lead to the introduction of extra amino acid residues to at least one end of the protein. The homologous recombination process on the other hand has the additional advantage of utilizing existing constructs without any need to modify the cloning site with LIC linkers, while being as high-throughput compatible.

4.7.5 The New, *E. coli*-Independent Site-Directed Mutagenesis Approach

A critical review of the classic SDM mechanism [267] was the necessary basis of attempting an *E. coli*-independent approach. In this method, a pair of oligonucleotides carrying the mutation is used in which one primer is the exact reverse complement of the other. Both will form a perfect short stretch of double-stranded DNA. In the presence of the plasmid template, a small but sufficient percentage of both primers also bind to their respective priming sites on the template DNA. A DNA polymerase extends each primer around the length of the plasmid until the very nucleotide behind the 5'-end of this same primer. Upon reaching this end, the enzyme stalls and falls off the double-stranded DNA, leaving behind a nick in the phosphodiester backbone. As a result of primer complementarity, the product of this SDM reaction exists in a non-covalently closed circular form in which the full length of both primers comprises the annealed single-stranded overlaps. Both nicks are repaired after transformation of the reaction product into *E. coli* [267].

Why Template Removal is necessary in Classic SDM

Due to the non-exponential nature of the mutagenesis step, the mutagenesis product is not in great excess over the unmutated template. Thus the latter needs to be removed by digestion with the restriction endonuclease *DpnI* which recognizes the template due to its *Dam*-mediated methylation obtained in the bacterial host from which it comes. Otherwise a great percentage of the picked clones will contain the original plasmid without the mutation. This methylation is not a feature of the mutated product generated *in vitro*, and *DpnI* recognizes and cleaves methylated and hemimethylated (consisting of heteroduplex DNA formed by template and mutagenesis product) double-stranded DNA. The recognition site (5'...G m6A⁺T C...3') consists of four base pairs and occurs quite frequently, so the unmutated DNA is cleaved into short fragments and thus efficiently removed. The remaining amount of mutagenized DNA is sufficient to chemically transform highly competent *E. coli* cells.

Due to Full Primer Complementarity, the Classic SDM is a Non-Exponential Reaction

The SDM reaction is, however, a non-exponential, linear copying rather than an exponential amplification of the template plasmid. The reason for this is again found in the absolute primer complementarity: the product of the first SDM cycle has, as

explained above, single-stranded ends that are comprised of the primers themselves. These in turn can again fully bind their respective counterpart, which, however, is an unproductive priming situation. As a result, the product of one SDM cycle can not serve as a template in the next one. The SDM method is designed based on the reasoning that sequence errors introduced by DNA polymerase nucleotide misincorporation should be kept at a minimum. If a nucleotide misincorporation were to occur in one cycle of an exponential, polymerase *chain* reaction, this error would be exponentially copied in subsequent cycles. This is simply prevented by the non-exponential nature of the SDM procedure as only the original can be copied in each mutagenesis cycle.

Designing a New Site-Specific Mutagenesis Procedure Based on Classic SDM

For introducing directed mutations into toxic or otherwise unstable DNA such as the *BSEP* and *MDR3* cDNA, a different approach than standard site-directed mutagenesis is needed, since the usage of *E. coli* must completely be avoided. It has been shown in Results 3.5 that only *intact BSEP* and *MDR3* plasmids (constructed by homologous recombination in and recovered from *S. cerevisiae*) could be maintained with sufficient stability in *E. coli*. The site-directed mutagenesis product, however, is not an intact, nick-free plasmid as discussed above. Sufficient amounts of plasmid template for the classic SDM approach can be obtained directly from yeast (see Results 3.5). However, all DNA in *S. cerevisiae* is unmethylated and thus cannot be removed from the final mutagenesis reaction mixture by *DpnI* digestion [268,269,270]. While it is possible to methylate the template DNA *in vitro*, this is hardly a practicable way as this constitutes several additional reaction steps, complicates handling, and a complete methylation can be considered unobtainable under *in vitro* conditions. If the template is not removed, the mutated product has to drastically outnumber the template for a suitable mutagenesis efficiency. Generating more product is also a prerequisite for the efficient transformation of yeast cells, as this requires more DNA than is generated during a SDM reaction. Finally, to obtain transformants directly from *S. cerevisiae*, the linear product obtained from a polymerase-based procedure needs to be precisely recircularized by its host, even after a change in primer design.

Turning the Classic SDM Reaction into a Genuine, Exponential PCR

By changing the mutagenesis primer design from a complete to a partial, 5′-overlap of the primer pair the mutant strand synthesis reaction from classic SDM is turned into an exponential, PCR-like reaction. Due to this extensive primer shift, a product is generated that carries terminal primer binding sites that can be used for productive priming. As a result, the mutagenesis product functions as a template in all subsequent reaction cycles. A similar shift of primer positions has previously been reported in a different context [271], where a more efficient simultaneous introduction of more than one mutation in *E. coli* was desired. By strictly keeping the annealing temperature above the T_m of the 5′-overlap of the primer pair ($T_{ann} = 60\text{ °C}$), the ends of the mutagenesis product should become double-stranded. The different impacts of both the classic and the new primer design on the mutagenesis are compared in detail in Figure 3. The new primers are constructed according to the following guidelines: both primers are about 50 nt in length, with the 5′-end consisting of 20 nt sequence overlap between the primers (lower panel, left).

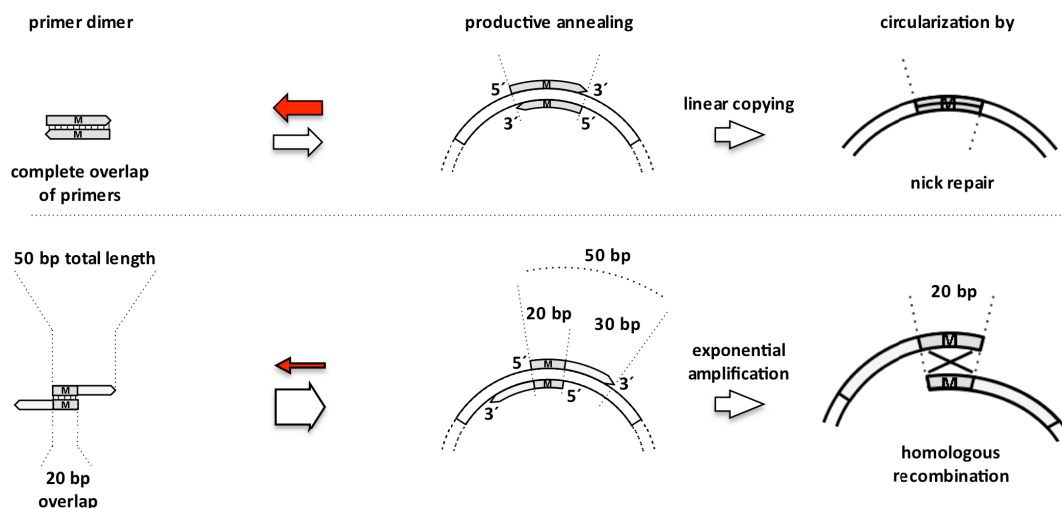


Figure 3. Impact of the different primer designs on template binding and *in vivo* product repair in site-directed mutagenesis. **Upper panel** Classic SDM. The primer pair forms a perfect double strand due to absolute complementarity. **Lower panel** New, *E. coli*-independent SDM. The primer pair forms only a partial double strand, while the full length of each oligonucleotide can bind to the template. Dark grey stretches indicate the reverse-complementary regions on the primers.

This simple, yet fundamental change in primer design is apt to instantly solve all problems encountered upon dismissal of *E. coli* for mutagenesis: I) *Template removal*. The unmutated template can be left in the reaction mixture. The exponentially generated reaction product significantly outcompetes the minute amount of used template (10 ng). Thus, the template can be unmethylated and come directly from yeast. II) *Yield*. A single reaction is now sufficient to chemically transform yeast cells. With the amounts obtained with classic SDM, many more reactions would need to be pooled, and this would inevitably result in a substantial number of false positive clones, because the mutagenesis template has, if toxic, to come directly from yeast, and then can not be removed. III) *Product repair in the target organism*. Instead of single-stranded overlaps made up by the mutagenic primer pair, the mutagenesis product by the different primer design is endowed with double-stranded ends of identical sequence that allow its precise recirculation by homologous recombination into an intact, selectable plasmid (Figure 3, lower panel, right). The 20 nt 5'-overlap is a minimum requirement for this [284]. At the same time it should not be too long as this results in an increase of unproductive primer dimerization against which the template has to compete (compare upper and lower panel, left and middle). As a rule, this stretch should never exceed 40 % of the whole primer length for preferred template binding. The modified primer design of the presented, yeast-based SDM is simple and like the classic SDM covers by definition all aspects of mutagenesis (Figure 4): mutation, insertion and deletion (including large deletions).

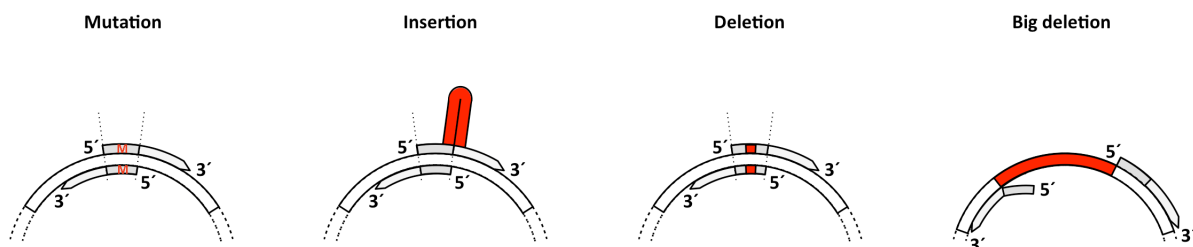


Figure 4. Mutation, insertion, and small or big deletions with the new SDM primer design. The shifted primer design of the exponential, *S. cerevisiae*-based SDM approach allows for any of the manipulations that the classic SDM permits. Dark grey boxed areas indicate the 20 nt stretch of reverse-complementary.

The primer pair for yeast-based SDM can easily be designed by the following basic rules: each oligonucleotide should be around 50 bases long, with 20 bases of 5' primer-to-primer overlap for an efficient recombination of the mutated plasmid ends in yeast, carrying the mutation, deletion or insertion in their middle, and 30 bases of 3'-sequence for template annealing. Due to the exponential nature of the new site-directed mutagenesis, the number of cycles is strictly kept at 18 as in the classic SDM protocol [285] to minimize PCR-introduced errors. Also, a proofreading DNA polymerase is used with an error rate equal to that of the *Pfu* Ultra enzyme in the commonly used Stratagene kit [273]. All analyzed clones so far faithfully replicate the template sequence in addition to the introduced mutation. Still, after obtaining the desired toxic gene mutation, one should confirm the integrity of all features needed for subsequent cloning steps of a project, e. g. before shuttling a mutated plasmid back into cell culture, the complete relevant sequence should be verified.

Restriction Sites as Markers for Successful Mutagenesis

Only some mutational changes that effect the change of an amino acid or its deletion result in the addition or disappearance of restriction sites on the mutated DNA. Since the primer cover a sequence of about 50 nucleotides, this stretch is bound to contain cryptic or complete restriction sites that can be activated or inactivated, respectively, by a second mutation encoded on the mutagenic primer. This second mutation then serves as a marker for the first, "restriction-silent" mutation in the subsequent analysis of transformant yeast clones by colony PCR. Additionally, it only needs to be designed into one of the primers when located outside the 20 nt 5', primer-primer overlap region. The only limitation for this analytical mutation is that it should not be among the first 10 bases of the oligonucleotide as this may compromise priming.

Figure 5 shows a detailed comparison of the *E. coli*- and yeast-based SDM procedures. In classic SDM (left side), the template has to compete with the oligonucleotides for priming because they allow for just as much base pairing as itself, if the primer-template mismatch due to the mutation is not taken into account. In contrast, the reduction of the primer complementarity to 20 nt (right side) greatly favors the annealing of the full 50 nt to the template in the first cycle (step 1 and 2). More importantly yet, it still outcompetes in subsequent cycles, when the shifted primers can not only again bind to the plasmid template at full length, but also to the

product template with 30 nt (step 3). While the 10 additional nt in comparison with the 20 nt primer-primer interaction may not drastically favor mutagenesis product priming in the second cycle, already at the end of this cycle the first product molecules with double-stranded ends appear, which subsequently are drastically preferred priming targets that, like the template, offer the full 50 nt of binding.

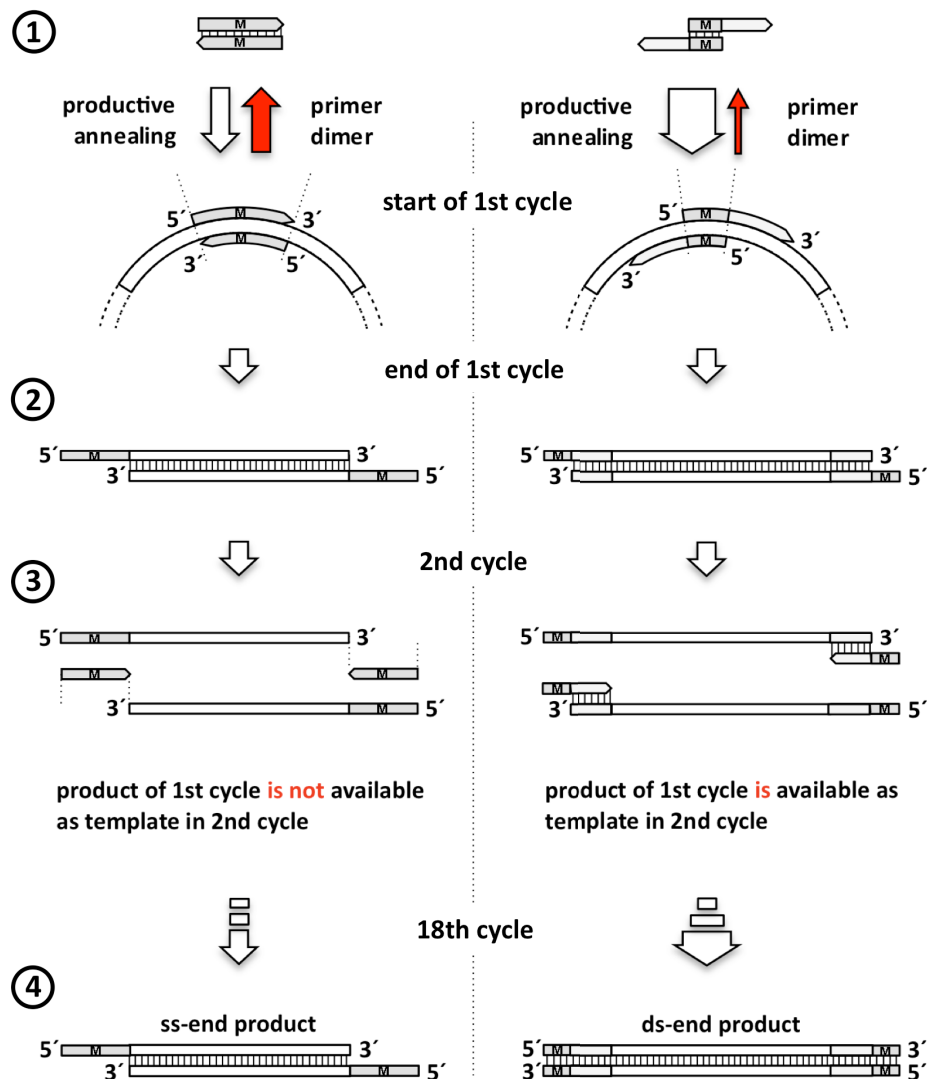


Figure 5. Comparison between the classic and the new, *E. coli*-independent site-directed mutagenesis method. Left cartoon side The classic site-directed mutagenesis (SDM). The mutagenesis primers perfectly overlap (step 1). As a result, the single-stranded ends of the product (steps 2 and 4) are not available as template in further cycles (step 3). **Right cartoon side** The change in primer design to a partial overlap results in preferred template binding (step 1). Thus, the ends of the product (steps 2 and 4) are available as productive priming sites in following reaction cycles (step 3). So already in third cycle, the first completely double-stranded product molecules appear.

Outlook

In the course of the practical work on this thesis, a complete workflow for the cloning and manipulation of unstable or otherwise toxic genes was established that consists of several, partially well-established procedures. It permits their quick cloning into any plasmid, the simultaneous construction and screening of several expression vectors, and the introduction of point mutations, utilizing a minimum of resources and hands-on time. This approach proved to be vital to this project as it gave the first-time heterologous overexpression of the unstable *BSEP* and *MDR3* cDNA in two yeast species. Due to the new, *E. coli*-independent mutagenesis method, both mechanistic and disease-associated mutations of these two human liver ABC transporters can now rapidly be generated and analyzed in cell culture or *in vitro*. Particularly the new approach to targeted mutagenesis should prove helpful in future endeavors where functionally relevant mutants of proteins up to now could not be studied due to limitations in their bacterial cloning.

Several novel clinical BSEP mutations have been recreated in cell culture models by the new mutagenesis method and are currently being studied on the cellular level.

The purification of BSEP and MDR3 is currently being optimized on both the genetic and the biochemical level. Future *in vitro* studies utilizing the two expression systems will aim at elucidating the function of these challenging membrane proteins in health and disease.

References

1. Lewin B (2007) *Cells*. Sudbury, Mass.: Jones and Bartlett Publishers. xix, 863 p. p.
2. Singer SJ, Nicolson GL (1972) The fluid mosaic model of the structure of cell membranes. *Science* 175: 720-731.
3. Vereb G, Szollosi J, Matko J, Nagy P, Farkas T, et al. (2003) Dynamic, yet structured: The cell membrane three decades after the Singer-Nicolson model. *Proc Natl Acad Sci U S A* 100: 8053-8058.
4. Saier MH, Jr. (1999) A functional-phylogenetic system for the classification of transport proteins. *J Cell Biochem Suppl* 32-33: 84-94.
5. Saier MH, Jr. (2000) A functional-phylogenetic classification system for transmembrane solute transporters. *Microbiol Mol Biol Rev* 64: 354-411.
6. Saier MH, Jr. (2000) Families of proteins forming transmembrane channels. *J Membr Biol* 175: 165-180.
7. Agre P, Kozono D (2003) Aquaporin water channels: molecular mechanisms for human diseases. *FEBS Lett* 555: 72-78.
8. Berg JM, Tymoczko JL, Stryer L (2002) *Biochemistry*. New York: W.H. Freeman. 1 v. (various pagings) p.
9. Serrano R (1978) Characterization of the plasma membrane ATPase of *Saccharomyces cerevisiae*. *Mol Cell Biochem* 22: 51-63.
10. Malpartida F, Serrano R (1980) Purification of the yeast plasma membrane ATPase solubilized with a novel zwitterionic detergent. *FEBS Lett* 111: 69-72.
11. Serrano R, Kielland-Brandt MC, Fink GR (1986) Yeast plasma membrane ATPase is essential for growth and has homology with (Na⁺ + K⁺), K⁺- and Ca²⁺-ATPases. *Nature* 319: 689-693.
12. Kaplan JH (2002) Biochemistry of Na,K-ATPase. *Annu Rev Biochem* 71: 511-535.
13. Skou JC (1957) The influence of some cations on an adenosine triphosphatase from peripheral nerves. *Biochim Biophys Acta* 23: 394-401.
14. Henderson R, Unwin PN (1975) Three-dimensional model of purple membrane obtained by electron microscopy. *Nature* 257: 28-32.
15. Holland IB (2003) *ABC proteins : from bacteria to man*. Amsterdam ; Boston: Academic Press. xxiii, 647 p. p.
16. Higgins CF, Haag PD, Nikaido K, Ardeshir F, Garcia G, et al. (1982) Complete nucleotide sequence and identification of membrane components of the histidine transport operon of *S. typhimurium*. *Nature* 298: 723-727.
17. Linton KJ, Higgins CF (1998) The *Escherichia coli* ATP-binding cassette (ABC) proteins. *Mol Microbiol* 28: 5-13.
18. Bauer BE, Wolfger H, Kuchler K (1999) Inventory and function of yeast ABC proteins: about sex, stress, pleiotropic drug and heavy metal resistance. *Biochim Biophys Acta* 1461: 217-236.
19. Dean M, Rzhetsky A, Allikmets R (2001) The human ATP-binding cassette (ABC) transporter superfamily. *Genome Res* 11: 1156-1166.
20. Dean M, Allikmets R (2001) Complete characterization of the human ABC gene family. *J Bioenerg Biomembr* 33: 475-479.
21. Higgins CF (1992) ABC transporters: from microorganisms to man. *Annu Rev Cell Biol* 8: 67-113.
22. Serres MH, Goswami S, Riley M (2004) GenProtEC: an updated and improved analysis of functions of *Escherichia coli* K-12 proteins. *Nucleic Acids Res* 32: D300-302.

23. Ernst R, Kueppers P, Stindt J, Kuchler K, Schmitt L (2010) Multidrug efflux pumps: Substrate selection in ATP-binding cassette multidrug efflux pumps - first come, first served? *FEBS Journal* 277: 540-549.
24. Kerr ID, Jones PM, George AM (2010) Multidrug efflux pumps: The structures of prokaryotic ATP-binding cassette transporter efflux pumps and implications for our understanding of eukaryotic P-glycoproteins and homologues. *FEBS Journal* 277: 550-563.
25. Crowley E, Callaghan R (2010) Multidrug efflux pumps: drug binding - gates or cavity? *FEBS Journal* 277: 530-539.
26. Borst P, Elferink RO (2002) Mammalian ABC transporters in health and disease. *Annu Rev Biochem* 71: 537-592.
27. Borst P, Jonkers J, Rottenberg S (2007) What makes tumors multidrug resistant? *Cell Cycle* 6: 2782-2787.
28. Dassa E (1993) Sequence-function relationships in MalG, an inner membrane protein from the maltose transport system in *Escherichia coli*. *Mol Microbiol* 7: 39-47.
29. Mourez M, Hofnung M, Dassa E (1997) Subunit interactions in ABC transporters: a conserved sequence in hydrophobic membrane proteins of periplasmic permeases defines an important site of interaction with the ATPase subunits. *EMBO J* 16: 3066-3077.
30. Biemans-Oldehinkel E, Doeven MK, Poolman B (2006) ABC transporter architecture and regulatory roles of accessory domains. *FEBS Lett* 580: 1023-1035.
31. Koch J, Guntrum R, Heintke S, Kyritsis C, Tampe R (2004) Functional dissection of the transmembrane domains of the transporter associated with antigen processing (TAP). *J Biol Chem* 279: 10142-10147.
32. Koch J, Guntrum R, Tampe R (2005) Exploring the minimal functional unit of the transporter associated with antigen processing. *FEBS Lett* 579: 4413-4416.
33. Schmitt L, Tampe R (2002) Structure and mechanism of ABC transporters. *Curr Opin Struct Biol* 12: 754-760.
34. Walker JE, Saraste M, Runswick MJ, Gay NJ (1982) Distantly related sequences in the alpha- and beta-subunits of ATP synthase, myosin, kinases and other ATP-requiring enzymes and a common nucleotide binding fold. *Embo J* 1: 945-951.
35. Zaitseva J, Jenewein S, Jumpertz T, Holland IB, Schmitt L (2005) H662 is the linchpin of ATP hydrolysis in the nucleotide-binding domain of the ABC transporter HlyB. *Embo J* 24: 1901-1910.
36. Vetter IR, Wittinghofer A (1999) Nucleoside triphosphate-binding proteins: different scaffolds to achieve phosphoryl transfer. *Q Rev Biophys* 32: 1-56.
37. Zaitseva J, Jenewein S, Oswald C, Jumpertz T, Holland IB, et al. (2005) A molecular understanding of the catalytic cycle of the nucleotide-binding domain of the ABC transporter HlyB. *Biochem Soc Trans* 33: 990-995.
38. Zaitseva J, Oswald C, Jumpertz T, Jenewein S, Wiedenmann A, et al. (2006) A structural analysis of asymmetry required for catalytic activity of an ABC-ATPase domain dimer. *EMBO J* 25: 3432-3443.
39. Higgins CF, Linton KJ (2004) The ATP switch model for ABC transporters. *Nat Struct Mol Biol* 11: 918-926.
40. Hopfner KP, Karcher A, Shin DS, Craig L, Arthur LM, et al. (2000) Structural biology of Rad50 ATPase: ATP-driven conformational control in DNA double-strand break repair and the ABC-ATPase superfamily. *Cell* 101: 789-800.
41. Locher KP, Lee AT, Rees DC (2002) The *E. coli* BtuCD structure: a framework for ABC transporter architecture and mechanism. *Science* 296: 1091-1098.

42. Fetsch EE, Davidson AL (2002) Vanadate-catalyzed photocleavage of the signature motif of an ATP-binding cassette (ABC) transporter. *Proc Natl Acad Sci U S A* 99: 9685-9690.
43. Abrahams JP, Leslie AG, Lutter R, Walker JE (1994) Structure at 2.8 Å resolution of F1-ATPase from bovine heart mitochondria. *Nature* 370: 621-628.
44. Story RM, Steitz TA (1992) Structure of the recA protein-ADP complex. *Nature* 355: 374-376.
45. Chen J, Lu G, Lin J, Davidson AL, Quijcho FA (2003) A tweezers-like motion of the ATP-binding cassette dimer in an ABC transport cycle. *Mol Cell* 12: 651-661.
46. Hung LW, Wang IX, Nikaido K, Liu PQ, Ames GF, et al. (1998) Crystal structure of the ATP-binding subunit of an ABC transporter. *Nature* 396: 703-707.
47. Verdon G, Albers SV, Dijkstra BW, Driessen AJ, Thunnissen AM (2003) Crystal structures of the ATPase subunit of the glucose ABC transporter from *Sulfolobus solfataricus*: nucleotide-free and nucleotide-bound conformations. *J Mol Biol* 330: 343-358.
48. Smith PC, Karpowich N, Millen L, Moody JE, Rosen J, et al. (2002) ATP binding to the motor domain from an ABC transporter drives formation of a nucleotide sandwich dimer. *Mol Cell* 10: 139-149.
49. Gaudet R, Wiley DC (2001) Structure of the ABC ATPase domain of human TAP1, the transporter associated with antigen processing. *Embo J* 20: 4964-4972.
50. Karpowich N, Martsinkevich O, Millen L, Yuan YR, Dai PL, et al. (2001) Crystal structures of the MJ1267 ATP binding cassette reveal an induced-fit effect at the ATPase active site of an ABC transporter. *Structure (Camb)* 9: 571-586.
51. Yuan YR, Blecker S, Martsinkevich O, Millen L, Thomas PJ, et al. (2001) The crystal structure of the MJ0796 ATP-binding cassette. Implications for the structural consequences of ATP hydrolysis in the active site of an ABC transporter. *J Biol Chem* 276: 32313-32321.
52. Lewis HA, Buchanan SG, Burley SK, Connors K, Dickey M, et al. (2004) Structure of nucleotide-binding domain 1 of the cystic fibrosis transmembrane conductance regulator. *Embo J* 23: 282-293.
53. Ward A, Reyes CL, Yu J, Roth CB, Chang G (2007) Flexibility in the ABC transporter MsbA: Alternating access with a twist. *Proc Natl Acad Sci U S A* 104: 19005-19010.
54. Dawson RJ, Locher KP (2006) Structure of a bacterial multidrug ABC transporter. *Nature* 443: 180-185.
55. Aller SG, Yu J, Ward A, Weng Y, Chittaboina S, et al. (2009) Structure of P-glycoprotein reveals a molecular basis for poly-specific drug binding. *Science* 323: 1718-1722.
56. Ehrmann M, Ehrle R, Hofmann E, Boos W, Schlosser A (1998) The ABC maltose transporter. *Mol Microbiol* 29: 685-694.
57. Benabdelhak H, Kiontke S, Horn C, Ernst R, Blight MA, et al. (2003) A specific interaction between the NBD of the ABC-transporter HlyB and a C-terminal fragment of its transport substrate haemolysin A. *J Mol Biol* 327: 1169-1179.
58. Jardetzky O (1966) Simple allosteric model for membrane pumps. *Nature* 211: 969-970.
59. Janas E, Hofacker M, Chen M, Gompf S, van der Does C, et al. (2003) The ATP hydrolysis cycle of the nucleotide-binding domain of the mitochondrial ATP-binding cassette transporter Mdl1p. *J Biol Chem* 278: 26862-26869.
60. Sauna ZE, Ambudkar SV (2001) Characterization of the catalytic cycle of ATP hydrolysis by human P-glycoprotein. The two ATP hydrolysis events in a single

- catalytic cycle are kinetically similar but affect different functional outcomes. *J Biol Chem* 276: 11653-11661.
61. Nikaido K, Liu PQ, Ames GF (1997) Purification and characterization of HisP, the ATP-binding subunit of a traffic ATPase (ABC transporter), the histidine permease of *Salmonella typhimurium*. Solubility, dimerization, and ATPase activity. *J Biol Chem* 272: 27745-27752.
 62. Zaitseva J, Jenewein S, Wiedenmann A, Benabdelhak H, Holland IB, et al. (2005) Functional characterization and ATP-induced dimerization of the isolated ABC-domain of the haemolysin B transporter. *Biochemistry* 44: 9680-9690.
 63. Liu CE, Liu PQ, Ames GF (1997) Characterization of the adenosine triphosphatase activity of the periplasmic histidine permease, a traffic ATPase (ABC transporter). *J Biol Chem* 272: 21883-21891.
 64. Liu PQ, Ames GF (1998) In vitro disassembly and reassembly of an ABC transporter, the histidine permease. *Proc Natl Acad Sci U S A* 95: 3495-3500.
 65. Pinkett HW, Lee AT, Lum P, Locher KP, Rees DC (2007) An inward-facing conformation of a putative metal-chelate-type ABC transporter. *Science* 315: 373-377.
 66. Khare D, Oldham ML, Orelle C, Davidson AL, Chen J (2030) Alternating Access in Maltose Transporter Mediated by Rigid-Body Rotations. *Molecular Cell* 33: 528-536.
 67. Hollenstein K, Dawson RJP, Locher KP (2007) Structure and mechanism of ABC transporter proteins. *Curr Opin Struct Biol* 17: 412-418.
 68. Dawson RJ, Locher KP (2007) Structure of the multidrug ABC transporter Sav1866 from *Staphylococcus aureus* in complex with AMP-PNP. *FEBS Lett* 581: 935-938.
 69. Scriver CR (1989) *The Metabolic basis of inherited disease*. New York: McGraw-Hill Information Services Co., Health Professions Division. 2 v. (xxviii, 3006, 3085 p.) p.
 70. Bodzioch M, Orso E, Klucken J, Langmann T, Bottcher A, et al. (1999) The gene encoding ATP-binding cassette transporter 1 is mutated in Tangier disease. *Nat Genet* 22: 347-351.
 71. Brooks-Wilson A, Marcil M, Clee SM, Zhang LH, Roomp K, et al. (1999) Mutations in ABC1 in Tangier disease and familial high-density lipoprotein deficiency. *Nat Genet* 22: 336-345.
 72. Marcil M, Brooks-Wilson A, Clee SM, Roomp K, Zhang LH, et al. (1999) Mutations in the ABC1 gene in familial HDL deficiency with defective cholesterol efflux. *Lancet* 354: 1341-1346.
 73. Rust S, Rosier M, Funke H, Real J, Amoura Z, et al. (1999) Tangier disease is caused by mutations in the gene encoding ATP-binding cassette transporter 1. *Nat Genet* 22: 352-355.
 74. Allikmets R (1997) A photoreceptor cell-specific ATP-binding transporter gene (ABCR) is mutated in recessive Stargardt macular dystrophy. *Nat Genet* 17: 122.
 75. Allikmets R, Shroyer NF, Singh N, Seddon JM, Lewis RA, et al. (1997) Mutation of the Stargardt disease gene (ABCR) in age-related macular degeneration. *Science* 277: 1805-1807.
 76. Martinez-Mir A, Paloma E, Allikmets R, Ayuso C, del Rio T, et al. (1998) Retinitis pigmentosa caused by a homozygous mutation in the Stargardt disease gene ABCR. *Nat Genet* 18: 11-12.
 77. Didier AD, Loor F (1995) Decreased biotolerability for ivermectin and cyclosporin A in mice exposed to potent P-glycoprotein inhibitors. *Int J Cancer* 63: 263-267.

78. Didier A, Loor F (1996) The abamectin derivative ivermectin is a potent P-glycoprotein inhibitor. *Anticancer Drugs* 7: 745-751.
79. Pouliot JF, L'Heureux F, Liu Z, Prichard RK, Georges E (1997) Reversal of P-glycoprotein-associated multidrug resistance by ivermectin. *Biochem Pharmacol* 53: 17-25.
80. Mealey KL, Northrup NC, Bentjen SA (2003) Increased toxicity of P-glycoprotein-substrate chemotherapeutic agents in a dog with the MDR1 deletion mutation associated with ivermectin sensitivity. *J Am Vet Med Assoc* 223: 1453-1455, 1434.
81. Roulet A, Puel O, Gesta S, Lepage JF, Drag M, et al. (2003) MDR1-deficient genotype in Collie dogs hypersensitive to the P-glycoprotein substrate ivermectin. *Eur J Pharmacol* 460: 85-91.
82. Oude Elferink RP, Groen AK (1995) The role of mdr2 P-glycoprotein in biliary lipid secretion. Cross-talk between cancer research and biliary physiology. *J Hepatol* 23: 617-625.
83. Ruetz S, Gros P (1994) Phosphatidylcholine translocase: a physiological role for the mdr2 gene. *Cell* 77: 1071-1081.
84. Noe J, Stieger B, Meier PJ (2002) Functional expression of the canalicular bile salt export pump of human liver. *Gastroenterology* 123: 1659-1666.
85. Zutz A, Gompf S, Schagger H, Tampe R (2009) Mitochondrial ABC proteins in health and disease. *Biochim Biophys Acta* 1787: 681-690.
86. Ballatori N, Hammond CL, Cunningham JB, Krance SM, Marchan R (2005) Molecular mechanisms of reduced glutathione transport: role of the MRP/CFTR/ABCC and OATP/SLC21A families of membrane proteins. *Toxicol Appl Pharmacol* 204: 238-255.
87. Quinton PM (1999) Physiological basis of cystic fibrosis: a historical perspective. *Physiol Rev* 79: S3-S22.
88. Inagaki N, Gonoi T, Clement JPt, Namba N, Inazawa J, et al. (1995) Reconstitution of IKATP: an inward rectifier subunit plus the sulfonylurea receptor. *Science* 270: 1166-1170.
89. Borst P, Evers R, Kool M, Wijnholds J (2000) A family of drug transporters: the multidrug resistance-associated proteins. *J Natl Cancer Inst* 92: 1295-1302.
90. Bakos E, Evers R, Calenda G, Tusnady GE, Szakacs G, et al. (2000) Characterization of the amino-terminal regions in the human multidrug resistance protein (MRP1). *J Cell Sci* 113 Pt 24: 4451-4461.
91. Shani N, Valle D (1998) Peroxisomal ABC transporters. *Methods Enzymol* 292: 753-776.
92. Bisbal C, Martinand C, Silhol M, Lebleu B, Salehzada T (1995) Cloning and characterization of a RNase L inhibitor. A new component of the interferon-regulated 2-5A pathway. *J Biol Chem* 270: 13308-13317.
93. Zimmerman C, Klein KC, Kiser PK, Singh AR, Firestein BL, et al. (2002) Identification of a host protein essential for assembly of immature HIV-1 capsids. *Nature* 415: 88-92.
94. Marton MJ, Vazquez de Aldana CR, Qiu H, Chakraborty K, Hinnebusch AG (1997) Evidence that GCN1 and GCN20, translational regulators of GCN4, function on elongating ribosomes in activation of eIF2alpha kinase GCN2. *Mol Cell Biol* 17: 4474-4489.
95. Tyzack JK, Wang X, Belsham GJ, Proud CG (2000) ABC50 interacts with eukaryotic initiation factor 2 and associates with the ribosome in an ATP-dependent manner. *J Biol Chem* 275: 34131-34139.

96. Chen H, Rossier C, Lalioti MD, Lynn A, Chakravarti A, et al. (1996) Cloning of the cDNA for a human homologue of the *Drosophila* white gene and mapping to chromosome 21q22.3. *Am J Hum Genet* 59: 66-75.
97. Klucken J, Buchler C, Orso E, Kaminski WE, Porsch-Ozcurumez M, et al. (2000) ABCG1 (ABC8), the human homolog of the *Drosophila* white gene, is a regulator of macrophage cholesterol and phospholipid transport. *Proc Natl Acad Sci U S A* 97: 817-822.
98. Sarkadi B, Ozvegy-Laczka C, Nemet K, Varadi A (2004) ABCG2 -- a transporter for all seasons. *FEBS Lett* 567: 116-120.
99. Spies T, DeMars R (1991) Restored expression of major histocompatibility class I molecules by gene transfer of a putative peptide transporter. *Nature* 351: 323-324.
100. Spies T, Bresnahan M, Bahram S, Arnold D, Blanck G, et al. (1990) A gene in the human major histocompatibility complex class II region controlling the class I antigen presentation pathway. *Nature* 348: 744-747.
101. Trowsdale J, Hanson I, Mockridge I, Beck S, Townsend A, et al. (1990) Sequences encoded in the class II region of the MHC related to the 'ABC' superfamily of transporters. *Nature* 348: 741-744.
102. Deverson EV, Gow IR, Coadwell WJ, Monaco JJ, Butcher GW, et al. (1990) MHC class II region encoding proteins related to the multidrug resistance family of transmembrane transporters. *Nature* 348: 738-741.
103. Powis SJ, Townsend AR, Deverson EV, Bastin J, Butcher GW, et al. (1991) Restoration of antigen presentation to the mutant cell line RMA-S by an MHC-linked transporter. *Nature* 354: 528-531.
104. van der Blik AM, Kooiman PM, Schneider C, Borst P (1988) Sequence of *mdr3* cDNA encoding a human P-glycoprotein. *Gene* 71: 401-411.
105. Schinkel AH, Roelofs EM, Borst P (1991) Characterization of the human MDR3 P-glycoprotein and its recognition by P-glycoprotein-specific monoclonal antibodies. *Cancer Res* 51: 2628-2635.
106. Elferink RP, Tytgat GN, Groen AK (1997) Hepatic canalicular membrane 1: The role of *mdr2* P-glycoprotein in hepatobiliary lipid transport. *FASEB J* 11: 19-28.
107. Allikmets R, Raskind WH, Hutchinson A, Schueck ND, Dean M, et al. (1999) Mutation of a putative mitochondrial iron transporter gene (ABC7) in X-linked sideroblastic anemia and ataxia (XLSA/A). *Hum Mol Genet* 8: 743-749.
108. Bekri S, Kispal G, Lange H, Fitzsimons E, Tolmie J, et al. (2000) Human ABC7 transporter: gene structure and mutation causing X-linked sideroblastic anemia with ataxia with disruption of cytosolic iron-sulfur protein maturation. *Blood* 96: 3256-3264.
109. Thompson R, Strautnieks S (2001) BSEP: function and role in progressive familial intrahepatic cholestasis. *Semin Liver Dis* 21: 545-550.
110. Keitel V, Burdelski M, Warskulat U, Kuhlkamp T, Keppler D, et al. (2005) Expression and localization of hepatobiliary transport proteins in progressive familial intrahepatic cholestasis. *Hepatology* 41: 1160-1172.
111. Dubin IN, Johnson FB (1954) Chronic idiopathic jaundice with unidentified pigment in liver cells; a new clinicopathologic entity with a report of 12 cases. *Medicine (Baltimore)* 33: 155-197.
112. Wada M, Toh S, Taniguchi K, Nakamura T, Uchiumi T, et al. (1998) Mutations in the canalicular multispecific organic anion transporter (cMOAT) gene, a novel ABC transporter, in patients with hyperbilirubinemia II/Dubin-Johnson syndrome. *Hum Mol Genet* 7: 203-207.

113. Ringpfeil F, Lebowitz MG, Christiano AM, Uitto J (2000) Pseudoxanthoma elasticum: mutations in the MRP6 gene encoding a transmembrane ATP-binding cassette (ABC) transporter. *Proc Natl Acad Sci U S A* 97: 6001-6006.
114. Riordan JR, Rommens JM, Kerem B, Alon N, Rozmahel R, et al. (1989) Identification of the cystic fibrosis gene: cloning and characterization of complementary DNA. *Science* 245: 1066-1073.
115. Kerem B, Rommens JM, Buchanan JA, Markiewicz D, Cox TK, et al. (1989) Identification of the cystic fibrosis gene: genetic analysis. *Science* 245: 1073-1080.
116. Rommens JM, Iannuzzi MC, Kerem B, Drumm ML, Melmer G, et al. (1989) Identification of the cystic fibrosis gene: chromosome walking and jumping. *Science* 245: 1059-1065.
117. Thomas PM, Cote GJ, Wohllk N, Haddad B, Mathew PM, et al. (1995) Mutations in the sulfonyleurea receptor gene in familial persistent hyperinsulinemic hypoglycemia of infancy. *Science* 268: 426-429.
118. Mosser J, Douar AM, Sarde CO, Kioschis P, Feil R, et al. (1993) Putative X-linked adrenoleukodystrophy gene shares unexpected homology with ABC transporters. *Nature* 361: 726-730.
119. Berge KE, Tian H, Graf GA, Yu L, Grishin NV, et al. (2000) Accumulation of dietary cholesterol in sitosterolemia caused by mutations in adjacent ABC transporters. *Science* 290: 1771-1775.
120. Lee MH, Lu K, Hazard S, Yu H, Shulenin S, et al. (2001) Identification of a gene, ABCG5, important in the regulation of dietary cholesterol absorption. *Nat Genet* 27: 79-83.
121. Lu K, Lee MH, Hazard S, Brooks-Wilson A, Hidaka H, et al. (2001) Two genes that map to the STSL locus cause sitosterolemia: genomic structure and spectrum of mutations involving sterolin-1 and sterolin-2, encoded by ABCG5 and ABCG8, respectively. *Am J Hum Genet* 69: 278-290.
122. Haussinger D, Kubitz R, Reinehr R, Bode JG, Schliess F (2004) Molecular aspects of medicine: from experimental to clinical hepatology. *Mol Aspects Med* 25: 221-360.
123. Chandra P, Brouwer KL (2004) The complexities of hepatic drug transport: current knowledge and emerging concepts. *Pharm Res* 21: 719-735.
124. Kullak-Ublick GA, Stieger B, Meier PJ (2004) Enterohepatic bile salt transporters in normal physiology and liver disease. *Gastroenterology* 126: 322-342.
125. Leslie EM, Deeley RG, Cole SP (2005) Multidrug resistance proteins: role of P-glycoprotein, MRP1, MRP2, and BCRP (ABCG2) in tissue defense. *Toxicol Appl Pharmacol* 204: 216-237.
126. Faber KN, Muller M, Jansen PL (2003) Drug transport proteins in the liver. *Adv Drug Deliv Rev* 55: 107-124.
127. Meier PJ, Eckhardt U, Schroeder A, Hagenbuch B, Stieger B (1997) Substrate specificity of sinusoidal bile acid and organic anion uptake systems in rat and human liver. *Hepatology* 26: 1667-1677.
128. Hagenbuch B, Stieger B, Foguet M, Lubbert H, Meier PJ (1991) Functional expression cloning and characterization of the hepatocyte Na⁺/bile acid cotransport system. *Proc Natl Acad Sci U S A* 88: 10629-10633.
129. Konig J, Nies AT, Cui Y, Leier I, Keppler D (1999) Conjugate export pumps of the multidrug resistance protein (MRP) family: localization, substrate specificity, and MRP2-mediated drug resistance. *Biochim Biophys Acta* 1461: 377-394.

130. Keppler D, Cui Y, Konig J, Leier I, Nies A (1999) Export pumps for anionic conjugates encoded by MRP genes. *Adv Enzyme Regul* 39: 237-246.
131. Arrese M, Ananthanarayanan M (2004) The bile salt export pump: molecular properties, function and regulation. *Pflugers Arch* 449: 123-131.
132. Micrograph LTS (2006) Used under the GNU Free Documentation License. Department of Histology, Jagiellonian University Medical College, Krakow, Poland.
133. Cartoon of Liver Cell Ultrastructure. Downloaded from www.irishhealth.com on 11.01.10.
134. Childs S, Yeh RL, Georges E, Ling V (1995) Identification of a sister gene to P-glycoprotein. *Cancer Res* 55: 2029-2034.
135. Gerloff T, Stieger B, Hagenbuch B, Madon J, Landmann L, et al. (1998) The sister of P-glycoprotein represents the canalicular bile salt export pump of mammalian liver. *J Biol Chem* 273: 10046-10050.
136. Meier PJ, Stieger B (2002) Bile salt transporters. *Annu Rev Physiol* 64: 635-661.
137. Aleksandrov L, Aleksandrov AA, Chang XB, Riordan JR (2002) The First Nucleotide Binding Domain of Cystic Fibrosis Transmembrane Conductance Regulator Is a Site of Stable Nucleotide Interaction, whereas the Second Is a Site of Rapid Turnover. *J Biol Chem* 277: 15419-15425.
138. Aleksandrov L, Mengos A, Chang X, Aleksandrov A, Riordan JR (2001) Differential interactions of nucleotides at the two nucleotide binding domains of the cystic fibrosis transmembrane conductance regulator. *J Biol Chem* 276: 12918-12923.
139. Chen M, Abele R, Tampe R (2004) Functional non-equivalence of ATP-binding cassette signature motifs in the transporter associated with antigen processing (TAP). *J Biol Chem* 279: 46073-46081.
140. Fickert P, Zollner G, Fuchsbichler A, Stumptner C, Pojer C, et al. (2001) Effects of ursodeoxycholic and cholic acid feeding on hepatocellular transporter expression in mouse liver. *Gastroenterology* 121: 170-183.
141. Karpen SJ (2002) Nuclear receptor regulation of hepatic function. *J Hepatol* 36: 832-850.
142. Schmitt M, Kubitz R, Lizun S, Wettstein M, Haussinger D (2001) Regulation of the dynamic localization of the rat Bsep gene-encoded bile salt export pump by anisoosmolarity. *Hepatology* 33: 509-518.
143. Kipp H, Arias IM (2002) Trafficking of canalicular ABC transporters in hepatocytes. *Annu Rev Physiol* 64: 595-608.
144. Kubitz R, Sutfels G, Kuhlkamp T, Kolling R, Haussinger D (2004) Trafficking of the bile salt export pump from the Golgi to the canalicular membrane is regulated by the p38 MAP kinase. *Gastroenterology* 126: 541-553.
145. Noe J, Hagenbuch B, Meier PJ, St-Pierre MV (2001) Characterization of the mouse bile salt export pump overexpressed in the baculovirus system. *Hepatology* 33: 1223-1231.
146. Pauli-Magnus C, Kerb R, Fattinger K, Lang T, Anwald B, et al. (2004) BSEP and MDR3 haplotype structure in healthy Caucasians, primary biliary cirrhosis and primary sclerosing cholangitis. *Hepatology* 39: 779-791.
147. Smith AJ, de Vree JM, Ottenhoff R, Oude Elferink RP, Schinkel AH, et al. (1998) Hepatocyte-specific expression of the human MDR3 P-glycoprotein gene restores the biliary phosphatidylcholine excretion absent in Mdr2 (-/-) mice. *Hepatology* 28: 530-536.
148. Crawford AR, Smith AJ, Hatch VC, Oude Elferink RP, Borst P, et al. (1997) Hepatic secretion of phospholipid vesicles in the mouse critically depends on mdr2 or

- MDR3 P-glycoprotein expression. Visualization by electron microscopy. *J Clin Invest* 100: 2562-2567.
149. Degiorgio D, Colombo C, Seia M, Porcaro L, Costantino L, et al. (2007) Molecular characterization and structural implications of 25 new ABCB4 mutations in progressive familial intrahepatic cholestasis type 3 (PFIC3). *Eur J Hum Genet* 15: 1230-1238.
 150. Mbongo-Kama E, Harnois F, Mennecier D, Leclercq E, Burnat P, et al. (2007) MDR3 mutations associated with intrahepatic and gallbladder cholesterol cholelithiasis: an update. *Ann Hepatol* 6: 143-149.
 151. Floreani A, Carderi I, Paternoster D, Soardo G, Azzaroli F, et al. (2008) Hepatobiliary phospholipid transporter ABCB4, MDR3 gene variants in a large cohort of Italian women with intrahepatic cholestasis of pregnancy. *Dig Liver Dis* 40: 366-370.
 152. Oude Elferink RP, Bakker CT, Roelofsen H, Middelkoop E, Ottenhoff R, et al. (1993) Accumulation of organic anion in intracellular vesicles of cultured rat hepatocytes is mediated by the canalicular multispecific organic anion transporter. *Hepatology* 17: 434-444.
 153. Benet LZ, Izumi T, Zhang Y, Silverman JA, Wachter VJ (1999) Intestinal MDR transport proteins and P-450 enzymes as barriers to oral drug delivery. *J Control Release* 62: 25-31.
 154. Cui Y, Konig J, Buchholz JK, Spring H, Leier I, et al. (1999) Drug resistance and ATP-dependent conjugate transport mediated by the apical multidrug resistance protein, MRP2, permanently expressed in human and canine cells. *Mol Pharmacol* 55: 929-937.
 155. Nies AT, Keppler D (2007) The apical conjugate efflux pump ABCC2 (MRP2). *Pflugers Arch* 453: 643-659.
 156. Fernandez SB, Hollo Z, Kern A, Bakos E, Fischer PA, et al. (2002) Role of the N-terminal transmembrane region of the multidrug resistance protein MRP2 in routing to the apical membrane in MDCKII cells. *J Biol Chem* 277: 31048-31055.
 157. Gao M, Yamazaki M, Loe DW, Westlake CJ, Grant CE, et al. (1998) Multidrug resistance protein. Identification of regions required for active transport of leukotriene C4. *J Biol Chem* 273: 10733-10740.
 158. Bakos E, Hegedus T, Hollo Z, Welker E, Tusnady GE, et al. (1996) Membrane topology and glycosylation of the human multidrug resistance-associated protein. *J Biol Chem* 271: 12322-12326.
 159. Hirohashi T, Suzuki H, Ito K, Ogawa K, Kume K, et al. (1998) Hepatic expression of multidrug resistance-associated protein-like proteins maintained in eisai hyperbilirubinemic rats. *Mol Pharmacol* 53: 1068-1075.
 160. Sprinz H, Nelson RS (1954) Persistent non-hemolytic hyperbilirubinemia associated with lipochrome-like pigment in liver cells: report of four cases. *Ann Intern Med* 41: 952-962.
 161. Jonker JW, Stedman CAM, Liddle C, Downes M (2009) Hepatobiliary ABC transporters: physiology, regulation and implications for disease. *Front Biosci* 14: 4904-4920.
 162. Yu L, Li-Hawkins J, Hammer RE, Berge KE, Horton JD, et al. (2002) Overexpression of ABCG5 and ABCG8 promotes biliary cholesterol secretion and reduces fractional absorption of dietary cholesterol. *J Clin Invest* 110: 671-680.
 163. Graf GA, Li WP, Gerard RD, Gelissen I, White A, et al. (2002) Coexpression of ATP-binding cassette proteins ABCG5 and ABCG8 permits their transport to the apical surface. *J Clin Invest* 110: 659-669.

164. Bull LN, van Eijk MJ, Pawlikowska L, DeYoung JA, Juijn JA, et al. (1998) A gene encoding a P-type ATPase mutated in two forms of hereditary cholestasis. *Nat Genet* 18: 219-224.
165. Simons K, Ikonen E (1997) Functional rafts in cell membranes. *Nature* 387: 569-572.
166. Brown DA, London E (2000) Structure and function of sphingolipid- and cholesterol-rich membrane rafts. *J Biol Chem* 275: 17221-17224.
167. Meder D, Moreno MJ, Verkade P, Vaz WLC, Simons K (2006) Phase coexistence and connectivity in the apical membrane of polarized epithelial cells. *Proc Natl Acad Sci USA* 103: 329-334.
168. Dos Santos SM, Weber C-C, Franke C, Müller WE, Eckert GP (2007) Cholesterol: Coupling between membrane microenvironment and ABC transporter activity. *Biochem Biophys Res Commun* 354: 216-221.
169. Klappe K, Hummel I, Hoekstra D, Kok JW (2009) Lipid dependence of ABC transporter localization and function. *Chem Phys Lipids* 161: 57-64.
170. Paulusma CC, Groen A, Kunne C, Ho-Mok KS, Spijkerboer AL, et al. (2006) Atp8b1 deficiency in mice reduces resistance of the canalicular membrane to hydrophobic bile salts and impairs bile salt transport. *Hepatology* 44: 195-204.
171. Oude Elferink RPJ, Paulusma CC (2007) Function and pathophysiological importance of ABCB4 (MDR3 P-glycoprotein). *Pflugers Arch* 453: 601-610.
172. Ortiz DF, St Pierre MV, Abdulmessih A, Arias IM (1997) A yeast ATP-binding cassette-type protein mediating ATP-dependent bile acid transport. *J Biol Chem* 272: 15358-15365.
173. Wagner S, Bader ML, Drew D, de Gier J-W (2006) Rationalizing membrane protein overexpression. *Trends Biotechnol* 24: 364-371.
174. Noé J, Stieger B, Meier PJ (2002) Functional expression of the canalicular bile salt export pump of human liver. *Gastroenterology* 123: 1659-1666.
175. Smith AJ, van Helvoort A, van Meer G, Szabo K, Welker E, et al. (2000) MDR3 P-glycoprotein, a phosphatidylcholine translocase, transports several cytotoxic drugs and directly interacts with drugs as judged by interference with nucleotide trapping. *J Biol Chem* 275: 23530-23539.
176. Hagmann W, Nies AT, König J, Frey M, Zentgraf H, et al. (1999) Purification of the human apical conjugate export pump MRP2 reconstitution and functional characterization as substrate-stimulated ATPase. *Eur J Biochem* 265: 281-289.
177. Hagmann W, Schubert J, König J, Keppler D (2002) Reconstitution of transport-active multidrug resistance protein 2 (MRP2; ABCC2) in proteoliposomes. *Biol Chem* 383: 1001-1009.
178. Mus-Veteau I (2010) Heterologous expression of membrane proteins for structural analysis. *Methods Mol Biol* 601: 1-16.
179. Evans GL, Ni B, Hrycyna CA, Chen D, Ambudkar SV, et al. (1995) Heterologous expression systems for P-glycoprotein: *E. coli*, yeast, and baculovirus. *J Bioenerg Biomembr* 27: 43-52.
180. Dean M, Hamon Y, Chimini G (2001) The human ATP-binding cassette (ABC) transporter superfamily. *J Lipid Res* 42: 1007-1017.
181. Kuchler K, Thorner J (1992) Functional expression of human *mdr1* in the yeast *Saccharomyces cerevisiae*. *Proc Natl Acad Sci USA* 89: 2302-2306.
182. Figler RA, Omote H, Nakamoto RK, Al-Shawi MK (2000) Use of chemical chaperones in the yeast *Saccharomyces cerevisiae* to enhance heterologous membrane protein expression: high-yield expression and purification of human P-glycoprotein. *Arch Biochem Biophys* 376: 34-46.

183. Lee SH, Altenberg GA (2003) Transport of leukotriene C₄ by a cysteine-less multidrug resistance protein 1 (MRP1). *Biochem J* 370: 357-360.
184. Lee SH, Altenberg GA (2003) Expression of functional multidrug-resistance protein 1 in *Saccharomyces cerevisiae*: effects of N- and C-terminal affinity tags. *Biochem Biophys Res Commun* 306: 644-649.
185. Bergman LW (2001) Growth and maintenance of yeast. *Methods Mol Biol* 177: 9-14.
186. Ernst R, Kueppers P, Klein CM, Schwarzmüller T, Kuchler K, et al. (2008) A mutation of the H-loop selectively affects rhodamine transport by the yeast multidrug ABC transporter Pdr5. *Proc Natl Acad Sci USA* 105: 5069-5074.
187. Ernst R, Klemm R, Schmitt L, Kuchler K (2005) Yeast ABC Transporters - Cellular Cleaning Pumps. *Methods Enzymol.*
188. Mamnun YM, Pandjaitan R, Mahe Y, Delahodde A, Kuchler K (2002) The yeast zinc finger regulators Pdr1p and Pdr3p control pleiotropic drug resistance (PDR) as homo- and heterodimers in vivo. *Mol Microbiol* 46: 1429-1440.
189. Rogers B, Decottignies A, Kolaczowski M, Carvajal E, Balzi E, et al. (2001) The pleiotropic drug ABC transporters from *Saccharomyces cerevisiae*. *J Mol Microbiol Biotechnol* 3: 207-214.
190. Wolfger H, Mamnun YM, Kuchler K (2001) Fungal ABC proteins: pleiotropic drug resistance, stress response and cellular detoxification. *Res Microbiol* 152: 375-389.
191. Kueppers P (2010) Molekulare Analyse des pleiotropen ABC-Transporters Pdr5 aus *S. cerevisiae*. Duesseldorf: Heinrich Heine Universitaet Duesseldorf.
192. Decottignies A, Grant AM, Nichols JW, de Wet H, McIntosh DB, et al. (1998) ATPase and multidrug transport activities of the overexpressed yeast ABC protein Yor1p. *J Biol Chem* 273: 12612-12622.
193. Nakamura K, Niimi M, Niimi K, Holmes AR, Yates JE, et al. (2001) Functional expression of *Candida albicans* drug efflux pump Cdr1p in a *Saccharomyces cerevisiae* strain deficient in membrane transporters. *Antimicrob Agents Chemother* 45: 3366-3374.
194. Mahé Y, Lemoine Y, Kuchler K (1996) The ATP binding cassette transporters Pdr5 and Snq2 of *Saccharomyces cerevisiae* can mediate transport of steroids in vivo. *J Biol Chem* 271: 25167-25172.
195. Lerner-Marmarosh N, Gimi K, Urbatsch IL, Gros P, Senior AE (1999) Large scale purification of detergent-soluble P-glycoprotein from *Pichia pastoris* cells and characterization of nucleotide binding properties of wild-type, Walker A, and Walker B mutant proteins. *J Biol Chem* 274: 34711-34718.
196. Cai J, Daoud R, Georges E, Gros P (2001) Functional expression of multidrug resistance protein 1 in *Pichia pastoris*. *Biochemistry* 40: 8307-8316.
197. Wang Z, Stalcup LD, Harvey BJ, Weber J, Chloupkova M, et al. (2006) Purification and ATP Hydrolysis of the Putative Cholesterol Transporters ABCG5 and ABCG8†. *Biochemistry* 45: 9929-9939.
198. Johnson BJH, Lee J-Y, Pickert A, Urbatsch IL (2010) Bile acids stimulate ATP hydrolysis in the purified cholesterol transporter ABCG5/G8. *Biochemistry* 49: 3403-3411.
199. Chloupková M, Pickert A, Lee J-Y, Souza S, Trinh YT, et al. (2007) Expression of 25 human ABC transporters in the yeast *Pichia pastoris* and characterization of the purified ABCG3 ATPase activity. *Biochemistry* 46: 7992-8003.
200. Cregg JM, Tolstorukov I, Kusari A, Sunga J, Madden K, et al. (2009) Expression in the yeast *Pichia pastoris*. *Methods Enzymol* 463: 169-189.

201. Bartosz G, König J, Keppler D, Hagmann W (1998) Human mast cells secreting leukotriene C₄ express the MRP1 gene-encoded conjugate export pump. *Biol Chem* 379: 1121-1126.
202. Scheffer GL, Kool M, Heijn M, de Haas M, Pijnenborg AC, et al. (2000) Specific detection of multidrug resistance proteins MRP1, MRP2, MRP3, MRP5, and MDR3 P-glycoprotein with a panel of monoclonal antibodies. *Cancer Res* 60: 5269-5277.
203. Keitel V, Burdelski M, Warskulat U, Köhlkamp T, Keppler D, et al. (2005) Expression and localization of hepatobiliary transport proteins in progressive familial intrahepatic cholestasis. *Hepatology* 41: 1160-1172.
204. Egner R, Mahé Y, Pandjaitan R, Kuchler K (1995) Endocytosis and vacuolar degradation of the plasma membrane-localized Pdr5 ATP-binding cassette multidrug transporter in *Saccharomyces cerevisiae*. *Mol Cell Biol* 15: 5879-5887.
205. Ernst R (2007) Molekulare Analyse von ABC-Transportern am Beispiel von Pdr5p aus *S. cerevisiae* und der isolierten NBD des humanen TAP1. Duesseldorf: Heinrich Heine Universitaet Duesseldorf.
206. Cui Y, König J, Buchholz JK, Spring H, Leier I, et al. (1999) Drug resistance and ATP-dependent conjugate transport mediated by the apical multidrug resistance protein, MRP2, permanently expressed in human and canine cells. *Mol Pharmacol* 55: 929-937.
207. Byrne JA, Strautnieks SS, Mieli-Vergani G, Higgins CF, Linton KJ, et al. (2002) The human bile salt export pump: characterization of substrate specificity and identification of inhibitors. *Gastroenterology* 123: 1649-1658.
208. Mumberg D, Müller R, Funk M (1995) Yeast vectors for the controlled expression of heterologous proteins in different genetic backgrounds. *Gene* 156: 119-122.
209. Mumberg D, Müller R, Funk M (1994) Regulatable promoters of *Saccharomyces cerevisiae*: comparison of transcriptional activity and their use for heterologous expression. *Nucleic Acids Res* 22: 5767-5768.
210. Keitel V, Burdelski M, Vojnisek Z, Schmitt L, Häussinger D, et al. (2009) De novo bile salt transporter antibodies as a possible cause of recurrent graft failure after liver transplantation: A novel mechanism of cholestasis. *Hepatology* 50: 510-517.
211. Hanahan D (1983) Studies on transformation of *Escherichia coli* with plasmids. *J Mol Biol* 166: 557-580.
212. Singh MV, Weil PA (2002) A method for plasmid purification directly from yeast. *Anal Biochem* 307: 13-17.
213. Lorenz RT, Parks LW (1990) Effects of lovastatin (mevinolin) on sterol levels and on activity of azoles in *Saccharomyces cerevisiae*. *Antimicrob Agents Chemother* 34: 1660-1665.
214. Mamnun YM, Schüller C, Kuchler K (2004) Expression regulation of the yeast PDR5 ATP-binding cassette (ABC) transporter suggests a role in cellular detoxification during the exponential growth phase. *FEBS Lett* 559: 111-117.
215. Serrano R (1988) H⁺-ATPase from plasma membranes of *Saccharomyces cerevisiae* and *Avena sativa* roots: purification and reconstitution. *Methods Enzymol* 157: 533-544.
216. Goffeau A, Dufour JP (1988) Plasma membrane ATPase from the yeast *Saccharomyces cerevisiae*. *Methods Enzymol* 157: 528-533.
217. Dufour JP, Amory A, Goffeau A (1988) Plasma membrane ATPase from the yeast *Schizosaccharomyces pombe*. *Methods Enzymol* 157: 513-528.
218. Bradford MM (1976) A rapid and sensitive method for the quantitation of microgram quantities of protein utilizing the principle of protein-dye binding. *Anal Biochem* 72: 248-254.

219. Godiska R, Mead D, Dhodda V, Wu C, Hochstein R, et al. (2010) Linear plasmid vector for cloning of repetitive or unstable sequences in *Escherichia coli*. *Nucleic Acids Res* 38: e88.
220. Falster DS, Nakken S, Bergem-Ohr M, Rodland EA, Breivik J (2010) Unstable DNA repair genes shaped by their own sequence modifying phenotypes. *J Mol Evol* 70: 266-274.
221. Vu K, Bautos J, Hong M-P, Gelli A (2009) The functional expression of toxic genes: Lessons learned from molecular cloning of CCH1, a high-affinity Ca²⁺ channel. *Anal Biochem* 393: 234-241.
222. Byrne JA, Strautnieks SS, Ihrke G, Pagani F, Knisely AS, et al. (2009) Missense mutations and single nucleotide polymorphisms in ABCB11 impair bile salt export pump processing and function or disrupt pre-messenger RNA splicing. *Hepatology* 49: 553-567.
223. Wang G, Christensen LA, Vasquez KM (2006) Z-DNA-forming sequences generate large-scale deletions in mammalian cells. *Proc Natl Acad Sci U S A* 103: 2677-2682.
224. Cheng SH, Gregory RJ, Marshall J, Paul S, Souza DW, et al. (1990) Defective intracellular transport and processing of CFTR is the molecular basis of most cystic fibrosis. *Cell* 63: 827-834.
225. Kielland-Brandt MCW, B.; Holmberg, S.; Litske Petersen J. G.; Nilsson-Tillgren T. (1980) Genetic Evidence for Nuclear Location of 2-Micron DNA in Yeast. *Carlsberg Res Commun* 45: 119-124.
226. Gerbaud CG, M. (1980) 2 um Plasmid Copy Number in Different Yeast Strains and Repartition of Endogenous and 2 um Chimeric Plasmids in Transformed Strains. *Current Genetics* 1: 219-228.
227. Qiang BQ, Schildkraut I (1984) A type II restriction endonuclease with an eight nucleotide specificity from *Streptomyces fimbriatus*. *Nucleic Acids Res* 12: 4507-4516.
228. Wentzell LM, Nobbs TJ, Halford SE (1995) The *Sfi*I restriction endonuclease makes a four-strand DNA break at two copies of its recognition sequence. *J Mol Biol* 248: 581-595.
229. Sambrook J, Russell DW (2001) *Molecular cloning : a laboratory manual*. Cold Spring Harbor, N.Y.: Cold Spring Harbor Laboratory Press.
230. Keitel V, Kartenbeck J, Nies AT, Spring H, Brom M, et al. (2000) Impaired protein maturation of the conjugate export pump multidrug resistance protein 2 as a consequence of a deletion mutation in Dubin-Johnson syndrome. *Hepatology* 32: 1317-1328.
231. Beck WT, Mueller TJ, Tanzer LR (1979) Altered surface membrane glycoproteins in Vinca alkaloid-resistant human leukemic lymphoblasts. *Cancer Res* 39: 2070-2076.
232. Kartner N, Evernden-Porelle D, Bradley G, Ling V (1985) Detection of P-glycoprotein in multidrug-resistant cell lines by monoclonal antibodies. *Nature* 316: 820-823.
233. Zhang G, Fedyunin I, Miekley O, Valleriani A, Moura A, et al. (2010) Global and local depletion of ternary complex limits translational elongation. *Nucleic Acids Research* 38: 4778-4787.
234. Sharp PM, Cowe E (1991) Synonymous codon usage in *Saccharomyces cerevisiae*. *Yeast* 7: 657-678.
235. Tao L, Jackson RE, Cheng Q (2005) Directed evolution of copy number of a broad host range plasmid for metabolic engineering. *Metab Eng* 7: 10-17.

236. Ma H, Kunes S, Schatz PJ, Botstein D (1987) Plasmid construction by homologous recombination in yeast. *Gene* 58: 201-216.
237. Gibson DG (2009) Synthesis of DNA fragments in yeast by one-step assembly of overlapping oligonucleotides. *Nucleic Acids Res* 37: 6984-6990.
238. Oldenburg KR, Vo KT, Michaelis S, Paddon C (1997) Recombination-mediated PCR-directed plasmid construction in vivo in yeast. *Nucleic Acids Res* 25: 451-452.
239. Jansen G, Wu C, Schade B, Thomas DY, Whiteway M (2005) Drag&Drop cloning in yeast. *Gene* 344: 43-51.
240. Kubitz R, Keitel V, Scheuring S, Kohrer K, Haussinger D (2006) Benign recurrent intrahepatic cholestasis associated with mutations of the bile salt export pump. *J Clin Gastroenterol* 40: 171-175.
241. Pauli-Magnus C, Lang T, Meier Y, Zodan-Marin T, Jung D, et al. (2004) Sequence analysis of bile salt export pump (ABCB11) and multidrug resistance p-glycoprotein 3 (ABCB4, MDR3) in patients with intrahepatic cholestasis of pregnancy. *Pharmacogenetics* 14: 91-102.
242. Brown CR, Hong-Brown LQ, Welch WJ (1997) Strategies for correcting the delta F508 CFTR protein-folding defect. *J Bioenerg Biomembr* 29: 491-502.
243. Welch WJ, Brown CR (1996) Influence of molecular and chemical chaperones on protein folding. *Cell Stress Chaperones* 1: 109-115.
244. Pomorski T, Lombardi R, Riezman H, Devaux PF, van Meer G, et al. (2003) Drs2p-related P-type ATPases Dnf1p and Dnf2p are required for phospholipid translocation across the yeast plasma membrane and serve a role in endocytosis. *Mol Biol Cell* 14: 1240-1254.
245. Raymond M, Gros P, Whiteway M, Thomas DY (1992) Functional complementation of yeast *ste6* by a mammalian multidrug resistance *mdr* gene. *Science* 256: 232-234.
246. Ruetz S, Raymond M, Gros P (1993) Functional expression of P-glycoprotein encoded by the mouse *mdr3* gene in yeast cells. *Proc Natl Acad Sci USA* 90: 11588-11592.
247. Raymond M, Ruetz S, Thomas DY, Gros P (1994) Functional expression of P-glycoprotein in *Saccharomyces cerevisiae* confers cellular resistance to the immunosuppressive and antifungal agent FK520. *Mol Cell Biol* 14: 277-286.
248. Ruetz S, Brault M, Kast C, Hemenway C, Heitman J, et al. (1996) Functional expression of the multidrug resistance-associated protein in the yeast *Saccharomyces cerevisiae*. *J Biol Chem* 271: 4154-4160.
249. Mao Q, Scarborough GA (1997) Purification of functional human P-glycoprotein expressed in *Saccharomyces cerevisiae*. *Biochim Biophys Acta* 1327: 107-118.
250. Niimi M, Wada S-i, Tanabe K, Kaneko A, Takano Y, et al. (2005) Functional analysis of fungal drug efflux transporters by heterologous expression in *Saccharomyces cerevisiae*. *Jpn J Infect Dis* 58: 1-7.
251. Leonard PJ, Rathod PK, Golin J (1994) Loss of function mutation in the yeast multiple drug resistance gene *PDR5* causes a reduction in chloramphenicol efflux. *Antimicrob Agents Chemother* 38: 2492-2494.
252. Kolaczowski M, van der Rest M, Cybularz-Kolaczowska A, Soumillion JP, Konings WN, et al. (1996) Anticancer drugs, ionophoric peptides, and steroids as substrates of the yeast multidrug transporter *Pdr5p*. *J Biol Chem* 271: 31543-31548.
253. Saeki T, Shimabuku AM, Azuma Y, Shibano Y, Komano T, et al. (1991) Expression of human P-glycoprotein in yeast cells--effects of membrane component sterols on the activity of P-glycoprotein. *Agric Biol Chem* 55: 1859-1865.

254. Staatz CE, Goodman LK, Tett SE (2010) Effect of CYP3A and ABCB1 Single Nucleotide Polymorphisms on the Pharmacokinetics and Pharmacodynamics of Calcineurin Inhibitors: Part II. *Clinical Pharmacokinetics* 49: 207-221.
255. Saeki T, Ueda K, Tanigawara Y, Hori R, Komano T (1993) Human P-glycoprotein transports cyclosporin A and FK506. *J Biol Chem* 268: 6077-6080.
256. Breuder T, Hemenway CS, Movva NR, Cardenas ME, Heitman J (1994) Calcineurin is essential in cyclosporin A- and FK506-sensitive yeast strains. *Proc Natl Acad Sci U S A* 91: 5372-5376.
257. Kim RB (2002) Drugs as P-glycoprotein substrates, inhibitors, and inducers. *Drug Metab Rev* 34: 47-54.
258. Endres CJ, Hsiao P, Chung FS, Unadkat JD (2006) The role of transporters in drug interactions. *Eur J Pharm Sci* 27: 501-517.
259. Keesler GA, Casey WM, Parks LW (1992) Stimulation by heme of steryl ester synthase and aerobic sterol exclusion in the yeast *Saccharomyces cerevisiae*. *Arch Biochem Biophys* 296: 474-481.
260. Jumpertz T, Tschapek B, Infed N, Smits SH, Ernst R, et al. (2011) High-throughput evaluation of the critical micelle concentration of detergents. *Anal Biochem* 408: 64-70.
261. Seret A, Bahri M-A (2009) The CMC-like behaviour of bile salts as probed by photoexcited Rose Bengal. *Colloids and Surfaces A: Physicochemical and Engineering Aspects* 339: 153-158.
262. Istvan ES, Deisenhofer J (2001) Structural mechanism for statin inhibition of HMG-CoA reductase. *Science* 292: 1160-1164.
263. Hirano M, Maeda K, Hayashi H, Kusuhara H, Sugiyama Y (2005) Bile salt export pump (BSEP/ABCB11) can transport a nonbile acid substrate, pravastatin. *J Pharmacol Exp Ther* 314: 876-882.
264. Sakaeda T, Takara K, Kakumoto M, Ohmoto N, Nakamura T, et al. (2002) Simvastatin and lovastatin, but not pravastatin, interact with MDR1. *J Pharm Pharmacol* 54: 419-423.
265. Zehnpfennig B, Urbatsch IL, Galla H-J (2009) Functional Reconstitution of Human ABCC3 into Proteoliposomes Reveals a Transport Mechanism with Positive Cooperativity. *Biochemistry* 48: 4423-4430.
266. Cregg JM, Russell KA (1998) Transformation. *Methods Mol Biol* 103: 27-39.
267. Braman J, Papworth C, Greener A (1996) Site-directed mutagenesis using double-stranded plasmid DNA templates. *Methods Mol Biol* 57: 31-44.
268. Feher Z, Kiss A, Venetianer P (1983) Expression of a bacterial modification methylase gene in yeast. *Nature* 302: 266-268.
269. Proffitt JH, Davie JR, Swinton D, Hattman S (1984) 5-Methylcytosine is not detectable in *Saccharomyces cerevisiae* DNA. *Mol Cell Biol* 4: 985-988.
270. Hattman S, Kenny C, Berger L, Pratt K (1978) Comparative study of DNA methylation in three unicellular eucaryotes. *J Bacteriol* 135: 1156-1157.
271. Liu H, Naismith JH (2008) An efficient one-step site-directed deletion, insertion, single and multiple-site plasmid mutagenesis protocol. *BMC Biotechnol* 8: 91.
272. Stratagene Inc. QuikChange II XL Site-Directed Mutagenesis Kit Instruction Manual. Revision B.
273. Stratagene Inc. PfuUltra High-Fidelity DNA Polymerase Instruction Manual. Revision #064001h.
274. Teo SH, Jackson SP (1997) Identification of *Saccharomyces cerevisiae* DNA ligase IV: involvement in DNA double-strand break repair. *EMBO J* 16: 4788-4795.

-
275. Romanos MA, Scorer CA, Clare JJ (1992) Foreign gene expression in yeast: a review. *Yeast* 8: 423-488.
 276. Tate CG (2001) Overexpression of mammalian integral membrane proteins for structural studies. *FEBS Letters* 504: 94-98.
 277. Aller SG, Yu J, Ward A, Weng Y, Chittaboina S, et al. (2009) Supporting Online Material for Structure of P-Glycoprotein Reveals a Molecular Basis for Poly-Specific Drug Binding. *Science* 323: 1718-1722.
 278. Urbatsch IL, Gimi K, Wilke-Mounts S, Lerner-Marmarosh N, Rousseau ME, et al. (2001) Cysteines 431 and 1074 are responsible for inhibitory disulfide cross-linking between the two nucleotide-binding sites in human P-glycoprotein. *J Biol Chem* 276: 26980-26987.
 279. Schmitt L, Benabdelhak H, Blight MA, Holland IB, Stubbs MT (2003) Crystal structure of the nucleotide-binding domain of the ABC-transporter haemolysin B: identification of a variable region within ABC helical domains. *J Mol Biol* 330: 333-342.
 280. Ernst R, Klemm R, Schmitt L, Kuchler K (2005) Yeast ATP-binding cassette transporters: cellular cleaning pumps. *Meth Enzymol* 400: 460-484.
 281. Holz C, Prinz B, Bolotina N, Sievert V, Bussow K, et al. (2003) Establishing the yeast *Saccharomyces cerevisiae* as a system for expression of human proteins on a proteome-scale. *J Struct Funct Genomics* 4: 97-108.
 282. Aslanidis C, de Jong PJ (1990) Ligation-independent cloning of PCR products (LIC-PCR). *Nucleic Acids Res* 18: 6069-6074.
 283. Geertsma ER, Poolman B (2007) High-throughput cloning and expression in recalcitrant bacteria. *Nat Methods* 4: 705-707.
 284. Manivasakam P, Weber SC, McElver J, Schiestl RH (1995) Micro-homology mediated PCR targeting in *Saccharomyces cerevisiae*. *Nucleic Acids Res* 23: 2799-2800.
 285. QuikChange II XL Site-Directed Mutagenesis Kit Instruction Manual. Revision D. Agilent Technologies Inc.

Abbreviations

(k)bp	(kilo) base pair
A.U.	arbitrary unit
ABC	ATP binding cassette
ALD	Adrenoleukodystrophy
AOX1	<i>Alcohol oxidase 1</i>
APS	ammoniumperoxo-disulphate
ATP	adenosine triphosphate
BCRP	breast cancer resistance protein
BRIC	benign recurrent intrahepatic cholestasis
BSA	bovine serum albumine
BSEP	bile salt export pump
CFTR	cystic fibrosis transmembrane conductance regulator
CIAP	calf intestinal alkaline phosphatase
cmc	critical micellar concentration
Ctrl	control
CYMAL	6-cyclohexylhexyl-beta-D-maltopyranoside
dd.	double-distilled
DDM	dodecyl maltopyranoside
DJS	Dubin-Johnson syndrome
DM	decyl maltopyranoside
DMSO	dimethyl sulfoxide
DNA	deoxyribonucleic acid
dNTP	deoxynucleotide triphosphate
<i>E. coli</i>	<i>Escherichia coli</i>
EDTA	ethylenediamine tetraacetic acid
ER	endoplasmic reticulum
EtBr	ethidium bromide
eYFP	enhanced yellow fluorescent protein
FOS-14 / -16	Fos-choline-14 / -16
FXR	farnesoid X receptor
GOI	gene of interest
GTQ	Gentechnik-Qualität
h	hour
HCl	hydrochloric acid
HDL	high density lipoprotein
HEK	human embryonal kidney
HEPES	4-(2-hydroxyethyl)-1-piperazineethanesulfonic acid
HepG2	human hepatoma cell line
His	histidine

HlyB	hemolysin B
HMG-CoA	3-hydroxy-3-methylglutaryl-Coenzyme A
HR	homologous recombination
HRP	horseradish peroxidase
IMAC	immobilized metal ion affinity chromatography
IPTG	Isopropyl-beta-D-thiogalactoside
LB	lysogeny beoth
MAPK	mitogen-activated protein kinase
MDCK	Madin Darby canine kidney
MDR1 / 3	multidrug resistance protein 1 / 3
MFS	major facilitator superfamily
min	minute
mRNA	messenger RNA
MRP2	multidrug resistance-associated protein 2
MWCO	molecular weight cut-off
NBD	nucleotide binding domain
nt	nucleotide
NTA	nitrilotriacetic acid
NTCP	sodium (Na) taurocholate co-transporting polypeptide
NTE	N-terminal extension
OABP	oligo-adenylate binding protein
OATP	organic anion transporting polypeptide
ORF	open reading frame
Ori	origin of replication
P	pellet
P-gp	P-glycoprotein
<i>P. pastoris</i>	<i>Pichia pastoris</i>
PC	phosphatidylcholine
PCR	polymerase chain reaction
PDR	pleiotropic drug resistance
PEG	poly ethylene glycol
PFIC	progressive familiar intrahepatic cholestase
Pfu	<i>Pyrococcus furiosus</i>
PKC	protein kinase C
PM	plasma membrane
Pmal	plasma membrane ATPase I
PNK	polynucleotide kinase
rpm	revolutions per minute
RT	room temperature
RXR	retinoic X receptor
<i>S. cerevisiae</i>	<i>Saccharomyces cerevisiae</i>

SBP	substrate binding protein
SDM	site-directed mutagenesis
SDS	sodium dodecyl sulphate
PAGE	poly acrylamide gel electrophoresis
SLC	solute carrier
SN	supernatant
TAP	transporter associated with antigen processing
TBS(-T)	Tris-buffered saline (-Tween)
T(D)C	tauro(deoxy)cholate
TCA	trichloroacetic acid
TEMED	tetramethylethylenediamine
TMD	transmembrane domain
Tris	tris-(hydroxymethyl)-aminomethan
UV	ultraviolet
V	Volt
v/v	volume per volume
w/v	weight per volume
wt	wild type
YFL	your favourite locus
YNB	yeast nitrogen broth
YPD	yeast peptone dextrose

Danksagung

An vorderster Stelle danke ich Prof. Dr. Lutz Schmitt, der niemals den Glauben an dieses immer wieder von Frustrationen und unerwarteten Herausforderungen geprägte Projekt verloren hat und jedem seiner Doktoranden eine lückenlose Finanzierung klarmacht. Hut ab dafür! Sein Enthusiasmus für die Forschung hat die vorliegende Doktorarbeit erst ermöglicht. Und mich von Apple abhängig gemacht.

Ich danke weiter PD. Dr. Ulrich Schulte für die Übernahme des Koreferats, insbesondere aber für seine unnachgiebigen Fragen in unseren Institutsseminaren, die oft genug Gedankenanstöße waren und den Blick auf die großen Zusammenhänge gelenkt haben. Und uns Doktoranden oft genug Wissenslücken aufgezeigt haben. Uli! Dieses Jahr werd ich die Gartenschweinchen aus Ton wieder los beim Schrottwichteln!

Ein großes Dankeschön geht an Dr. Sander H. J. Smits für seine kontinuierliche Unterstützung und viele produktive und nervenaufreibende (BSEP hat zuerst meine, ich dann seine Nerven zerfasert) Diskussionen rund um mein Projekt. Vielen Dank dafür! und außerdem für das Korrekturlesen und Aufspüren vieler Sätze von epischer Länge in dieser Arbeit.

Ich möchte außerdem Dr. Verena Keitel, Dr. Claudia Stross und Prof. Dr. Ralf Kubitz herzlich danken für die Unterstützung, die sie mir als unsere Kooperationspartner im SFB575 zuteil werden ließen: Western Blots auf Filmmaterial, Reagenzien und Konstrukte sowie Transfektionen und Fluoreszenzmikroskopie.

Besonderer Dank für fünf produktive Jahre Ausnahmezustand gilt allen meinen Kolleginnen und Kollegen: von der Aufreinigung eines Proteins bis zu der Gewissheit, daß ein Edding nicht sicherer in der eigenen Schublade liegt als ein Eppiständer, habe ich einiges von Euch lernen können. André, Britta, Marianne, Martina, Nacera, Nils, Ninotschka, Patrick, Petra, Philipp, Robert, Silke und Silke, Stefan, Susanne, Rakesh (science and cuisine in personal union), Tatuschka, Veronique, und Prof. em. Dr. Manfred Grieshaber: Dank Euch allen für so manche Hilfe, gute Kritik und das Miteinander inner- und außerhalb des Mikrokosmos Institut. Mitge- und ertragen haben diesen Ausnahmezustand auch Freunde von "draußen", die trotz eines "Lebens für die Forschung" gottseidank noch so zahlreich sind, daß ich sie hier nicht aufzählen kann.

Dr. rer. nat. Petra Küppers: großen Respekt für die von Dir an dem PDR5-Projekt geleistete Arbeit! Da hab ich noch einiges lernen können. Vielen Dank auch an Dich für das Durchsehen der Arbeit sowie Deinen Input in privaten wie projektgebundenen Diskussionen, in denen unsere Sicht der Dinge oft gleich war, doch die Kommunikation wie zwei parallele Linien: gleicher Natur, doch erst im Unendlichen konvergierend.

An Marianne Kluth und Philipp Ellinger geht besonderer Dank für den Fleiß und die Mühe, die beide in dieses Projekt im Rahmen ihrer Bachelorarbeit haben fließen lassen. Ich bin sicher, daß beide auf ihrem jeweiligen Forschungsweg weiterhin sehr erfolgreich sein werden. Marianne, Du hast tapfer mit mir gegen MDR3 gekämpft und gewonnen! Ein ganz expliziter Dank an Philipp, der nach seinem USA-Aufenthalt zurückkam, um in seiner Master- und derzeit Doktorarbeit weiter die Reihen im Kampf gegen die menschliche Leber (und ihr ABC-Transporterrepertoire) zu stärken, für viele Diskussionen und Denkrunden als Masterstudent, in denen er sich so manche ausschweifende Satzgefüge aus meinem Mund anzuhören nicht zu schade war. Das Resultat waren immer häufiger wissenschaftliche Debatten, in denen die glänzenden Degen des Halbwissens aufeinanderprallten, um oft genug festzustellen, daß ein Gefecht nicht lohnt, wenn man die Waffe nicht beherrscht. So wurden aus uns beiden Wissenschaftler. "Challenge", Dir gehört jetzt die Zukunft!

Die wichtigste Danksagung aber kommt zuletzt: die an meine Familie. Dieser Dank gebührt ganz besonders meiner Mutter Karin und meinem Vater Klaus, die mich stets in allen Belangen unterstützt und mir in vielen Dingen den Rücken freigehalten haben. Birte, Thomas, Tanja und jüngst auch Paul, Ihr habt mich, jeder auf seine Weise, immer wieder auf den Boden der Tatsachen zurückgeholt, wenn mein Dasein zu "akademisch" wurde. Dank Euch dafür, daß wir als Familie immer zusammengestanden haben.

Erklärung

Hiermit erkläre ich, daß ich die vorliegende Arbeit selbständig verfaßt und nur die angegebenen Hilfsmittel benutzt habe. Diese Arbeit wurde an keiner anderen Fakultät eingereicht oder anderweitig veröffentlicht.

Düsseldorf, den 15.11.2010

Jan Stindt

Lebenslauf

Persönliche Daten

Geboren am 13.1.1978 in Kiel
Familienstand ledig
Nationalität deutsch

Hochschulausbildung

Seit 2007 Mitglied des Integrierten Graduiertenkollegs im SFB575 "Experimentelle Hepatologie" (Teilprojekt A9 - *In vitro* Charakterisierung von ABC Transportern der humanen Leber)

2005 Beginn der Promotion im Institut für Biochemie - Arbeitsgruppe Membrantransport an der Heinrich Heine Universität Düsseldorf bei Prof. Dr. Lutz Schmitt
Thema: "Molekulare Analyse von ABC-Transportern der humanen Leber"

Dezember 2004 Abschluss zum Diplombiologen an der Freien Universität Berlin. Thema der Diplomarbeit: "Analyse des *peptide loading complex* (PLC) in HCMV-infizierten humanen Fibroblasten"

WS2000-SS2004 Hauptstudium Biologie an der Freien Universität Berlin. Arbeit als studentische Hilfskraft im Institut für Neurobiologie. Mehrmonatige freie Mitarbeiter am Institut für angewandte Genetik, Institut für Mikrobiologie und Robert Koch Institut. Arbeit als Tutor im Institut für Pflanzenphysiologie (2001-2004)

WS1998-SS2000 Grundstudium Biologie an der Georg August Universität Göttingen. Arbeit als studentische Hilfskraft am Institut für Anthropologie und am Institut für Palynologie und Quartärwissenschaften

1997-1998 Zivildienst bei der Arbeiterwohlfahrt e.V. Kiel

Schulbildung

1988-1997 Thor-Heyerdahl-Gymnasium in Kiel (Allgemeine Hochschulreife)
1984-1988 Grundschule am Heidenberger Teich in Kiel

Leistungen

- 2009 Gordon Research Conference on "Multidrug Efflux Systems. Understanding And Overcoming Multi-Drug Efflux Pumps In Disease". Galveston, Texas, USA
Registration Fee Reimbursement Grant
Poster: Jan Stindt, Petra Kueppers, Sander H.J. Smits and Lutz Schmitt. "Homologous and heterologous overexpression of PDR and MDR Efflux pumps in yeast"
- 2008 Konferenz des SFB575 "Regenerative Hepatology". Düsseldorf, Nordrhein-Westfalen.
Short Talk: "*In vitro* characterization of human liver ABC transporters". **Poster:** Jan Stindt, Petra Küppers and Lutz Schmitt. "A system for overexpression of eukaryotic membrane proteins".
- 2008 FEMS Young Scientist Meeting Grant (YSMG)
2nd FEBS Special Meeting Co-sponsored by FEMS "ATP Binding Cassette (ABC) Transporter Proteins: From Multidrug Resistance to Genetic Diseases". Innsbruck, Österreich
Poster: Jan Stindt, Petra Kueppers, Robert Ernst and Lutz Schmitt. "Homologous and heterologous overexpression of eukaryotic membrane proteins in yeast"
- 2007 58. Mosbacher Kolloquium "Protein and lipid sorting in health and disease". Mosbach, Baden-Württemberg
Poster: Petra Küppers, Jan Stindt, Robert Ernst, Karl Kuchler and Lutz Schmitt. "Functional overexpression and characterization of the yeast ABC transporter Pdr5p"

Publikationen

Stindt J, Ellinger P, Stross C, Keitel V, Kubitz R, Häussinger D, Smits S H J, Schmitt L. Yeast as a Tool for Handling unstable DNA: Cloning, Expression and Mutagenesis of the Human Bile Salt Export Pump (ABCB11).

Manuscript in preparation

Kueppers P, Ernst R, **Stindt J**, Smits S H J, Kuchler K, Schmitt L. A TMD mutation changes ATPase activity and drug susceptibility in the yeast ABC transporter Pdr5.

Manuscript in preparation

Halenius A, Hauka S, Dölken L, **Stindt J**, Reinhard H, Wiek C, Hanenberg H, Koszinowski U H, Momburg F, Hengel H. Human Cytomegalovirus Targets the MHC Class I Peptide Loading Complex (PLC) and Inhibits Tapasin Gene Transcription.

Submitted

Ernst R, Kueppers P, **Stindt J**, Kuchler K, Schmitt L (2010) Multidrug efflux pumps: Substrate selection in ATP-binding cassette multidrug efflux pumps - first come, first served? FEBS Journal 277: 540-549.

Menzel R, Greggers U, Smith A, Berger S, Brandt R, Brunke S, Bundrock G, Huelse S, Pluempe T, Schaupp F, Schuettler E, Stach S, **Stindt J**, Stollhoff N, Watzl S (2005) Honey bees navigate according to a map-like spatial memory. Proc Natl Acad Sci U S A 102: 3040-3045.